

EFFICIENCY-AWARE AND ENERGY-AWARE DATA COLLECTION VIA A
UAV WITH LIMITED-CAPACITY BATTERY IN ROBOTIC WIRELESS
SENSOR NETWORKS

A THESIS SUBMITTED TO
THE GRADUATE SCHOOL OF NATURAL AND APPLIED SCIENCES
OF
MIDDLE EAST TECHNICAL UNIVERSITY

BY

ÖMER MELİH GÜL

IN PARTIAL FULFILLMENT OF THE REQUIREMENTS
FOR
THE DEGREE OF DOCTOR OF PHILOSOPHY
IN
ELECTRICAL AND ELECTRONICS ENGINEERING

DECEMBER 2020

Approval of the thesis:

**EFFICIENCY-AWARE AND ENERGY-AWARE DATA COLLECTION VIA A
UAV WITH LIMITED-CAPACITY BATTERY IN ROBOTIC WIRELESS
SENSOR NETWORKS**

submitted by **ÖMER MELİH GÜL** in partial fulfillment of the requirements for the degree of **Doctor of Philosophy in Electrical and Electronics Engineering Department, Middle East Technical University** by,

Prof. Dr. Halil Kalıpçılar
Dean, Graduate School of Natural and Applied Sciences _____

Prof. Dr. İlkey Ulusoy
Head of Department, **Electrical and Electronics Engineering** _____

Prof. Dr. Aydan Müşerref Erkmen
Supervisor, **Electrical and Electronics Engineering, METU** _____

Examining Committee Members:

Prof. Dr. Umut Orguner
Electrical and Electronics Engineering, METU _____

Prof. Dr. Aydan Müşerref Erkmen
Electrical and Electronics Engineering, METU _____

Prof. Dr. Klaus Werner Schmidt
Electrical and Electronics Engineering, METU _____

Prof. Dr. Huriye Işıl Bozma
Electrical and Electronics Engineering, Boğaziçi University _____

Assist. Prof. Dr. Yakup Özkazanç
Electrical and Electronics Engineering, Hacettepe University _____

Date: 17.12.2020



I hereby declare that all information in this document has been obtained and presented in accordance with academic rules and ethical conduct. I also declare that, as required by these rules and conduct, I have fully cited and referenced all material and results that are not original to this work.

Name, Surname: Ömer Melih Gül

Signature :

ABSTRACT

EFFICIENCY-AWARE AND ENERGY-AWARE DATA COLLECTION VIA A UAV WITH LIMITED-CAPACITY BATTERY IN ROBOTIC WIRELESS SENSOR NETWORKS

Gül, Ömer Melih

Ph.D., Department of Electrical and Electronics Engineering

Supervisor: Prof. Dr. Aydan Müşerref Erkmén

December 2020, 193 pages

This thesis investigates efficiency-aware and energy-aware data-collection problems by an unmanned aerial vehicle (UAV) with limited-capacity battery, in a clustered robot network. In each cluster, a cluster head (CH) robot allocates tasks to remaining robots and collects data from them. Firstly, we consider this problem by focusing on minimizing energy consumption of UAV coupled to minimum cost data collection from CH robots by visiting optimal portion of CH robots. UAV decides the CH robots to visit by considering both their locations and its battery capacity. If it cannot visit all CH robots, each nonvisited CH robot forwards its data to another CH robot. Cost optimization includes decision of transmission paths of transmitting robots. Optimal approach is derived, and total energy consumption of CH robots are compared for various numbers of clusters under different strategies. Secondly, we consider the problem by defining the priority set of CH robots which UAV needs to visit. We aim to minimize the total energy consumption of CH robots by visiting optimally a portion of CH robots including priority set. Energy consumptions of CH robots under different strategies are evaluated for various numbers of CH robots and priority sets. Thirdly, we tackle the problem by considering not only different locations but also

different data efficiencies for different CH robots. We aim to minimize total joint cost of energy consumption and data efficiencies of CH robots by visiting optimal set of CH robots. Total joint costs of CH robots under different strategies are evaluated for various numbers of CH robots.

Keywords: cluster-based routing, robotic network, energy efficient routing, unmanned aerial vehicle (UAV), wireless sensor network (WSN).



ÖZ

ROBOTİK KABLOSUZ DUYARGA AĞLARINDA SINIRLI KAPASİTELİ PİLE SAHİP BİR İHA İLE VERİMLİLİK-FARKINDA VE ENERJİ-FARKINDA VERİ TOPLAMA

Gül, Ömer Melih

Doktora, Elektrik ve Elektronik Mühendisliği Bölümü

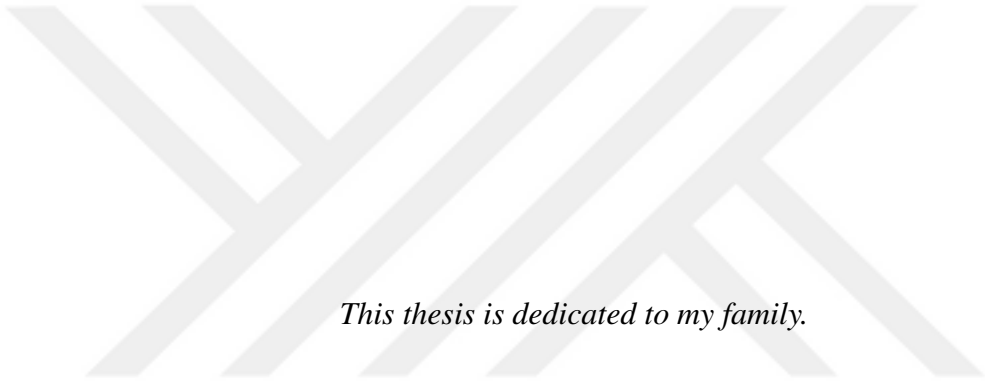
Tez Yöneticisi: Prof. Dr. Aydan Müşerref Erkmn

Aralık 2020 , 193 sayfa

Bu tez, kümelenen bir robot ağında sınırlı kapasiteli pile sahip bir insansız hava aracının (İHA) verimlilik-farkında ve enerji-farkında veri toplama problemleri incelemektedir. Her kümede, bir küme başı (KB) robotu kalan robotlara görevler atamakta ve onlardan veri toplamaktadır. İlk olarak, İHA'nın enerji harcamasını en aza indirerek KB robotlardan en iyi bir kısmını ziyaret ederek KB robotlardan en az maliyetli veri toplamasına odaklanarak bu problemi ele almaktayız. İHA, hem onların konumlarını hem de pil kapasitesini göz önünde bulundurarak ziyaret edeceği KB robotlara karar vermektedir. Eğer tüm KB robotlarını ziyaret edemezse ziyaret edilmemiş bir KB robot verisini başka bir KB robotuna iletirmektedir. Maliyet en iyileştirmesi, ileten robotların iletim yollarının kararlarını da içermektedir. En iyi yaklaşım elde edilmiş ve KB robotlarının toplam enerji harcaması farklı stratejiler altında farklı sayıda kümeler için karşılaştırılmıştır. İkinci olarak, İHA'ların gezmesi gereken KB robotlarından oluşan öncelik kümesi tanımlayarak bu problemi ele almaktayız. Öncelik kümesini de içeren en iyi KB robot kümesini ziyaret ederek KB robotlarının toplam enerji har-

camasını minimize etmeyi hedeflemekteyiz. Farklı stratejiler altında KB robotlarının toplam enerji harcaması farklı sayıda KB robot kümeleri ve öncelik kümeleri için değerlendirilmiştir. Üçüncü olarak, farklı KB robotlar için sadece farklı konumlar değil aynı zamanda farklı veri verimliliklerini de göz önünde bulundurarak bu problemi ele almaktayız. En iyi KB robot kümesini ziyaret ederek KB robotlarının toplam enerji harcaması ve veri verimliliklerinden oluşan toplam birleşik maliyetini en aza indirmeyi hedeflemekteyiz. Farklı stratejiler altında KB robotlarının toplam birleşik maliyetleri farklı sayıda KB robotları için değerlendirilmiştir.

Anahtar Kelimeler: Küme tabanlı rotalama, robot ağları, enerji verimli rotalama, insansız hava aracı (İHA), kablosuz duyarga ağları (KDA)



This thesis is dedicated to my family.

ACKNOWLEDGMENTS

I would like to thank firstly my supervisor Professor Aydan Müşerref Erkmen for her support, guidance and friendship. It was a great honor and experience to work with her for the last six years and our cooperation influenced my academical and world view highly. I would also like to thank Professor Umut Orguner and Assistant Professor Yakup Özkazanç for their guidance in the thesis monitoring committee meetings which help me very much. In addition, I would like to thank my thesis jury members Professor Klaus Werner Schmidt and Professor Huriye Işıl Bozma for their comments and suggestions which help us very much while editing this thesis. I also would like to thank Professor Mübeccel Demirekler for her valuable time and support during my studies. I owe her very much.

I thank my friends with whom I made projects, shared knowledge and spent time together at METU. I am quite lucky to be a colleague and friend of Ziya Özkan at the same time. He has been interested and helpful in the success of my work. I cannot forget his friendly attitude and help. In addition to Ziya, I would like to thank my friends Ali Hamidoğlu, Güner Velioğlu, Çağrı Batıhan, Mekki Uludağ, Naki Güler, Mustafa Mızrak, Hakan Aydoğdu, Sifatullah, Mehmet Sedat Feyat, Mehmet Ali Öztürk, Eray Şentürk, Ozan Koçak, Alim Yolalmaz, and Özgür Yalçın in the guesthouse. I appreciate their earnest friendship. I am also thankful to Özlem Tuğfe Demir, Ali Bulut Üçüncü, Ömer Çayır, Gökhan Koray Gültekin, and Serhat Emir Oğan.

I also thank my friends in IEEE Turkey Young Professionals Team, especially Göksel Uçtu ve Murat Yazıcı. In the toughest year 2020, we not only have done amazing work but also shared experience. I am honored to be chair of such a great team. I would also like to thank Professor Hasan Fatih Uğurdağ, IEEE Turkey Section Chair. I have learned a lot from him about not only volunteership but also academia and life.

Lastly but not the least, I would like to express my gratitude to my family for their love and care which has been an essential motivation to complete this study.

TABLE OF CONTENTS

ABSTRACT	v
ÖZ	vii
ACKNOWLEDGMENTS	x
TABLE OF CONTENTS	xi
LIST OF TABLES	xviii
LIST OF FIGURES	xxiv
LIST OF ABBREVIATIONS	xxxii
CHAPTERS	
1 INTRODUCTION	1
1.1 Motivation	1
1.2 Our Contributions	5
1.3 Organization	7
2 RELATED WORK	9
2.1 Energy-Aware, Cluster-Based Routing Protocols with Static Sink	9
2.2 Energy-Aware, Cluster-Based Routing Protocols with Mobile Sink	15
2.3 The related work with orienteering problem	18
3 ENERGY-AWARE CLUSTER-BASED DATA COLLECTION BY A UAV WITH A LIMITED-CAPACITY BATTERY IN ROBOTIC WIRELESS SENSOR NETWORKS	21

3.1	System Model and Problem Definition	21
3.1.1	Motivation and Problem Definition	21
3.1.2	Our Problem Approach Formulation	26
3.2	Sufficient Battery Capacity to Visit All CH Robots	28
3.3	Our Novel Approach: Total Energy Minimization Problem	28
3.3.1	Optimal Data Forwarding Strategy of CH Robots	29
3.3.2	Optimal Strategy for the UAV	34
3.4	Numerical Results	44
3.4.1	5-CH case	45
3.4.1.1	UAV-Oriented Strategy	45
3.4.1.2	Optimal Strategy (GAMEDFS)	47
3.4.1.3	Performance Comparison	50
3.4.2	6-CH case	51
3.4.2.1	UAV-Oriented Strategy	52
3.4.2.2	Optimal Strategy (GAMEDFS)	52
3.4.2.3	Performance Comparison	56
3.4.3	7-CH Case	57
3.4.3.1	UAV-Oriented Strategy	57
3.4.3.2	Optimal Strategy (GAMEDFS)	59
3.4.3.3	Performance Comparison	61
3.4.4	8-CH case	63
3.4.4.1	UAV-Oriented Strategy	63
3.4.4.2	Optimal Strategy (GAMEDFS)	65

3.4.4.3	Performance Comparison	68
3.4.5	9-CH case	70
3.4.5.1	UAV-Oriented Strategy	70
3.4.5.2	Optimal Strategy (GAMEDFS)	71
3.4.5.3	Performance Comparison	75
3.4.6	10-CH Case	77
3.4.6.1	UAV-Oriented Strategy	78
3.4.6.2	Optimal Strategy (GAMEDFS)	78
3.4.6.3	Performance Comparison	82
4	ENERGY-AWARE DATA COLLECTION WITH PRIORITY BY A UAV WITH A LIMITED-CAPACITY BATTERY IN ROBOTIC WIRELESS SENSOR NETWORKS	85
4.1	System Model and Problem Definition	85
4.1.1	Motivation and Problem Definition	85
4.1.2	Our Problem Approach Formulation	87
4.2	Total Energy Minimization by Visiting Priority Set with Limited Battery Capacity	89
4.3	Numerical Results	92
4.3.1	5-CH case	92
4.3.1.1	UAV-Oriented Strategy	92
4.3.1.2	Optimal Strategy with no priority set (GAMEDFS)	93
4.3.1.3	Optimal Strategy with Priori Set {CH 1}	93
4.3.1.4	Optimal Strategy with Priori Set {CH 1, 2}	94
4.3.1.5	Selecting Nearest Cluster Heads Strategy (SNCHS)	97

4.3.1.6	Performance Comparison	97
4.3.2	7-CH case	97
4.3.2.1	UAV-Oriented Strategy	97
4.3.2.2	Optimal Strategy with no priority set (GAMEDFS)	98
4.3.2.3	Optimal Strategy with Priori Set {CH 1}	98
4.3.2.4	Optimal Strategy with Priori Set {CH 1, 2}	99
4.3.2.5	Optimal Strategy with Priori Set {CH 1, 2, 3}	99
4.3.2.6	Selecting Nearest Cluster Heads Strategy (SNCHS)	100
4.3.2.7	Performance Comparison	101
4.3.3	10-CH case	102
4.3.3.1	UAV-Oriented Strategy	102
4.3.3.2	Optimal Strategy with no priori set (GAMEDFS)	103
4.3.3.3	Optimal Strategy with Priori Set {CH 1}	105
4.3.3.4	Optimal Strategy with Priori Set {CH 1, 2}	105
4.3.3.5	Optimal Strategy with Priori Set {CH 1, 2, 3}	107
4.3.3.6	Optimal Strategy with Priori Set {CH 1, 2, 3, 4}	108
4.3.3.7	Selecting Nearest Cluster Heads Strategy (SNCHS)	108
4.3.3.8	Performance Comparison	109

5 EFFICIENCY-AWARE AND ENERGY-AWARE DATA COLLECTION VIA A UAV WITH LIMITED-CAPACITY BATTERY IN ROBOTIC WIRELESS SENSOR NETWORKS 111

5.1 System Model and Problem Definition 111

5.1.1 Motivation and Problem Definition 111

5.1.2 Problem Formulation 113

5.2	Joint Energy-Efficiency Cost Minimization Problem by UAV with Limited-Capacity Battery	115
5.2.1	Data Forwarding Strategy for CH Robots	117
5.2.2	Optimal Strategy for the UAV	118
5.3	Numerical Results	120
5.3.1	5-CH case	121
5.3.1.1	UAV-Oriented Strategy	121
5.3.1.2	GAMEDFS	122
5.3.1.3	EEADCS	124
5.3.1.4	Performance Comparison	124
5.3.2	6-CH case	125
5.3.2.1	UAV-Oriented Strategy	125
5.3.2.2	GAMEDFS	127
5.3.2.3	EEADCS	128
5.3.2.4	Performance Comparison	130
5.3.3	7-CH case	130
5.3.3.1	UAV-Oriented Strategy	131
5.3.3.2	GAMEDFS	132
5.3.3.3	EEADCS	134
5.3.3.4	Performance Comparison	135
5.3.4	8-CH case	135
5.3.4.1	UAV-Oriented Strategy	136
5.3.4.2	GAMEDFS	137

5.3.4.3	EEADCS	138
5.3.4.4	Performance Comparison	140
5.3.5	9-CH case	140
5.3.5.1	UAV-Oriented Strategy	141
5.3.5.2	GAMEDFS	142
5.3.5.3	EEADCS	144
5.3.5.4	Performance Comparison	145
5.3.6	10-CH case	146
5.3.6.1	UAV-Oriented Strategy	147
5.3.6.2	GAMEDFS	148
5.3.6.3	EEADCS	149
5.3.6.4	Performance Comparison	152
6	SENSITIVITY ANALYSIS UNDER HOP CONSTRAINTS FOR DATA FORWARDING	155
6.1	5-CH case	157
6.1.1	EEADCS with 1-hop constraint	157
6.1.2	Performance Comparison	158
6.2	7-CH case	160
6.2.1	EEADCS with 3-hop constraint	161
6.2.2	EEADCS with 2-hop constraint	161
6.2.3	EEADCS with 1-hop constraint	162
6.2.4	Performance Comparison	164
6.3	10-CH case	165

6.3.1	EEADCS with 3-hop constraint	166
6.3.2	EEADCS with 2-hop constraint	167
6.3.3	EEADCS with 1-hop constraint	169
6.3.4	Performance Comparison	171
7	CONCLUSION	175
	REFERENCES	179
	CURRICULUM VITAE	191



LIST OF TABLES

TABLES

Table 3.1 Symbols and Notation	22
Table 3.2 The table shows indices of the nonvisited CH robots depending on battery capacity of UAV in Figure 3.8. "None" implies that UAV visits all CH robots if $B = 45$ or $B = 50$. "×" implies that the UAV-Oriented Strategy is infeasible for that battery capacity.	50
Table 3.3 The table shows total energy consumption of nonvisited CH robots depending on battery capacity of UAV in Figure 3.9. "×" implies that the UAV-Oriented strategy is infeasible for that battery capacity.	51
Table 3.4 The table shows indices of the nonvisited CH robots depending on battery capacity of UAV in Figure 3.10. "None" implies that the UAV visits all CH robots if $B = 35, 40, 45, 50$. "×" implies that the UAV-Oriented strategy is infeasible for that battery capacity.	56
Table 3.5 The table shows total energy consumption of nonvisited CH robots depending on battery capacity of UAV in Figure 3.11. "×" implies that the UAV-Oriented strategy is infeasible for that battery capacity.	57
Table 3.6 The table shows indices of the nonvisited CH robots depending on battery capacity of UAV in Figure 3.12. "None" implies that the UAV visits all CH robots if $B = 35, 40, 45, 50$. "×" implies that the UAV-oriented strategy is infeasible for that battery capacity.	62
Table 3.7 The table shows total energy consumption of nonvisited CH robots depending on battery capacity of UAV in Figure 3.13. "×" implies that the UAV-oriented strategy is infeasible for that battery capacity.	62

Table 3.8	The table shows indices of the nonvisited CH robots depending on battery capacity of UAV in Figure 3.14. "None" implies that the UAV visits all CH robots if $B = 35, 40, 45, 50$. "×" implies that the UAV-Oriented strategy is infeasible for that battery capacity.	69
Table 3.9	The table shows total energy consumption of nonvisited CH robots depending on battery capacity of UAV in Figure 3.15. "×" implies that the UAV-Oriented strategy is infeasible for that battery capacity.	69
Table 3.10	The table shows indices of the nonvisited CH robots depending on battery capacity of UAV in Figure 3.16. "None" implies that the UAV visits all CH robots if $B = 35, 40, 45, 50$. "×" implies that the UAV-Oriented strategy is infeasible for that battery capacity.	76
Table 3.11	The table shows total energy consumption of nonvisited CH robots depending on battery capacity of UAV in Figure 3.17. "×" implies that the UAV-Oriented strategy is infeasible for that battery capacity.	76
Table 3.12	The table shows indices of the nonvisited CH robots depending on battery capacity of UAV in Figure 3.18. "None" implies that the UAV visits all CH robots if $B = 45$ or $B = 50$	83
Table 3.13	The table shows total energy consumption of nonvisited CH robots depending on battery capacity of UAV in Figure 3.19.	83
Table 4.1	The table shows indices of the nonvisited CH robots depending on battery capacity of UAV and priority set in the 5-CH robot scenario in Figure 4.2. "None" implies that UAV visits all CH robots if $B = 45$ or $B = 50$. "no priority" means that UAV can desist from any CH robots. "×" implies that visiting that priority set with that battery capacity is infeasible.	96

Table 4.2 The table shows the total energy consumption of nonvisited CH robots depending on battery capacity of UAV and priority set in the 5-CH robot scenario in Figure 4.2. "no priority" means that UAV can desist from any CH robots. "×" implies that visiting that priority set with that battery capacity is infeasible. 96

Table 4.3 The table shows indices of the nonvisited CH robots depending on battery capacity of the UAV and the priority set in the 7-CH robot scenario in Figure 4.4. "None" implies that UAV visits all CH robots if $B = 35, 40, 45, 50$. "no priority" means that the UAV can desist from any CH robots. "×" implies that visiting that priority set with that battery capacity is infeasible. 102

Table 4.4 The table shows the total energy consumption of the nonvisited CH robots depending on battery capacity of the UAV and the priority set in the 7-CH robot scenario in Figure 4.4. "no priority" means that the UAV can desist from any CH robots. "×" implies that visiting that priority set with that battery capacity is infeasible. 103

Table 4.5 The table shows indices of the nonvisited CH robots depending on battery capacity of UAV and priority set in the 10-CH robot scenario in Figure 4.6. "None" implies that UAV visits all CH robots if $B = 45$ or $B = 50$. "no priority" means that UAV can desist from any CH robots. "×" implies that visiting that priority set with that battery capacity is infeasible. 109

Table 4.6 The table shows total energy consumption of (the nonvisited) CH robots depending on battery capacity of UAV and priority set in the 10-CH robot scenario in Figure 4.6. "no priority" means that UAV can desist from any CH robots. "×" implies that visiting that priority set with that battery capacity is infeasible. 110

Table 5.1 The table shows indices of the nonvisited CH robots depending on battery capacity of UAV in Figure 5.2. "None" implies that UAV visits all CH robots if $B = 45$ or $B = 50$. "×" implies that the UAV-oriented Strategy is infeasible for that battery capacity. 126

Table 5.2 The table shows total joint cost of energy consumption and data efficiencies of the nonvisited CH robots depending on battery capacity of UAV in Figure 5.3. "×" implies that the UAV-oriented strategy is infeasible for that battery capacity. 126

Table 5.3 The table shows indices of the nonvisited CH robots depending on battery capacity of UAV in Figure 5.4. "None" implies that the UAV visits all CH robots if $B = 25, 30, 35, 40, 45, 50$. "×" implies that the UAV-oriented strategy is infeasible for that battery capacity. 130

Table 5.4 The table shows total joint cost of energy consumption and data efficiencies of the nonvisited CH robots depending on battery capacity of UAV in Figure 5.5. "×" implies that the UAV-oriented strategy is infeasible for that battery capacity. 131

Table 5.5 The table shows indices of the nonvisited CH robots depending on battery capacity of UAV in Figure 5.6. "None" implies that the UAV visits all CH robots if $B = 35, 40, 45, 50$. "×" implies that the UAV-oriented strategy is infeasible for that battery capacity. 135

Table 5.6 The table shows total joint cost of energy consumption and data efficiencies of the nonvisited CH robots depending on battery capacity of UAV in Figure 5.7. "×" implies that the UAV-oriented strategy is infeasible for that battery capacity. 136

Table 5.7 The table shows indices of the nonvisited CH robots depending on battery capacity of UAV in Figure 5.8. "None" implies that the UAV visits all CH robots if $B = 25, 30, 35, 40, 45, 50$. "×" implies that the UAV-oriented strategy is infeasible for that battery capacity. 140

Table 5.8 The table shows total joint cost of energy consumption and data efficiencies of the nonvisited CH robots depending on battery capacity of UAV in Figure 5.9. "×" implies that the UAV-oriented strategy is infeasible for that battery capacity. 141

Table 5.9 The table shows indices of the nonvisited CH robots depending on battery capacity of UAV in Figure 5.10. "None" implies that the UAV visits all CH robots if $B = 25, 30, 35, 40, 45, 50$. "×" implies that the UAV-oriented strategy is infeasible for that battery capacity. 146

Table 5.10 The table shows total joint cost of energy consumption and data efficiencies of the nonvisited CH robots depending on battery capacity of UAV in Figure 5.11. "×" implies that the UAV-oriented strategy is infeasible for that battery capacity. 146

Table 5.11 The table shows indices of the nonvisited CH robots depending on battery capacity of UAV in Figure 5.12. "None" implies that the UAV visits all CH robots if $B = 45$ or $B = 50$ 152

Table 5.12 The table shows total joint cost of energy consumption and data efficiencies of the nonvisited CH robots depending on battery capacity of UAV in Figure 5.13. 153

Table 6.1 The table shows indices of the nonvisited CH robots depending on battery capacity of UAV in Figure 6.1. "None" implies that UAV visits all CH robots if $B = 45$ or $B = 50$. "×" implies that the UAV-oriented Strategy is infeasible for that battery capacity. 160

Table 6.2 The table shows total joint cost of energy consumption and data efficiencies of the nonvisited CH robots depending on battery capacity of UAV in Figure 6.2. "×" implies that the UAV-oriented strategy is infeasible for that battery capacity. 161

Table 6.3	The table shows indices of the nonvisited CH robots depending on battery capacity of UAV in Figure 6.3. "None" implies that the UAV visits all CH robots if $B = 35, 40, 45, 50$. "×" implies that the UAV-oriented strategy is infeasible for that battery capacity.	165
Table 6.4	The table shows total joint cost of energy consumption and data efficiencies of the nonvisited CH robots depending on battery capacity of UAV in Figure 6.4. "×" implies that the UAV-oriented strategy is infeasible for that battery capacity.	166
Table 6.5	The table shows indices of the nonvisited CH robots depending on battery capacity of UAV in Figure 6.5. "None" implies that the UAV visits all CH robots if $B = 45$ or $B = 50$	172
Table 6.6	The table shows total joint cost of energy consumption and data efficiencies of the nonvisited CH robots depending on battery capacity of UAV in Figure 6.6.	173

LIST OF FIGURES

FIGURES

- Figure 3.1 The whole multi-robot system includes a fusion center (FC) and five clusters of robots around FC. Red dots are the cluster head (CH) robots whereas the orange ones are the remaining robots which collect (environmental monitoring) data from the sensors (the black dots) in their cluster and send their data to the CH robot of their cluster. There are 19 robots in total and the UAV in the system. The UAV initially stands on the FC to charge its battery. After the UAV collects data from all CH robots directly or indirectly, it returns to FC to send all data to FC and recharge its battery for the next path. 23
- Figure 3.2 The whole multi-robot system consists of a fusion center (FC) where the UAV starts its route and six clusters of robots around FC. The red circles show the locations of the six cluster head (CH) robots in their robot cluster. *The UAV uses the strategy π_0 for the data collection.* With respect to this initial position of the UAV at $\xi_0 = (0, 0)$, the positions of the CH robots are $(\xi_1, \xi_2, \xi_3, \xi_4, \xi_5, \xi_6) = ((-16, 12), (9, 16), (-13, 16), (-7, 24), (0, 24), (6, 32))$ units. 31
- Figure 3.3 The whole multi-robot system consists of a fusion center (FC) where the UAV starts its route and 6 cluster of robots around FC. The red circles show the locations of the cluster head (CH) robots in their robot cluster. *The UAV uses the strategy π_1 for the data collection.* With respect to this initial position of the UAV at $\xi_0 = (0, 0)$, the positions of the CH robots are $(\xi_1, \xi_2, \xi_3, \xi_4, \xi_5, \xi_6) = ((-16, 12), (9, 16), (-13, 16), (-7, 24), (0, 24), (6, 32))$ units. 35

Figure 3.4 The whole multi-robot system consists of a fusion center (FC) where the UAV starts its route and 6 cluster of robots around FC. The red circles show the locations of the cluster head (CH) robots in their robot cluster. *The UAV uses the strategy π_2 for the data collection.* With respect to this initial position of the UAV at $\xi_0 = (0, 0)$, the positions of the CH robots are $(\xi_1, \xi_2, \xi_3, \xi_4, \xi_5, \xi_6) = ((-16, 12), (9, 16), (-13, 16), (-7, 24), (0, 24), (6, 32))$ units. 36

Figure 3.5 The whole multi-robot system consists of a fusion center (FC) where the UAV starts its route and 7 cluster head (CH) robots around FC. The red circles show the locations of the cluster head (CH) robots in their robot cluster. *The UAV uses an optimal strategy such that it visits CH 1, CH 2, CH 3, CH 4, CH 5, CH 6, and CH 7 in order (The path has a length of 244 m).* With respect to the initial position at $\xi_0 = (0, 0)$, the positions of the CH robots are $(\xi_1, \xi_2, \xi_3, \xi_4, \xi_5, \xi_6, \xi_7) = ((24, -32), (48, -25), (72, -32), (72, 7), (48, 0), (48, 25), (24, 32))$ m. . 38

Figure 3.6 The whole multi-robot system consists of a fusion center (FC) where the UAV starts its route and 7 cluster head (CH) robots around FC. The red circles show the locations of the cluster head (CH) robots in their robot cluster. *The UAV uses an optimal strategy such that it visits CH 1, CH 2, CH 4, CH 5, CH 6, and CH 7 in order (The path has a length of 220 m).* With respect to the initial position at $\xi_0 = (0, 0)$, the positions of the CH robots are $(\xi_1, \xi_2, \xi_3, \xi_4, \xi_5, \xi_6, \xi_7) = ((24, -32), (48, -25), (72, -32), (72, 7), (48, 0), (48, 25), (24, 32))$ m. . 40

Figure 3.7 The whole multi-robot system consists of a fusion center (FC) where the UAV starts its route and 7 cluster head (CH) robots around FC. The red circles show the locations of the cluster head (CH) robots in their robot cluster. *The UAV uses an optimal strategy such that it visits CH 1, CH 2, CH 5, CH 4, CH 6 and CH 7 in order (The path has a length of 210 m).* With respect to the initial position at $\xi_0 = (0, 0)$, the positions of the CH robots are $(\xi_1, \xi_2, \xi_3, \xi_4, \xi_5, \xi_6, \xi_7) = ((24, -32), (48, -25), (72, -32), (72, 7), (48, 0), (48, 25), (24, 32))$ m. . 41

Figure 3.8	Nodes show that the locations (positions) of the five CH robots. The weight of a link shows the square of distance between the two nodes connected via that link.	46
Figure 3.9	The total energy consumption of the five CH robots in Figure 3.8 under the strategies, UAV-Oriented and GAMEDFS for varying battery capacities of the UAV from $B = 5 \times C_{UAV}$ to $B = 50 \times C_{UAV}$	48
Figure 3.10	Nodes show that the locations of the 6 CH robots. The weight of a link shows the square of distance between the two nodes connected via that link.	53
Figure 3.11	The total energy consumption of the 6 CH robots in Figure 3.10 under the strategies, UAV-Oriented and GAMEDFS for varying battery capacities of the UAV from $B = 5 \times C_{UAV}$ to $B = 50 \times C_{UAV}$. The units for energy consumption of the UAV and total energy consumption of the nonvisited CH robots are C_{UAV} and C_{CH} , respectively. These constants depend on the type of the UAV and the CH robots.	54
Figure 3.12	Nodes show that the locations of the seven CH robots. The weight of a link shows the square of distance between the two nodes connected via that link.	58
Figure 3.13	The total energy consumption of the seven CH robots in Figure 3.12 under the strategies, UAV-Oriented and GAMEDFS for varying battery capacities of the UAV from $B = 5 \times C_{UAV}$ to $B = 50 \times C_{UAV}$. The units for energy consumption of the UAV and total energy consumption of the nonvisited CH robots are C_{UAV} and C_{CH} , respectively. These constants depend on the type of the UAV and the CH robots.	60
Figure 3.14	Nodes show that the locations of the 8 CH robots. The weight of a link shows the square of distance between the two nodes connected via that link.	64

Figure 3.15 The total energy consumption of the 8 CH robots in Figure 3.14 under the strategies, UAV-Oriented and GAMEDFS for varying battery capacities of the UAV from $B = 5 \times C_{UAV}$ to $B = 50 \times C_{UAV}$. The units for energy consumption of the UAV and total energy consumption of the nonvisited CH robots are C_{UAV} and C_{CH} , respectively. These constants depend on the type of the UAV and the CH robots. 65

Figure 3.16 Nodes show that the locations of the 9 CH robots. The weight of a link shows the square of distance between the two nodes connected via that link. 71

Figure 3.17 The total energy consumption of the 9 CH robots in Figure 3.16 under the strategies, UAV-Oriented and GAMEDFS for varying battery capacities of the UAV from $B = 5 \times C_{UAV}$ to $B = 50 \times C_{UAV}$. The units for energy consumption of the UAV and total energy consumption of the nonvisited CH robots are C_{UAV} and C_{CH} , respectively. These constants depend on the type of the UAV and the CH robots. 72

Figure 3.18 Nodes show that the locations of the 10 CH robots. The weight of a link shows the square of distance between the two nodes connected via that link. 77

Figure 3.19 The total energy consumption of the 10 CH robots in Figure 3.18 under the strategies, UAV-Oriented and GAMEDFS for varying battery capacities of the UAV from $B = 5 \times C_{UAV}$ to $B = 50 \times C_{UAV}$. The units for energy consumption of the UAV and total energy consumption of the nonvisited CH robots are C_{UAV} and C_{CH} , respectively. These constants depend on the type of the UAV and the CH robots. 80

Figure 4.1 In this system, red dots are cluster head (CH) robots whereas the orange ones are the remaining robots. UAV starts its trajectory from FC. After UAV collects data from all CH robots, it returns to FC to send all data to FC and charge its battery for next path. 86

Figure 4.2	Nodes show that the locations of the 5 CH robots. The weight of a link shows the square of distance between the two nodes connected via that link.	94
Figure 4.3	Total energy consumption of the 5 CH robots in Figure 4.2 under UAV-Oriented strategy, GAMEDFS, OSPS and SNCHS for varying battery capacities of the UAV from $B = 5 \times C_{UAV}$ to $B = 50 \times C_{UAV}$. The units for energy consumption of the UAV and total energy consumption of the nonvisited CH robots are C_{UAV} and C_{CH} , respectively. These constants depend on the type of the UAV and the CH robots. . . .	95
Figure 4.4	Nodes show that the locations of the 7 CH robots. The weight of a link shows the square of distance between the two nodes connected via that link.	100
Figure 4.5	The total energy consumption of the 7 CH robots in Figure 4.4 under UAV-Oriented Strategy, GAMEDFS, OSPS and SNCHS for varying battery capacities of the UAV from $B = 5 \times C_{UAV}$ to $B = 50 \times C_{UAV}$. The units for energy consumption of the UAV and total energy consumption of the nonvisited CH robots are C_{UAV} and C_{CH} , respectively. These constants depend on the type of the UAV and the CH robots.	101
Figure 4.6	Nodes show that the locations of the 10 CH robots. The weight of a link shows the square of distance between the two nodes connected via that link.	104
Figure 4.7	The total energy consumption of the 10 CH robots in Figure 4.6 under UAV-oriented Strategy, GAMEDFS, OSPS and SNCHS for varying battery capacities of the UAV from $B = 5 \times C_{UAV}$ to $B = 50 \times C_{UAV}$. The units for energy consumption of the UAV and total energy consumption of the nonvisited CH robots are C_{UAV} and C_{CH} , respectively. These constants depend on the type of the UAV and the CH robots.	106

Figure 5.1	The system consists of base station (BS), a UAV and 5 cluster of robots. Red dots are CH robots whereas orange dots represent remained robots. UAV starts its trajectory from BS. After UAV collects data from CH robots, it returns to BS to bring data there and charge its battery for next path.	112
Figure 5.2	Nodes show locations of 5 CH robots. The weight of a link shows square of distance between two nodes connected by the link. . . .	122
Figure 5.3	Total joint cost of data efficiency and energy consumption of the 5 CH robots in Figure 3.8 under UAV-Oriented strategy, GAMEDFS and EEADCS, vs. battery capacity of UAV from $B = 5 \times C_{UAV}$ to $B = 50 \times C_{UAV}$. The units for energy consumption of the UAV and total joint cost of the CH robots are C_{UAV} and C_{CH} , respectively. These constants depend on the type of the UAV and the CH robots.	125
Figure 5.4	Nodes show the locations of the 6 CH robots. The weight of a link shows square of distance between two nodes connected by the link.	127
Figure 5.5	Total joint cost of data efficiency and energy consumption of the 6 CH robots in Figure 5.4 under UAV-Oriented strategy, GAMEDFS and EEADCS, vs. battery capacity of UAV from $B = 5 \times C_{UAV}$ to $B = 50 \times C_{UAV}$. The units for energy consumption of the UAV and total joint cost of the CH robots are C_{UAV} and C_{CH} , respectively. These constants depend on the type of the UAV and the CH robots.	129
Figure 5.6	Nodes show the locations of the 7 CH robots. The weight of a link shows square of distance between two nodes connected by the link.	132
Figure 5.7	Total joint cost of data efficiency and energy consumption of the 7 CH robots in Figure 5.6 under UAV-Oriented strategy, GAMEDFS and EEADCS, vs. battery capacity of UAV from $B = 5 \times C_{UAV}$ to $B = 50 \times C_{UAV}$. The units for energy consumption of the UAV and total joint cost of the CH robots are C_{UAV} and C_{CH} , respectively. These constants depend on the type of the UAV and the CH robots.	133

Figure 5.8 Nodes show the locations of the 8 CH robots. The weight of a link shows square of distance between two nodes connected by the link. 137

Figure 5.9 Total joint cost of data efficiency and energy consumption of the 8 CH robots in Figure 5.8 under UAV-Oriented strategy, GAMEDFS and EEADCS, vs. battery capacity of UAV from $B = 5 \times C_{UAV}$ to $B = 50 \times C_{UAV}$. The units for energy consumption of the UAV and total joint cost of the CH robots are C_{UAV} and C_{CH} , respectively. These constants depend on the type of the UAV and the CH robots. 139

Figure 5.10 Nodes show the locations of the 9 CH robots. The weight of a link shows square of distance between two nodes connected by the link. 142

Figure 5.11 Total joint cost of data efficiency and energy consumption of the 9 CH robots in Figure 5.10 under UAV-Oriented strategy, GAMEDFS and EEADCS, vs. battery capacity of UAV from $B = 5 \times C_{UAV}$ to $B = 50 \times C_{UAV}$. The units for energy consumption of the UAV and total joint cost of the CH robots are C_{UAV} and C_{CH} , respectively. These constants depend on the type of the UAV and the CH robots. 145

Figure 5.12 Nodes show locations of 10 CH robots. The weight of a link shows square of distance between two nodes connected by the link. . . . 147

Figure 5.13 Total joint cost of data efficiency and energy consumption of 10 CH robots in Figure 5.12 under UAV-Oriented strategy, GAMEDFS and EEADCS, vs. battery capacity of UAV from $B = 5 \times C_{UAV}$ to $B = 50 \times C_{UAV}$. The units for energy consumption of the UAV and total joint cost of the CH robots are C_{UAV} and C_{CH} , respectively. These constants depend on the type of the UAV and the CH robots. 150

Figure 6.1 Nodes show locations of 5 CH robots. The weight of a link shows square of distance between two nodes connected by the link. . . . 157

Figure 6.2	Total joint cost of data efficiency and energy consumption of the 5 CH robots in Figure 6.1 under UAV-Oriented strategy, GAMEDFS and EEADCS (with various hop constraints), for varying battery capacities of UAV. The units for energy consumption of the UAV and total joint cost of the CH robots are C_{UAV} and C_{CH} , respectively. These constants depend on the type of the UAV and the CH robots.	159
Figure 6.3	Nodes show locations of 7 CH robots. The weight of a link shows square of distance between two nodes connected by the link. . . .	162
Figure 6.4	Total joint cost of data efficiency and energy consumption of the 7 CH robots in Figure 6.3 under UAV-Oriented strategy, GAMEDFS and EEADCS (with various hop constraints), for varying battery capacities of UAV. The units for energy consumption of the UAV and total joint cost of the CH robots are C_{UAV} and C_{CH} , respectively. These constants depend on the type of the UAV and the CH robots.	163
Figure 6.5	Nodes show locations of 10 CH robots. The weight of a link shows square of distance between two nodes connected by the link. . . .	167
Figure 6.6	Total joint cost of data efficiency and energy consumption of the 10 CH robots in Figure 6.5 under UAV-Oriented strategy, GAMEDFS and EEADCS (with various hop constraints), for varying battery capacities of UAV. The units for energy consumption of the UAV and total joint cost of the CH robots are C_{UAV} and C_{CH} , respectively. These constants depend on the type of the UAV and the CH robots.	170

LIST OF ABBREVIATIONS

IoT	Internet of Things
WSN	Wireless Sensor Network
CPS	Cyber-physical system
IoRT	Internet of Robotic Things
RSSI	Received signal strength indication
UAV	Unmanned Aerial Vehicle
CH	Cluster head
RWSN	Robotic Wireless Sensor Network
LEACH	Low-energy adaptive clustering approach
TDMA	Time Division Multiple Access
CDMA	Code Division Multiple Access
LELE	Leader Election with Load Balancing Energy
HEED	Hybrid Energy Efficient Distributed
SCHE	Stable Cluster Head Election
ALEACH	Advanced LEACH
TB-LEACH	Time-based LEACH
DEESO	Distributed and energy-efficient self organization
ACA	Adaptive channel assignment
LEACH-IMP	Improved LEACH
TSCHS	two-step cluster head selection
ModLEACH	Modified LEACH
SEP	Stable Election Protocol
DEEC	Distributed Energy-Efficient Clustering
EAMR	Energy-aware multi-hop Routing

PEER	Progressive Energy-Efficient Routing
MANET	Mobile ad hoc network
EE-OLSR	Energy-efficient Optimized Link State Routing
RP	rendezvous point
EAPC	Energy-aware path construction
WRP	Weighted Rendezvous Points
ECDRA	Energy-efficient cluster-based dynamic routing algorithm
CCMAR	Cluster-chain mobile agent routing
MIEEPB	mobile sink improved energy-efficient power-efficient gathering in sensor information system-based routing protocol
DT	Direct transmission
EETP	Energy efficient trajectory planning
PSO	particle swarm optimization
MOPSO	multi-objective particle swarm optimization
PSO-RPS	PSO-based RPs selection
ACO	Ant Colony Optimization
WCHS	Weight-based cluster head selection
PSRS	Pair-based sink relocation scheme
DODAG	Destination-oriented directed acyclic graph
QDVGDD	Query-Driven Virtual Grid based Data Dissemination
DEDC	delay aware, energy-efficient data communication protocol
CM	Cluster member
OP	Orienteering Problem
TSP	Travelling Salesman Problem
StPSO	Strengthened Particle Swarm Optimization
DStPSO	Discrete Strengthened PSO
ML-VNS	Multi-level VNS

TS	Tabu Search
PSDA	Probabilistic Solution Discovery Algorithm
PR	Path Relinking
GRASP	Greedy Randomized Adaptive Search Procedure
MSPDFS	Multi Shortest Path Data Forwarding Strategy
GAMEDFS	Genetic Algorithm with Minimum Energy for Data Forwarding Strategy
EEADCS	Efficiency and Energy-Aware Data Collection Strategy



CHAPTER 1

INTRODUCTION

1.1 Motivation

Internet of Things (IoT) is a smart sizable communication infrastructure of uniquely attributable wireless equipments which are able to communicate with each other via Internet [1]. IoT has been considered as one of the most promising networking paradigms that fill the gap between the physical and cyber world. In the IoT structures, the devices are generally equipped with wireless sensors [2] which enables efficient data transmission and collection anywhere [3]. Wireless sensor networks (WSNs) have numerous applications, such as smart cities [4], structural health monitoring [5], agriculture [6], frost monitoring [7] and ambient air monitoring [8].

For the last two decades, robotics and wireless sensor networks (WSN) have been very well-investigated separately and so they are very well-known fields. On the other hand, there exist many new opportunities and research directions at the junction of these research fields which combines robot networks and WSNs in one single hybrid network, a robotic wireless sensor network, where robot networks cooperate with WSN to relieve individual disadvantages. There are many applications where robots and wireless sensors help each other in the network. The survey [10] reviews robotic applications in WSN. Distributing the sensor nodes randomly in the WSN may cause some of the nodes to be located outside of communication range of their neighbors or located in an area outside its node task. A mobile robot can help reposition the nodes in optimal locations, which improves operation, lifetime, and energy efficiency of the network greatly [11]. Robotics can assist in WSNs by servicing the network, in ways such as repositioning nodes, replacing broken nodes, and recharging batteries.

The work [12] investigates the problems of robot task allocation and fulfillment to optimally serve WSNs such as recharging batteries and replacing broken or depleted nodes via single-task and multi-task robots.

In [13], the robot replaces the sensors which almost deplete their energy and send out a help localizing signal to it by navigating the WSN based on received signal strength indication (RSSI) from the neighbor nodes and following the route determined by the WSN. Moreover, the robot can help collect data from sensors and fuse these data [14]. The robots can also be used as data mules, which is investigated as the traveling salesman problem in [15] and with the multiple robot case in [16]. However, data muling can cause very long waiting times in transporting data; therefore, the work [17] proposes a clustering method among the data mules to save time. The robot can be used to localize sensors in WSN [18].

Secondly, main applications of WSNs in robotics can be considered as path sensing, mapping, planning, and localization of robots. The WSN help the robots choose the optimal path and avoid dangerous areas [19]. In [20], a modified SLAM algorithm is used for robots. The work [21, 22] use particle filters instead of Kalman filters in SLAM algorithm. Beside these, WSNs can provide many tools for coordinating multiple robots and swarm robotics [23]. Using robotics with WSNs makes it easy to share real-time sensor data. Combining these technologies makes sense for a large number of applications. Some applications of WSN using robotics can be listed as military use, weather forecasting, health care, and transport monitoring. Besides these, energy harvesting and low-power WSN may be another possible application area. Furthermore, using both robotics and WSNs with internet in cyber-physical systems (CPS) leads to the Internet of Robotic Things (IoRT), which has brought several changes in various domains that cover several applications in challenging environments. For example, IoRT systems can be used in manufacturing industries to execute difficult tasks such as assembling, packaging, welding, managing quality control, and so on autonomously and remotely [24].

For the last two decades, numerous papers have investigated the energy-efficient data collection problem with a static sink, a fusion center, which collects data from sensor nodes. In these papers, the network is divided into clusters where the cluster head

node collects data from the other nodes and send the data to the FC directly or indirectly (forward the data to another cluster head node). The aim is to reduce the energy consumption of the network and thus increase the network lifetime. Although several papers have proposed efficient algorithms to reduce the energy consumption for the problem with static sink, for less energy consumption of cluster head nodes, UAV can be used to collect data from the cluster head nodes and to bring the data to the fusion center. Using UAV has the following advantages. It can access the locations which people or land vehicles can only access with difficulty and risk. UAV can be used when it is expensive and impractical to rent manned aerial vehicles [25]. Therefore, researchers have recently investigated the problem with a mobile sink instead of the static sink in order to reduce the total energy consumption of the network more. In the related literature considering the problem with the mobile sink, there exist many papers which consider the consumed-energy minimization problem as a traveling salesman problem for the cases in which the UAV has sufficient energy to visit all or a constant portion (like half) of CH nodes for data collection. However, to visit a constant portion of the CH nodes, the mobile sink needs a varying battery capacity depending on the locations of the CH robots, which is not practical.

We investigate a data collection problem by a mobile sink, an unmanned aerial vehicle (UAV) with limited battery capacity, in a robot network divided into several robot clusters, each of which has a cluster head (CH) robot, cluster member robots which collect data from the surrounding sensor nodes. Due to the limit on its battery capacity, UAV faces a lack of energy to be able to visit all CH robots depending on their locations and its battery capacity. This battery constraint discriminates our problem from the classical traveling salesman problem where the UAV always has sufficient battery capacity to visit all CH robots. However, the battery capacity of the UAV is constant. Thus, in our problem, the UAV may generally visit a variable number of CH nodes rather than a constant portion of the CH nodes as considered in the recent literature. Our innovative contribution beyond current approaches considers not only variable parametric number of nodes but an optimized CH transmission costs of non-visited CH robots. If the UAV cannot visit all of CH robots due to the limited battery capacity, then each CH robot not visited by the UAV forwards their data to the CH robots. The UAV aims to minimize total energy consumption of the CH robots by

visiting a varying optimized portion of the CH robots. For this purpose, the UAV decides which CH robots to visit by considering not only the locations of CH robots but also its battery capacity. We also tackle the energy-aware data collection problem with priority set of CH robots which must be visited by the UAV.

We also tackle another problem by a UAV with limited-capacity battery in a clustered robot network where each cluster consists of a cluster head (CH) robot, cluster member robots which collect data from surrounding sensors. A cluster head (CH) robot allocates tasks to cluster member robots. In this problem, we also consider all of limited battery capacity of UAV, locations of CH robots and various efficiency of data for different CH robots. Because of its limited-capacity battery, UAV cannot guarantee for visiting each CH robot depending on location of each CH robot. The battery limit differs our problem from travel salesman problem (TSP) in which UAV has enough battery capacity for visiting each of CH robots which is impractical due to fact that UAV has constant-capacity battery. Therefore, UAV may generally visit a variable number of CH nodes rather than a constant portion of CH nodes which was focus of the recent literature except our previous paper [76]. Our innovative contribution beyond current approaches consider not only variable parametric number of nodes but also an optimized joint costs of energy consumptions and data efficiencies of nonvisited CH robots. Unless UAV can travel to each CH robot because of its constrained-capacity battery, each nonvisited CH robot forwards data to an other CH robot through data hopping. UAV aims to minimize total joint costs of energy consumptions and data efficiencies of CH robots by visiting a varying optimized portion of CH robots. UAV decides which CH robots to visit by considering all of its battery capacity, locations and data efficiencies of CH robots.

The proposed algorithms aim to minimize total energy consumption of nonvisited CH robots; therefore, they consider energy consumption of CH robots while making the decision of the CH robots to visit (energy-awareness). In addition, the recent algorithm, EEADCS, aims to minimize total joint cost of energy consumption of nonvisited CH robots; therefore, they consider not only energy consumption but also data efficiencies of CH robots while making the decision of the CH robots to visit (both energy-awareness and efficiency awareness).

In our RWSN, the sensors in different positions may collect data with different accuracy. The cluster member robots which collect data from the surrounding sensors may execute their assigned tasks with different accuracy, which can result in different efficiency for different CM robots in the same cluster. After a cluster head (CH) collects the resultant data from the CM robots in its cluster, it evaluates the data and has a data efficiency. This data efficiency of a CH robot may be different from another CH robot even if the evaluated data is exactly same. This difference between data efficiency of CH robots comes from the difference between the types/structures of CH robots. Hence, when we consider all the differences between sensors, CM robots and CH robots, data efficiency of a CH robot may differ from data efficiency of another CH robot.

1.2 Our Contributions

The main contributions of this thesis can be summarized as follows:

- To the best of our knowledge, our work in Chapter 3 is the first work in which the UAV considers minimizing total energy consumption of the CH robots by visiting a varying optimized portion or all of the CH robots depending on the constant capacity of its battery, whereas the related literature considers the minimum energy path for the mobile sink by visiting all or half of the CH robots/nodes.
- We propose a two-stage solution for this problem. Our method of optimizing the visited subset of CH, taking into account also the transmission of leftout nonvisited CH, is derived from a traveling salesman problem when the UAV visits a constant portion of CHs. Chapter 3 will explicitly provide this derivation and then clearly provide the innovative abilities of our approach by removing a varying portion of the CH robots from the path in order to reduce the energy consumption of the UAV below the battery capacity of the UAV. For this purpose, the UAV considers both the locations of CH robots and its battery capacity along with transmission hops in energy usage of the nonvisited CH robots. As a result, the UAV desists to visit the CH robots which consume less

energy for forwarding their data and which the UAV requires more energy to visit.

- In Chapter 3, we also find optimal data forwarding strategies for all nonvisited CH robots by considering all possible transmission paths in each case. Here, we consider each combination (subset) of CH robots as a separate case in which each CH robot in this combination (subset) of CH robots looks for an optimal transmission path to forward its data to the UAV via data hopping (via other CH robots).
- To the best of our knowledge, our work in Chapter 4 is the first work where minimizing total energy consumption of CH robots is tackled with a priority set of CH robots (the set of CH robots which must be visited by the UAV) by visiting a varying optimized portion of CH robots depending on its battery capacity.
- To the best of our knowledge, our work in Chapter 5 is the first work which considers not only a limit on battery capacity of the UAV but also various efficiency of data for different CH robots in the data collection problem.
- Our work in Chapter 5 proposes a solution which includes a strategy for the UAV to visit a varying optimized portion of CH robots and strategies for each nonvisited CH robot to forward its data to the UAV.
- Our work in Chapter 5 exhibits optimality of the proposed solution for the non-visited CH robots to forward their data to UAV.
- Our work in Chapter 5 exhibits optimality of the proposed solution for the UAV to visit a varying optimized portion of CH robots to minimize the cost which depends on not only total energy consumption of the nonvisited CH robots but also the efficiency of data at the nonvisited CH robots.
- Chapter 6 makes the sensitivity analysis of the algorithm proposed in Chapter 5 with respect to hop constraints for data forwarding and evaluate its performance for various battery capacities and various hop constraints.

1.3 Organization

The remainder of this thesis is organized as follows.

In Chapter 2, we provide the related work about energy-aware, cluster-based routing protocols with both static sink and mobile sink cases.

In Chapter 3, we consider energy-aware cluster-based data collection via a UAV with limited-capacity battery in robotic wireless sensor networks. The problem definition along with the system model are given in Section 3.1. In Section 3.2, we consider the case in that the UAV has sufficient energy to visit all CH robots for data collection that will help us explicitly derive our novel approach which will be the focus of Section 3.3. In Section 3.4, we provide numerical results for total energy consumption of CH robots in different scenarios.

In Chapter 4, we consider energy-efficient data collection with priority by a UAV with a limited-capacity battery in robotic wireless sensor networks. In Section 4.1, we give our problem definition and system model. Our novel approach is derived explicitly in Section 4.2. In Section 4.3, we make performance comparison in different scenarios.

In Chapter 5, we consider efficiency-aware and energy-aware data collection by a UAV with a limited-capacity battery in robotic wireless sensor networks. In Section 5.1, we give our problem definition and system model. In Section 5.2, we investigate the problem and develop our novel approach which considers not only energy consumption of CH robots and UAV but also data efficiencies of CH robots. In Section 5.3, we evaluate performances of strategies in various scenarios.

Chapter 6 makes the sensitivity analysis of the algorithm proposed in Chapter 5 with respect to hop constraints for data forwarding and evaluate its performance for various battery capacities and various hop constraints.

Chapter 7 concludes the thesis and provides future work.



CHAPTER 2

RELATED WORK

In this chapter, we provide the related work about energy-aware, cluster-based routing protocols with both static sink and mobile sink cases. As we also consider difference between efficiencies of data collected by different CH robots in Chapter 5, our problem in Chapter 5 becomes similar to orienteering problem. Therefore, we also survey several papers considering orienteering problem.

2.1 Energy-Aware, Cluster-Based Routing Protocols with Static Sink

Power consumed by the sensors has a significant influence on the network lifetime. If a sensor node sends data directly to the base station, the energy consumed in this transmission is much greater than the energy consumed in inter-sensor communication since the distance between the base station and a sensor is generally much greater than the distance between two neighboring sensors. To deal with this problem, many cluster-based routing protocols have been proposed for the last two decades. These protocols first divide the WSNs into regions—"clusters"—then, a cluster head is selected in each cluster to collect data from the other sensors in its cluster and send data to the base station. To distribute the extra power consumption of being cluster head, each cluster-head sensor leaves this responsibility to another sensor in the cluster after a while.

In the work [26,27], the authors propose a cluster-based protocol, low-energy adaptive clustering hierarchy (LEACH), which makes randomized rotation of cluster-heads to equally distribute the energy consumption among the sensors in the same cluster. LEACH assumes that all sensors are homogeneous (have same properties), energy-

limited (but still enough to send data to base station/fusion center for many times), and immobile (static); the base station is far from the sensors (the reason why the authors suggest cluster-based routing policies). LEACH uses localized coordination for enabling robustness and scalability in dynamic networks. Under LEACH, the cluster head sensors collect data from the remaining sensor nodes and reduce their amount of data by aggregating them. As the amount of data transmitted to the base station decrease, the power consumption decreases. In LEACH protocol, each cluster head schedules the sensors via TDMA for the intra-cluster data collection and different CDMA is used for inter-cluster traffic to prevent the data transmissions from the interference. LEACH reduces the energy consumption eight times and increases the network lifetime two times compared to the previous protocols of direct transmission, minimum transmission energy, multi-hop routing, and static clustering. Here, the authors considers the network lifetime as the number of rounds when first node dies and the number of rounds when first node dies, separately. Then, the authors derived the lifetime results of all policies for different amounts of initial energy numerically.

In [28], the authors propose a new protocol, leader election with load balancing energy (LELE). This protocol considers the remaining energy of the sensors and the distances between the sensors while LEACH do not consider these two factors and make decisions based only on the probability and a threshold limit. However, LELE protocol neglects the fact that learning the battery states of each neighboring sensor brings another additional energy consumption. In the work [29], the authors propose a cluster head election protocol which do not use location information or localization methods. In this work, the mobility of the sensors is modelled with the mobility model of Random Walk with Reflection (or Brownian Motion) [30], which was described mathematically first by Einstein in 1926 [31]. The protocol selects the optimal cluster head by using the updated information of the network topology which has Random Walk mobility model. However, this mobility models cannot be applied to many robotic wireless sensor networks because the cluster member robots move toward a target to complete a task assigned by the cluster head and their path to execute the assigned tasks may be different than the mobility models. The papers [32] and [33] propose a low-complexity cluster-based routing algorithm, Hybrid Energy Efficient Distributed (HEED). It can be considered as an extended version of tradi-

tional LEACH [12], [27]. Primary concern of HEED protocol is the remaining energy in the sensors. It considers network topology features like inter-sensor distances, sensor degree (hop) as secondary parameters. The secondary ones are just used for breaking tie between two sensors while selecting cluster head to evenly distribute the power among the sensors in the cluster. However, setting a hierarchy between remained energy and other parameters cannot guarantee optimality and even near-optimality in mobile wireless sensor networks such as multi-robot systems where the distances between sensors dynamically change depending on the changing position of the sensors (or robots).

In the work [34], the authors consider that a cluster-head spends more energy than the others while it collects data from cluster members, fuses data to decrease its size, or transmits the aggregated data to a base station. Regarding each sensor as an ant and each cluster as a nest in this work, the authors propose a novel clustering mechanism based on ANTCLUST [35] where clusters are organized in a distributed and energy-efficient way through local communication among neighboring sensor nodes. It is numerically shown that the ANTCLUST based algorithm can collect data from more than 80% of the sensors longer than LEACH by over 25% and it also extends the network lifetime 150% compared with LEACH. In the work [36], the authors propose a cluster-based routing protocol, stable cluster head election (SCHE). SCHE differs from LEACH such that SCHE does not change the cluster heads in each round whereas the traditional LEACH changes the cluster heads in each round. Thus, SCHE reduces energy consumption very much compared with the LEACH (up to 90%).

In the paper [37], the authors propose a cluster head election protocol, advanced LEACH (ALEACH). LEACH makes decisions independent from the energy remained (present energy condition) in sensors, which is an important drawback of LEACH. ALEACH overcomes this problem by introducing two terms, general probability and current probability, in the threshold equation. In the work [38], the authors propose an energy-efficient routing protocol, time-based LEACH (TB-LEACH) which just changes the cluster head election. Thus, it improves the cluster partition and forms uniform and balanced clusters. In the work [39], the authors propose an energy-aware routing protocol, distributed and energy-efficient self organization (DEESO). Electing the cluster head is adjusted to the remained energy in the battery of sensors. It is

a completely distributed approach and adaptive channel assignment (ACA) is applied for addressing the on-off mode changes of sensors in the network topology. Thus, it increases the network lifetime and transmits three times more data compared with LEACH.

In the work [40], the authors propose a clustering protocol, LEACH-IMP. This protocol determines the optimal cluster heads by considering the positions of the sensors. By keeping the cluster head constant, LEACH-IMP is much more energy efficient than LEACH. In the work [41], the authors propose an energy-aware routing protocol. Different from LEACH [26] and LEACH-F [27], this protocol uses dynamic round times; in other words, it changes the round times depending on the remained energy of the sensors. Thus, this protocol consumes considerably less energy and increases the network lifetime compared with LEACH and LEACH-F. In the paper [42], the authors propose a new routing protocol, two-step cluster head selection (TSCHS) routing protocol. TSCHS aims to solve an important problem of LEACH, the variability of the number of cluster heads. This protocol has two stages to select the cluster heads. In the work [43], the authors propose an energy-aware routing protocol, modified LEACH (ModLEACH). Different from the LEACH, ModLEACH introduces an efficient cluster head replacement scheme with dual transmission power levels which are used for decreasing interference and collisions. Thus, ModLEACH decreases packet drop ratio.

In the papers [44], [45], the authors propose heterogeneous cluster-based routing protocols for the wireless sensors networks where some sensors are more powerful than the other sensors (heterogeneity of the power levels in different sensors). In the paper [44], Stable Election Protocol (SEP) is proposed. SEP selects the cluster heads with an approach based on a weighted election probability. Advanced sensors which have additional energy forces them to be elected as cluster heads. In the paper [45], distributed energy-efficient clustering (DEEC) is proposed. This protocol selects the cluster heads via a probability function depending on the ratio between the remained energy of each sensor and the average energy in the wireless sensor network. If a sensor has high remained energy, then it is more likely to be selected as a cluster head.

In the paper [46], the authors propose an energy-aware multi-hop routing (EAMR) protocol for a WSN. EAMR distinguishes from the former energy-aware routing protocols since EAMR reduces the excessive overhead commonly seen in many routing protocols by employing all fixed clustering, multi-hop routing and threshold based cluster head selection mechanisms together. Reducing the overhead prolongs the lifetime as energy consumption in the sensor nodes can be decreased via an energy-efficient protocol. Moreover, implementing relay nodes allows all of the received data in the cluster to be transmitted thru inter cluster transmissions. On the other hand, the main consideration in mobile wireless sensor networks not always take into account the energy consumption. However, it has still an important influence on the network lifetime since those energy resources can be easily replaced or rechargeable by the users or the operators. Hence, a higher concern is given in those networks to quality of service such as higher performances. However, energy efficiency is a very critical performance metric in mobile wireless sensor networks, imminently determining the network lifetime [47].

The work [48] presents a literature survey of the energy-aware routing protocols proposed for the routing problem in mobility case, i. e., the sensor nodes are mobile.

In the paper [49], the authors exhibit that that many minimum energy routing protocols could fail unless they consider the routing overhead involved and mobility of the sensors. They propose a simple energy-aware routing protocol, Progressive Energy Efficient Routing (PEER) protocol, so as to improve the performance in mobility scenarios. The energy-aware routing protocol, PEER, has considerably better performance than that of a normal energy-based routing protocol.

In the paper [50], the authors design a heterogeneous mobile adhoc network (MANET) which consists of traditional and mobile nodes with limited energy and a few controllable mobile relay nodes with more abundant energy resources. The authors propose a framework for relay deployment that predicts mobility of the nodes and operates in tandem with the underlying MANET routing protocol to define the mobility of the relay nodes optimally. Together with the solutions, they present two cases for the relay deployment problem to achieve different goals. Case 1, named Min-Total, aims to minimize the total energy consumed across all the traditional nodes for trans-

mitting data, whereas the goal in case 2, named Min-Max, is to minimize the maximum energy consumed by a traditional node for transmitting data. The solutions also prioritise individual nodes depending on remaining energy profiles and contextual significance. They investigate the performance of the proposed framework under different mobility prediction schemes. When the relay nodes constitute a small fraction of the total nodes in the network, the proposed framework results in significant energy savings. Furthermore, we observed that while both the schemes have their potential advantages, the differences between these two optimization schemes become more obvious in larger networks. The main drawback of that paper is that its mobility prediction scheme considers no acceleration for cluster member robots which can be quite common in robotic wireless sensor networks due to the forces for connectivity maintenance, collision and obstacle avoidance, task allocation and friction. In the paper [51], the authors propose an energy efficient routing protocol, an Energy-Efficient Optimized Link State Routing (EE-OLSR). As a proactive protocol, OLSR [52] finds a route between two nodes in the network in very quickly. However, it spends lots of resources while selecting the Multi Point Relays and exchanging the information of topology control. The authors modified the multi point relay selection mechanism in the OLSR protocol so as to extend the network lifetime without losses from throughput, end-to-end delay or overhead. Moreover, they show that extinguishing the energy consumption caused by overhearing can extend the network lifetime without compromising the operation of OLSR. In the paper [53], the authors propose an energy efficient and robust location service. Thus, they can do hierarchical geographic clustering structure and considers energy during the election of cluster leader. Moreover, this localization service is adaptive to mobility due to the mobility prediction model using classical Kalman filter. They proposed a protocol in which the location servers estimate the locations of the mobile sensors based on the last location information. The performance of the proposed protocol is evaluated. The main drawbacks of this work are only considering the distances of sensor nodes to the center of the cluster and considering the lowest mobility among the nodes while electing a cluster head among the nodes.

Although the protocols with static sink give good results, by visiting cluster heads, the mobile sink reduces the distance between itself and the cluster heads which transmits

data to the mobile sink. The decrease in the transmission distance between the mobile sink and cluster head nodes results in decrease in total energy consumption of the network and so increase in network lifetime. Therefore, the protocols with mobile sink have been investigated and preferred more in recent years. We consider the problem with mobile sink as well. In the next section, the protocols with mobile sink are surveyed.

2.2 Energy-Aware, Cluster-Based Routing Protocols with Mobile Sink

Collecting data using mobile sink provides an effective solution to the energy-hole problem¹ in WSN, which may be faced in WSNs with static sink where sensor nodes forward their data towards static sink. The approaches using mobile sink for this problem can be divided into two main categories: direct and rendezvous approaches. With direct approaches, the mobile sink collects data from each node based on one hop distance metrics. With rendezvous approach, the mobile sink travels just a limited number of nodes named as rendezvous points (RP) and establishes the local routing for data collection from all other nodes to primary sensor nodes [55]. In our problem, the UAV collects data from the CH robots; therefore, the papers considering the problem with mobile sink are closer to our work than the ones tackling the problem with static sink. In this section, we survey the main existing approaches in the related literature considering the data collection problem with mobile sinks.

In [56], an energy-aware path construction (EAPC) policy is proposed for collecting data based on environmental monitoring. With EAPC, the mobile sink chooses a suitable set of locations for collecting data and plans a path for collecting data; then, it starts data collection from the points burdened with data. In terms of energy consumption and network lifetime, EAPC is more efficient than weighted rendezvous points (WRP) policy, which assigns a weight to each sensor and considers the nodes with the highest weight as data collection points [57].

In the paper [58], first, the number of clusters is determined and the whole sensor field

¹ The distance between the static sink and sensors is much larger than the distance between sensors. Therefore, the CH sensors especially the ones closer to static sink consumes very much energy to transmit the aggregated data to the static sink. This is the energy-hole problem.

is divided into sectors with the number of clusters angularly (cluster-forming phase). In each cluster, by considering the ratio of residual energy of a sensor node to its distance to the sink as the weight of that sensor, the algorithm calculates the weights of cluster members and selects a cluster head (CH). Member nodes search for the optimal scenario by calculating energy consumption of different routing paths. Then, CHs form connections for intercluster communication via a greedy policy. The proposed algorithm performs better than two algorithms (considering the similar problems), the energy-efficient cluster-based dynamic routing algorithm (ECDRA) [59] and the cluster-chain mobile agent routing (CCMAR) [60]. The work [61] considers a network which consists of static sensor nodes distributed uniformly randomly and a mobile sink with unlimited battery capacity. The authors propose the MIEEPB-DT protocol which combines direct transmission (DT) protocol with the mobile sink improved energy-efficient power-efficient gathering in sensor information system-based routing protocol (MIEEPB) [62] for the efficient usage of the limited energy of nodes. MIEEPB-DT performs better than DT and MIEEPB for network lifetime and energy efficiency.

The paper [63] considers a data collection problem in WSNs via a mobile sink with unlimited battery capacity. An energy-efficient trajectory planning (EETP) technique is proposed using multi-objective particle swarm optimization (MOPSO) for balancing the load of rendezvous nodes and shortening the path of the mobile sink. EETP performs much better than WRP [57], CB in terms of energy consumption, and thus network lifetime. The work [65] considers a network where a mobile sink collects data from sensor nodes by using rendezvous points (RP). It has already been proven that meta-heuristics such as particle swarm optimization (PSO) shows a feasible and promising performance for forming the trajectory. The work [65] proposes a PSO-based RPs selection (PSO-RPS) technique which outperforms against the methods in related literature in terms of trajectory length. In [66], a hyperheuristic framework is proposed and it can construct high-level heuristics automatically for path planning by using the genetic algorithm. This algorithm prolongs the network lifetime.

The paper [67] proposes a cluster-based data collection protocol where the optimal cluster heads are selected to reduce energy consumption. The optimal path a mobile sink plans the optimal path by ant colony optimization (ACO) algorithm [68]- [70].

The mobile sink with unlimited battery capacity plans an efficient path for data collection along with the cluster centroid. The proposed method is analyzed in terms of lifetime and energy usage. The paper [71] proposes a five-stage solution for the cluster-based routing problem. First, the network is divided into multiple regions by quad tree combined binary tree policy. Secondly, the authors carry out weight-based cluster head selection (WCHS) method to select a cluster head in each partition. Then, it uses a novel pair-based sink relocation scheme (PSRS) for relocating the sink node. After then, the authors execute a destination-oriented directed acyclic graph (DODAG)-based route adjustment by considering three rules. Finally, type-2 fuzzy-based adaptive medium access (MAC) scheduling is used. This protocol decreases energy consumption up to 20% and so extends the network lifetime up to 30% compared with Grid Routing (GR) [72] and Query-Driven Virtual Grid based Data Dissemination (QDVGDD) [73] methods.

The paper [74] proposes a joint density-aware and energy-limited path construction algorithm for data collection (DEDC) aiming to select as much as possible appropriate anchors under the path length constraint for prolonging the network lifetime. Initially, the proposed DEDC determines the grid size according to the path length constraint, partitions the monitoring region into several grids, and identifies the grids to be balance or unbalance grids. Based on the partitioned grids, the proposed DEDC constructs a regular path and then further adjusts the path segments for these unbalanced grids. The regular path construction and path adjustment aim to construct a path passing through as more as possible anchors for balancing the forwarding loads and prolonging the network lifetime. Performance evaluations reveal that the proposed DEDC outperforms existing data collection mechanisms in terms of energy consumption, network lifetime, and SD energy consumptions.

The paper [75] proposes two data collection policies for cluster-based WSN: (1) WSN-oriented and (2) UAV-oriented. In the WSN-oriented approach, nodes within each cluster member (CM), send information to their cluster head (CH) and for collection, the UAV visits all CHs. As the UAV visits many CHs, the flight time is increased. In the UAV-Oriented approach, all CHs send data from their CMs to a sink node (the CH chosen by the UAV as sink); hence, the UAV only visits this node, reducing the flying time but with a higher system energy cost (total energy consump-

tion). To find the most suitable scheme for different monitoring conditions in terms of the average energy consumption and the buffer capacity of the system, the authors develop a mathematical model that considers both the dynamics of the WSN along with the UAV.

In the related literature, the papers investigate the problem without considering any limit on the battery capacity of the mobile sink. They consider the problem with a mobile sink visiting a constant portion of cluster heads like visiting half of them. However, visiting a constant portion of CH nodes requires varying battery capacity of the mobile sink depending on the topology of the network, which is impossible for the UAV (battery capacity of the mobile sink cannot vary). In this chapter, we fill this gap in the literature by considering the limited-capacity battery for the UAV. In our innovative approach, by choosing an energy optimally varying portion of the CH robots to visit, the UAV with finite constant-capacity battery aims to minimize total energy consumption of the nonvisited CH robots that will be transmitting data by multiple hops through other nonvisited CH to a visited CH robot. In our work [76], deciding the subset of CH robots to visit depends on not only the locations of CH robots but also its battery capacity. Please notice that as we consider a RWSN instead of WSN, the UAV cannot form the clusters or assign robots as CH robot in our problem. The UAV can only choose a subset or all of CH robots to visit and thus, it collects data from them.

2.3 The related work with orienteering problem

We consider not only a limit on battery capacity of the UAV but also the differences between data efficiencies of different CH robots in the data collection problem. Therefore, our problem is similar to the reward maximization problem with limited path length which is the classical orienteering problem (OP), first introduced in [77]. Consequently, we survey the recent work on the orienteering problem.²

OP combines selecting a group of nodes and finding shortest path between those se-

² In orienteering problem, the competitor/collector tries to maximize the total profit collected score there is no cost for the remained scores which are not collected by the competitor/collector. On the other hand, orienteering problem does not consider data forwarding strategies at all, which differs our problem much from orienteering problem.

lected nodes [78]. It aims to maximize total reward by choosing some nodes where because of the limited time resource, the mobile sink cannot visit all available nodes. Travelling Salesman Problem considers finding shortest path between a group of nodes. On the other hand, Knapsack Problem considers maximizing the total collected profit by choosing from a set of non-divisible projects or tasks (CH robots in our problem) under a fixed budget such as battery capacity of UAV. As a result, OP combines Travelling Salesman Problem and Knapsack Problem [79]. Due to this similarity between our problem and orienteering problem, we survey the recent work on the orienteering problem.

As a recent work which considers the UAV trajectory design problem as OP, in the work [80], a UAV flies over multiple locations and serves as many users as possible in limited time. Optimal trajectory design problem was defined as a mixed-integer linear programming in that paper which suggests and propose a greedy poliy by considering the problem as an OP. It is numerically shown that proposed algorithm is fast and a near-optimal solution.

The paper [81] proposes Strengthened Particle Swarm Optimization (StPSO) by modifying pioneering-particles which achieves the swarm's experience. Each pioneer-particle is processed in two steps, initiating an external local search and assigning a random velocity. By introducing two steps of modification, the exploration mechanism of PSO is further improved and premature convergence can be avoided. Two sub-variants by only including one of two possible steps, namely Diversification Strengthened PSO and Intensification Strengthened PSO, are also introduced. [82] proposes Discrete Strengthened PSO (DStPSO) which focuses on modifying pioneering-particles achieving optimality via Reduced Variable Neighborhood Search.

[83] investigates OP for undirected and directed graphs. It proposes a $(2 + \delta)$ -approximation algorithm and an $O(\log^2 OPT)$ approximation algorithm for undirected graphs and directed graphs, respectively. [84] develops Multi-Level VNS (ML-VNS) which solves certain identical instances concurrently by reducing computational and search resources. Three sets of large-sized OP instances are used for comparing with ML-VNS against Tabu Search (TS) [85] and Probabilistic Solution Discovery Algorithm (PSDA) [86]. In addition to using the set of instances in [86], they

generate new instances with larger number of nodes. PSDA is only applied to the new instance sets. ML-VNS achieves better the solution quality than both PSDA and TS for all sets of instances. Nevertheless, ML-VNS has more computational complexity than TS.

[87] proposes a method based on Path Relinking (PR) and Greedy Randomized Adaptive Search Procedure (GRASP) strategies [88]. This work explores various constructive methods and two neighborhoods in the local search of GRASP. PR is then adapted in the context of GRASP. [89] proposes Memetic-GRASP by combining GRASP, evolutionary algorithm and two local search procedures. Memetic-GRASP solves only 87 benchmark instances [90,91].

In our innovative approach in this thesis, by choosing an efficiency and energy-optimally varying portion of the CH robots to visit, the UAV with finite constant-capacity battery aims to minimize the joint cost of data efficiencies and energy consumption of the nonvisited CH robots which send data via other nonvisited CH robots until a visited CH robot. In our work, deciding the subset of CH robots to visit depends on not only locations of CH robots and its battery capacity but also data efficiencies of CH robots.

CHAPTER 3

ENERGY-AWARE CLUSTER-BASED DATA COLLECTION BY A UAV WITH A LIMITED-CAPACITY BATTERY IN ROBOTIC WIRELESS SENSOR NETWORKS

3.1 System Model and Problem Definition

This section focuses on defining our problem and generates our system approach. Table 3.1 summarizes the notation and symbols commonly used in this chapter for ease of reference.

3.1.1 Motivation and Problem Definition

We will present here a motivating scenario and formulate the problem based on this motivation. We interchangeably use robot, node, and sensor in the rest of this chapter. We consider a robotic network which consists of M clusters of mobile robots, an unmanned aerial vehicle (UAV) with limited battery capacity and the fusion center where the UAV charges its battery. The responsibility of the robotic network is to collect data from the sensors which monitor environmental changes such as temperature, humidity, noise, etc.

Each cluster has a cluster head (CH) robot which allocates tasks to the remaining robots in the cluster. The remaining robots execute the tasks assigned to them (such as monitoring the environment and detecting unusual cases) and send the resultant data (obtained using their sensors) to the CH robot in its cluster. The responsibility of a CH robot is to collect data from the robots in its cluster and then transmit data to the UAV directly or indirectly (by sending its data to another CH robot to forward to the

Table 3.1: Symbols and Notation

Places	Explanations
M	The number of all CH robots
S	The index set of all CH robots
ξ_i	The position of the CH robot i
ξ_0	The initial position of the UAV
$E_{UAV}(i, j)$	The energy consumed by the UAV for the path from CH robot i to CH robot j
C_{UAV}	The constant ratio between the energy consumption of the UAV and the distance it travels
$E_{CH}(i, j)$	The energy consumed by CH robot i to transmit data to CH robot j
C_{CH}	The ratio between energy consumption of a CH robot and the square of length of the path it forwarded its data
$\pi(\xi_i, \xi_j)$	The linear path from CH robot i to CH robot j
P	The set of all possible paths between the CH robots
π	The strategy, the set of the linear paths followed by the UAV for the data collection
E_{UAV}^π	Energy consumption of the UAV under strategy π
u_i	The data forwarding strategy of CH robot i not visited by the UAV
u	The set of all data forwarding strategies for all CH robots
$E_i^\pi(u_i)$	Energy consumption of CH robot i under strategies π, u_i
$E_{ACH}^\pi(u_i)$	Energy consumption of all CH robots under strategies π, u

UAV). In this network, UAV visits some of the CH robots or all of them depending on their locations and the battery capacity of the UAV. Please see Figure 3.1. If the UAV cannot visit all of CH robots due to its limited battery capacity, then the CH robots which are not visited by the UAV send their data to one of neighboring CH through multiple hops via other nonvisited CH neighbors.

The index set of all CH robots in the network is denoted by $S \triangleq \{1, 2, \dots, M\}$. In the multi-robot system, each CH robot collects data from the remaining robots (in its

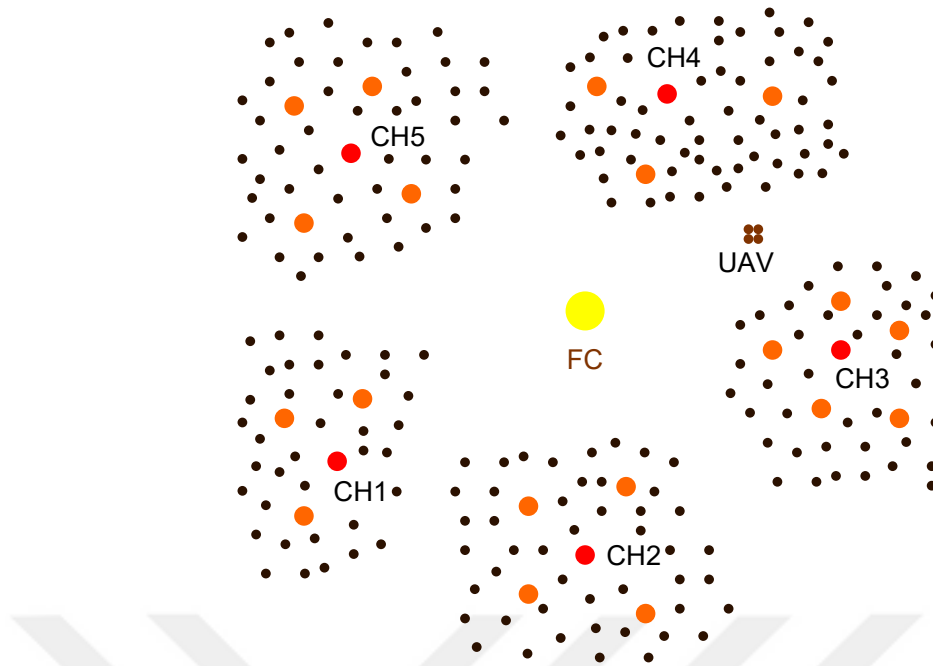


Figure 3.1: The whole multi-robot system includes a fusion center (FC) and five clusters of robots around FC. Red dots are the cluster head (CH) robots whereas the orange ones are the remaining robots which collect (environmental monitoring) data from the sensors (the black dots) in their cluster and send their data to the CH robot of their cluster. There are 19 robots in total and the UAV in the system. The UAV initially stands on the FC to charge its battery. After the UAV collects data from all CH robots directly or indirectly, it returns to FC to send all data to FC and recharge its battery for the next path.

cluster) to aggregate and transmit to the UAV. Each robot in that cluster aggregates data from the sensors surrounding it and the resultant data after executing the task assigned to it by the CH robot. The battery capacity of the UAV is denoted by B .

A CH robot spends significant energy for data aggregation and transmission to the UAV or the neighboring CH robot. If a CH robot moves like the remaining robots in its cluster, then the energy level of the CH robot will decrease below the critical energy level quickly. Falling below the critical level fast causes frequent CH election which is a very time and energy consuming process. It may also cause a CH robot which allocates tasks very efficiently to leave being CH robot a result of inefficient energy consumption due to moving like other robots in the cluster. Hence, it is

reasonable to make the following assumption.

Assumption 1. *A CH robot does not move during its CH mission to avoid additional energy consumption.*¹

Remark 1. *From Assumption 1, each robot in that cluster aggregates data from the sensors surrounding it and the resultant data after executing the task assigned to it by the CH robot. Therefore, the sensors and the robots except CH robots and the UAV will not be shown in the following figures except Figure 3.1.*

Initially, we aim to focus on the distances for calculating the costs of energy consumption. Therefore, we make the following assumption.

Assumption 2. *Each CH robot sends the same amount of data without latency to the UAV (directly or indirectly by forwarding its data).*²

The positions of the CH robots and initial position of the UAV are denoted by using Cartesian coordinates. The position (vertice of the network) of the CH robot i (of the cluster i) is denoted by $\xi_i \triangleq (x_i, y_i)$. The initial position of the UAV is denoted by $\xi_0 \triangleq (x_0, y_0)$.

From the related literature, it is assumed that the energy consumption of the UAV is proportional to the distance it travels. To illustrate, the energy consumed by the UAV from CH robot i to CH robot j is denoted by $E_{UAV}(i, j)$ and this energy cost is defined as

$$\begin{aligned} E_{UAV}(i, j) &\triangleq C_{UAV} \|\xi_i - \xi_j\| \\ &= C_{UAV} \sqrt{(x_i - x_j)^2 + (y_i - y_j)^2} \end{aligned} \quad (3.1)$$

where C_{UAV} is the constant ratio between the energy consumption of the UAV and the distance it travels, which represents the direct proportionality. On the other hand, from the related literature, it is assumed that the energy consumption (for data transmission) of a CH robot is proportional to the square of the distance between itself and

¹ Despite the motivation given for this assumption, CH robots may need to move in some scenarios while performing the CH mission. In this case, the mobility for CH robots need to be considered in the system model.

² Although we assume that the homogeneity (same amount) of transmitted data for each CH robot, CH robots may send data in different amount and different efficiency.

the next hop. (The next hop may be a neighboring CH robot or the UAV depending on the path the UAV for data collection.)

To illustrate, the energy consumed by the CH robot i to transmit data to CH robot j is denoted by $E_{CH}(i, j)$ and this energy cost is defined as

$$\begin{aligned} E_{CH}(i, j) &\triangleq C_{CH} \|\xi_i - \xi_j\|^2 \\ &= C_{CH} [(x_i - x_j)^2 + (y_i - y_j)^2] \end{aligned} \quad (3.2)$$

where C_{CH} is the constant ratio between the energy consumption of a CH robot and the square of distance between it and the next hop (neighboring robot), which represents the quadratic proportionality (From Assumption 2, the amount of data to send is same for each CH robot in a round. Therefore, C_{CH} is constant for each CH robot).

In the related literature, it is assumed that the robots or nodes have sufficient energy to transmit their data to the FC which is the initial position of the UAV. During the path, it is very probable that the UAV may pass through a closer point for each CH robot. In the worst case, the UAV can collect data from some CH robots when it is standing on the FC (the initial position of the UAV). Therefore, we make the following assumption in this work.

Assumption 3. *A CH robot has sufficient energy to transmit its data directly to the UAV when the UAV stands at its initial position before starting to its trajectory.*

Data transmission rate while communicating with the UAV is constant for all CH robots because this is more energy efficient from the fact that data transmission rate is a concave function of data transmission power.

Assumption 4. *A CH robot transmits data to the UAV or another CH robot with constant rate.*

In other words, if a CH robot i consumes α_1 units energy to transmit β_1 bits and α_2 units energy to transmit β_2 bits, then a CH robot i consumes $\alpha_1 + \alpha_2$ units energy to transmit $\beta_1 + \beta_2$ bits. Depending on the battery capacity of the UAV, it may visit a portion of CH robots instead of all CH robots due to the lack of energy. As this problem considers efficient energy usage of the UAV beside the CH robots, we make the following assumption.

Assumption 5. *The UAV visits each CH robot at most once.*

Under these assumptions, we will define the problem more precisely in the following subsection.

3.1.2 Our Problem Approach Formulation

In this work, the UAV aims to plan such a path that it can complete with the energy in its full battery. Although each CH robot has sufficient energy to transmit their data in one round, it is not desired that the CH robots spend much energy for this data transmission. *The UAV aims to minimize the total energy consumption of the CH robots by planning the path through which it visits the CH robots.*

Definition 1 (Path Set, P). *Let's define the path set as the set of all $M \times (M + 1)$ the linear paths between the positions of the M CH robots and the initial position of the UAV which are denoted by*

$$P \triangleq \{p(\xi_0, \xi_1), p(\xi_0, \xi_2), \dots, p(\xi_0, \xi_M), \dots, p(\xi_i, \xi_j), \dots, p(\xi_M, \xi_{M-1})\}. \quad (3.3)$$

where $p(\xi_i, \xi_j)$ is the linear path (edge of the network) from CH robot i to CH robot j if $i \neq 0$ and $j \neq 0$ and the length of $p(\xi_i, \xi_j)$ is equals to $\|\xi_i - \xi_j\|$. (Notice that $p(\xi_0, \xi_j)$ is the linear path (edge of the network) from the initial position of the UAV to CH robot j and $p(\xi_i, \xi_0)$ is the linear path from CH robot i to the initial position of the UAV.)

Definition 2 (Strategy of the UAV, π). *Let us define the strategy of the UAV as the set of the linear paths followed by the UAV for the data collection, which is a subset of the path set, i.e., $\pi \subseteq P$.*

Definition 3 (Data forwarding strategy of CH robot i , u_i). *Let us define the data forwarding strategy of CH robot i as the set of the linear paths followed by the CH robot i for forwarding data to a CH robot on the route (visited by the UAV). Notice that $u_i = \emptyset$ for all CH robot i visited by the UAV. The data forwarding strategy is a subset of the path set, i. e., $u_i \subseteq P$.*

Definition 4 (The set of data forwarding strategies of CH robots, u). *Let us define the set of data forwarding strategies of CH robots as the set of all data forwarding*

strategies of CH robots such that $u = \{u_1, u_2, \dots, u_M\}$, where $u_i = \emptyset$ for all CH robot i visited by the UAV.

Definition 5 (Indicator function). The indicator function is a binary function which takes a value of 1 for true event A , i. e.,

$$I_{\{A\}} \triangleq \begin{cases} 1 & \text{if event } A \text{ is true} \\ 0 & \text{if event } A \text{ is false} \end{cases} \quad (3.4)$$

Definition 6 (Energy consumption of the UAV under strategy π , E_{UAV}^π). Let us define energy consumption of the UAV under strategy π as the total energy consumed by the UAV whenever the strategy π is applied, i.e.,

$$E_{UAV}^\pi \triangleq \left[\sum_{j=1}^M \sum_{i=1}^M E_{UAV}(i, j) I_{\{p(\xi_i, \xi_j) \in \pi\}} \right] \quad (3.5)$$

From Equation (4.1), Equation (3.5) yields

$$E_{UAV}^\pi = \left[\sum_{j=1}^M \sum_{i=1}^M C_{UAV} \|\xi_i - \xi_j\| I_{\{p(\xi_i, \xi_j) \in \pi\}} \right]. \quad (3.6)$$

Remark 2. Notice that if a CH robot i is not visited by the UAV, then

$$\sum_{j=1}^M I_{\{p(\xi_i, \xi_j) \in \pi\}} = 0. \quad (3.7)$$

Definition 7 (Energy consumption of CH robot i under strategy π , u_i , $E_i^\pi(u_i)$). Using the data forwarding strategy u_i , a CH robot i not visited by the UAV under strategy π consumes $E_i^\pi(u_i)$. If a CH robot i is visited by the UAV under strategy π , $E_i^\pi(u_i) = 0$ (no need for data forwarding strategy).

Definition 8 (Total energy consumption of all CH robots under strategies π , u , $E_{ACH}^\pi(u)$). Let us define energy consumption of all CH robots under strategy π as the total energy consumed by all CH robots whenever the strategy π is applied, i. e.,

$$E_{ACH}^\pi(u) \triangleq \sum_{i=1}^M \left[E_i^\pi(u_i) \left(1 - \sum_{j=1}^M I_{\{p(\xi_i, \xi_j) \in \pi\}} \right) \right]. \quad (3.8)$$

Under Assumptions 1–5, we formulate our approach precisely as in Problem 1.

Problem 1. Minimizing total energy consumption of CH robots via a UAV with limited-capacity battery

$$\begin{aligned} \min_{u, \pi} \quad & E_{ACH}^\pi(u) \\ \text{s.t.} \quad & E_{UAV}^\pi \leq B \end{aligned}$$

3.2 Sufficient Battery Capacity to Visit All CH Robots

In this section, we consider the case in that the UAV has sufficient energy to visit all CH robots for data collection. First, we will consider the problem as a traveling salesman problem and then look for the shortest path. Thus, we can obtain a lower bound for the amount of energy which the UAV needs to be able to visit all CH robots.

Definition 9 (Minimum battery capacity for the UAV to visit all CH robots, B_{TSP}). *The energy required for visiting all CH robots under the optimum strategy in the traveling salesman problem is the minimum battery capacity for the UAV to visit all CH robots.*

To find this minimum battery capacity to visit all CH robots, we consider the problem as the classical traveling salesman problem. To find a robust optimal solution for the traveling salesman problem at hand, we consider the following remark.

Remark 3. *In a multirobot network system, one actually deals with hundreds of robots at most, which implies that at most tens of CH robots exist in the network. Roughly speaking, square root of the number of robots can be taken in this process to find the number of CH robots approximately.*

From Remark 3, we can find optimal solution for the TSP by using common techniques in the literature, like the genetic algorithm (GA) or the particle swarm optimization algorithm (PSO). We use GA to solve TSP. Thus, for our network including the UAV and CH robots, we apply GA as optimal solution³ in case the UAV has sufficient battery capacity to visit all CH robots for data collection.

3.3 Our Novel Approach: Total Energy Minimization Problem

The main novelty in this chapter comes from the case investigated in this section. Although there exist many papers considering the first case described in Section 3.2, to

³ As in our scenarios, we consider scenarios with tens of CH robots and related literature consider 5% of sensor nodes as CH sensors (not more than 1000 sensors so at most 50 sensors become CH nodes). As we consider robots which have much less number than sensors, the number of all robots in our system can be considered as 200 robots at most (which implies 10 CH robots at most). In this case, genetic algorithm can give optimal solution when UAV consider to visit all CH robots in a combination of CH robots in our scenarios (the robot scenarios with at most 10-CH robot).

date, there exists no paper considering the limited-capacity battery considered in this section. (In the related literature, the second case is considered as visiting a constant portion of the cluster heads, like visiting half of them. However, for visiting constant portion of the cluster heads, the UAV needs a varying battery capacity depending on the locations of the CH robots, which is not practical.)

In order to motivate our novelty, the UAV has *insufficient battery capacity* to visit all CH robots. In this case, by choosing an energy optimally varying portion of the CH robots to visit, the UAV aims to minimize total energy consumption of the nonvisited CH robots that will be transmitting data by multiple hops through other nonvisited CH until a visited CH node. Therefore, we will focus on minimizing energy consumption of each nonvisited CH robot under strategy π . In the next subsection, we will investigate optimal strategies for the nonvisited CH robots to forward their data to another CH robot until a visited CH robot.

3.3.1 Optimal Data Forwarding Strategy of CH Robots

If a CH robot i is visited by the UAV, then there is no need for the data forwarding strategy and so $u_i = \emptyset$. On the other hand, if a CH robot i is not visited by the UAV, then it should look for the shortest path to each CH robot and take the minimum of all shortest paths. From Equation (3.2), the squares of the distances between the neighboring CH robots are considered to calculate the shortest path between the CH robots. Thus, we can derive optimal data forwarding strategy for each CH robot. Please notice that each of the nonvisited CH robots considers each of the visited CH robots visited by the UAV as a possible target CH robot to find the optimal data forwarding strategy for itself.

Definition 10 (Minimum energy consumption of CH robot i not visited under strategy π , γ_i^π). Let us define minimum energy consumption of CH robot i not visited by the UAV under strategy π , i. e.,

$$\gamma_i^\pi = \min_{u_i} E_i^\pi(u_i) \quad (3.9)$$

for a CH robot i not visited by the UAV where u_i is data forwarding strategy of CH robot i .

The following example is given to better understand Definition 10.

Example 1. *Let us consider the multirobot system in Figure 3.2, where the UAV collects data from 6 CH robots by only visiting two of them under strategy π_0 .*

Under the strategy π_0 , the UAV visits CH 1 and CH 2 (they are on the route) so $E_1^{\pi_0}(u_1) = E_2^{\pi_0}(u_2) = 0$. Therefore, $\gamma_1^{\pi_0} = \gamma_2^{\pi_0} = 0$.

If CH 3 chooses CH 1 to forward its data under strategy u_3 , then its energy consumption will be minimum, i. e., $\gamma_3^{\pi_0} = C_{CH}\|\xi_3 - \xi_1\|^2 = 25$ for $C_{CH} = 1$ from Equation (3.2). Similarly, if CH 5 chooses CH 2 to forward its data under strategy u_5 , then its energy consumption will be minimums, i. e., $\gamma_5^{\pi_0} = C_{CH}\|\xi_5 - \xi_2\|^2 = 225$ for $C_{CH} = 1$ from Equation (3.2).

If CH 4 forwards its data directly to CH 2, $E_4^{\pi_0}(u_4) = C_{CH}\|\xi_4 - \xi_2\|^2 = 400$ for $C_{CH} = 1$ from Equation (3.2). If CH 4 forwards its data directly to CH 1, $E_4^{\pi_0}(u_4) = C_{CH}\|\xi_4 - \xi_1\|^2 = 225$ for $C_{CH} = 1$ from Equation (3.2). If CH 4 forwards its data first to CH 5 then forwards it to CH 2, $E_4^{\pi_0}(u_4) = C_{CH}[\|\xi_4 - \xi_5\|^2 + \|\xi_5 - \xi_2\|^2] = 49 + 225 = 274$ for $C_{CH} = 1$ from Equation (3.2). If CH 4 forwards its data first to CH 3 then forwards it to CH 1, $E_4^{\pi_0}(u_4) = C_{CH}[\|\xi_4 - \xi_3\|^2 + \|\xi_3 - \xi_1\|^2] = 100 + 25 = 125$ for $C_{CH} = 1$ from Equation (3.2). Hence, $\gamma_4^{\pi_0} = 125$.

If CH 6 forwards its data directly to CH 2, $E_6^{\pi_0}(u_6) = C_{CH}\|\xi_6 - \xi_2\|^2 = 409$ for $C_{CH} = 1$ from Equation (3.2). If CH 6 forwards its data first to CH 5 then to forwards CH 2, $E_6^{\pi_0}(u_6) = C_{CH}[\|\xi_6 - \xi_5\|^2 + \|\xi_5 - \xi_2\|^2] = 100 + 225 = 325$ for $C_{CH} = 1$ from Equation (3.2). On the other hand, if CH 6 forwards its data directly to CH 1, $E_6^{\pi_0}(u_6) = C_{CH}\|\xi_6 - \xi_1\|^2 = 884$ for $C_{CH} = 1$ from Equation (3.2). If CH 6 forwards its data first to CH 5 then forwards it to CH 1, $E_6^{\pi_0}(u_6) = C_{CH}[\|\xi_6 - \xi_5\|^2 + \|\xi_5 - \xi_1\|^2] = 100 + 400 = 500$ for $C_{CH} = 1$ from Equation (3.2). If CH 6 forwards its data first to CH 4 then forwards it to CH 1, $E_6^{\pi_0}(u_6) = C_{CH}[\|\xi_6 - \xi_4\|^2 + \|\xi_4 - \xi_1\|^2] = 233 + 225 = 458$ for $C_{CH} = 1$ from Equation (3.2). If CH 6 forwards its data first to CH 5, then forwards it to CH 4 and finally then forwards it to CH 1, $E_6^{\pi_0}(u_6) = C_{CH}[\|\xi_6 - \xi_5\|^2 + \|\xi_5 - \xi_4\|^2 + \|\xi_4 - \xi_1\|^2] = 100 + 49 + 225 = 374$ for $C_{CH} = 1$ from Equation (3.2). If CH 6 forwards its data first to CH 5, then forwards it to CH 4, after then forwards it to CH 3 and finally then forwards it to CH 1, $E_6^{\pi_0}(u_6) = C_{CH}[\|\xi_6 - \xi_5\|^2 + \|\xi_5 - \xi_4\|^2 + \|\xi_4 - \xi_3\|^2 + \|\xi_3 - \xi_1\|^2] = 100 + 49 + 100 + 25 = 274$

for $C_{CH} = 1$ from Equation (3.2). Hence, $\gamma_6^{\pi_0} = 274$.

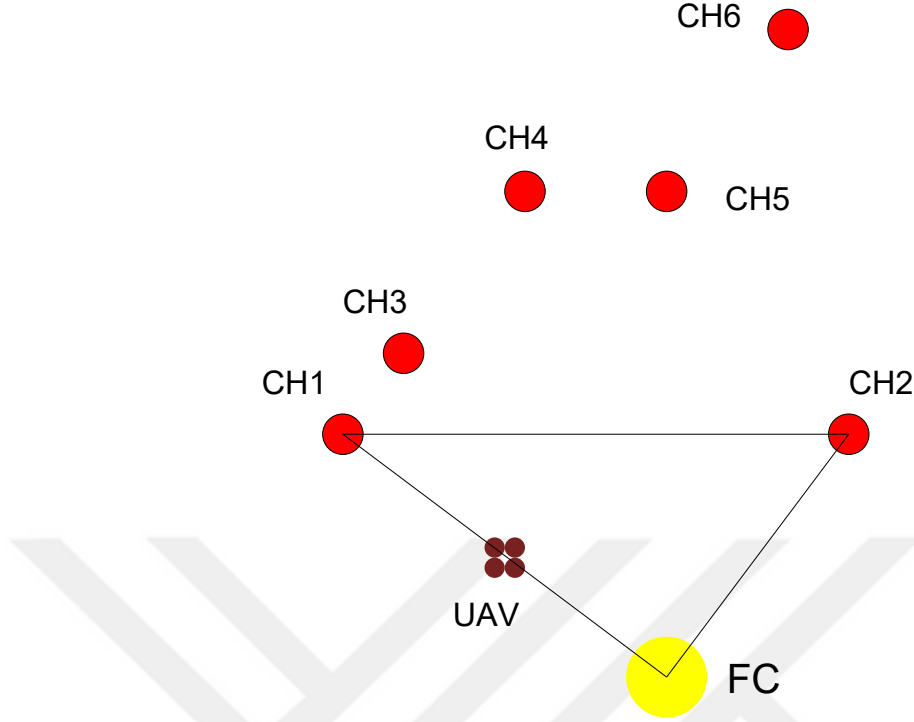


Figure 3.2: The whole multi-robot system consists of a fusion center (FC) where the UAV starts its route and six clusters of robots around FC. The red circles show the locations of the six cluster head (CH) robots in their robot cluster. *The UAV uses the strategy π_0 for the data collection.* With respect to this initial position of the UAV at $\xi_0 = (0, 0)$, the positions of the CH robots are $(\xi_1, \xi_2, \xi_3, \xi_4, \xi_5, \xi_6) = ((-16, 12), (9, 16), (-13, 16), (-7, 24), (0, 24), (6, 32))$ units.

Following remarks will be useful for proposing the data forwarding strategy for CH robots.

Remark 4. *In Example 1, notice that the best data forwarding strategy for CH 6 is to forward its data to CH 1 (the visited CH robot farther to CH 6) using CH 5, CH 4, or CH 3 instead of forwarding its data to CH 2 (the closer CH robot farther to CH 6).*

Remark 5. *The data forwarding strategy of a CH robot i not visited by the UAV, u_i , depends only on the positions of the CH robots, both the CH robots on the trajectory of the UAV and the ones not on the trajectory of the UAV. Notice that u_i does not depend on the order by which the UAV visits those CH robots. As an example, data*

forwarding strategies for a CH robot i is same for following two cases: 1) the UAV visits CH robots p, q, r, s in order, 2) the UAV visits CH robots q, p, s, r , in order ($i \notin \{p, q, r, s\}$).

By the motivation from Remark 5, we make the following definition to propose the data forwarding strategy for CH robots more precisely.

Definition 11 (*K*-element combinations of the CH robots). Let S_a^K be a K -element subset of the M -element set of all CH robots, i. e., $S_a^K \subseteq S$ and $|S_a^K| = K$ for $1 \leq a \leq \binom{M}{K}$. Let $S^K(B)$ be the set of all feasible K -element combinations which can be visited by the UAV with battery capacity B . $S_a^K(j)$ represents as the j^{th} element in the combination S_a^K .

From Remark 4, the data forwarding strategy needs to consider the sum of squares of distances between CH robots instead of the sum of distances between CH robots. From Remark 5, the data forwarding strategy depends only on the positions of the CH robots not visited by the UAV and the ones visited by the UAV whereas the strategy does not depend on the order in which the UAV visits them. Thus, Remark 4 and Remark 5 provide us the motivation to propose optimal data forwarding strategy for a CH robot, Algorithm 1, by using Definition 11.

Remark 6. Finding a shortest path is feasible in real time. Here instead of finding a short path to only one visited CH robot, whereas each nonvisited CH robot consider finding one shortest path to each visited CH robot. After finding all shortest paths, each nonvisited CH robot chooses the visited CH robot which can be reached via the minimum of the shortest paths from that nonvisited CH robot. Hence, Algorithm 1 is feasible in real-time.

Generally shortest path algorithms with single input-single output has a computational complexity of $O(V + E)$ where V denotes the number of vertices (a visited CH robot and the nonvisited CH robots in our case) and E denotes the edge between the vertices. If UAV visits K CH robots, then $V = M - K + 1$ and $E = V(V - 1)$ and so $V + E = V^2$. Therefore, the shortest path algorithms with single nonvisited CH robot-single visited CH robot has a computational complexity of $O(V + E) = O(V^2) = O((M - K + 1)^2)$. In our shortest path algorithm, each of $M - K$ nonvisited CH

Algorithm 1 Multi Shortest Path Data Forwarding Strategy (MSPDFS)

Initialization: Assume that the UAV chose a K -element combination from M CH robots, S_a^K , to look for a trajectory to visit all CH robots in that combination. $|S_a^K|$ is cardinality of the set S_a^K . Given the combination S_a^K , data forwarding strategy is formed as follows.

Algorithm:

for $i = 1 : M$ **do**

 # Comment: If CH robot i is on the trajectory of the UAV

if $i \in S_a^K$ **then**

 # Comment: No need to forward data to another CH robot

$u_i = \emptyset$ and $\gamma_i^\pi = 0$

else

 # Comment: Calculate shortest paths for all CH robot on the trajectory of the UAV.

for $j = 1 : |S_a^K|$ **do**

 Find shortest path (minimum energy path strategy for data forwarding) from the position of CH robot i to the position of CH robot $S_a^K(j)$.

end for

 Compare it with the shortest path to origin (initial position of the UAV) and choose the shorter one. Find the optimal strategy $u_i^* = \arg \min_{u_i} E_i^\pi(u_i)$ by comparing the energy cost of the best strategy for each destination, $S_a^K(j)$.

end if

end for

Output: The optimal data forwarding strategy u_i^* for each CH robot i given S_a^K

robot considers each of K visited CH robot as target and take the minimum of the K shortest path (one for one visited CH robot). Hence, computational complexity of our shortest path algorithm is $O(K \times (M - K + 1)^2)$.

3.3.2 Optimal Strategy for the UAV

As it is exhibited in the previous section, if the UAV has sufficient battery capacity to visit all CH robots, then Problem 1 can be considered as a TSP problem and an optimal strategy can be obtained by common techniques in the literature. On the other hand, if the UAV has a battery capacity less than B_{TSP} , then considering Problem 1 as a TSP problem does not guarantee to obtain an optimal strategy.

In this case, we need to consider not only the energy consumption of the UAV below its battery capacity but also the minimum energy consumption of the nonvisited CH robots and the data forwarding strategies for the nonvisited CH robots (These strategies are investigated in the previous subsection.) This is shown as in the following proposition. Let π^* denote the optimal strategy for Problem 1.

Proposition 1. *For $B < B_{TSP}$, π_{TSP}^{max} does not necessarily imply the optimality condition for the Problem 1, where π_{TSP}^{max} is the strategy by which the TSP can visit the maximum number of CH robots.*

Proof. This proposition will be proved by a counter example system in Figures 3.3 and 3.4. In this example, we take the initial position of the UAV as $\xi_0 = (0, 0)$. With respect to this initial position, the positions of the CH robots are $(\xi_1, \xi_2, \xi_3, \xi_4, \xi_5, \xi_6) = ((-16, 12), (9, 16), (-13, 16), (-7, 24), (0, 24), (6, 32))$.

With respect to these positions, we obtain the distance between the CH robots. $\|\xi_1 - \xi_3\| = 5$, $\|\xi_3 - \xi_4\| = 10$, $\|\xi_4 - \xi_5\| = 7$, $\|\xi_5 - \xi_2\| = 15$, $\|\xi_6 - \xi_5\| = 10$, $\|\xi_1 - \xi_5\| = 20$, $\|\xi_0 - \xi_1\| = 20$, $\|\xi_0 - \xi_2\| = 15$ where ξ_0 is the initial point of route (trajectory) of UAV.

Assume that $B = 70$ and let's investigate the cost of the following two strategies, π_1 as shown in Figure 3.3 and π_2 as shown in Figure 3.4.

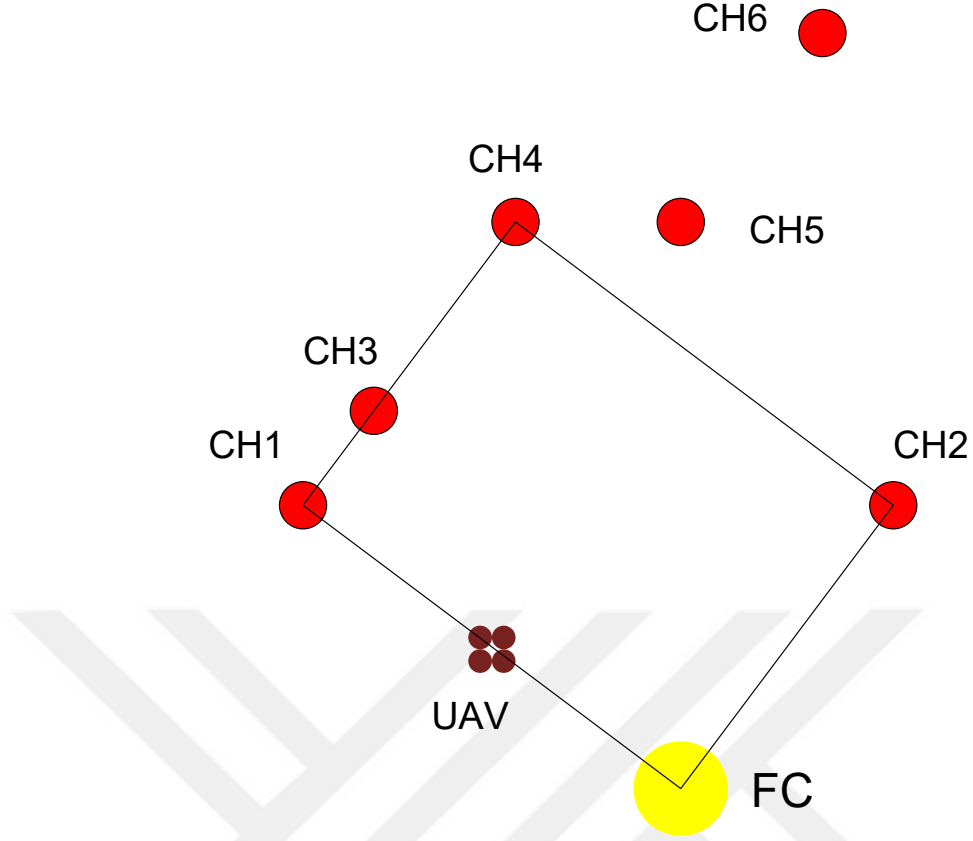


Figure 3.3: The whole multi-robot system consists of a fusion center (FC) where the UAV starts its route and 6 cluster of robots around FC. The red circles show the locations of the cluster head (CH) robots in their robot cluster. *The UAV uses the strategy π_1 for the data collection.* With respect to this initial position of the UAV at $\xi_0 = (0, 0)$, the positions of the CH robots are $(\xi_1, \xi_2, \xi_3, \xi_4, \xi_5, \xi_6) = ((-16, 12), (9, 16), (-13, 16), (-7, 24), (0, 24), (6, 32))$ units.

$$\pi_1 = \{p(\xi_0, \xi_1), p(\xi_1, \xi_3), p(\xi_3, \xi_4), p(\xi_4, \xi_2), p(\xi_2, \xi_0)\} \quad (3.10)$$

$$\pi_2 = \{p(\xi_0, \xi_1), p(\xi_1, \xi_5), p(\xi_5, \xi_2), p(\xi_2, \xi_0)\} \quad (3.11)$$

The UAV consumes the following energies under these two strategies.

$$E_{UAV}^{\pi_1} = \|\xi_0 - \xi_1\| + \|\xi_1 - \xi_3\| + \|\xi_3 - \xi_4\| + \|\xi_4 - \xi_2\| + \|\xi_2 - \xi_0\| \quad (3.12)$$

$$E_{UAV}^{\pi_2} = \|\xi_0 - \xi_1\| + \|\xi_1 - \xi_5\| + \|\xi_5 - \xi_2\| + \|\xi_2 - \xi_0\| \quad (3.13)$$

From Equations (3.12) and (3.13), $E_{UAV}^{\pi_1} = E_{UAV}^{\pi_2} = 70$ which equals to the battery

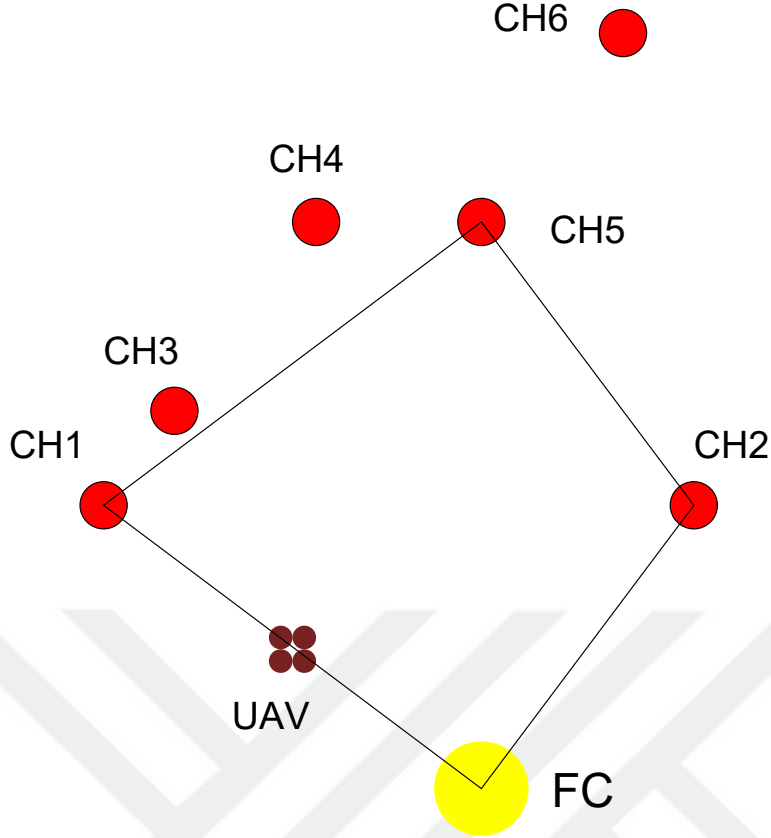


Figure 3.4: The whole multi-robot system consists of a fusion center (FC) where the UAV starts its route and 6 cluster of robots around FC. The red circles show the locations of the cluster head (CH) robots in their robot cluster. *The UAV uses the strategy π_2 for the data collection.* With respect to this initial position of the UAV at $\xi_0 = (0, 0)$, the positions of the CH robots are $(\xi_1, \xi_2, \xi_3, \xi_4, \xi_5, \xi_6) = ((-16, 12), (9, 16), (-13, 16), (-7, 24), (0, 24), (6, 32))$ units.

capacity of the UAV, B . In this case, $\pi_1 = \pi_{TSP}^{max}$ because it visits maximum number of CH robots, 4.

Let's compare the cost of these two strategies π_1 and π_2 for Problem 1.

The total energy consumption of the CH robots under the strategy π_1 is

$$E_{ACH}^{\pi_1} = \sum_{i=1}^6 \left[\gamma_i^{\pi_1} \left(1 - \sum_{j=1}^6 I_{\{p(\xi_i, \xi_j) \in \pi_1\}} \right) \right], \quad (3.14)$$

$$= \gamma_5^{\pi_1} + \gamma_6^{\pi_1}, \quad (3.15)$$

$$= \|\xi_5 - \xi_4\|^2 + [\|\xi_5 - \xi_4\|^2 + \|\xi_6 - \xi_5\|^2] \quad (3.16)$$

The total energy consumption of the CH robots under the strategy π_2 is

$$E_{ACH}^{\pi_2} = \sum_{i=1}^6 \left[\gamma_i^{\pi_2} \left(1 - \sum_{j=1}^6 I_{\{p(\xi_i, \xi_j) \in \pi_2\}} \right) \right], \quad (3.17)$$

$$= \gamma_3^{\pi_1} + \gamma_4^{\pi_1} + \gamma_6^{\pi_1}, \quad (3.18)$$

$$= \|\xi_3 - \xi_1\|^2 + \|\xi_5 - \xi_4\|^2 + \|\xi_6 - \xi_5\|^2 \quad (3.19)$$

From Equations (3.16) and (3.19),

$$\begin{aligned} E_{ACH}^{\pi_1} - E_{ACH}^{\pi_2} &= \|\xi_5 - \xi_4\|^2 - \|\xi_3 - \xi_1\|^2 \\ E_{ACH}^{\pi_1} &> E_{ACH}^{\pi_2} \end{aligned} \quad (3.20)$$

As it can be seen from Figure 3.3, $\pi_2 = \pi^*$ for Problem 1. Remind that $\pi_1 = \pi_{TSP}^{max}$ is the optimal strategy for the TSP which aims to visit the maximum number of CH robots, 4 in this example. From Equation (3.20),

$$E_{ACH}^{\pi_{TSP}^{max}} > E_{ACH}^* \quad (3.21)$$

which yields π_{TSP}^{max} cannot achieve optimality in this example. Hence, it is proved. \square

As the UAV with battery capacity $B < B_{TSP}$ does not have sufficient energy to visit all CH robots, it needs to desist from visiting some of the CH robots. The problem is to choose a subset of CH robots to desist from visiting them such that the total energy consumption of those unvisited CH robots will be minimum. The following remark will be useful in analyzing the desisting process.

Remark 7. *To solve the problem for the UAV with battery capacity $B < B_{TSP}$, (Let us remind that from Definition 9, B_{TSP} is the minimum energy required for the UAV to visit all CH robots.) our strategy will start at a point $B = B_{TSP}$, then the strategy will decrease the energy consumption of the UAV by desisting from visiting some CH robots. The decrease needs to be at least $B_{TSP} - B$.*

The following lemma is useful to search for a path after desisting from visiting a set of CH robots.

Lemma 1. *Assume that the UAV with battery capacity B_1 can follow an optimal route such that it visit CH robot i , j , and k successively on the optimal route by which the*

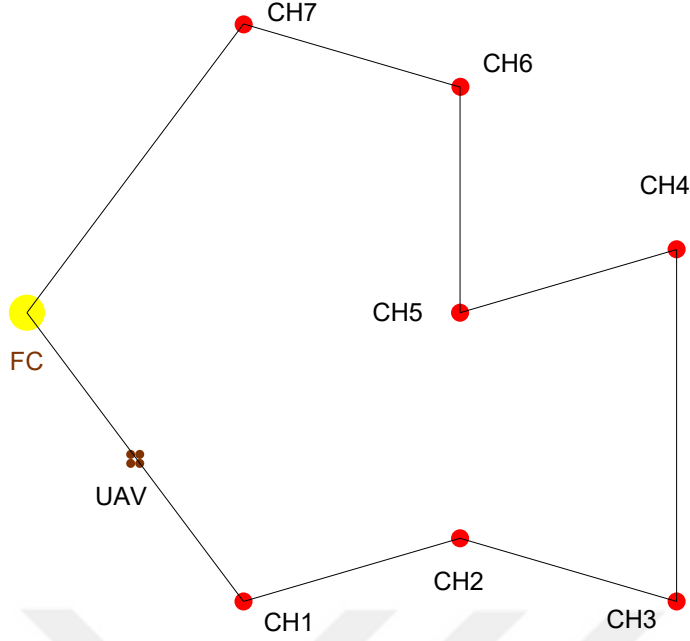


Figure 3.5: The whole multi-robot system consists of a fusion center (FC) where the UAV starts its route and 7 cluster head (CH) robots around FC. The red circles show the locations of the cluster head (CH) robots in their robot cluster. *The UAV uses an optimal strategy such that it visits CH 1, CH 2, CH 3, CH 4, CH 5, CH 6, and CH 7 in order (The path has a length of 244 m). With respect to the initial position at $\xi_0 = (0, 0)$, the positions of the CH robots are $(\xi_1, \xi_2, \xi_3, \xi_4, \xi_5, \xi_6, \xi_7) = ((24, -32), (48, -25), (72, -32), (72, 7), (48, 0), (48, 25), (24, 32))$ m.*

UAV visits $K < M$ CH robots (B_1 is the minimum energy required to follow that path). If the battery capacity of UAV decreased slightly such that $B_2 < B_1$ and the UAV decided to desist from visiting CH robot j , simply visiting CH robot k just after visiting CH robot i (the direct line from CH robot i to CH robot j would not guarantee optimality to plan a route with the remaining $K - 1$ CH robots except CH robot j).

Proof. The proof will be done by contradiction. Consider a multi-robot system in Figure 3.5 which consists of a fusion center (FC) where the UAV starts its route and 7 cluster head (CH) robots around FC. The red circles show the locations of the cluster head (CH) robots in their robot cluster (to focus on the CH robots, the other robots are not shown in Figures 3.5–3.7). It is assumed that the initial position of the UAV, the position of the fusion center is $\xi_0 = (0, 0)$. With respect

to this initial position, the positions of the CH robots are $(\xi_1, \xi_2, \xi_3, \xi_4, \xi_5, \xi_6, \xi_7) = ((24, -32), (48, -25), (72, -32), (72, 7), (48, 0), (48, 25), (24, 32))$ *m*. The UAV uses an optimal strategy such that it visits CH 1, CH 2, CH 3, CH 4, CH 5, CH 6 and CH 7 in order. To follow that route, the UAV needs exactly the following amount of energy

$$\begin{aligned}
E_{UAV}^\pi &= E_{UAV}(0, 1) + E_{UAV}(1, 2) + E_{UAV}(2, 3) + E_{UAV}(3, 4) + E_{UAV}(4, 5) \\
&+ E_{UAV}(5, 6) + E_{UAV}(6, 7) + E_{UAV}(7, 0) \\
&= C_{UAV} \times [\|\xi_0 - \xi_1\| + \|\xi_1 - \xi_2\| + \|\xi_2 - \xi_3\| + \|\xi_3 - \xi_4\| + \|\xi_4 - \xi_5\| \\
&+ \|\xi_5 - \xi_6\| + \|\xi_6 - \xi_7\| + \|\xi_7 - \xi_0\|] \\
&= C_{UAV} \times [40 + 25 + 25 + 39 + 25 + 25 + 25 + 40] \\
&= 244 \times C_{UAV}
\end{aligned} \tag{3.22}$$

From Equations (3.22), if $B < 244 \times C_{UAV}$, then the UAV needs to desist from visiting at least one CH robot. Assume that the UAV decided to desist from visiting CH 3 and then search for an optimal route to visit all CH robots except CH 3.

Consider a multi-robot system in Figure 3.6 which is the same system in Figure 3.5.

The UAV uses a strategy such that it visits CH 1, CH 2, CH 4, CH 5, CH 6, and CH 7 in order. In this strategy, instead of visiting CH 3, the UAV visits CH 4 just after visiting CH 2 (reconstructing the route with a direct line from CH 2 to CH 4) To follow that route, the UAV needs exactly the following amount of energy

$$\begin{aligned}
E_{UAV}^\pi &= E_{UAV}(0, 1) + E_{UAV}(1, 2) + E_{UAV}(2, 4) + E_{UAV}(4, 5) + E_{UAV}(5, 6) \\
&+ E_{UAV}(6, 7) + E_{UAV}(7, 0) \\
&= C_{UAV} \times [\|\xi_0 - \xi_1\| + \|\xi_1 - \xi_2\| + \|\xi_2 - \xi_4\| + \|\xi_4 - \xi_5\| + \|\xi_5 - \xi_6\| \\
&+ \|\xi_6 - \xi_7\| + \|\xi_7 - \xi_0\|] \\
&= C_{UAV} \times [40 + 25 + 40 + 25 + 25 + 25 + 40] \\
&= 220 \times C_{UAV}
\end{aligned} \tag{3.23}$$

Consider a multi-robot system in Figure 3.7 which is the same system in Figure 3.5. The UAV uses a strategy such that it visits CH 1, CH 2, CH 5, CH 4, CH 6, and CH 7 in order. To follow that route, the UAV needs exactly the following amount of energy

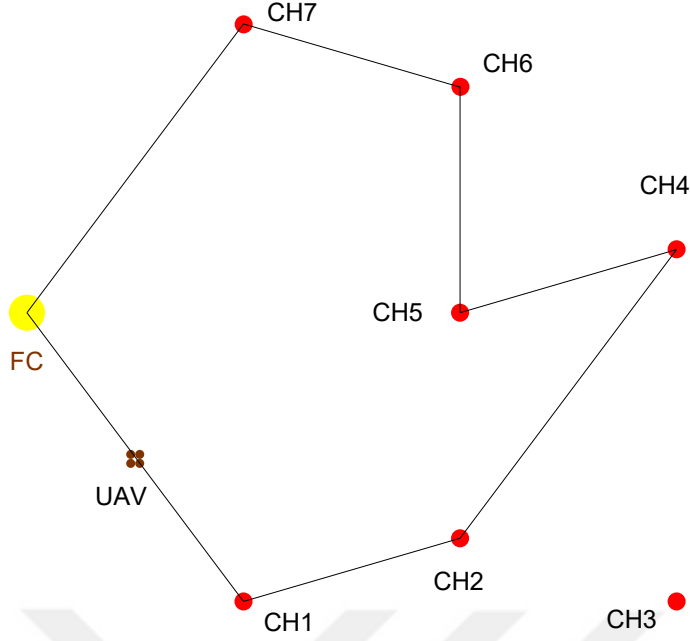


Figure 3.6: The whole multi-robot system consists of a fusion center (FC) where the UAV starts its route and 7 cluster head (CH) robots around FC. The red circles show the locations of the cluster head (CH) robots in their robot cluster. *The UAV uses an optimal strategy such that it visits CH 1, CH 2, CH 4, CH 5, CH 6, and CH 7 in order (The path has a length of 220 m). With respect to the initial position at $\xi_0 = (0, 0)$, the positions of the CH robots are $(\xi_1, \xi_2, \xi_3, \xi_4, \xi_5, \xi_6, \xi_7) = ((24, -32), (48, -25), (72, -32), (72, 7), (48, 0), (48, 25), (24, 32))$ m.*

$$\begin{aligned}
E_{UAV}^\pi &= E_{UAV}(0, 1) + E_{UAV}(1, 2) + E_{UAV}(2, 5) + E_{UAV}(5, 4) + E_{UAV}(4, 6) \\
&\quad + E_{UAV}(6, 7) + E_{UAV}(7, 0) \\
&= C_{UAV} \times [\|\xi_0 - \xi_1\| + \|\xi_1 - \xi_2\| + \|\xi_2 - \xi_5\| + \|\xi_5 - \xi_4\| + \|\xi_4 - \xi_6\| \\
&\quad + \|\xi_6 - \xi_7\| + \|\xi_7 - \xi_0\|] \\
&= C_{UAV} \times [40 + 25 + 25 + 25 + 30 + 25 + 40] \\
&= 210 \times C_{UAV}
\end{aligned} \tag{3.24}$$

From Equations (3.23) and (3.24), using a direct line from CH 2 to CH 4 does not provide the optimal route for visiting all CH robots except CH 3. By this contradiction, the lemma is proved. \square

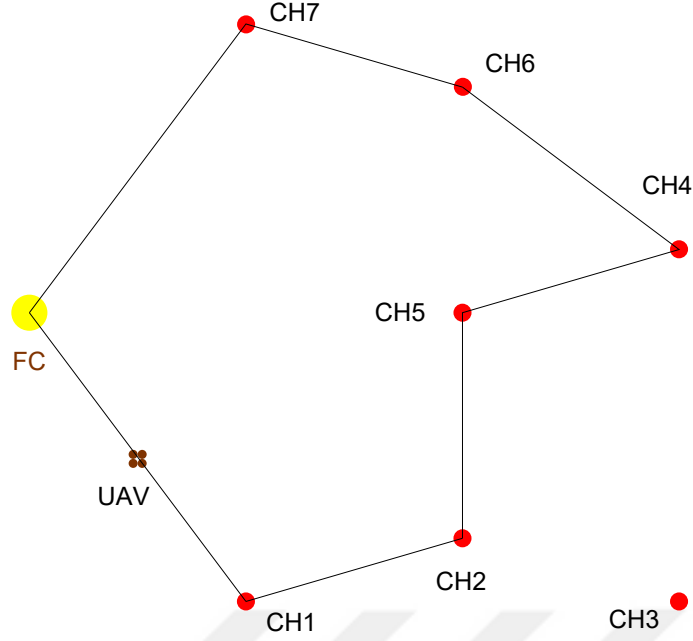


Figure 3.7: The whole multi-robot system consists of a fusion center (FC) where the UAV starts its route and 7 cluster head (CH) robots around FC. The red circles show the locations of the cluster head (CH) robots in their robot cluster. *The UAV uses an optimal strategy such that it visits CH 1, CH 2, CH 5, CH 4, CH 6 and CH 7 in order (The path has a length of 210 m). With respect to the initial position at $\xi_0 = (0, 0)$, the positions of the CH robots are $(\xi_1, \xi_2, \xi_3, \xi_4, \xi_5, \xi_6, \xi_7) = ((24, -32), (48, -25), (72, -32), (72, 7), (48, 0), (48, 25), (24, 32))$ m.*

From Remark 5, The data forwarding strategy of a CH robot not visited by the UAV depends only on the positions of the CH robots on the trajectory of the UAV and the ones not on the trajectory of the UAV. The data forwarding strategies do not depend on the order in which the UAV visits them. This need to be considered for finding optimal data forwarding strategies. From Lemma 1, if the UAV desists to visit a CH robot j , instead of simply passing from the previous CH robot i to the next CH robot k according to the visiting order (i, j, k are the consecutive CH robots according to the order), the UAV needs to consider the path planning problem again as a TSP problem for finding the optimal path (trajectory). Therefore, the UAV can find the optimal path only considering path planning problem as a TSP problem for each combination of CH robots from Definition 11. Thus, Remark 5 and Lemma 1 provide us the motivation to propose Algorithm 2 by using Definition 11.

Algorithm 2 Genetic Algorithm with Minimum Energy for Data Forwarding Strategy (GAMEDFS)

Initialize: Battery capacity of the UAV is insufficient for visiting all CH robots, i.e., $B < B_{TSP}$.

Algorithm:

for $K = (M - 1) : 1$ **do**

Comment: Choose K CH robots and desist from visiting other CH robots.

Find all $\binom{M}{K}$ combinations of the CH robots.

Comment: For each of the $\binom{M}{K}$ combinations of CH robots.

for $a = 1 : \binom{M}{K}$ **do**

Comment: Check whether the UAV can find a route to visit all CH robots in the combination S_a^K .

if $\min_{\pi} E_{UAV}^{\pi} \leq B$ **for** S_a^K **then**

Comment: S_a^K is a feasible K -element combination, i.e., $S_a^K \in S^K(B)$.

find the minimum energy consumption of the CH robots in $S - S_a^K$.

Use Algorithm 1 for each CH robot $i \in S - S_a^K$. Find $\sum_{i \in S - S_a^K} \gamma_i^{\pi}$

end if

end for

Comment: If there exists at least a feasible K -element combination, find the K -element combination S_a^K by which energy consumption of CH robots in $S - S_a^K$ will be minimum.

if $S^K(B) \neq \emptyset$ **then**

Find $\min_{S_a^K \in S^K(B)} \sum_{i \in S - S_a^K} \gamma_i^{\pi}$

end if

end for

Comment: Find the combination S_a^K by which the minimum energy consumption of the CH robots in $S - S_a^K$ will be minimum (In this step, all combinations with all K values are considered so this is the step to find the minimum of minimum).

Find $\min_K \left[\min_{S_a^K \in S^K(B)} \sum_{i \in S - S_a^K} \gamma_i^{\pi} \right]$.

Comment: As output, provide the result of K and the combination S_a^K .

Output: $(K, S_a^K) = \arg \min \sum_{i \in S - S_a^K} \gamma_i^{\pi}$

Remark 8. *Our algorithm uses a kind of exhaustive search algorithm. It considers all the combinations and then chooses the feasible combination which gives us minimum among the total joint costs of all feasible CH robots. For this purpose, it applies minimum energy for data forwarding strategy to each feasible combination. (Remind that minimum energy for data forwarding strategy is the multi shortest path for data forwarding strategy (MSPDFS) proposed as Algorithm 1).*

Here, we check the feasibility of a combination of CH robots by considering to visit all CH robots in the combination as TSP. To solve this TSP problem and check the feasibility of a combination, our strategy applies genetic algorithm. That is the reason why our strategy includes genetic-algorithm based strategy in its name.

Theorem 1. *Algorithm 2 is optimal for Problem 1.*

Proof. From Definition 8, Problem 1 can be converted into the following problem

$$\begin{aligned} \min_{\pi \subseteq P} \min_{u_i} & \sum_{i=1}^M (E_i^\pi(u_i) I_{\{i \in S - S_a^K\}}) \\ \text{s.t.} & E_{UAV}^\pi \leq B \end{aligned} \quad (3.25)$$

S_a^K be a K -element subset of the M -element set of all CH robots, i.e., $S_a^K \subseteq S$ and $|S_a^K| = K$ for $1 \leq a \leq \binom{M}{K}$.

From Definition 10, the problem in (3.25) can be converted into the following problem

$$\begin{aligned} \min_{\pi \subseteq P} & \sum_{i=1}^M [\gamma_i^\pi I_{\{i \in S - S_a^K\}}] \\ \text{s.t.} & E_{UAV}^\pi \leq B \end{aligned} \quad (3.26)$$

From Remark 7, the UAV with battery capacity $B < B_{TSP}$ cannot visit all M CH robots; therefore, the UAV needs to desist from visiting a subset of the CH robots.

From Remark 5, the strategy of a CH robot i not visited by the UAV, u_i , depends only on the positions of the CH robots. u_i does not depend on the route on which the UAV visit the CH robots. Therefore, the total energy consumption of the CH robots depends on the combination whereby the UAV determines the CH robots to visit.

If $\min_{\pi} E_{UAV}^{\pi} > B$ for S_a^K , then the combination S_a^K is such an infeasible combination that the UAV with battery capacity B cannot visit all the CH robots in that combination S_a^K . Therefore, it is unnecessary to find $\sum_{i \in S - S_a^K} \gamma_i^{\pi}$ for S_a^K such that $\min_{\pi} E_{UAV}^{\pi} > B$ for S_a^K .

Algorithm 2 finds all $\sum_{i \in S - S_a^K} \gamma_i^{\pi}$ for $S_a^K \in S^K(B)$ (recall that $\min_{\pi} E_{UAV}^{\pi} \leq B$ for $S_a^K \in S^K(B)$ from Definition 11) and then takes the minimum of $\sum_{i \in S - S_a^K} \gamma_i^{\pi}$ values.

From Proposition 1, the following inequality cannot be guaranteed

$$\min_{S_a^K \in S^K(B)} \sum_{i \in S - S_a^K} \gamma_i^{\pi} \leq \min_{S_a^{K-1} \in S^{K-1}(B)} \sum_{i \in S - S_a^{K-1}} \gamma_i^{\pi} \quad (3.27)$$

Therefore, the algorithm considers all K values such that $1 \leq K \leq M-1$ for optimal solution. In other words, an algorithm needs to find $\min_K \left[\min_{S_a^K \in S^K(B)} \sum_{i \in S - S_a^K} \gamma_i^{\pi} \right]$ to guarantee optimality.

Thus, Algorithm 2 guarantees optimality for the problem in 3.26. Hence, Algorithm 2 guarantees the optimality for Problem 1. \square

Remark 9. *As we consider all combinations of M CH robots (totally 2^M combination), our algorithm GAMEDFS has exponential complexity with respect to the number of CH robots. Therefore, it is not scalable with the number of CH robots.*

For each combination of K CH robots, obtaining the optimal strategies requires $O((M-K)K(M-K+1)^2)$ computations which takes its maximum value when $K = \frac{M+1}{2}$. Therefore, obtaining the optimal strategies requires $O(\frac{M^4}{16})$ computations. Hence, computational complexity of GAMEDFS is $O(2^{M-4} \times M^4)$.

3.4 Numerical Results

In this section, we will evaluate the performance of the strategies for varying battery capacities and varying number of CH robots. We consider three scenarios with varying number of CH robots, namely 5-CH robot scenario, 7-CH robot scenario, and

10-CH robot scenario. In each scenario, the locations of CH robots are randomly generated. For different battery capacities, the performance of different strategies are investigated.

In these scenarios, we observe that the path length for the UAV to visit all CH robots is less than 50 units. This means that the sufficient battery capacity for the UAV to visit all CH robots is less than $50 \times C_{UAV}$ (recall that C_{UAV} is the energy consumption of the UAV per unit distance travel). In these scenarios, we evaluate the performances of two strategies, namely, our optimal strategy (GAMEDFS) and UAV-Oriented strategy in [75]. Please notice that we investigate all decisions taken by both strategies for each battery level varying from $B = 50 \times C_{UAV}$ to $B = 5 \times C_{UAV}$ in each of 5-CH, 7-CH and 10-CH robot scenarios. We also calculate the resultant energy consumption of the UAV and CH robots.

3.4.1 5-CH case

Figure 3.8 shows the locations of the five CH robots and the weights of the links between them. With respect to this initial position of the UAV $(0,0)$, the positions of the CH robots are $(\xi_1, \xi_2, \xi_3, \xi_4, \xi_5) = ((-8, 5), (2, 2), (6, 10), (-2, -3), (-5, -5)) m$. In the configuration in Figure 3.8, the total energy consumption is $296 \times C_{CH}$ if all CH robots send their data directly to the FC at $\xi_0 = (0, 0)$ (the UAV visits no CH robot).

3.4.1.1 UAV-Oriented Strategy

By applying the UAV-Oriented strategy, the UAV travels only to CH robot 2 ($\xi_2 = (2, 2)$) and collects all data of the CH robots from there if the UAV has sufficient battery capacity (to travel there and return back to the FC), which is

$$\begin{aligned}
 B &= 2 \times \|\xi_2 - \xi_0\| \\
 &= 2 \times \sqrt{(2-0)^2 + (2-0)^2} \times C_{UAV} \\
 &\approx 5.66 \times C_{UAV} \\
 &< 10 \times C_{UAV},
 \end{aligned} \tag{3.28}$$

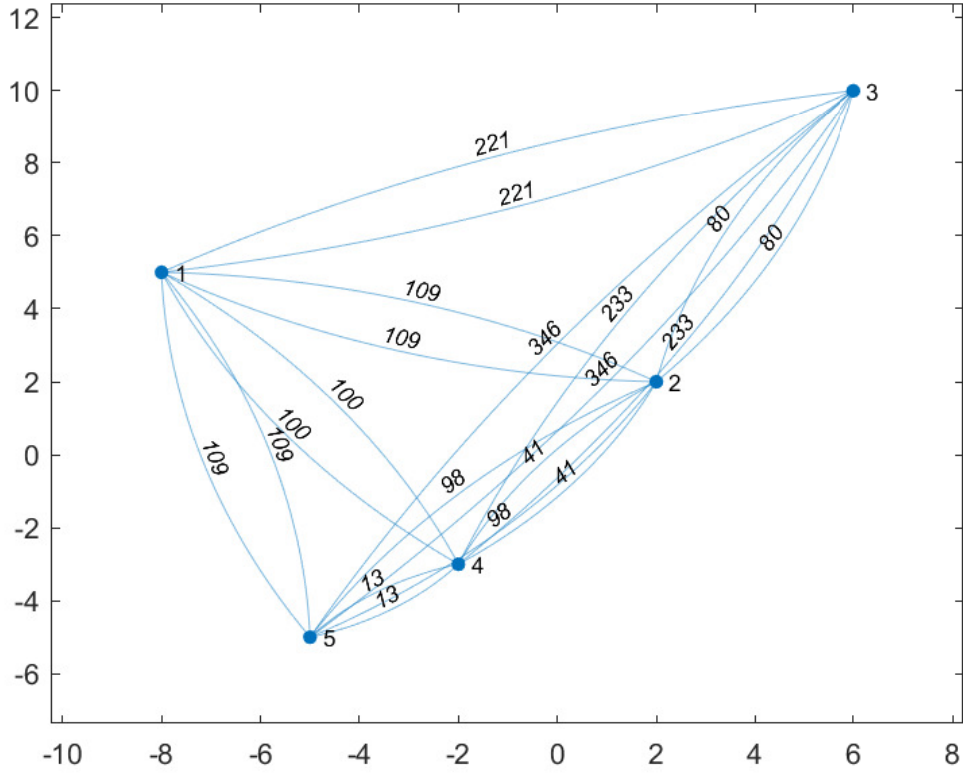


Figure 3.8: Nodes show that the locations (positions) of the five CH robots. The weight of a link shows the square of distance between the two nodes connected via that link.

by which the UAV can apply the UAV-Oriented strategy which results in the total energy consumption of the CH robots as follows

$$\begin{aligned}
 E_{ACH}^{\pi^{UAV-Oriented}}(u) &= \|\xi_1 - \xi_2\|^2 + \|\xi_3 - \xi_2\|^2 + \|\xi_4 - \xi_2\|^2 + \|\xi_5 - \xi_2\|^2 \\
 &= (109 + 80 + 41 + 98) \times C_{CH} \\
 &= 328 \times C_{CH} \\
 &> 296 \times C_{CH},
 \end{aligned} \tag{3.29}$$

which yields an interesting result that the UAV-Oriented strategy causes more energy consumption of CH robots than no strategy (the UAV visits no CH robots) in the configuration in Figure 3.8. If $B = 5$, then the UAV-Oriented strategy is not applicable because the UAV cannot travel to CH robot 2 and none of the other CH robots are closer to the origin than CH robot 2.

3.4.1.2 Optimal Strategy (GAMEDFS)

The performance of optimal strategy (GAMEDFS) is investigated for battery capacities varying from $B = 5$ to $B = 50$ in the configuration in Figure 3.8. In Figure 3.9, by applying optimal strategy, the UAV with $B = 45 \times C_{UAV}$ or $B = 50 \times C_{UAV}$ can make the CH robots consume no energy for forwarding data ($E_{UAV}^{\pi^*}(u) = 0$). Notice that if the problem is considered as a TSP problem for the configuration in Figure 3.8, the energy required for the UAV to visit all CH robots is

$$\begin{aligned} E_{UAV}^{\pi^*}(u) &= \|\xi_0 - \xi_2\| + \|\xi_2 - \xi_3\| + \|\xi_3 - \xi_1\| + \|\xi_1 - \xi_5\| + \|\xi_5 - \xi_4\| + \|\xi_4 - \xi_0\| \\ &= (\sqrt{8} + \sqrt{80} + \sqrt{221} + \sqrt{109} + \sqrt{13} + \sqrt{13}) \times C_{UAV} \\ &\approx 44.29 \times C_{UAV} \end{aligned} \quad (3.30)$$

which yields that the UAV with $B = 44.29$ needs to desist from visiting at least one CH robot. The UAV with $B = 35$ or $B = 40 \times C_{UAV}$ desists from visiting CH robot 3 which results in

$$E_{ACH}^{\pi^{GAMEDFS}}(u) = 80 \times C_{CH} \quad (3.31)$$

total energy consumption of CH robots. Thus, the UAV consumes

$$\begin{aligned} E_{UAV}^{\pi^*}(u) &= \|\xi_0 - \xi_2\| + \|\xi_2 - \xi_1\| + \|\xi_1 - \xi_5\| + \|\xi_5 - \xi_4\| + \|\xi_4 - \xi_0\| \\ &= (\sqrt{8} + \sqrt{109} + \sqrt{109} + \sqrt{13} + \sqrt{13}) \times C_{UAV} \\ &\approx 30.92 \times C_{UAV} \end{aligned} \quad (3.32)$$

The UAV with $B = 30 \times C_{UAV}$ desists from visiting CH robot 3 and CH robot 5, which results in

$$\begin{aligned} E_{ACH}^{\pi^{GAMEDFS}}(u) &= (80 + 13) \times C_{CH} \\ &= 93 \times C_{CH} \end{aligned} \quad (3.33)$$

total energy consumption of CH robots. Thus, the UAV consumes

$$\begin{aligned} E_{UAV}^{\pi^*}(u) &= \|\xi_0 - \xi_2\| + \|\xi_2 - \xi_1\| + \|\xi_1 - \xi_4\| + \|\xi_4 - \xi_0\| \\ &= (\sqrt{8} + \sqrt{109} + \sqrt{100} + \sqrt{13}) \times C_{UAV} \\ &\approx 26.87 \times C_{UAV} \end{aligned} \quad (3.34)$$

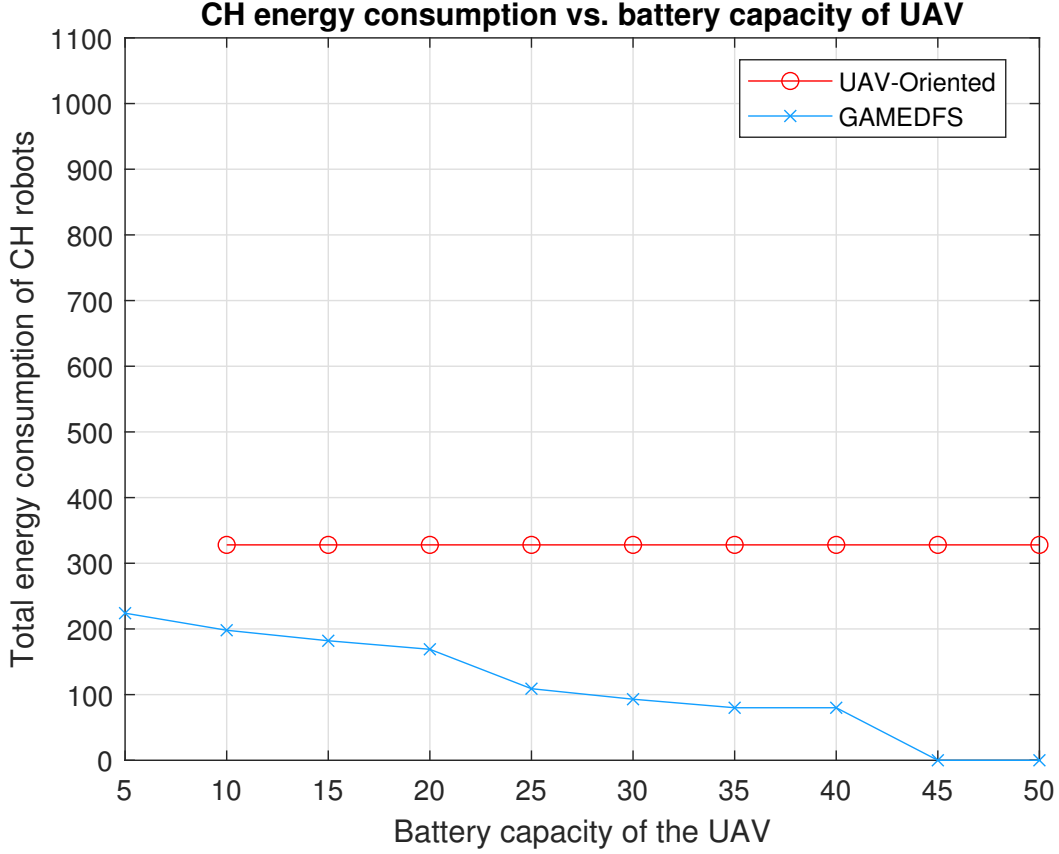


Figure 3.9: The total energy consumption of the five CH robots in Figure 3.8 under the strategies, UAV-Oriented and GAMEDFS for varying battery capacities of the UAV from $B = 5 \times C_{UAV}$ to $B = 50 \times C_{UAV}$.

The UAV with $B = 25 \times C_{UAV}$ desists from visiting CH robot 3, CH robot 2, and CH robot 5 which results in

$$\begin{aligned}
 E_{ACH}^{\pi^{GAMEDFS}}(u) &= ((80 + 8) + 8 + 13) \times C_{CH} \\
 &= 109 \times C_{CH}
 \end{aligned} \tag{3.35}$$

total energy consumption of CH robots (CH 3 robot sends its data to CH robot 2 to forward it to the UAV at FC). Thus, the UAV consumes

$$\begin{aligned}
 E_{UAV}^{\pi^*}(u) &= \|\xi_0 - \xi_1\| + \|\xi_1 - \xi_4\| + \|\xi_4 - \xi_0\| \\
 &= (\sqrt{89} + \sqrt{100} + \sqrt{13}) \times C_{UAV} \\
 &\approx 23.04 \times C_{UAV}
 \end{aligned} \tag{3.36}$$

The UAV with $B = 20 \times C_{UAV}$ desists from visiting CH robot 3 and CH robot 1

which results in

$$\begin{aligned} E_{ACH}^{\pi^{GAMEDFS}}(u) &= (80 + 89) \times C_{CH} \\ &= 169 \times C_{CH} \end{aligned} \quad (3.37)$$

total energy consumption of CH robots. Thus, the UAV consumes

$$\begin{aligned} E_{UAV}^{\pi^*}(u) &= \|\xi_0 - \xi_2\| + \|\xi_2 - \xi_5\| + \|\xi_5 - \xi_4\| + \|\xi_4 - \xi_0\| \\ &= (\sqrt{8} + \sqrt{98} + \sqrt{13} + \sqrt{13}) \times C_{UAV} \\ &\approx 19.94 \times C_{UAV} \end{aligned} \quad (3.38)$$

The UAV with $B = 15 \times C_{UAV}$ desists from visiting CH robot 3, CH robot 5, and CH robot 1 which results in

$$\begin{aligned} E_{ACH}^{\pi^{GAMEDFS}}(u) &= (80 + 13 + 89) \times C_{CH} \\ &= 182 \times C_{CH} \end{aligned} \quad (3.39)$$

total energy consumption of CH robots. Thus, the UAV consumes

$$\begin{aligned} E_{UAV}^{\pi^*}(u) &= \|\xi_0 - \xi_2\| + \|\xi_2 - \xi_4\| + \|\xi_4 - \xi_0\| \\ &= (\sqrt{8} + \sqrt{41} + \sqrt{13}) \times C_{UAV} \\ &\approx 12.84 \times C_{UAV} \end{aligned} \quad (3.40)$$

The UAV with $B = 10 \times C_{UAV}$ desists from visiting CH robot 3, CH robot 2, CH robot 5, and CH robot 1 which results in

$$\begin{aligned} E_{ACH}^{\pi^{GAMEDFS}}(u) &= ((80 + 8) + 8 + 13 + 89) \times C_{CH} \\ &= 198 \times C_{CH} \end{aligned} \quad (3.41)$$

total energy consumption of CH robots. Thus,

$$\begin{aligned} E_{UAV}^{\pi^*}(u) &= \|\xi_0 - \xi_4\| + \|\xi_4 - \xi_0\| \\ &= (\sqrt{13} + \sqrt{13}) \times C_{UAV} \\ &\approx 7.21 \times C_{UAV} \end{aligned} \quad (3.42)$$

The UAV with $B = 5 \times C_{UAV}$ cannot travel to any CH robots which results in

$$\begin{aligned} E_{ACH}^{\pi^{GAMEDFS}}(u) &= ((80 + 8) + 8 + (13 + 13) + 13 + 89) \times C_{CH} \\ &= 224 \times C_{CH} \end{aligned} \quad (3.43)$$

total energy consumption of CH robots (CH 3 robot and CH robot 5 send its data to CH robot 2 and CH robot 4, respectively, in order to forward it to the UAV at the origin). Even without visiting any CH robot, optimal strategy performs better than no strategy and the UAV-Oriented strategy.

3.4.1.3 Performance Comparison

Table 3.2 summarizes indices of the nonvisited CH robots which the strategies decide to desist from visiting in the configuration of Figure 3.8. Similarly, Table 3.3 summarizes total energy consumption of the nonvisited CH robots which the strategies decides to desist from visiting. From these tables, it can be observed how UAV decides to desist from visiting a subset of CH robots depending on its battery capacity in the configuration of Figure 3.8. Furthermore, the total energy consumption of the nonvisited CH robots depends on the desisting decisions taken by UAV and so the battery capacity of the UAV. Besides these, the total energy consumption of the nonvisited CH robots also depends on the network topology, the locations of all CH robots.

Table 3.2: The table shows indices of the nonvisited CH robots depending on battery capacity of UAV in Figure 3.8. "None" implies that UAV visits all CH robots if $B = 45$ or $B = 50$. " \times " implies that the UAV-Oriented Strategy is infeasible for that battery capacity.

Strategy	B = 5	B = 10	B = 15	B = 20	B = 25
UAV-Oriented Strategy	\times	1,3-5	1,3-5	1,3-5	1,3-5
Optimal Strategy (GAMEDFS)	1-5	1-3,5	1,3,5	2-5	2,3,5
Strategy	B = 30	B = 35	B = 40	B = 45	B = 50
UAV-Oriented Strategy	1,3-5	1,3-5	1,3-5	1,3-5	1,3-5
Optimal Strategy (GAMEDFS)	3,5	3	3	None	None

We compare the performances of UAV-Oriented strategy and our two-stage optimal strategy for battery capacities varying from $B = 5$ to $B = 50$ in the configuration in Figure 3.8. From Figure 3.9, the following observations can be made. Applying the UAV-Oriented strategy results in $328 \times C_{CH}$ for battery capacities from $B = 10$ to

Table 3.3: The table shows total energy consumption of nonvisited CH robots depending on battery capacity of UAV in Figure 3.9. "×" implies that the UAV-Oriented strategy is infeasible for that battery capacity.

Strategy	B = 5	B = 10	B = 15	B = 20	B = 25
UAV-Oriented Strategy	×	328	328	328	328
Optimal Strategy (GAMEDFS)	224	198	182	135	109
Strategy	B = 30	B = 35	B = 40	B = 45	B = 50
UAV-Oriented Strategy	328	328	328	328	328
Optimal Strategy (GAMEDFS)	93	80	80	0	0

$B = 50$, it is not applicable for $B = 5$ which is insufficient battery capacity for the UAV to travel any CH robot and turn back to the FC. This strategy performs worse than no strategy by which the UAV standing on the FC collects data from all CH robots (no strategy results in $296 \times C_{CH} < 328 \times C_{CH}$). On the other hand, the two-stage optimal strategy achieves zero total energy consumption of all CH robots for $B = 45$ and $B = 50$. Optimal strategy results in $80 \times C_{CH}$ total energy consumption, only one fourth of that by the UAV-Oriented strategy for $B = 35$ and $B = 40$. Optimal strategy results in $93 \times C_{CH}$ and $109 \times C_{CH}$ total energy consumption, less than one third of that by the UAV-Oriented strategy, for $B = 30$ and $B = 25$, respectively. For $B = 20$, $B = 15$ and $B = 10$, optimal strategy results in $169 \times C_{CH}$, $182 \times C_{CH}$ and $198 \times C_{CH}$ total energy consumption, respectively, still less than 61% of that by the UAV-Oriented strategy. Even for $B = 5$, optimal strategy results in $224 \times C_{CH}$ total energy consumption, still less than 76% of that by no strategy. Remind that UAV-Oriented strategy is not applicable for $B = 5$.

3.4.2 6-CH case

In Figure 3.10 shows the locations of the 6 CH robots and the weights of the links between them. With respect to this initial position of the UAV (0,0), the positions of the CH robots are $(\xi_1, \xi_2, \xi_3, \xi_4, \xi_5, \xi_6) = ((-3, 1), (1, -7), (1, -1), (4, -7), (7, 3), (7, -9))m$. In the configuration in Figure 3.10, total energy consumption is $315 \times C_{CH}$ if all CH robots send their data directly to the FC at $\xi_0 = (0, 0)$.

3.4.2.1 UAV-Oriented Strategy

By applying UAV-Oriented strategy, the UAV travels only to CH robot 3 ($\xi_3 = (-1, -1)$) and collect all data of the CH robots from there if the UAV has sufficient battery capacity (to travel there and return back to the FC), which is

$$\begin{aligned}
B &= 2 \times \|\xi_3 - \xi_0\| \\
&= 2 \times \sqrt{(-1-0)^2 + (-1-0)^2} \times C_{UAV} \\
&\approx 2.83 \times C_{UAV} \\
&< 5 \times C_{UAV},
\end{aligned} \tag{3.44}$$

by which the UAV can apply UAV-Oriented strategy which results in the total energy consumption of the CH robots as follows

$$\begin{aligned}
E_{ACH}^{\pi^{UAV-Oriented}}(u) &= \|\xi_1 - \xi_3\|^2 + \|\xi_2 - \xi_3\|^2 + \|\xi_4 - \xi_3\|^2 + \|\xi_5 - \xi_3\|^2 + \|\xi_6 - \xi_3\|^2 \\
&= (20 + 36 + 45 + 52 + 100) \times C_{CH} \\
&= 253 \times C_{CH}
\end{aligned} \tag{3.45}$$

3.4.2.2 Optimal Strategy (GAMEDFS)

In Figure 3.11, by applying optimal strategy (GAMEDFS), the UAV with $B = 40 \times C_{UAV}$ or $B = 45 \times C_{UAV}$ or $B = 50 \times C_{UAV}$ can make the CH robots consume no energy for forwarding data ($E_{UAV}^{\pi^*}(u) = 0$). Notice that if the problem is considered as a TSP problem for the configuration in Figure 3.10, the energy required for the UAV to visit all CH robots is

$$\begin{aligned}
E_{UAV}^{\pi^*}(u) &= \|\xi_0 - \xi_1\| + \|\xi_1 - \xi_2\| + \|\xi_2 - \xi_4\| + \|\xi_4 - \xi_6\| + \|\xi_6 - \xi_5\| \\
&+ \|\xi_5 - \xi_3\| + \|\xi_3 - \xi_0\| \\
&= (\sqrt{10} + \sqrt{80} + 3 + \sqrt{13} + 12 + \sqrt{52} + \sqrt{2}) \times C_{UAV} \\
&\approx 39.34 \times C_{UAV}
\end{aligned} \tag{3.46}$$

which yields that the UAV with $B < 39.34 \times C_{UAV}$ needs to desist from visiting at least one CH robot. The UAV with $B = 35 \times C_{UAV}$ desists from visiting CH robot 1 which results in

$$E_{ACH}^{\pi^{GAMEDFS}}(u) = 10 \times C_{CH} \tag{3.47}$$

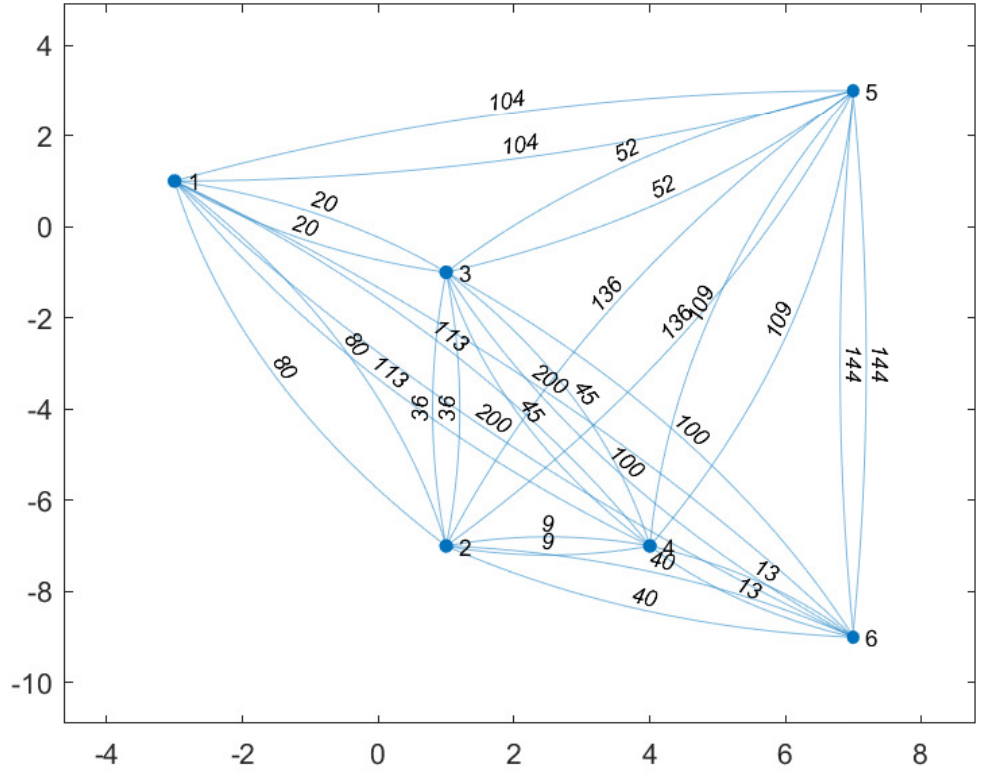


Figure 3.10: Nodes show that the locations of the 6 CH robots. The weight of a link shows the square of distance between the two nodes connected via that link.

total energy consumption of CH robots. Thus, the UAV consumes

$$\begin{aligned}
 E_{UAV}^{\pi^*}(u) &= \|\xi_0 - \xi_3\| + \|\xi_3 - \xi_2\| + \|\xi_2 - \xi_4\| + \|\xi_4 - \xi_6\| + \|\xi_6 - \xi_5\| + \|\xi_5 - \xi_0\| \\
 &= (\sqrt{2} + 6 + 3 + \sqrt{13} + 12 + \sqrt{58}) \times C_{UAV} \\
 &\approx 33.64 \times C_{UAV}
 \end{aligned} \tag{3.48}$$

The UAV with $B = 30 \times C_{UAV}$ desists from visiting CH robot 1 and CH robot 5 which results in

$$\begin{aligned}
 E_{ACH}^{\pi^{GAMEDFS}}(u) &= (10 + 13) \times C_{CH} \\
 &= 23 \times C_{CH}
 \end{aligned} \tag{3.49}$$

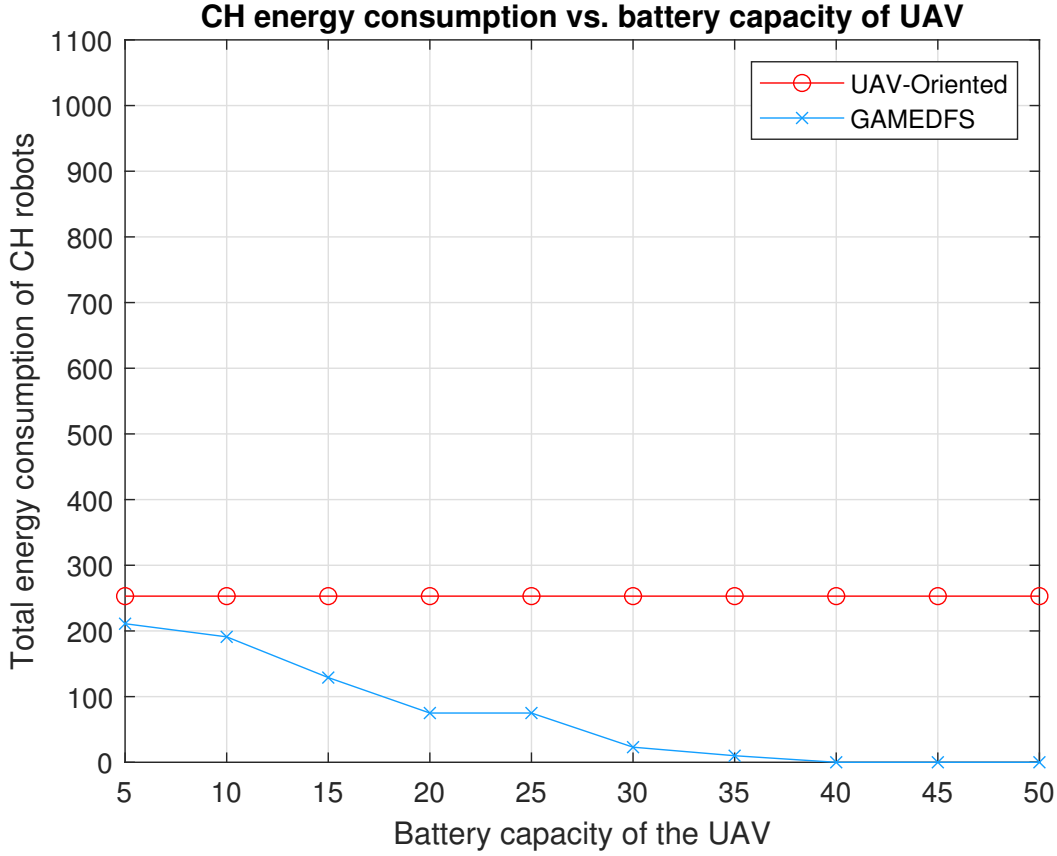


Figure 3.11: The total energy consumption of the 6 CH robots in Figure 3.10 under the strategies, UAV-Oriented and GAMEDFS for varying battery capacities of the UAV from $B = 5 \times C_{UAV}$ to $B = 50 \times C_{UAV}$. The units for energy consumption of the UAV and total energy consumption of the nonvisited CH robots are C_{UAV} and C_{CH} , respectively. These constants depend on the type of the UAV and the CH robots.

total energy consumption of CH robots. Thus, the UAV consumes

$$\begin{aligned}
 E_{UAV}^{\pi^*}(u) &= \|\xi_0 - \xi_3\| + \|\xi_3 - \xi_2\| + \|\xi_2 - \xi_4\| + \|\xi_4 - \xi_5\| + \|\xi_5 - \xi_0\| \\
 &= (\sqrt{2} + 6 + 3 + \sqrt{109} + \sqrt{58}) \times C_{UAV} \\
 &\approx 28.47 \times C_{UAV}
 \end{aligned} \tag{3.50}$$

The UAV with $B = 25 \times C_{UAV}$ or $B = 20 \times C_{UAV}$ desists from visiting CH robot 1, CH robot 5 and CH robot 6 which results in

$$\begin{aligned}
 E_{ACH}^{\pi^{GAMEDFS}}(u) &= (10 + 52 + 13) \times C_{CH} \\
 &= 75 \times C_{CH}
 \end{aligned} \tag{3.51}$$

total energy consumption of CH robots. Thus, the UAV consumes

$$\begin{aligned}
E_{UAV}^{\pi^*}(u) &= \|\xi_0 - \xi_3\| + \|\xi_3 - \xi_4\| + \|\xi_4 - \xi_2\| + \|\xi_2 - \xi_0\| \\
&= (\sqrt{2} + \sqrt{45} + 3 + \sqrt{50}) \times C_{UAV} \\
&\approx 18.19 \times C_{UAV}
\end{aligned} \tag{3.52}$$

The UAV with $B = 15 \times C_{UAV}$ visits CH robot 3 and CH robot 2 which results in

$$\begin{aligned}
E_{ACH}^{\pi^{GAMEDFS}}(u) &= (10 + 9 + 52 + (13 + 45)) \times C_{CH} \\
&= 129 \times C_{CH}
\end{aligned} \tag{3.53}$$

total energy consumption of CH robots. Thus, the UAV consumes

$$\begin{aligned}
E_{UAV}^{\pi^*}(u) &= \|\xi_0 - \xi_3\| + \|\xi_3 - \xi_2\| + \|\xi_2 - \xi_0\| \\
&= (\sqrt{2} + 6 + \sqrt{50}) \times C_{UAV} \\
&\approx 14.49 \times C_{UAV}
\end{aligned} \tag{3.54}$$

The UAV with $B = 10 \times C_{UAV}$ visits CH robot 1 and CH robot 3 which results in

$$\begin{aligned}
E_{ACH}^{\pi^{GAMEDFS}}(u) &= (36 + 45 + 52 + (13 + 45)) \times C_{CH} \\
&= 191 \times C_{CH}
\end{aligned} \tag{3.55}$$

total energy consumption of CH robots. Thus, the UAV consumes

$$\begin{aligned}
E_{UAV}^{\pi^*}(u) &= \|\xi_0 - \xi_3\| + \|\xi_3 - \xi_1\| + \|\xi_1 - \xi_0\| \\
&= (\sqrt{2} + \sqrt{20} + \sqrt{10}) \times C_{UAV} \\
&\approx 9.05 \times C_{UAV}
\end{aligned} \tag{3.56}$$

The UAV with $B = 5 \times C_{UAV}$ cannot travel to any CH robots which results in

$$\begin{aligned}
E_{ACH}^{\pi^{GAMEDFS}}(u) &= (10 + (36 + 2) + 2 + (45 + 2) + (52 + 2) \\
&\quad + (13 + 45 + 2)) \times C_{CH} \\
&= 211 \times C_{CH}
\end{aligned} \tag{3.57}$$

total energy consumption of CH robots (CH 2 robot, CH 4 robot and CH robot 5 send its data to CH robot 3 to forward it to the UAV at FC. Similarly, CH 6 robot forwards its data to CH robot 4). *Even without visiting any CH robot, optimal strategy performs better than no strategy and the UAV-Oriented strategy.*

3.4.2.3 Performance Comparison

Table 3.4 summarizes indices of the nonvisited CH robots which the strategies decide to desist from visiting in the configuration of Figure 3.10. Similarly, Table 3.5 summarizes total energy consumption of the nonvisited CH robots which the strategies decide to desist from visiting. From these tables, it can be observed how UAV decides to desist from visiting a subset of CH robots depending on its battery capacity in the configuration of Figure 3.10. Furthermore, the total energy consumption of the nonvisited CH robots depends on the desisting decisions taken by UAV and so the battery capacity of the UAV. Besides these, the total energy consumption of the nonvisited CH robots also depends on the network topology, the locations of all CH robots.

Table 3.4: The table shows indices of the nonvisited CH robots depending on battery capacity of UAV in Figure 3.10. "None" implies that the UAV visits all CH robots if $B = 35, 40, 45, 50$. " \times " implies that the UAV-Oriented strategy is infeasible for that battery capacity.

Strategy	B = 5	B = 10	B = 15	B = 20	B = 25
UAV-Oriented Strategy	1,2,4-6	1,2,4-6	1,2,4-6	1,2,4-6	1,2,4-6
Optimal Strategy (GAMEDFS)	1,2,4-6	2,4-6	1,4-6	1,5,6	1,5,6
Strategy	B = 30	B = 35	B = 40	B = 45	B = 50
UAV-Oriented Strategy	1,2,4-6	1,2,4-6	1,2,4-6	1,2,4-6	1,2,4-6
Optimal Strategy (GAMEDFS)	1,5	1	None	None	None

We compare the performances of the UAV-Oriented strategy and our two-stage optimal strategy for battery capacities varying from $B = 5$ to $B = 50$ in the configuration in Figure 3.10. From Figure 3.11, the following observations can be made. Applying the UAV-Oriented strategy results in $253 \times C_{CH}$ for all battery capacities $B = 5, 10, 15, 20, 25, 30, 35, 40, 45, 50$. On the other hand, the two-stage optimal strategy achieves zero total energy consumption of all CH robots for $B = 40, B = 45$ and $B = 50$. Optimal strategy results in $10 \times C_{CH}$ total energy consumption, less than 4% of that by the UAV-Oriented strategy for $B = 35$. Optimal strategy results in $23 \times C_{CH}$ total energy consumption, only one eleventh of that by the UAV-Oriented

Table 3.5: The table shows total energy consumption of nonvisited CH robots depending on battery capacity of UAV in Figure 3.11. "×" implies that the UAV-Oriented strategy is infeasible for that battery capacity.

Strategy	B = 5	B = 10	B = 15	B = 20	B = 25
UAV-Oriented Strategy	253	253	253	253	253
Optimal Strategy (GAMEDFS)	211	191	129	75	75
Strategy	B = 30	B = 35	B = 40	B = 45	B = 50
UAV-Oriented Strategy	253	253	253	253	253
Optimal Strategy (GAMEDFS)	23	10	0	0	0

strategy for $B = 30$. For $B = 20, 25$, optimal strategy results in $75 \times C_{CH}$, less than 30% of that by the UAV-Oriented strategy. For $B = 15$, optimal strategy results in $129 \times C_{CH}$ total energy consumption, nearly half of that by the UAV-Oriented strategy. For $B = 10$, optimal strategy results in $191 \times C_{CH}$ total energy consumption, less than 80% of that by the UAV-Oriented strategy. Even for $B = 5$, optimal strategy results in $211 \times C_{CH}$ total energy consumption, still nearly five sixth of that by no strategy.

3.4.3 7-CH Case

Figure 3.12 shows the locations of the seven CH robots and the weights of the links between them. With respect to this initial position of the UAV (0,0), the positions of the CH robots are $(\xi_1, \xi_2, \xi_3, \xi_4, \xi_5, \xi_6, \xi_7) = ((9, 6), (3, 9), (3, 2), (7, 8), (8, -1), (7, 5), (2, 2))m$. In the configuration in Figure 3.12, the total energy consumption is $480 \times C_{CH}$ if all CH robots send their data directly to the FC at $\xi_0 = (0, 0)$ (the UAV visit no CH robot).

3.4.3.1 UAV-Oriented Strategy

By applying the UAV-Oriented strategy, the UAV travels only to CH robot 6 ($\xi_6 = (7, 5)$) and collect all data of the CH robots from there if the UAV has sufficient battery

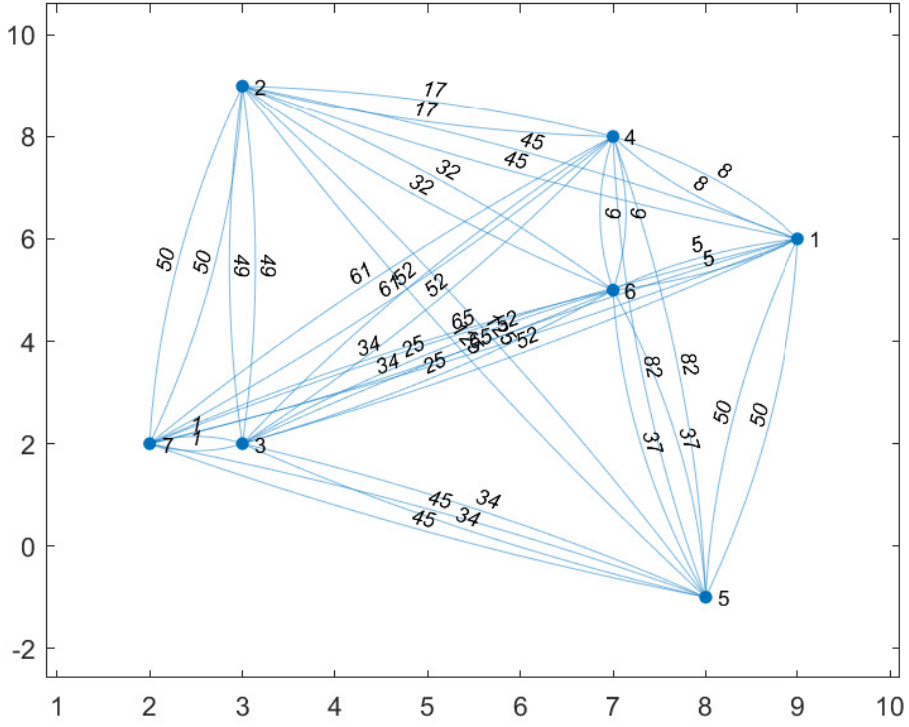


Figure 3.12: Nodes show that the locations of the seven CH robots. The weight of a link shows the square of distance between the two nodes connected via that link.

capacity (to travel there and return back to the FC), which is

$$\begin{aligned}
 B &= 2 \times \|\xi_6 - \xi_0\| \\
 &= 2 \times \sqrt{(7-0)^2 + (5-0)^2} \\
 &\approx 17.2 \times C_{UAV} \\
 &< 20 \times C_{UAV},
 \end{aligned} \tag{3.58}$$

by which the UAV can apply the UAV-Oriented strategy which results in the total energy consumption of the CH robots as follows

$$\begin{aligned}
 E_{ACH}^{\pi_{UAV-Oriented}}(u) &= \|\xi_1 - \xi_6\|^2 + \|\xi_2 - \xi_6\|^2 + \|\xi_3 - \xi_6\|^2 + \|\xi_4 - \xi_6\|^2 \\
 &+ \|\xi_5 - \xi_6\|^2 + \|\xi_7 - \xi_6\|^2 \\
 &= (5 + 32 + 25 + 9 + 37 + 34) \times C_{CH} \\
 &= 142 \times C_{CH}
 \end{aligned} \tag{3.59}$$

If $B = 10$ or $B = 15$, the UAV can travel to CH robot 3 which is closer to the origin than CH robot 6. Similar to Equation (3.59), $E_{ACH}^{\pi^{UAV-Oriented}}(u) = 213 \times C_{CH}$. However, if $B = 5$, then the UAV-oriented strategy is not applicable because the UAV cannot travel to any CH robot.

3.4.3.2 Optimal Strategy (GAMEDFS)

The performance of optimal strategy (GAMEDFS) is investigated for battery capacities varying from $B = 5$ to $B = 50$ in the configuration in Figure 3.12. In Figure 3.13, by applying optimal strategy, the UAV with $B = 35 \times C_{UAV}$ or $B = 40 \times C_{UAV}$ or $B = 45 \times C_{UAV}$ or $B = 50 \times C_{UAV}$ can make the CH robots consume no energy for forwarding data ($E_{UAV}^{\pi^*}(u) = 0$). Notice that if the problem is considered as a TSP problem for the configuration in Figure 3.12, the energy required for the UAV to visit all CH robots is

$$\begin{aligned}
E_{UAV}^{\pi^*}(u) &= \|\xi_0 - \xi_2\| + \|\xi_2 - \xi_4\| + \|\xi_4 - \xi_1\| + \|\xi_1 - \xi_6\| + \|\xi_6 - \xi_5\| \\
&+ \|\xi_5 - \xi_3\| + \|\xi_3 - \xi_7\| + \|\xi_7 - \xi_0\| \\
&= (\sqrt{90} + \sqrt{17} + \sqrt{8} + \sqrt{5} + \sqrt{37} + \sqrt{34} + 1 + \sqrt{8}) \times C_{UAV} \\
&\approx 34.42 \times C_{UAV}
\end{aligned} \tag{3.60}$$

which yields that the UAV with $B < 34.42 \times C_{UAV}$ needs to desist from visiting at least one CH robot. The UAV with $B = 30 \times C_{UAV}$ desists from visiting CH robot 5 which results in

$$E_{ACH}^{\pi^{GAMEDFS}}(u) = 34 \times C_{CH} \tag{3.61}$$

total energy consumption of CH robots. Thus, the UAV consumes

$$\begin{aligned}
E_{UAV}^{\pi^*}(u) &= \|\xi_0 - \xi_2\| + \|\xi_2 - \xi_4\| + \|\xi_4 - \xi_1\| + \|\xi_1 - \xi_6\| + \|\xi_6 - \xi_3\| \\
&+ \|\xi_3 - \xi_7\| + \|\xi_7 - \xi_0\| \\
&= (\sqrt{90} + \sqrt{17} + \sqrt{8} + \sqrt{5} + 5 + 1 + \sqrt{8}) \times C_{UAV} \\
&\approx 27.50 \times C_{UAV}
\end{aligned} \tag{3.62}$$

The UAV with $B = 25 \times C_{UAV}$ desists from visiting CH robot 2 and CH robot 5

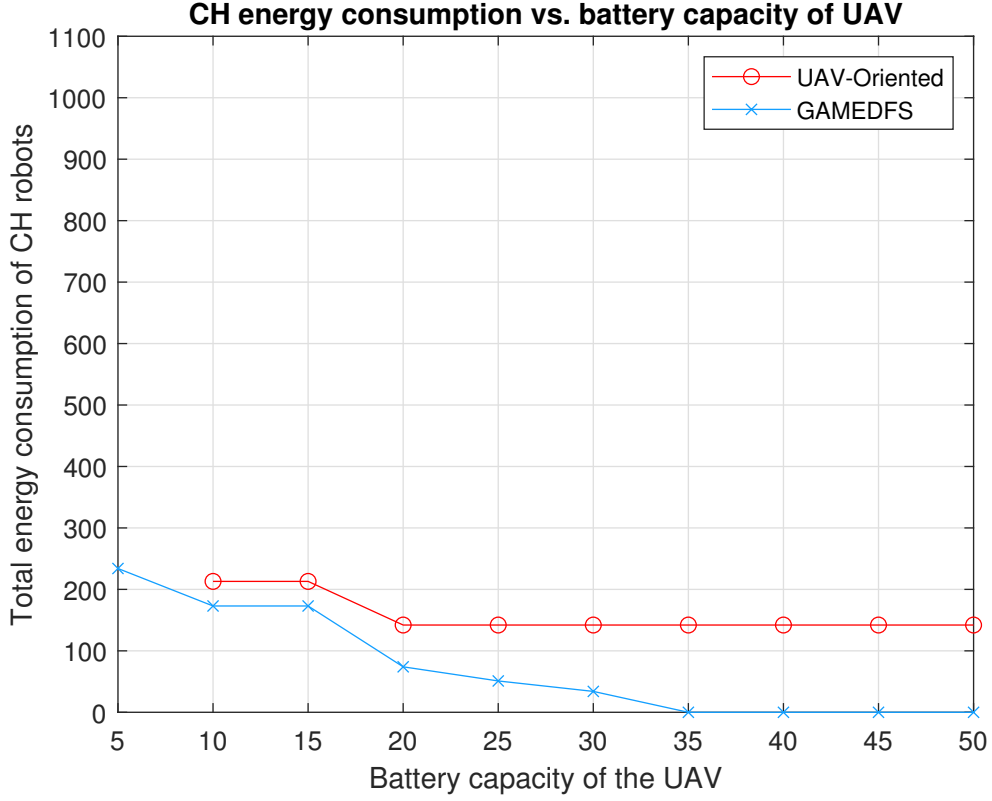


Figure 3.13: The total energy consumption of the seven CH robots in Figure 3.12 under the strategies, UAV-Oriented and GAMEDFS for varying battery capacities of the UAV from $B = 5 \times C_{UAV}$ to $B = 50 \times C_{UAV}$. The units for energy consumption of the UAV and total energy consumption of the nonvisited CH robots are C_{UAV} and C_{CH} , respectively. These constants depend on the type of the UAV and the CH robots.

which results in

$$\begin{aligned}
 E_{ACH}^{\pi^{GAMEDFS}}(u) &= (17 + 34) \times C_{CH} \\
 &= 51 \times C_{CH}
 \end{aligned} \tag{3.63}$$

total energy consumption of CH robots. Thus, the UAV consumes

$$\begin{aligned}
 E_{UAV}^*(u) &= \|\xi_0 - \xi_4\| + \|\xi_4 - \xi_1\| + \|\xi_1 - \xi_6\| + \|\xi_6 - \xi_3\| + \|\xi_3 - \xi_7\| \\
 &\quad + \|\xi_7 - \xi_0\| \\
 &= (\sqrt{113} + \sqrt{8} + \sqrt{5} + 5 + 1 + \sqrt{8}) \times C_{UAV} \\
 &\approx 24.52 \times C_{UAV}
 \end{aligned} \tag{3.64}$$

The UAV with $B = 20 \times C_{UAV}$ desists from visiting CH robot 1, CH robot 2, CH robot 4, and CH robot 5 which results in

$$\begin{aligned} E_{ACH}^{\pi^{GAMEDFS}}(u) &= (5 + (17 + 9) + 9 + 34) \times C_{CH} \\ &= 74 \times C_{CH} \end{aligned} \quad (3.65)$$

total energy consumption of CH robots. Thus, the UAV consumes

$$\begin{aligned} E_{UAV}^{\pi^*}(u) &= \|\xi_0 - \xi_6\| + \|\xi_6 - \xi_3\| + \|\xi_3 - \xi_7\| + \|\xi_7 - \xi_0\| \\ &= (\sqrt{74} + 5 + 1 + \sqrt{8}) \times C_{UAV} \\ &\approx 17.43 \times C_{UAV} \end{aligned} \quad (3.66)$$

The UAV with $B = 10 \times C_{UAV}$ or $B = 15 \times C_{UAV}$ desists from visiting CH robot 1, CH robot 2, CH robot 4, CH robot 5, and CH robot 6 which results in

$$\begin{aligned} E_{ACH}^{\pi^{GAMEDFS}}(u) &= ((5 + 25) + 50 + (9 + 25) + 34 + 25) \times C_{CH} \\ &= 173 \times C_{CH} \end{aligned} \quad (3.67)$$

total energy consumption of CH robots. Thus, the UAV consumes

$$\begin{aligned} E_{UAV}^{\pi^*}(u) &= \|\xi_0 - \xi_3\| + \|\xi_3 - \xi_7\| + \|\xi_7 - \xi_0\| \\ &= (\sqrt{13} + 1 + \sqrt{8}) \times C_{UAV} \\ &\approx 7.43 \times C_{UAV} \end{aligned} \quad (3.68)$$

The UAV with $B = 5 \times C_{UAV}$ cannot travel to any CH robots which results in

$$\begin{aligned} E_{ACH}^{\pi^{GAMEDFS}}(u) &= ((5 + 25 + 1 + 8) + (50 + 8) + (1 + 8) + (9 + 25 + 1 + 8) \\ &\quad + (34 + 1 + 8) + (25 + 1 + 8) + 8) \times C_{CH} \\ &= 234 \times C_{CH} \end{aligned} \quad (3.69)$$

total energy consumption of CH robots (All CH robots send their data directly or indirectly to CH robot 7 to forward it to the UAV at FC). Even visiting no CH robot, optimal strategy performs better than no strategy.

3.4.3.3 Performance Comparison

Table 3.6 summarizes indices of the nonvisited CH robots which the strategies decide to desist from visiting in the configuration of Figure 3.12. Similarly, Table 3.7 sum-

marizes total energy consumption of the nonvisited CH robots which the strategies decide to desist from visiting. From these tables, it can be observed how UAV decides to desist from visiting a subset of CH robots depending on its battery capacity in the configuration of Figure 3.12. Furthermore, the total energy consumption of the nonvisited CH robots depends on the desisting decisions taken by UAV and so the battery capacity of the UAV. Besides these, the total energy consumption of the nonvisited CH robots also depends on the network topology, the locations of all CH robots.

Table 3.6: The table shows indices of the nonvisited CH robots depending on battery capacity of UAV in Figure 3.12. "None" implies that the UAV visits all CH robots if $B = 35, 40, 45, 50$. "×" implies that the UAV-oriented strategy is infeasible for that battery capacity.

Strategy	B = 5	B = 10	B = 15	B = 20	B = 25
UAV-Oriented Strategy	×	1,2,4-7	1,2,4-7	1-5,7	1-5,7
Optimal Strategy (GAMEDFS)	1-7	1,2,4-6	1,2,4-6	1,2,4,5	2,5
Strategy	B = 30	B = 35	B = 40	B = 45	B = 50
UAV-Oriented Strategy	1-5,7	1-5,7	1-5,7	1-5,7	1-5,7
Optimal Strategy (GAMEDFS)	5	None	None	None	None

Table 3.7: The table shows total energy consumption of nonvisited CH robots depending on battery capacity of UAV in Figure 3.13. "×" implies that the UAV-oriented strategy is infeasible for that battery capacity.

Strategy	B = 5	B = 10	B = 15	B = 20	B = 25
UAV-Oriented Strategy	×	213	213	142	142
Optimal Strategy (GAMEDFS)	234	173	173	74	51
Strategy	B = 30	B = 35	B = 40	B = 45	B = 50
UAV-Oriented Strategy	142	142	142	142	142
Optimal Strategy (GAMEDFS)	34	0	0	0	0

We compare the performances of the UAV-oriented strategy and our two-stage optimal strategy for battery capacities varying from $B = 5$ to $B = 50$ in the configuration

in Figure 3.12. From Figure 3.13, the following observations can be made. Applying the UAV-oriented strategy results in $142 \times C_{CH}$ and $213 \times C_{CH}$ for battery capacities $B = 20, 25, 30, 35, 40, 45, 50$ and $B = 10, 15$, respectively. It is not applicable for $B = 5$ which is insufficient battery capacity for the UAV to travel any CH robot and turn back to the FC. On the other hand, the two-stage optimal strategy achieves zero energy consumption of all CH robots for $B = 35, B = 40, B = 45$ and $B = 50$. Optimal strategy results in $34 \times C_{CH}$ total energy consumption, only one fourth of that by the UAV-oriented strategy for $B = 30$. Optimal strategy results in $51 \times C_{CH}$, less than 36% of that by the UAV-oriented strategy for $B = 25$. For $B = 20$, optimal strategy results in $51 \times C_{CH}$, nearly half of that by the UAV-oriented strategy. For $B = 10$ and $B = 15$, optimal strategy results in $173 \times C_{CH}$ total energy consumption, nearly 81% of that by the UAV-oriented strategy. Even for $B = 5$, optimal strategy results in $234 \times C_{CH}$ total energy consumption, still less than half of that by no strategy. Remember that the UAV-oriented strategy is not applicable for $B = 5$.

3.4.4 8-CH case

In Figure 3.14 shows the locations of the 8 CH robots and the weights of the links between them. With respect to this initial position of the UAV $(0,0)$, the positions of the CH robots are $(\xi_1, \xi_2, \xi_3, \xi_4, \xi_5, \xi_6, \xi_7, \xi_8) = ((-4, 1), (8, -6), (6, 8), (9, -9), (6, -7), (5, 5), (1, -6), (6, -2))m$. In the configuration in Figure 3.14, the total energy consumption is $591 \times C_{CH}$ if all CH robots send their data directly to the FC at $\xi_0 = (0, 0)$.

3.4.4.1 UAV-Oriented Strategy

By applying UAV-Oriented strategy, the UAV travels only to CH robot 8 ($\xi_8 = (-2, 6)$) and collect all data of the CH robots from there if the UAV has sufficient battery capacity (to travel there and return back to the FC), which is

$$\begin{aligned}
B &= 2 \times \|\xi_8 - \xi_0\| \\
&= 2 \times \sqrt{(-2 - 0)^2 + (6 - 0)^2} \times C_{UAV} \\
&\approx 12.65 \times C_{UAV} \\
&< 15 \times C_{UAV},
\end{aligned} \tag{3.70}$$

by which the UAV can apply UAV-Oriented strategy which results in the total energy consumption of the CH robots as follows

$$\begin{aligned}
E_{ACH}^{\pi^{UAV-Oriented}}(u) &= \|\xi_1 - \xi_8\|^2 + \|\xi_2 - \xi_8\|^2 + \|\xi_3 - \xi_8\|^2 + \|\xi_4 - \xi_8\|^2 \\
&+ \|\xi_5 - \xi_8\|^2 + \|\xi_6 - \xi_8\|^2 + \|\xi_7 - \xi_8\|^2 \\
&= (109 + 20 + 100 + 58 + 25 + 50 + 41) \times C_{CH} \\
&= 403 \times C_{CH}
\end{aligned} \tag{3.71}$$

If $B = 10$, the UAV can travel to CH robot 1 which is closer to the origin than CH robot 8. Similar to Equation (3.71), $E_{ACH}^{\pi^{UAV-Oriented}}(u) = 1055 \times C_{CH} > 591 \times C_{CH}$ which yields that for $B = 10$, the UAV-oriented strategy causes more energy consumption of CH robots than no strategy (the UAV visits no CH robots) in the configuration in Figure 3.14. On the other hand, if $B = 5$, then the UAV-oriented strategy is not applicable because the UAV cannot travel to any CH robot.

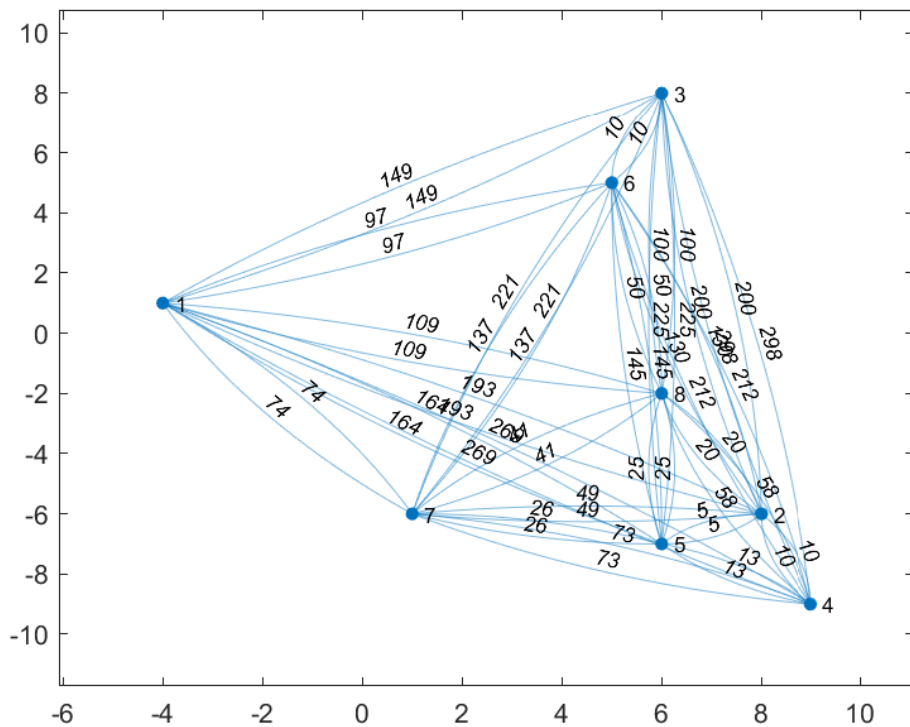


Figure 3.14: Nodes show that the locations of the 8 CH robots. The weight of a link shows the square of distance between the two nodes connected via that link.

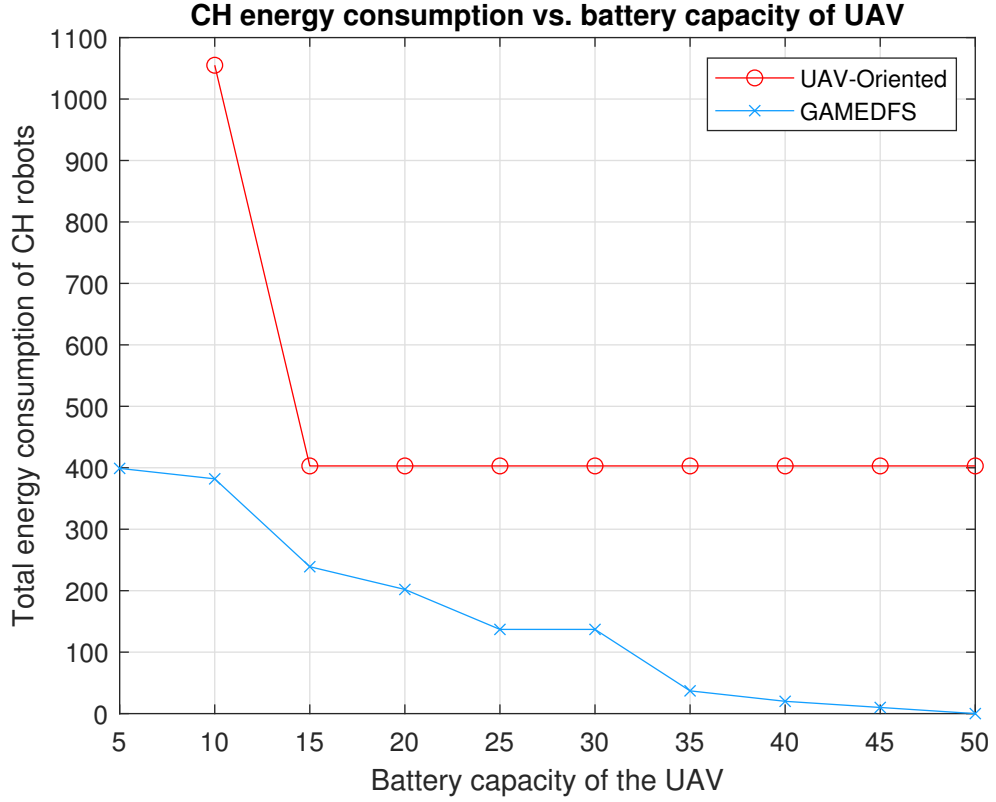


Figure 3.15: The total energy consumption of the 8 CH robots in Figure 3.14 under the strategies, UAV-Oriented and GAMEDFS for varying battery capacities of the UAV from $B = 5 \times C_{UAV}$ to $B = 50 \times C_{UAV}$. The units for energy consumption of the UAV and total energy consumption of the nonvisited CH robots are C_{UAV} and C_{CH} , respectively. These constants depend on the type of the UAV and the CH robots.

3.4.4.2 Optimal Strategy (GAMEDFS)

In Figure 3.15, by applying optimal strategy (GAMEDFS), the UAV with $B = 50 \times C_{UAV}$ can make the CH robots consume no energy for forwarding data ($E_{UAV}^{\pi^*}(u) = 0$). Notice that if the problem is considered as a TSP problem for the configuration in Figure 3.14, the energy required for the UAV to visit all CH robots is

$$\begin{aligned}
E_{UAV}^{\pi^*}(u) &= \|\xi_0 - \xi_1\| + \|\xi_1 - \xi_3\| + \|\xi_3 - \xi_6\| + \|\xi_6 - \xi_8\| + \|\xi_8 - \xi_2\| \\
&\quad + \|\xi_2 - \xi_4\| + \|\xi_4 - \xi_5\| + \|\xi_5 - \xi_7\| + \|\xi_7 - \xi_0\| \\
&= (\sqrt{17} + \sqrt{149} + \sqrt{10} + \sqrt{50} + \sqrt{20} + \sqrt{10} + \sqrt{13} + \sqrt{26} + \sqrt{37}) \times C_{UAV} \\
&\approx 48.98 \times C_{UAV}
\end{aligned} \tag{3.72}$$

which yields that the UAV with $B < 48.98 \times C_{UAV}$ needs to desist from visiting at least one CH robot. The UAV with $B = 45 \times C_{UAV}$ desists from visiting CH robot 4 which results in

$$E_{ACH}^{\pi^{GAMEDFS}}(u) = 10 \times C_{CH} \quad (3.73)$$

total energy consumption of CH robots. Thus, the UAV consumes

$$\begin{aligned} E_{UAV}^{\pi^*}(u) &= \|\xi_0 - \xi_1\| + \|\xi_1 - \xi_3\| + \|\xi_3 - \xi_6\| + \|\xi_6 - \xi_8\| + \|\xi_8 - \xi_2\| \\ &+ \|\xi_2 - \xi_5\| + \|\xi_5 - \xi_7\| + \|\xi_7 - \xi_0\| \\ &= (\sqrt{17} + \sqrt{149} + \sqrt{10} + \sqrt{50} + \sqrt{20} + \sqrt{5} + \sqrt{26} + \sqrt{37}) \times C_{UAV} \\ &\approx 44.45 \times C_{UAV} \end{aligned} \quad (3.74)$$

The UAV with $B = 40 \times C_{UAV}$ desists from visiting CH robot 3 and CH robot 4 which results in

$$\begin{aligned} E_{ACH}^{\pi^{GAMEDFS}}(u) &= (10 + 10) \times C_{CH} \\ &= 20 \times C_{CH} \end{aligned} \quad (3.75)$$

total energy consumption of CH robots. Thus, the UAV consumes

$$\begin{aligned} E_{UAV}^{\pi^*}(u) &= \|\xi_0 - \xi_1\| + \|\xi_1 - \xi_6\| + \|\xi_6 - \xi_8\| + \|\xi_8 - \xi_2\| + \|\xi_2 - \xi_5\| \\ &+ \|\xi_5 - \xi_7\| + \|\xi_7 - \xi_0\| \\ &= (\sqrt{17} + \sqrt{97} + \sqrt{50} + \sqrt{20} + \sqrt{5} + \sqrt{26} + \sqrt{37}) \times C_{UAV} \\ &\approx 38.93 \times C_{UAV} \end{aligned} \quad (3.76)$$

The UAV with $B = 35 \times C_{UAV}$ desists from visiting CH robot 1, CH robot 3 and CH robot 4 which results in

$$\begin{aligned} E_{ACH}^{\pi^{GAMEDFS}}(u) &= (17 + 10 + 10) \times C_{CH} \\ &= 37 \times C_{CH} \end{aligned} \quad (3.77)$$

total energy consumption of CH robots. Thus, the UAV consumes

$$\begin{aligned} E_{UAV}^{\pi^*}(u) &= \|\xi_0 - \xi_6\| + \|\xi_6 - \xi_8\| + \|\xi_8 - \xi_2\| + \|\xi_2 - \xi_5\| + \|\xi_5 - \xi_7\| + \|\xi_7 - \xi_0\| \\ &= (\sqrt{50} + \sqrt{50} + \sqrt{20} + \sqrt{5} + \sqrt{26} + \sqrt{37}) \times C_{UAV} \\ &\approx 32.03 \times C_{UAV} \end{aligned} \quad (3.78)$$

The UAV with $B = 25 \times C_{UAV}$ or $B = 30 \times C_{UAV}$ desists from visiting CH robot 1, CH robot 3, CH robot 4 and CH robot 6 which results in

$$\begin{aligned} E_{ACH}^{\pi^{GAMEDFS}}(u) &= (17 + (10 + 50) + 10 + 50) \times C_{CH} \\ &= 137 \times C_{CH} \end{aligned} \quad (3.79)$$

total energy consumption of CH robots. Thus, the UAV consumes

$$\begin{aligned} E_{UAV}^{\pi^*}(u) &= \|\xi_0 - \xi_8\| + \|\xi_8 - \xi_2\| + \|\xi_2 - \xi_5\| + \|\xi_5 - \xi_7\| + \|\xi_7 - \xi_0\| \\ &= (\sqrt{40} + \sqrt{20} + \sqrt{5} + \sqrt{26} + \sqrt{37}) \times C_{UAV} \\ &\approx 24.21 \times C_{UAV} \end{aligned} \quad (3.80)$$

The UAV with $B = 20 \times C_{UAV}$ visits only CH robot 7 and CH robot 8 which results in

$$\begin{aligned} E_{ACH}^{\pi^{GAMEDFS}}(u) &= (17 + 20 + (10 + 50) + (10 + 20) + 25 + 50) \times C_{CH} \\ &= 202 \times C_{CH} \end{aligned} \quad (3.81)$$

total energy consumption of CH robots. Thus, the UAV consumes

$$\begin{aligned} E_{UAV}^{\pi^*}(u) &= \|\xi_0 - \xi_8\| + \|\xi_8 - \xi_7\| + \|\xi_7 - \xi_0\| \\ &= (\sqrt{40} + \sqrt{41} + \sqrt{37}) \times C_{UAV} \\ &\approx 18.81 \times C_{UAV} \end{aligned} \quad (3.82)$$

The UAV with $B = 15 \times C_{UAV}$ visits only CH robot 8 which results in

$$\begin{aligned} E_{ACH}^{\pi^{GAMEDFS}}(u) &= (17 + 20 + (10 + 50) + (10 + 20) + 25 + 50 + 37) \times C_{CH} \\ &= 239 \times C_{CH} \end{aligned} \quad (3.83)$$

total energy consumption of CH robots. Thus, the UAV consumes

$$\begin{aligned} E_{UAV}^{\pi^*}(u) &= \|\xi_0 - \xi_8\| + \|\xi_8 - \xi_0\| \\ &= (\sqrt{40} + \sqrt{40}) \times C_{UAV} \\ &\approx 12.65 \times C_{UAV} \end{aligned} \quad (3.84)$$

The UAV with $B = 10 \times C_{UAV}$ visits only CH robot 1 which results in

$$\begin{aligned} E_{ACH}^{\pi^{GAMEDFS}}(u) &= ((20 + 40) + (10 + 50) + (10 + 20 + 40) + (25 + 40) + 50 \\ &\quad + 37 + 40) \times C_{CH} \\ &= 382 \times C_{CH} \end{aligned} \quad (3.85)$$

total energy consumption of CH robots. Thus, the UAV consumes

$$\begin{aligned}
E_{UAV}^{\pi^*}(u) &= \|\xi_0 - \xi_1\| + \|\xi_1 - \xi_0\| \\
&= (\sqrt{17} + \sqrt{17}) \times C_{UAV} \\
&\approx 8.25 \times C_{UAV}
\end{aligned} \tag{3.86}$$

The UAV with $B = 5 \times C_{UAV}$ cannot travel to any CH robots which results in

$$\begin{aligned}
E_{ACH}^{\pi^{GAMEDFS}}(u) &= (17 + (20 + 40) + (10 + 50) + (10 + 20 + 40) + (25 + 40) \\
&\quad + 50 + 37 + 40) \times C_{CH} \\
&= 399 \times C_{CH}
\end{aligned} \tag{3.87}$$

total energy consumption of CH robots. *Even without visiting any CH robot, optimal strategy performs better than no strategy and the UAV-Oriented strategy.*

3.4.4.3 Performance Comparison

Table 3.8 summarizes indices of the nonvisited CH robots which the strategies decide to desist from visiting in the configuration of Figure 3.14. Similarly, Table 3.9 summarizes total energy consumption of the nonvisited CH robots which the strategies decide to desist from visiting. From these tables, it can be observed how UAV decides to desist from visiting a subset of CH robots depending on its battery capacity in the configuration of Figure 3.14. Furthermore, the total energy consumption of the nonvisited CH robots depends on the desisting decisions taken by UAV and so the battery capacity of the UAV. Besides these, the total energy consumption of the nonvisited CH robots also depends on the network topology, the locations of all CH robots.

We compare the performances of the UAV-Oriented strategy and our two-stage optimal strategy for battery capacities varying from $B = 5$ to $B = 50$ in the configuration in Figure 3.14. From Figure 3.15, the following observations can be made. Applying the UAV-Oriented strategy results in $403 \times C_{CH}$ and $1055 \times C_{CH}$ for battery capacities $B = 15, 20, 25, 30, 35, 40, 45, 50$ and $B = 10$, respectively. It is not applicable for $B = 5$ which is insufficient battery capacity for the UAV to travel any CH robot

Table 3.8: The table shows indices of the nonvisited CH robots depending on battery capacity of UAV in Figure 3.14. "None" implies that the UAV visits all CH robots if $B = 35, 40, 45, 50$. "×" implies that the UAV-Oriented strategy is infeasible for that battery capacity.

Strategy	B = 5	B = 10	B = 15	B = 20	B = 25
UAV-Oriented Strategy	×	2-8	1-7	1-7	1-7
Optimal Strategy (GAMEDFS)	1-8	2-8	1-7	1-6	1,3,4,6
Strategy	B = 30	B = 35	B = 40	B = 45	B = 50
UAV-Oriented Strategy	1-7	1-7	1-7	1-7	1-7
Optimal Strategy (GAMEDFS)	1,3,4,6	1,3,4	3,4	4	None

Table 3.9: The table shows total energy consumption of nonvisited CH robots depending on battery capacity of UAV in Figure 3.15. "×" implies that the UAV-Oriented strategy is infeasible for that battery capacity.

Strategy	B = 5	B = 10	B = 15	B = 20	B = 25
UAV-Oriented Strategy	×	1055	403	403	403
Optimal Strategy (GAMEDFS)	399	382	239	202	137
Strategy	B = 30	B = 35	B = 40	B = 45	B = 50
UAV-Oriented Strategy	403	403	403	403	403
Optimal Strategy (GAMEDFS)	137	37	20	10	0

and turn back to the FC. On the other hand, the two-stage optimal strategy achieves zero energy consumption of all CH robots for $B = 50$. Optimal strategy results in $10 \times C_{CH}$ total energy consumption, only one fortieth of that by the UAV-Oriented strategy for $B = 45$. Optimal strategy results in $20 \times C_{CH}$ total energy consumption, only one twentieth of that by the UAV-Oriented strategy for $B = 40$. For $B = 35$, optimal strategy results in $37 \times C_{CH}$ total energy consumption, less than one tenth of that by the UAV-Oriented strategy. Optimal strategy results in $137 \times C_{CH}$ total energy consumption, nearly one third of that by the UAV-Oriented strategy for $B = 25, 30$. Optimal strategy results in $202 \times C_{CH}$, nearly half of that by the UAV-Oriented strategy for $B = 20$. For $B = 15$, optimal strategy results in $239 \times C_{CH}$, nearly half of that

by the UAV-Oriented strategy. For $B = 10$, optimal strategy results in $382 \times C_{CH}$ total energy consumption, less than that by the UAV-Oriented strategy. Even for $B = 5$, optimal strategy results in $399 \times C_{CH}$ total energy consumption, less than two fifth of that by no strategy. Recall that the UAV-Oriented strategy is not applicable for $B = 5$.

3.4.5 9-CH case

In Figure 3.16 shows the locations of the 9 CH robots and the weights of the links between them. With respect to this initial position of the UAV $(0,0)$, the positions of the CH robots are $(\xi_1, \xi_2, \xi_3, \xi_4, \xi_5, \xi_6, \xi_7, \xi_8, \xi_9) = ((7, 5), (6, -1), (7, 3), (5, 10), (-4, 3), (3, -7), (-3, 10), (9, 8), (1, -4))m$. In the configuration in Figure 3.16, the total energy consumption is $648 \times C_{CH}$ if all CH robots send their data directly to the FC at $\xi_0 = (0, 0)$ (the UAV visit no CH robot).

3.4.5.1 UAV-Oriented Strategy

By applying UAV-Oriented strategy, the UAV travels only to CH robot 3 ($\xi_3 = (7, 3)$) and collects all data of the CH robots from there if the UAV has sufficient battery capacity (to travel there and return back to the FC), which is

$$\begin{aligned}
B &= 2 \times \|\xi_3 - \xi_0\| \\
&= 2 \times \sqrt{(7-0)^2 + (3-0)^2} \times C_{UAV} \\
&\approx 15.23 \times C_{UAV} \\
&< 20 \times C_{UAV},
\end{aligned} \tag{3.88}$$

by which the UAV can apply UAV-Oriented strategy which results in the total energy consumption of the CH robots as follows

$$\begin{aligned}
E_{ACH}^{\pi^{UAV-Oriented}}(u) &= \|\xi_1 - \xi_3\|^2 + \|\xi_2 - \xi_3\|^2 + \|\xi_4 - \xi_3\|^2 + \|\xi_5 - \xi_3\|^2 \\
&+ \|\xi_6 - \xi_3\|^2 + \|\xi_7 - \xi_3\|^2 + \|\xi_8 - \xi_3\|^2 + \|\xi_9 - \xi_3\|^2 \\
&= (4 + 17 + 53 + 121 + 116 + 149 + 29 + 85) \times C_{CH} \\
&= 574 \times C_{CH}
\end{aligned} \tag{3.89}$$

If $B = 15$, the UAV can travel to CH robot 2 which is closer to the origin than CH robot 3. Similar to Equation (3.89), $E_{ACH}^{\pi^{UAV-Oriented}}(u) = 663 \times C_{CH} > 574 \times C_{CH}$

which yields that the UAV-Oriented strategy causes more energy consumption of CH robots than no strategy. If $B = 10$, the UAV can travel to CH robot 9 which is closer to the origin than CH robot 3. Similar to Equation (3.89), $E_{ACH}^{\pi^{UAV-Oriented}}(u) = 955 \times C_{CH} > 574 \times C_{CH}$ which yields that the UAV-Oriented strategy causes more energy consumption of CH robots than no strategy. However, if $B = 5$, then the UAV-Oriented strategy is not applicable because the UAV cannot travel to any CH robot.

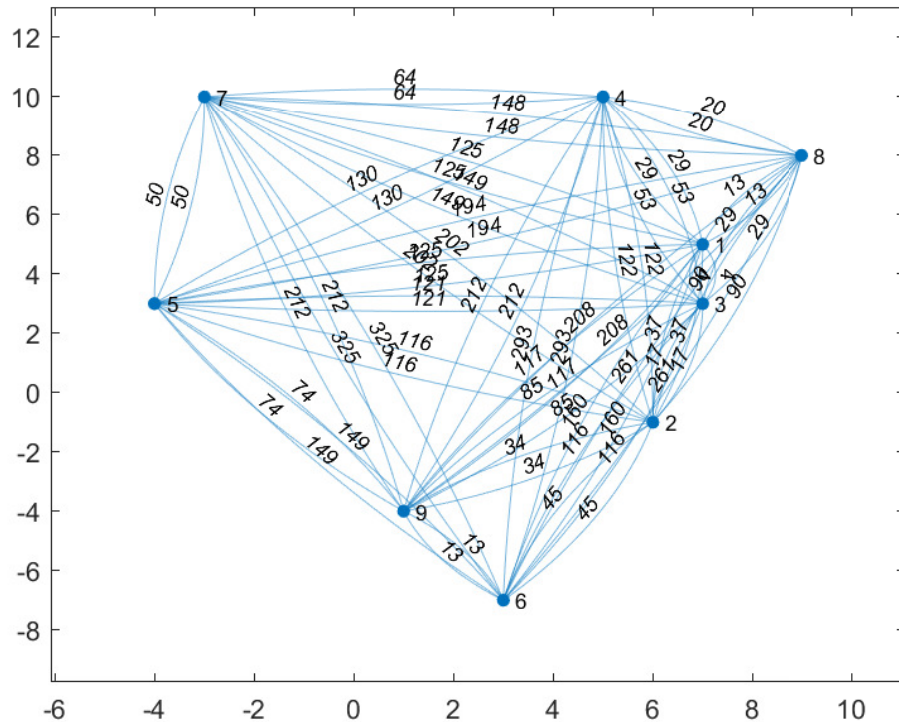


Figure 3.16: Nodes show that the locations of the 9 CH robots. The weight of a link shows the square of distance between the two nodes connected via that link.

3.4.5.2 Optimal Strategy (GAMEDFS)

In Figure 3.17, by applying optimal strategy (GAMEDFS), the UAV with $B = 50 \times C_{UAV}$ can make the CH robots consume no energy for forwarding data ($E_{UAV}^{\pi^*}(u) = 0$). Notice that if the problem is considered as a TSP problem for the configuration in Figure 3.16, the energy required for the UAV to visit all CH robots is

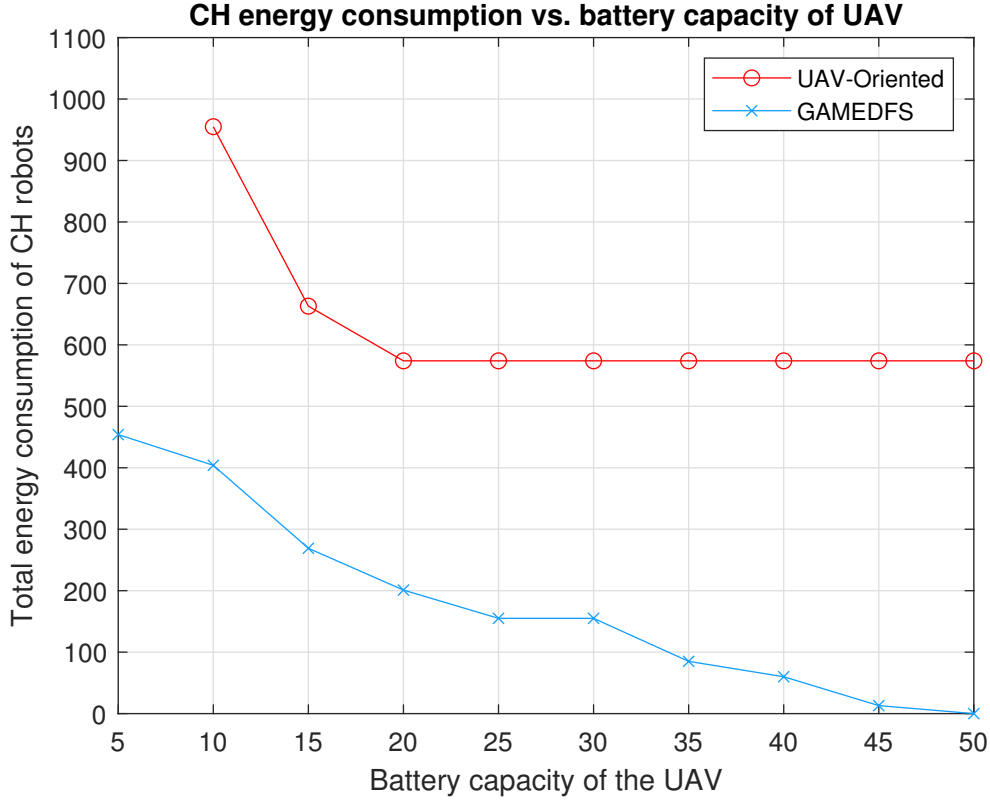


Figure 3.17: The total energy consumption of the 9 CH robots in Figure 3.16 under the strategies, UAV-Oriented and GAMEDFS for varying battery capacities of the UAV from $B = 5 \times C_{UAV}$ to $B = 50 \times C_{UAV}$. The units for energy consumption of the UAV and total energy consumption of the nonvisited CH robots are C_{UAV} and C_{CH} , respectively. These constants depend on the type of the UAV and the CH robots.

$$\begin{aligned}
E_{UAV}^{\pi^*}(u) &= \|\xi_0 - \xi_5\| + \|\xi_5 - \xi_7\| + \|\xi_7 - \xi_4\| + \|\xi_4 - \xi_8\| + \|\xi_8 - \xi_1\| \\
&\quad + \|\xi_1 - \xi_3\| + \|\xi_3 - \xi_2\| + \|\xi_2 - \xi_6\| + \|\xi_6 - \xi_9\| + \|\xi_9 - \xi_0\| \\
&= (5 + \sqrt{50} + 8 + \sqrt{20} + \sqrt{13} + 2 + \sqrt{17} + \sqrt{45} + \sqrt{13} + \sqrt{17}) \times C_{UAV} \\
&\approx 48.71 \times C_{UAV}
\end{aligned} \tag{3.90}$$

which yields that the UAV with $B < 48.71 \times C_{UAV}$ needs to desist from visiting at least one CH robot. The UAV with $B = 45 \times C_{UAV}$ desists from visiting CH robot 6 which results in

$$E_{ACH}^{\pi^{GAMEDFS}}(u) = 13 \times C_{CH} \tag{3.91}$$

total energy consumption of CH robots. Thus, the UAV consumes

$$\begin{aligned}
E_{UAV}^{\pi^*}(u) &= \|\xi_0 - \xi_5\| + \|\xi_5 - \xi_7\| + \|\xi_7 - \xi_4\| + \|\xi_4 - \xi_8\| + \|\xi_8 - \xi_1\| \\
&+ \|\xi_1 - \xi_3\| + \|\xi_3 - \xi_2\| + \|\xi_2 - \xi_9\| + \|\xi_9 - \xi_0\| \\
&= (5 + \sqrt{50} + 8 + \sqrt{20} + \sqrt{13} + 2 + \sqrt{17} + \sqrt{34} + \sqrt{17}) \times C_{UAV} \\
&\approx 44.26 \times C_{UAV}
\end{aligned} \tag{3.92}$$

The UAV with $B = 40 \times C_{UAV}$ desists from visiting CH robot 6, CH robot 8 and CH robot 9 which results in

$$\begin{aligned}
E_{ACH}^{\pi^{GAMEDFS}}(u) &= ((13 + 17) + 13 + 17) \times C_{CH} \\
&= 60 \times C_{CH}
\end{aligned} \tag{3.93}$$

total energy consumption of CH robots. Thus, the UAV consumes

$$\begin{aligned}
E_{UAV}^{\pi^*}(u) &= \|\xi_0 - \xi_5\| + \|\xi_5 - \xi_7\| + \|\xi_7 - \xi_4\| + \|\xi_4 - \xi_1\| + \|\xi_1 - \xi_3\| \\
&+ \|\xi_3 - \xi_2\| + \|\xi_2 - \xi_0\| \\
&= (5 + \sqrt{50} + 8 + \sqrt{29} + 2 + \sqrt{17} + \sqrt{37}) \times C_{UAV} \\
&\approx 37.66 \times C_{UAV}
\end{aligned} \tag{3.94}$$

The UAV with $B = 35 \times C_{UAV}$ desists from visiting CH robot 1, CH robot 2, CH robot 6, CH robot 8 and CH robot 9 which results in

$$\begin{aligned}
E_{ACH}^{\pi^{GAMEDFS}}(u) &= (4 + 17 + (13 + 17) + (13 + 4) + 17) \times C_{CH} \\
&= 85 \times C_{CH}
\end{aligned} \tag{3.95}$$

total energy consumption of CH robots. Thus, the UAV consumes

$$\begin{aligned}
E_{UAV}^{\pi^*}(u) &= \|\xi_0 - \xi_5\| + \|\xi_5 - \xi_7\| + \|\xi_7 - \xi_4\| + \|\xi_4 - \xi_3\| + \|\xi_3 - \xi_0\| \\
&= (5 + \sqrt{50} + 8 + \sqrt{53} + \sqrt{58}) \times C_{UAV} \\
&\approx 34.97 \times C_{UAV}
\end{aligned} \tag{3.96}$$

The UAV with $B = 25 \times C_{UAV}$ or $B = 30 \times C_{UAV}$ desists from visiting CH robot 4, CH robot 5, CH robot 6, CH robot 7 and CH robot 8 which results in

$$\begin{aligned}
E_{ACH}^{\pi^{GAMEDFS}}(u) &= (29 + 25 + 13 + (50 + 25) + 13) \times C_{CH} \\
&= 155 \times C_{CH}
\end{aligned} \tag{3.97}$$

total energy consumption of CH robots. Thus, the UAV consumes

$$\begin{aligned}
E_{UAV}^{\pi^*}(u) &= \|\xi_0 - \xi_9\| + \|\xi_9 - \xi_2\| + \|\xi_2 - \xi_3\| + \|\xi_3 - \xi_1\| + \|\xi_1 - \xi_0\| \\
&= (\sqrt{17} + \sqrt{34} + \sqrt{17} + 2 + \sqrt{74}) \times C_{UAV} \\
&\approx 24.68 \times C_{UAV}
\end{aligned} \tag{3.98}$$

The UAV with $B = 20 \times C_{UAV}$ visit CH robot 2 and CH robot 3 which results in

$$\begin{aligned}
E_{ACH}^{\pi^{GAMEDFS}}(u) &= (4 + (29 + 4) + 25 + (13 + 17) + (50 + 25) + (13 + 4) \\
&\quad + 17) \times C_{CH} \\
&= 201 \times C_{CH}
\end{aligned} \tag{3.99}$$

total energy consumption of CH robots. Thus, the UAV consumes

$$\begin{aligned}
E_{UAV}^{\pi^*}(u) &= \|\xi_0 - \xi_2\| + \|\xi_2 - \xi_3\| + \|\xi_3 - \xi_0\| \\
&= (\sqrt{37} + \sqrt{17} + \sqrt{58}) \times C_{UAV} \\
&\approx 17.82 \times C_{UAV}
\end{aligned} \tag{3.100}$$

The UAV with $B = 15 \times C_{UAV}$ visits only CH robot 2 which results in

$$\begin{aligned}
E_{ACH}^{\pi^{GAMEDFS}}(u) &= ((4 + 17) + 17 + (29 + 4 + 17) + 25 + (13 + 17) + (50 + 25) \\
&\quad + (13 + 4 + 17) + 17) \times C_{CH} \\
&= 269 \times C_{CH}
\end{aligned} \tag{3.101}$$

total energy consumption of CH robots. Thus, the UAV consumes

$$\begin{aligned}
E_{UAV}^{\pi^*}(u) &= \|\xi_0 - \xi_2\| + \|\xi_2 - \xi_0\| \\
&= (\sqrt{37} + \sqrt{37}) \times C_{UAV} \\
&\approx 12.17 \times C_{UAV}
\end{aligned} \tag{3.102}$$

The UAV with $B = 10 \times C_{UAV}$ visits only CH robot 9 which results in

$$\begin{aligned}
E_{ACH}^{\pi^{GAMEDFS}}(u) &= ((4 + 17 + 37) + 37 + (17 + 37) + (29 + 4 + 17 + 37) \\
&\quad + (13 + 17) + 50 + (13 + 4 + 17 + 37) + 17) \times C_{CH} \\
&= 404 \times C_{CH}
\end{aligned} \tag{3.103}$$

total energy consumption of CH robots. Thus, the UAV consumes

$$\begin{aligned}
E_{UAV}^{\pi^*}(u) &= \|\xi_0 - \xi_5\| + \|\xi_5 - \xi_0\| \\
&= (5 + 5) \times C_{UAV} \\
&= 10 \times C_{UAV}
\end{aligned} \tag{3.104}$$

The UAV with $B = 5 \times C_{UAV}$ cannot travel to any CH robots which results in

$$\begin{aligned}
E_{ACH}^{\pi^{GAMEDFS}}(u) &= ((4 + 17 + 37) + 37 + (17 + 37) + (29 + 4 + 17 + 37) + 25 \\
&\quad + (13 + 17) + (50 + 25) + (13 + 4 + 17 + 37) + 17) \times C_{CH} \\
&= 454 \times C_{CH}
\end{aligned} \tag{3.105}$$

total energy consumption of CH robots. *Even without visiting any CH robot, optimal strategy performs better than no strategy and the UAV-Oriented strategy.*

3.4.5.3 Performance Comparison

Table 3.10 summarizes indices of the nonvisited CH robots which the strategies decide to desist from visiting in the configuration of Figure 3.16. Similarly, Table 3.11 summarizes total energy consumption of the nonvisited CH robots which the strategies decide to desist from visiting. From these tables, it can be observed how UAV decides to desist from visiting a subset of CH robots depending on its battery capacity in the configuration of Figure 3.16. Furthermore, the total energy consumption of the nonvisited CH robots depends on the desisting decisions taken by UAV and so the battery capacity of the UAV. Besides these, the total energy consumption of the nonvisited CH robots also depends on the network topology, the locations of all CH robots.

We compare the performances of the UAV-Oriented strategy and our two-stage optimal strategy for battery capacities varying from $B = 5$ to $B = 50$ in the configuration in Figure 3.16. From Figure 3.17, the following observations can be made. Applying the UAV-Oriented strategy results in $574 \times C_{CH}$, $663 \times C_{CH}$ and $955 \times C_{CH}$ for battery capacities $B = 20, 25, 30, 35, 40, 45, 50$, $B = 15$, and $B = 10$, respectively. It is not applicable for $B = 5$ which is insufficient battery capacity for the UAV to

Table 3.10: The table shows indices of the nonvisited CH robots depending on battery capacity of UAV in Figure 3.16. "None" implies that the UAV visits all CH robots if $B = 35, 40, 45, 50$. "×" implies that the UAV-Oriented strategy is infeasible for that battery capacity.

Strategy	B = 5	B = 10	B = 15	B = 20	B = 25
UAV-Oriented Strategy	×	1-8	1,3-9	1,2,4-9	1,2,4-9
Optimal Strategy (GAMEDFS)	1-9	1-8	1,3-9	1,4-9	4-8
Strategy	B = 30	B = 35	B = 40	B = 45	B = 50
UAV-Oriented Strategy	1,2,4-9	1,2,4-9	1,2,4-9	1,2,4-9	1,2,4-9
Optimal Strategy (GAMEDFS)	4-8	1,2,6,8,9	6,8,9	6	None

Table 3.11: The table shows total energy consumption of nonvisited CH robots depending on battery capacity of UAV in Figure 3.17. "×" implies that the UAV-Oriented strategy is infeasible for that battery capacity.

Strategy	B = 5	B = 10	B = 15	B = 20	B = 25
UAV-Oriented Strategy	×	955	663	574	574
Optimal Strategy (GAMEDFS)	454	404	269	201	155
Strategy	B = 30	B = 35	B = 40	B = 45	B = 50
UAV-Oriented Strategy	574	574	574	574	574
Optimal Strategy (GAMEDFS)	155	85	60	13	0

travel any CH robot and turn back to the FC. On the other hand, the two-stage optimal strategy achieves zero total energy consumption of all CH robots for $B = 50$. Optimal strategy results in $13 \times C_{CH}$ total energy consumption, only one fourth of that by the UAV-Oriented strategy for $B = 45$. Optimal strategy results in $60 \times C_{CH}$ total energy consumption, nearly one tenth of that by the UAV-Oriented strategy for $B = 40$. For $B = 35$, optimal strategy results in $85 \times C_{CH}$ total energy consumption, less than one seventh of that by the UAV-Oriented strategy. Optimal strategy results in $155 \times C_{CH}$ total energy consumption, nearly one fourth of that by the UAV-Oriented strategy for $B = 25, 30$. Optimal strategy results in $201 \times C_{CH}$, nearly one third of that by the UAV-Oriented strategy for $B = 20$. For $B = 15$, optimal strategy results

in $269 \times C_{CH}$, nearly two fifth of that by the UAV-Oriented strategy. For $B = 10$, optimal strategy results in $404 \times C_{CH}$ total energy consumption, nearly two fifth of that by the UAV-Oriented strategy. Even for $B = 5$, optimal strategy results in $454 \times C_{CH}$ total energy consumption. Recall that the UAV-Oriented strategy is not applicable for $B = 5$.

3.4.6 10-CH Case

Figure 3.18 shows the locations of the 10 CH robots and the weights of the links between them. With respect to this initial position of the UAV $(0,0)$, the positions of the CH robots are $(\xi_1, \xi_2, \xi_3, \xi_4, \xi_5, \xi_6, \xi_7, \xi_8, \xi_9, \xi_{10}) = ((6, -7), (-5, 3), (2, 4), (-4, 7), (-2, 2), (2, -7), (-1, -2), (4, -8), (-1, 5), (7, -6))m$. In the configuration in Figure 3.18, the total energy consumption is $461 \times C_{CH}$ if all CH robots send their data directly to the FC at $\xi_0 = (0, 0)$ (the UAV visit no CH robot).

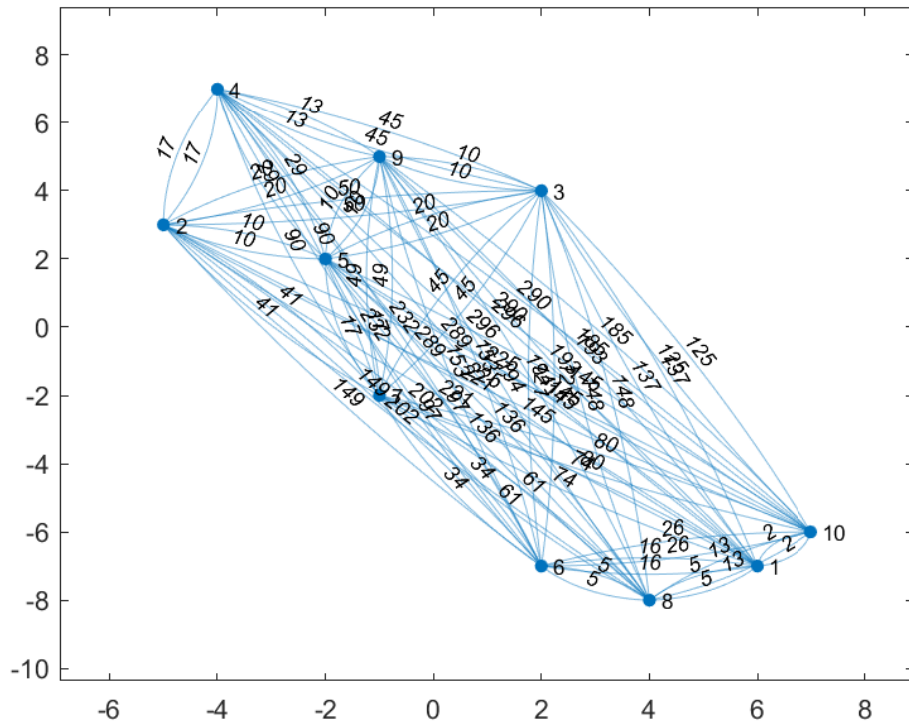


Figure 3.18: Nodes show that the locations of the 10 CH robots. The weight of a link shows the square of distance between the two nodes connected via that link.

3.4.6.1 UAV-Oriented Strategy

By applying the UAV-Oriented strategy, the UAV travels only to CH robot 7 ($\xi_7 = (-1, -2)$) and collects all data of the CH robots from there if the UAV has sufficient battery capacity (to travel there and return back to the FC), which is

$$\begin{aligned}
B &= 2 \times \|\xi_7 - \xi_0\| \\
&= 2 \times \sqrt{(-1 - 0)^2 + (2 - 0)^2} \times C_{UAV} \\
&\approx 4.47 \times C_{UAV} \\
&< 5 \times C_{UAV},
\end{aligned} \tag{3.106}$$

by which the UAV can apply the UAV-Oriented strategy which results in the total energy consumption of the CH robots as follows

$$\begin{aligned}
E_{ACH}^{\pi^{UAV-Oriented}}(u) &= \|\xi_1 - \xi_7\|^2 + \|\xi_2 - \xi_7\|^2 + \|\xi_3 - \xi_7\|^2 + \|\xi_4 - \xi_7\|^2 + \|\xi_5 - \xi_7\|^2 \\
&\quad + \|\xi_6 - \xi_7\|^2 + \|\xi_8 - \xi_7\|^2 + \|\xi_9 - \xi_7\|^2 + \|\xi_{10} - \xi_7\|^2 \\
&= (74 + 41 + 45 + 90 + 17 + 34 + 61 + 49 + 80) \times C_{CH} \\
&= 491 \times C_{CH}
\end{aligned} \tag{3.107}$$

which yields an interesting result that the UAV-Oriented strategy causes more energy consumption of CH robots than no strategy (the UAV visits no CH robots) in the configuration in Figure 3.18.

3.4.6.2 Optimal Strategy (GAMEDFS)

The performance of optimal strategy (GAMEDFS) is investigated for battery capacities varying from $B = 5$ to $B = 50$ in the configuration in Figure 3.18. In Figure 3.19, by applying optimal strategy, the UAV with $B = 45 \times C_{UAV}$ or $B = 50 \times C_{UAV}$ can make the CH robots consume no energy for forwarding data ($E_{UAV}^{\pi^*}(u) = 0$). Notice that if the problem is considered as a TSP problem for the configuration in Figure 3.18, the energy required for the UAV to visit all CH robots is

$$\begin{aligned}
E_{UAV}^{\pi^*}(u) &= \|\xi_0 - \xi_5\| + \|\xi_5 - \xi_2\| + \|\xi_2 - \xi_4\| + \|\xi_4 - \xi_9\| + \|\xi_9 - \xi_3\| + \|\xi_3 - \xi_{10}\| \\
&\quad + \|\xi_{10} - \xi_1\| + \|\xi_1 - \xi_8\| + \|\xi_8 - \xi_6\| + \|\xi_6 - \xi_7\| + \|\xi_7 - \xi_0\| \\
&= (\sqrt{8} + \sqrt{10} + \sqrt{17} + \sqrt{13} + \sqrt{10} + \sqrt{125} + \sqrt{2} + \sqrt{5} + \sqrt{5} \\
&\quad + \sqrt{34} + \sqrt{5}) \times C_{UAV} \\
&\approx 42.02 \times C_{UAV}
\end{aligned} \tag{3.108}$$

which yields that the UAV with $B < 42.02 \times C_{UAV}$ needs to desist from visiting at least one CH robot. The UAV with $B = 40 \times C_{UAV}$ desists from visiting CH robot 2 which results in

$$E_{ACH}^{\pi^{GAMEDFS}}(u) = 10 \times C_{CH} \tag{3.109}$$

total energy consumption of CH robots.

Thus, the UAV consumes

$$\begin{aligned}
E_{UAV}^{\pi^*}(u) &= \|\xi_0 - \xi_5\| + \|\xi_5 - \xi_4\| + \|\xi_4 - \xi_9\| + \|\xi_9 - \xi_3\| + \|\xi_3 - \xi_{10}\| \\
&\quad + \|\xi_{10} - \xi_1\| + \|\xi_1 - \xi_8\| + \|\xi_8 - \xi_6\| + \|\xi_6 - \xi_7\| + \|\xi_7 - \xi_0\| \\
&= (\sqrt{8} + \sqrt{20} + \sqrt{13} + \sqrt{10} + \sqrt{125} + \sqrt{2} + \sqrt{5} + \sqrt{5} + \sqrt{34} \\
&\quad + \sqrt{5}) \times C_{UAV} \\
&\approx 39.21 \times C_{UAV}
\end{aligned} \tag{3.110}$$

The UAV with $B = 35 \times C_{UAV}$ desists from visiting CH robot 2 and CH robot 4 which results in

$$\begin{aligned}
E_{ACH}^{\pi^{GAMEDFS}}(u) &= (10 + 13) \times C_{CH} \\
&= 23 \times C_{CH}
\end{aligned} \tag{3.111}$$

total energy consumption of CH robots. Thus, the UAV consumes

$$\begin{aligned}
E_{UAV}^{\pi^*}(u) &= \|\xi_0 - \xi_5\| + \|\xi_5 - \xi_9\| + \|\xi_9 - \xi_3\| + \|\xi_3 - \xi_{10}\| + \|\xi_{10} - \xi_1\| \\
&\quad + \|\xi_1 - \xi_8\| + \|\xi_8 - \xi_6\| + \|\xi_6 - \xi_7\| + \|\xi_7 - \xi_0\| \\
&= (\sqrt{8} + \sqrt{10} + \sqrt{10} + \sqrt{125} + \sqrt{2} + \sqrt{5} + \sqrt{5} + \sqrt{34} + \sqrt{5}) \times C_{UAV} \\
&\approx 34.29 \times C_{UAV}
\end{aligned} \tag{3.112}$$

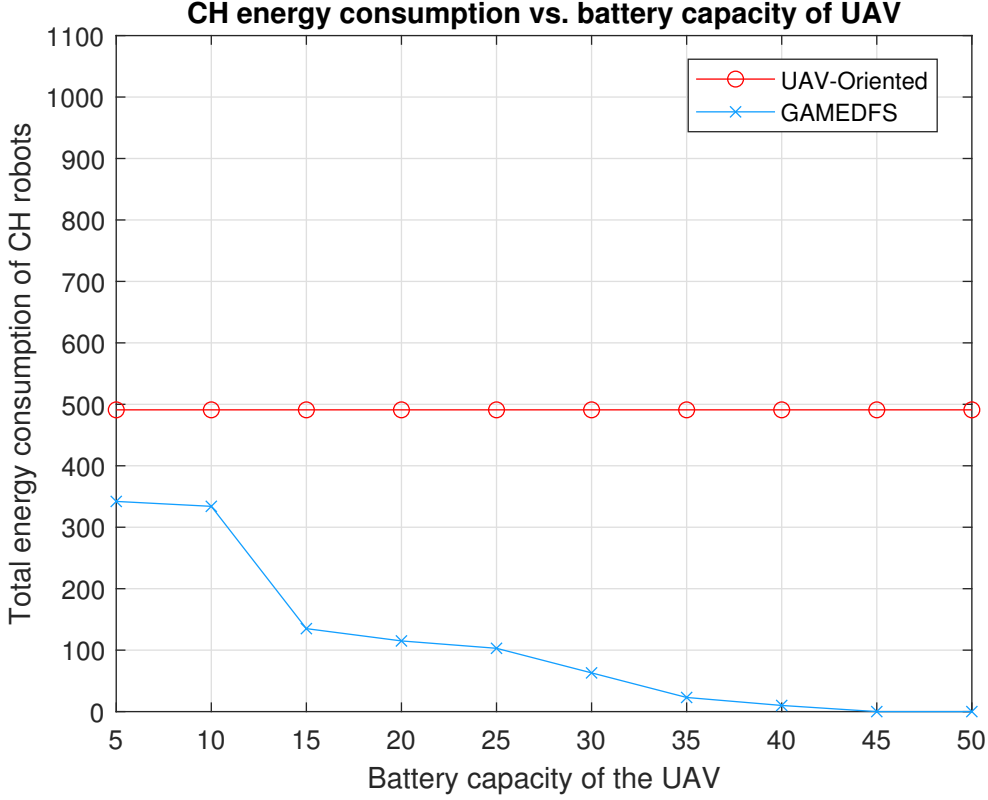


Figure 3.19: The total energy consumption of the 10 CH robots in Figure 3.18 under the strategies, UAV-Oriented and GAMEDFS for varying battery capacities of the UAV from $B = 5 \times C_{UAV}$ to $B = 50 \times C_{UAV}$. The units for energy consumption of the UAV and total energy consumption of the nonvisited CH robots are C_{UAV} and C_{CH} , respectively. These constants depend on the type of the UAV and the CH robots.

The UAV with $B = 30 \times C_{UAV}$ desists from visiting CH robot 2, CH robot 3, CH robot 4, and CH robot 9 which results in

$$\begin{aligned}
 E_{ACH}^{\pi^{GAMEDFS}}(u) &= (10 + 20 + (13 + 10) + 10) \times C_{CH} \\
 &= 63 \times C_{CH}
 \end{aligned} \tag{3.113}$$

total energy consumption of CH robots. Thus, the UAV consumes

$$\begin{aligned}
 E_{UAV}^{\pi^*}(u) &= \|\xi_0 - \xi_5\| + \|\xi_5 - \xi_{10}\| + \|\xi_{10} - \xi_1\| + \|\xi_1 - \xi_8\| + \|\xi_8 - \xi_6\| \\
 &+ \|\xi_6 - \xi_7\| + \|\xi_7 - \xi_0\| \\
 &= (\sqrt{8} + \sqrt{145} + \sqrt{2} + \sqrt{5} + \sqrt{5} + \sqrt{34} + \sqrt{5}) \times C_{UAV} \\
 &\approx 28.83 \times C_{UAV}
 \end{aligned} \tag{3.114}$$

The UAV with $B = 25 \times C_{UAV}$ desists from visiting CH robot 2, CH robot 3, CH robot 4, CH robot 5, and CH robot 9 which results in

$$\begin{aligned} E_{ACH}^{\pi^{GAMEDFS}}(u) &= ((10 + 8) + (20 + 8) + (13 + 10 + 8) + 8 + (10 + 8)) \times C_{CH} \\ &= 103 \times C_{CH} \end{aligned} \quad (3.115)$$

total energy consumption of CH robots. Thus, the UAV consumes

$$\begin{aligned} E_{UAV}^{\pi^*}(u) &= \|\xi_0 - \xi_{10}\| + \|\xi_{10} - \xi_1\| + \|\xi_1 - \xi_8\| + \|\xi_8 - \xi_6\| + \|\xi_6 - \xi_7\| + \|\xi_7 - \xi_0\| \\ &= (\sqrt{85} + \sqrt{2} + \sqrt{5} + \sqrt{5} + \sqrt{34} + \sqrt{5}) \times C_{UAV} \\ &\approx 23.17 \times C_{UAV} \end{aligned} \quad (3.116)$$

The UAV with $B = 20 \times C_{UAV}$ desists from visiting CH robot 1, CH robot 2, CH robot 3, CH robot 4, CH robot 5, CH robot 9, and CH robot 10 which results in

$$\begin{aligned} E_{ACH}^{\pi^{GAMEDFS}}(u) &= (5 + (10 + 8) + (20 + 8) + (13 + 10 + 8) + 8 + (10 + 8) \\ &\quad + (2 + 5)) \times C_{CH} \\ &= 115 \times C_{CH} \end{aligned} \quad (3.117)$$

total energy consumption of CH robots. Thus, the UAV consumes

$$\begin{aligned} E_{UAV}^{\pi^*}(u) &= \|\xi_0 - \xi_8\| + \|\xi_8 - \xi_6\| + \|\xi_6 - \xi_7\| + \|\xi_7 - \xi_0\| \\ &= (\sqrt{80} + \sqrt{5} + \sqrt{34} + \sqrt{5}) \times C_{UAV} \\ &\approx 19.25 \times C_{UAV} \end{aligned} \quad (3.118)$$

The UAV with $B = 15 \times C_{UAV}$ visits only CH robot 6 which results in

$$\begin{aligned} E_{ACH}^{\pi^{GAMEDFS}}(u) &= ((5 + 5) + (10 + 8) + (20 + 8) + (13 + 10 + 8) + 8 + 5 \\ &\quad + (10 + 8) + 5 + (2 + 5 + 5)) \times C_{CH} \\ &= 135 \times C_{CH} \end{aligned} \quad (3.119)$$

total energy consumption of CH robots. Thus, the UAV consumes

$$\begin{aligned} E_{UAV}^{\pi^*}(u) &= \|\xi_0 - \xi_6\| + \|\xi_6 - \xi_0\| \\ &= (\sqrt{53} + \sqrt{53}) \times C_{UAV} \\ &\approx 14.56 \times C_{UAV} \end{aligned} \quad (3.120)$$

The UAV with $B = 10 \times C_{UAV}$ visits only CH robot 5 and CH robot 7 which results in

$$\begin{aligned}
E_{ACH}^{\pi^{GAMEDFS}}(u) &= ((5 + 5 + 53) + (10 + 8) + (20 + 8) + (13 + 10 + 8) + 53 \\
&\quad + (10 + 8) + (5 + 53) + (2 + 5 + 5 + 53)) \times C_{CH} \\
&= 334 \times C_{CH}
\end{aligned} \tag{3.121}$$

total energy consumption of CH robots. Thus, the UAV consumes

$$\begin{aligned}
E_{UAV}^{\pi^*}(u) &= \|\xi_0 - \xi_5\| + \|\xi_5 - \xi_7\| + \|\xi_7 - \xi_0\| \\
&= (\sqrt{8} + \sqrt{17} + \sqrt{5}) \times C_{UAV} \\
&\approx 9.19 \times C_{UAV}
\end{aligned} \tag{3.122}$$

The UAV with $B = 5 \times C_{UAV}$ visit only CH robot 7 which results in

$$\begin{aligned}
E_{ACH}^{\pi^{GAMEDFS}}(u) &= ((5 + 5 + 53) + (10 + 8) + (20 + 8) + (13 + 10 + 8) + 8 + 53 \\
&\quad + (10 + 8) + (5 + 53) + (2 + 5 + 5 + 53)) \times C_{CH} \\
&= 342 \times C_{CH}
\end{aligned} \tag{3.123}$$

total energy consumption of CH robots. Even with $B = 5$, optimal strategy performs better than no strategy and the UAV-Oriented strategy.

3.4.6.3 Performance Comparison

Table 3.12 summarizes indices of the nonvisited CH robots which the strategies decide to desist from visiting in the configuration of Figure 3.18. Similarly, Table 3.13 summarizes total energy consumption of the nonvisited CH robots which the strategies decide to desist from visiting. From these tables, it can be observed how UAV decides to desist from visiting a subset of CH robots depending on its battery capacity in the configuration of Figure 3.18. Furthermore, the total energy consumption of the nonvisited CH robots depends on the desisting decisions taken by UAV and so the battery capacity of the UAV. Besides these, the total energy consumption of the nonvisited CH robots also depends on the network topology, the locations of all CH robots.

Table 3.12: The table shows indices of the nonvisited CH robots depending on battery capacity of UAV in Figure 3.18. "None" implies that the UAV visits all CH robots if $B = 45$ or $B = 50$.

Strategy	B = 5	B = 10	B = 15	B = 20	B = 25
UAV-Oriented Strategy	1-6,8-10	1-6,8-10	1-6,8-10	1-6,8-10	1-6,8-10
Optimal (GAMEDFS)	1-6,8-10	1-4,6,8-10	1-5,7-10	1-5,9,10	2-5,9
Strategy	B = 30	B = 35	B = 40	B = 45	B = 50
UAV-Oriented Strategy	1-6,8-10	1-6,8-10	1-6,8-10	1-6,8-10	1-6,8-10
Optimal (GAMEDFS)	2-4,9	2,4	2	None	None

Table 3.13: The table shows total energy consumption of nonvisited CH robots depending on battery capacity of UAV in Figure 3.19.

Strategy	B = 5	B = 10	B = 15	B = 20	B = 25
UAV-Oriented Strategy	491	491	491	491	491
Optimal Strategy (GAMEDFS)	342	334	135	105	103
Strategy	B = 30	B = 35	B = 40	B = 45	B = 50
UAV-Oriented Strategy	491	491	491	491	491
Optimal Strategy (GAMEDFS)	63	23	10	0	0

We compare the performances of the UAV-Oriented strategy and our two-stage optimal strategy for battery capacities varying from $B = 5$ to $B = 50$ in the configuration in Figure 3.18. From Figure 3.19, the following observations can be made. Applying the UAV-Oriented strategy results in $491 \times C_{CH}$ for battery capacities from $B = 10$ to $B = 50$. This strategy performs worse than no strategy by which the UAV standing on the FC collects data from all CH robots (no strategy results in $461 \times C_{CH} < 491 \times C_{CH}$). On the other hand, the two-stage optimal strategy achieves zero energy consumption of all CH robots for $B = 45$ and $B = 50$. Optimal strategy results in $10 \times C_{CH}$ total energy consumption, only 2% of that by UAV-Oriented strategy for $B = 40$. Optimal strategy results in $23 \times C_{CH}$, less than 5% of that by UAV-Oriented strategy for $B = 35$. For $B = 30$, optimal strategy results in $63 \times C_{CH}$,

less than 13% of that by UAV-Oriented strategy. For $B = 25$, $B = 20$ and $B = 15$, optimal strategy results in $103 \times C_{CH}$, $115 \times C_{CH}$ and $135 \times C_{CH}$ total energy consumption, respectively, still less than 28% of that by the UAV-Oriented strategy. For $B = 10$, optimal strategy results in $334 \times C_{CH}$, nearly 68% of that by the UAV-Oriented strategy. Even for $B = 5$, optimal strategy results in $342 \times C_{CH}$ total energy consumption, still less than 75% of that by no strategy.



CHAPTER 4

ENERGY-AWARE DATA COLLECTION WITH PRIORITY BY A UAV WITH A LIMITED-CAPACITY BATTERY IN ROBOTIC WIRELESS SENSOR NETWORKS

4.1 System Model and Problem Definition

This section focuses on defining our problem and generates our system approach.

4.1.1 Motivation and Problem Definition

We present a motivating scenario based on which we formulate our problem in this section. We consider a M -clustered robotic network where a UAV with limited battery capacity collects data from M robots which perform as cluster head (CH) robots in their clusters. This robotic network is responsible for collecting data from sensors monitoring environmental changes. Please see Figure 4.1.

Each cluster has a cluster head (CH) robot which allocates tasks to the cluster member (CM) robots in the cluster which execute the assigned tasks and send resultant data (obtained by using the sensors to monitor environment) to the CH robot. *A CH robot is responsible for collecting data from the robots in its cluster and then transmit data to UAV directly or indirectly.* UAV visits a varying portion of CH robots depending on its battery capacity and their locations. If the UAV cannot visit all CH robots due to its limited battery capacity, then nonvisited CH robots send their data to one of neighboring CH through multiple hops via other nonvisited CH neighbors. $S \triangleq \{1, 2, \dots, M\}$ denotes the index set of CH robots. B denotes battery capacity of UAV. Each CH robot collects data from the CM robots to aggregate and send to UAV.

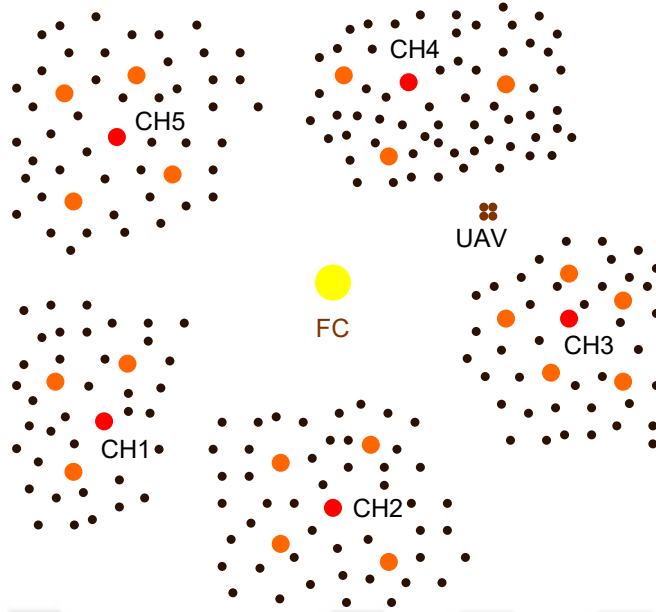


Figure 4.1: In this system, red dots are cluster head (CH) robots whereas the orange ones are the remaining robots. UAV starts its trajectory from FC. After UAV collects data from all CH robots, it returns to FC to send all data to FC and charge its battery for next path.

A CH robot spends significant energy to aggregate data and send it to UAV or neighboring CH robot. If a CH robot moves like the remaining robots in its cluster, then the energy level of the CH robot will decrease below the critical energy level quickly. Falling below the critical level fast causes frequent CH election which is a very time and energy consuming process. It may also cause a CH robot which allocates tasks efficiently to leave being CH robot a result of inefficient energy consumption. Hence, the following assumption is made.

Assumption 6. *No CH robot moves in order to avoid extra energy consumption.*

Remark 10. *From Assumption 6, we focus on battery capacity of UAV and locations of CH robots. Therefore, the sensors and the robots except CH robots and the UAV will not be shown in the following figures different from Figure 4.1.*

We consider distances to calculate total cost of consumed energy by nonvisited CH robots so Assumption 7 is made.

Assumption 7. *All CH robots have equal amount of data to transmit without latency.*

$\xi_0 \triangleq (x_0, y_0)$ denotes initial position of UAV. $\xi_i \triangleq (x_i, y_i)$ denotes position of CH robot i . We assume that UAV consumes energy proportional to the distance it travels. To illustrate, the energy consumed by UAV from CH robot i to j is denoted by

$$\begin{aligned} E_{UAV}(i, j) &\triangleq C_{UAV} \|\xi_i - \xi_j\| \\ &= C_{UAV} \sqrt{(x_i - x_j)^2 + (y_i - y_j)^2} \end{aligned} \quad (4.1)$$

where C_{UAV} is the constant ratio between energy consumed by UAV and the distance it travels, which represents the direct proportionality. On the other hand, we assume that energy consumed by a CH robot is proportional to the square of the distance between itself and the next hop. To illustrate, the energy consumed by CH robot i to send data to CH robot j is denoted by $E_{CH}(i, j)$ and this energy cost is defined as

$$\begin{aligned} E_{CH}(i, j) &\triangleq C_{CH} \|\xi_i - \xi_j\|^2 \\ &= C_{CH} [(x_i - x_j)^2 + (y_i - y_j)^2] \end{aligned} \quad (4.2)$$

where C_{CH} is the constant ratio between energy consumption of a CH robot and square of distance between it and the next hop, which represents the quadratic proportionality.

During the path, it is very probable that UAV may pass through a closer point for a CH robot. In worst case, UAV can collect data from some CH robots before starting trajectory. Therefore, we make the following assumption.

Assumption 8. *CH robots have enough energy to send their data to UAV directly if the UAV stands at its initial position.*

Assumption 9. *CH robots sends data to UAV or another CH robot with constant rate.*

4.1.2 Our Problem Approach Formulation

UAV aims to plan such a path that it can complete in its full battery capacity. Although each CH robot has sufficient energy to transmit their data in one round, CH robots are desired to spend less energy for this data transmission. *The UAV aims to minimize total energy consumption of CH robots by planning the path through which it visits the CH robots.*

Definition 12. Path Set, P is set of all linear paths between positions of M CH robots and initial position of UAV, denoted by $P \triangleq \{p(\xi_0, \xi_1), p(\xi_0, \xi_2), \dots, p(\xi_0, \xi_M), \dots, p(\xi_i, \xi_j), \dots, p(\xi_M, \xi_{M-1})\}$, where $p(\xi_i, \xi_j)$ denotes the linear path from CH robot i to j and its length equals to $\|\xi_i - \xi_j\|$.¹

Definition 13. Strategy of UAV, π is defined as the set of linear paths followed by the UAV for data collection, a subset of the path set, i. e., $\pi \subseteq P$.

Definition 14. Energy consumption of UAV with strategy π , E_{UAV}^π is energy consumed by UAV with strategy π , i. e.,

$$E_{UAV}^\pi \triangleq \left[\sum_{j=1}^M \sum_{i=1}^M C_{UAV} \|\xi_i - \xi_j\| I_{\{p(\xi_i, \xi_j) \in \pi\}} \right]. \quad (4.3)$$

where $I_{\{A\}}$ is indicator function becoming 1 for true event A .

Definition 15. Energy consumption of CH robot i under strategy π , u_i , $E_i^\pi(u_i)$ is the energy consumed by nonvisited CH robot i with data forwarding strategy u_i .

$E_i^\pi(u_i) = 0$ for each visited CH robot i under strategy π .

Definition 16. Priority set, S_{pr} , is the set of all CH robots which the UAV must visit on its trajectory. In other words, visiting them are mandatory.

Definition 17. Total energy consumption of all CH robots under strategies π , u , $E_{ACH}^\pi(u)$ is total energy consumed by all CH robots under strategy π , i. e.,

$$E_{ACH}^\pi(u) \triangleq \sum_{i=1}^M \left[E_i^\pi(u_i) \left(1 - \sum_{j=1}^M I_{\{p(\xi_i, \xi_j) \in \pi\}} \right) \right]. \quad (4.4)$$

Under Assumptions 6-9, we define our problem as follows.

Problem 2. Minimizing total energy consumption of CH robots via an limited-battery UAV with priority set

$$\begin{aligned} \min_{u, \pi} \quad & E_{ACH}^\pi(u) \\ \text{s.t.} \quad & E_{UAV}^\pi \leq B \\ & S_{pr} \subseteq S - S_{non}^\pi \end{aligned}$$

where S_{non}^π is the set of the nonvisited CH robots under strategy π .

¹ Notice that $p(\xi_0, \xi_j)$ is the linear path from initial position of UAV to CH robot j ; $p(\xi_i, \xi_0)$ is linear path from CH robot i to initial position of UAV.

4.2 Total Energy Minimization by Visiting Priority Set with Limited Battery Capacity

We first tackle the case in that UAV has sufficient energy to visit all CH robots. First, we consider the problem as a travel salesman problem (TSP) and then look for shortest path via genetic algorithm. Thus, we can obtain a lower bound for the amount of energy which UAV needs for visiting all CH robots.

Definition 18. (*Minimum battery capacity for the UAV to visit all CH robots, B_{TSP}*)
The energy required to visit all CH robots under the optimum strategy for TSP is the minimum battery capacity for the UAV to visit all CH robots.

In the case of sufficient battery capacity of UAV, by choosing an energy-optimally varying portion of the CH robots to visit, the UAV aims to minimize total energy consumption of nonvisited CH robots that will be sending data by multiple hops through other nonvisited CH until a visited CH node. As a result, we focus on minimizing energy consumption of each nonvisited CH robots. We need to consider optimal strategies for the nonvisited CH robots to forward their data.

A nonvisited CH robot i should look for the shortest path to each visited CH robot and take the minimum of all shortest paths. From Equation (4.2), squares of the distances between neighbor CH robots are used for calculating shortest path between CH robots. Thus, we can derive optimal data forwarding strategy for each CH robot. Note that each nonvisited CH robot considers each visited CH robot as a possible target to find the optimal data forwarding strategy for itself.

Definition 19. *K -element combinations of the CH robots, S_a^K , is a K -element subset of all CH robots, i. e., $S_a^K \subseteq S$ and $|S_a^K| = K$ for $1 \leq a \leq \binom{M}{K}$. Let $S^K(B)$ be the set of all feasible K -element combinations which can be visited by the UAV with battery capacity B .*

If the UAV has sufficient battery capacity to visit all CH robots, then Problem 2 can be considered as a TSP problem and an optimal strategy can be obtained by common techniques in the literature. On the other hand, if the UAV has a battery capacity less than B_{TSP} , then considering Problem 2 as a TSP problem does not guarantee to obtain

an optimal strategy. In this case, we should consider minimizing energy consumption of both UAV and nonvisited CH robots. The following proposition shows this. Let π^* denote the optimal strategy for Problem 2.

Proposition 2. *For $B < B_{TSP}$, π_{TSP}^{max} does not necessarily imply the optimality condition for the Problem 2, where π_{TSP}^{max} be the strategy by which the TSP can visit the maximum number of CH robots.*

Proof. The proof is quite similar to the proof of Proposition 1 in Chapter 3. The difference is that we should consider only the $M - |S_{pr}|$ CH robots not included by the priority set. \square

As UAV has insufficient battery capacity, $B < B_{TSP}$, to visit all CH robots, it desists from visiting some CH robots. Remark 11 can be used for this desisting process.

Remark 11. *To solve the problem for the UAV with battery capacity $B < B_{TSP}$, our strategy will start at a point $B = B_{TSP}$, then the strategy will decrease the energy consumption of the UAV by desisting from visiting some CH robots.*

Lemma 2 is useful to search for a path after desisting from visiting some CH robots.

Lemma 2. *Assume that the UAV with battery capacity B_1 can follow an optimal route such that it visits CH robot i , j and k successively on the optimal route by which the UAV visits $K < M$ CH robots (B_1 is the minimum energy required to follow that path). If UAV with slightly less battery capacity $B_2 < B_1$ decided to desist from visiting CH robot j , simply visiting CH robot k just after visiting CH robot i (the direct line from CH robot i to CH robot j) would not guarantee optimality to plan a route with the remaining $K - 1$ CH robots except CH robot j .*

Proof. The proof is quite similar to Lemma 1 in Chapter 3. The difference is that we should consider only the $M - |S_{pr}|$ CH robots not included by the priority set. \square

The data forwarding strategy depends only on locations of CH robots, not order by which UAV visits CH robots. This needs to be considered for finding optimal data forwarding strategies. From Lemma 2, if UAV desists to visit a CH robot j , instead

of simply passing from the previous CH robot i to the next CH robot k according to the visiting order (i, j, k are the consecutive CH robots according to the order), UAV needs to consider the path planning problem again as a TSP for finding the optimal path. Therefore, UAV can find the optimal path only considering path planning problem as a TSP for each combination of CH robots from Definition 19. Thus, Lemma 2 motivates us to propose Algorithm 3.

Algorithm 3 Optimal Strategy with Priority Set (OSPS)

Initialization: Battery capacity of the UAV is insufficient for visiting all CH robots, i.e., $B < B_{TSP}$.

Algorithm:

for $K = (M - 1) : 1$ **do**

Find all $\binom{M}{K}$ combinations of the CH robots.

for $a = 1 : \binom{M}{K}$ **do**

if $(\min_{\pi} E_{UAV}^{\pi} \leq B \text{ for } S_a^K) \& (S_a^K \cup S_{pr} = S_a^K)$ **then**

Use the data forwarding strategy, MSPDFS, for each CH robot $i \in S - S_a^K$.

Find $\sum_{i \in S - S_a^K} \min_{u_i} E_i^{\pi}(u_i)$

end if

end for

if $S^K(B) \neq \emptyset$ **then**

Find $\min_{S_a^K \in S^K(B)} \sum_{i \in S - S_a^K} \min_{u_i} E_i^{\pi}(u_i)$

end if

end for

Find $\min_K \left[\min_{S_a^K \in S^K(B)} \sum_{i \in S - S_a^K} \min_{u_i} E_i^{\pi}(u_i) \right]$.

Output: $(K, S_a^K) = \arg \min \sum_{i \in S - S_a^K} \min_{u_i} E_i^{\pi}(u_i)$

Theorem 2. Algorithm 3 is optimal for Problem 2.

Proof. The proof is similar to the Theorem 1 in Chapter 3. If the cardinality of priority set is N , then the UAV need to consider all K values from M to N . We will look for each CH robot $i \in S - S_{pr}$ and try to add them to trajectory depending on its battery capacity. As the rest of proof is similar to Theorem 1 in Chapter 3. \square

4.3 Numerical Results

We evaluate the performance of the strategies for varying battery capacities, various priority set of CH robots and number of CH robots. We consider three scenarios with varying number of CH robots, namely, 5-CH, 7-CH, and 10-CH robot scenarios by randomly generating locations of CH robots.

In these scenarios, we observe that path length for UAV to visit all CH robots is less than 50 units. If UAV has a battery capacity less than $50 \times C_{UAV}$, it can visit all CH robots. We evaluate the performances of OSPS, GAMEDFS, SNCHS and UAV-Oriented strategy in [75] with respect to different priority sets. In each scenario, we form the priority sets upto first $\lceil 0.4 \times M \rceil$ CH robots with respect to indices of CH robots. *We calculate the resultant energy consumption of the UAV and CH robots.*

4.3.1 5-CH case

Figure 4.2 shows the locations of the 5 CH robots and the weights of the links between them. With respect to this initial position of the UAV (0,0), the positions of the CH robots are $(\xi_1, \xi_2, \xi_3, \xi_4, \xi_5) = ((-8, 5), (2, 2), (6, 10), (-2, -3), (-5, -5)) m$.

4.3.1.1 UAV-Oriented Strategy

By applying UAV-Oriented strategy, the UAV travels only to CH robot 2 ($\xi_2 = (2, 2)$) and collect all data of the CH robots from there if

$$\begin{aligned}
 B &= 2 \times \|\xi_2 - \xi_0\| \\
 &= 2 \times \sqrt{(2-0)^2 + (2-0)^2} \times C_{UAV} \\
 &\approx 5.66 \times C_{UAV} \\
 &< 10 \times C_{UAV},
 \end{aligned} \tag{4.5}$$

which yields an interesting result that the UAV-Oriented strategy cause more energy consumption of CH robots than no strategy in the configuration in Figure 4.2. If $B = 5$, then the UAV-Oriented strategy is not applicable because the UAV cannot travel to CH robot 2 and the other CH robots are farther to origin than CH robot 2.

4.3.1.2 Optimal Strategy with no priority set (GAMEDFS)

The performance of optimal strategy with no priority set (equivalent to GAMEDFS proposed in Chapter 3) is tackled for battery capacities varying from $B = 5$ to $B = 50$ in the configuration in Figure 4.2. In Figure 4.3, by applying optimal strategy, the UAV with $B = 45 \times C_{UAV}$ or $B = 50 \times C_{UAV}$ can visit all CH robots, i. e., $E_{ACH}^{\pi^*}(u) = 0$. In the configuration in Figure 4.2, the energy required for the UAV to visit all CH robots is $E_{UAV}^{\pi^*}(u) \approx 44.29 \times C_{UAV}$. The UAV with $B = 35$ or $B = 40 \times C_{UAV}$ desists from visiting CH robot 3 which results in $E_{ACH}^{\pi^*}(u) = 80 \times C_{CH}$. Thus, the UAV consumes $E_{UAV}^{\pi^*}(u) \approx 30.92 \times C_{UAV}$. The UAV with $B = 30 \times C_{UAV}$ desists from visiting CH robot 3 and 5 which results in $E_{ACH}^{\pi^*}(u) = 93 \times C_{CH}$. Thus, the UAV consumes $E_{UAV}^{\pi^*}(u) \approx 26.87 \times C_{UAV}$. The UAV with $B = 25 \times C_{UAV}$ desists from visiting CH robot 2, 3 and 5 which results in $E_{ACH}^{\pi^*}(u) = 109 \times C_{CH}$ and $E_{UAV}^{\pi^*}(u) \approx 23.04 \times C_{UAV}$. The UAV with $B = 20 \times C_{UAV}$ desists from visiting CH robot 1 and 3 which results in $E_{ACH}^{\pi^*}(u) = 169 \times C_{CH}$ and $E_{UAV}^{\pi^*}(u) \approx 19.94 \times C_{UAV}$. UAV with $B = 15 \times C_{UAV}$ desists from visiting CH robot 1, 3 and 5 which results in $E_{ACH}^{\pi^*}(u) = 182 \times C_{CH}$ and $E_{UAV}^{\pi^*}(u) \approx 12.84 \times C_{UAV}$. UAV with $B = 10 \times C_{UAV}$ desists from visiting CH robot 1, 2, 3, and 5 which results in $E_{ACH}^{\pi^*}(u) = 198 \times C_{CH}$ and $E_{UAV}^{\pi^*}(u) \approx 7.21 \times C_{UAV}$. UAV with $B = 5 \times C_{UAV}$ can travel to no CH robot which results in $E_{ACH}^{\pi^*}(u) = 224 \times C_{CH}$. *Even without visiting any CH robot, optimal strategy performs better than UAV-Oriented strategy.*

4.3.1.3 Optimal Strategy with Priori Set {CH 1}

If the priority set consists of CH robot 1, UAV must visit CH 1, for which it needs

$$\begin{aligned}
 E_{UAV}^{\pi^*}(u) &= \|\xi_0 - \xi_1\| + \|\xi_1 - \xi_0\| \\
 &= (2 \times \sqrt{89}) \times C_{UAV} \\
 &\approx 18.87 \times C_{UAV}
 \end{aligned} \tag{4.6}$$

which means that the battery capacities $B = 5, 10, 15 \times C_{UAV} < 18.87 \times C_{UAV}$ are not feasible. For $B = 45, 50 \times C_{UAV}$, UAV can visit all CH robots as the case with no priority set, i. e., $E_{ACH}^{\pi^*}(u) = 0$. For $B = 20, 25, 30, 35, 40 \times C_{UAV}$, optimal strategy with priority set of CH robot 1 is same with GAMEDFS because UAV with

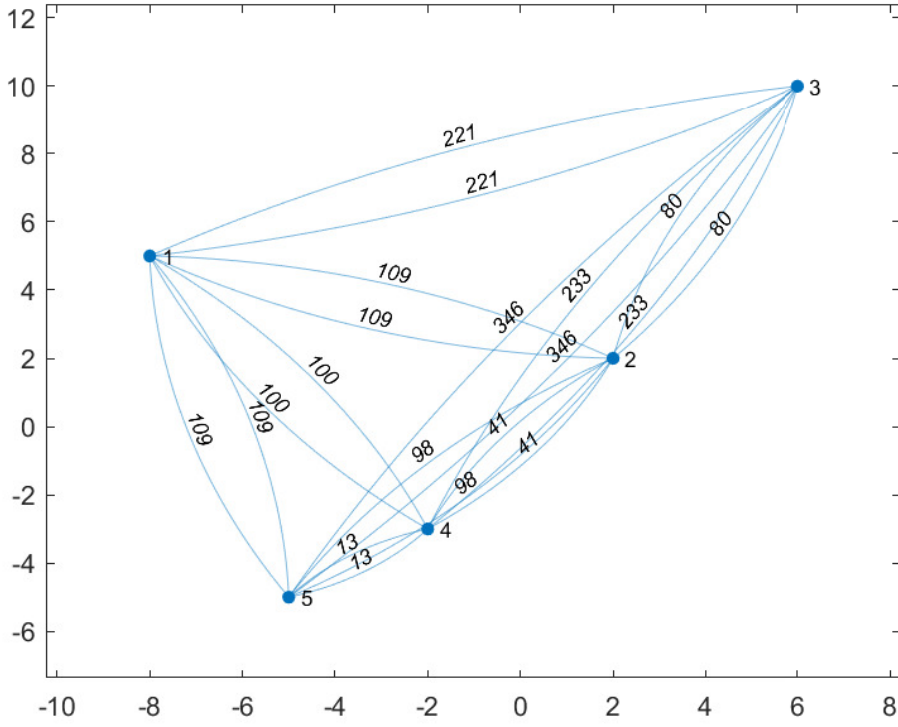


Figure 4.2: Nodes show that the locations of the 5 CH robots. The weight of a link shows the square of distance between the two nodes connected via that link.

those battery capacities does not desist from visiting CH 1 robot.

4.3.1.4 Optimal Strategy with Priors Set {CH 1, 2}

If the priority set consists of CH robot 1 and CH robot 2, then the UAV must visit CH robot 1 and 2, for which it needs

$$\begin{aligned}
 E_{UAV}^{\pi^*}(u) &= \|\xi_0 - \xi_1\| + \|\xi_1 - \xi_2\| + \|\xi_2 - \xi_0\| \\
 &= (\sqrt{89} + \sqrt{109} + \sqrt{8}) \times C_{UAV} \\
 &\approx 22.70 \times C_{UAV}
 \end{aligned} \tag{4.7}$$

which means that the battery capacities $B = 5, 10, 15, 20 \times C_{UAV} < 22.70 \times C_{UAV}$ are not feasible. For $B = 45, 50 \times C_{UAV}$, UAV can visit all CH robots as the case with no priority set, i.e., $E_{ACH}^{\pi^*}(u) = 0$. For $B = 30, 35, 40 \times C_{UAV}$, the optimal strategy

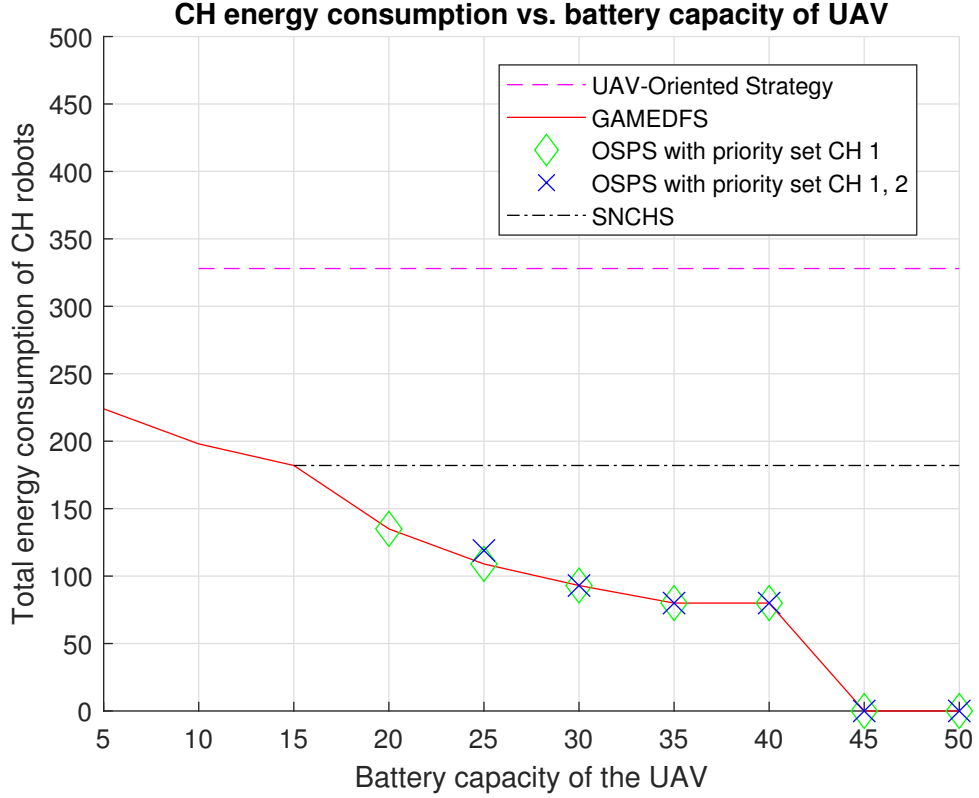


Figure 4.3: Total energy consumption of the 5 CH robots in Figure 4.2 under UAV-Oriented strategy, GAMEDFS, OSPS and SNCHS for varying battery capacities of the UAV from $B = 5 \times C_{UAV}$ to $B = 50 \times C_{UAV}$. The units for energy consumption of the UAV and total energy consumption of the nonvisited CH robots are C_{UAV} and C_{CH} , respectively. These constants depend on the type of the UAV and the CH robots.

with priority set of CH 1 and 2 is same with the optimal strategy with priority set of CH 1 because UAV with those battery capacities desists from visiting neither CH 1 nor CH 2. However, for $B = 25 \times C_{UAV}$, optimal strategy with priority set of CH 1 and 2 differs from optimal strategy with priority set of CH 1. By applying optimal strategy with priority set of CH1, UAV with $B = 25 \times C_{UAV}$ desists from visiting CH 3, 4 and 5 instead of desisting from CH 2, 3 and 5. In this case, total energy consumption of CH robots is

$$\begin{aligned}
 E_{ACH}^{\pi^*}(u) &= [\|\xi_4 - \xi_0\|^2 + (\|\xi_5 - \xi_4\|^2 + \|\xi_4 - \xi_0\|^2) + \|\xi_3 - \xi_2\|^2] \\
 &= [13 + (13 + 13) + 80] \times C_{CH} \\
 &= 119 \times C_{CH}
 \end{aligned} \tag{4.8}$$

Table 4.1: The table shows indices of the nonvisited CH robots depending on battery capacity of UAV and priority set in the 5-CH robot scenario in Figure 4.2. "None" implies that UAV visits all CH robots if $B = 45$ or $B = 50$. "no priority" means that UAV can desist from any CH robots. "×" implies that visiting that priority set with that battery capacity is infeasible.

Priority set	B=5	B=10	B=15	B=20	B=25
no priority	1-5	1-3,5	1,3,5	2-5	2,3,5
CH 1	×	×	×	2-5	2,3,5
CH 1,2	×	×	×	×	3,4,5
Priority set	B=30	B=35	B=40	B=45	B=50
no priority	3,5	3	3	None	None
CH 1	3,5	3	3	None	None
CH 1,2	3,5	3	3	None	None

Table 4.2: The table shows the total energy consumption of nonvisited CH robots depending on battery capacity of UAV and priority set in the 5-CH robot scenario in Figure 4.2. "no priority" means that UAV can desist from any CH robots. "×" implies that visiting that priority set with that battery capacity is infeasible.

Priority set	B=5	B=10	B=15	B=20	B=25
no priority	224	198	182	135	109
CH 1	×	×	×	135	109
CH 1,2	×	×	×	×	119
Priority set	B=30	B=35	B=40	B=45	B=50
no priority	93	80	80	0	0
CH 1	93	80	80	0	0
CH 1,2	93	80	80	0	0

4.3.1.5 Selecting Nearest Cluster Heads Strategy (SNCHS)

UAV selects the nearest two CH robots, CH robot 2 and 4 in this scenario. Therefore, UAV with $B = 15 \times C_{UAV}$ desists from visiting CH robot 1, 3 and 5 which results in

$$\begin{aligned} E_{ACH}^{\pi^*}(u) &= (80 + 13 + 89) \times C_{CH} \\ &= 182 \times C_{CH} \end{aligned} \quad (4.9)$$

and $E_{UAV}^{\pi^*}(u) \approx 12.84 \times C_{UAV}$, under which value SNCHS is not applicable.

4.3.1.6 Performance Comparison

We compare the performances of UAV-Oriented strategy, GAMEDFS, OSPS and SNCHS for battery capacities varying from $B = 5$ to $B = 50$ in the configuration in Figure 4.2. From Figure 4.3, the following observations can be made. Even for $B = 20$, optimal strategy consumes nearly half of the energy consumed by UAV-Oriented strategy. Besides this, SNCHS consumes nearly half of the energy consumed by UAV-Oriented strategy. For $B = 15$, SNCHS coincides with GAMEDFS.

4.3.2 7-CH case

Figure 4.4 shows the locations of the 7 CH robots and the weights of the links between them. With respect to initial position of UAV $(0,0)$, positions of CH robots are $(\xi_1, \xi_2, \xi_3, \xi_4, \xi_5, \xi_6, \xi_7) = ((9, 6), (3, 9), (3, 2), (7, 8), (8, -1), (7, 5), (2, 2)) m$.

4.3.2.1 UAV-Oriented Strategy

By applying UAV-Oriented strategy, UAV travels only to CH robot 6 ($\xi_6 = (7, 5)$) and collects all data of the CH robots from there if

$$\begin{aligned} B &= 2 \times \|\xi_6 - \xi_0\| \\ &= (2 \times \sqrt{(7-0)^2 + (5-0)^2}) \times C_{UAV} \\ &\approx 17.2 \times C_{UAV} \\ &< 20 \times C_{UAV}, \end{aligned} \quad (4.10)$$

In this case, total energy consumption of CH robots is $E_{ACH}^{\pi^{UAV-Oriented}}(u) = 142 \times C_{CH}$. If $B = 10$ or $B = 15$, the UAV can travel to CH robot 3, closer to the origin than CH robot 6, which results in $E_{ACH}^{\pi^{UAV-Oriented}}(u) = 213 \times C_{CH}$. However, if $B = 5$, UAV-oriented strategy is not applicable since UAV can visit no CH robot.

4.3.2.2 Optimal Strategy with no priority set (GAMEDFS)

The performance of optimal strategy with no priority set (equivalent to GAMEDFS proposed in Chapter 3) with battery capacities varying from $B = 5$ to $B = 50$ in the configuration in Figure 4.4. In Figure 4.5, by applying optimal strategy, UAV with $B = 35 \times C_{UAV}$ or $B = 40 \times C_{UAV}$ or $B = 45 \times C_{UAV}$ or $B = 50 \times C_{UAV}$ can visit all CH robots, i. e., $E_{ACH}^{\pi^{GAMEDFS}}(u) = 0$. In the configuration in Figure 4.4, the energy required for UAV to visit all CH robots is $E_{UAV}^{\pi^{GAMEDFS}}(u) \approx 34.42 \times C_{UAV}$. UAV with $B = 30 \times C_{UAV}$ desists from visiting CH robot 5 which results in $E_{ACH}^{\pi^{GAMEDFS}}(u) = 34 \times C_{CH}$ and $E_{UAV}^{\pi^{GAMEDFS}}(u) \approx 27.50 \times C_{UAV}$. UAV with $B = 25 \times C_{UAV}$ desists from visiting CH robot 1, 2, 4 and 5 which results in $E_{ACH}^{\pi^{GAMEDFS}}(u) = 51 \times C_{CH}$ and $E_{UAV}^{\pi^{GAMEDFS}}(u) \approx 24.52 \times C_{UAV}$. UAV with $B = 20 \times C_{UAV}$ desists from visiting CH robot 1, 2, 4 and 5 which results in $E_{ACH}^{\pi^{GAMEDFS}}(u) = 74 \times C_{CH}$ and $E_{UAV}^{\pi^{GAMEDFS}}(u) \approx 17.43 \times C_{UAV}$. UAV with $B = 10 \times C_{UAV}$ or $B = 15 \times C_{UAV}$ desists from visiting CH robot 1, 2, 4, 5 and 6 which results in $E_{ACH}^{\pi^{GAMEDFS}}(u) = 173 \times C_{CH}$ and $E_{UAV}^{\pi^{GAMEDFS}}(u) \approx 7.43 \times C_{UAV}$. UAV with $B = 5 \times C_{UAV}$ can visit no CH robot which results in $E_{ACH}^{\pi^{GAMEDFS}}(u) = 234 \times C_{CH}$. *Even visiting no CH robot, optimal strategy performs better than no strategy.*

4.3.2.3 Optimal Strategy with Prior Set {CH 1}

If the priority set consists of CH 1, UAV must visit CH 1, for which it needs

$$\begin{aligned}
E_{UAV}^{\pi^*}(u) &= \|\xi_0 - \xi_1\| + \|\xi_1 - \xi_0\| \\
&= (2 \times \sqrt{117}) \times C_{UAV} \\
&\approx 21.63 \times C_{UAV}
\end{aligned} \tag{4.11}$$

which means that the battery capacities $B = 5, 10, 15, 20, 25 \times C_{UAV} < 21.63 \times C_{UAV}$ are not feasible. For $B = 35, 40, 45, 50 \times C_{UAV}$, UAV can visit all CH robots as the

case with no priority set, i. e., $E_{ACH}^{\pi^*}(u) = 0$. For $B = 25, 30 \times C_{UAV}$, the optimal strategy with priority set of CH1 robot is same with GAMEDFS because UAV with those battery capacities does not desist from visiting CH 1 robot.

4.3.2.4 Optimal Strategy with Priori Set {CH 1, 2}

If the priority set consists of CH robot 1 and 2, the UAV must visit CH robot 1 and 2, for which it needs

$$\begin{aligned}
 E_{UAV}^{\pi^*}(u) &= \|\xi_0 - \xi_1\| + \|\xi_1 - \xi_2\| + \|\xi_2 - \xi_0\| \\
 &= (\sqrt{117} + \sqrt{45} + \sqrt{90}) \times C_{UAV} \\
 &\approx 27.01 \times C_{UAV}
 \end{aligned} \tag{4.12}$$

which means that the battery capacities $B = 5, 10, 15, 20 \times C_{UAV} < 27.01 \times C_{UAV}$ are not feasible. For $B = 35, 40, 45, 50 \times C_{UAV}$, UAV can visit all CH robots as GAMEDFS, i. e., $E_{ACH}^{\pi^*}(u) = 0$. For $B = 30 \times C_{UAV}$, the optimal strategy with priority set of CH 1 and 2 is same with the optimal strategy with priority set of CH 1 since UAV with those battery capacities desists from visiting neither CH 1 nor CH 2.

4.3.2.5 Optimal Strategy with Priori Set {CH 1, 2, 3}

If the priority set consists of CH robot 1, 2 and 3, then the UAV must visit CH robot 1, 2 and 3, for which it needs

$$\begin{aligned}
 E_{UAV}^{\pi^*}(u) &= \|\xi_0 - \xi_3\| + \|\xi_3 - \xi_1\| + \|\xi_1 - \xi_2\| + \|\xi_2 - \xi_0\| \\
 &= (\sqrt{13} + \sqrt{52} + \sqrt{45} + \sqrt{90}) \times C_{UAV} \\
 &\approx 27.01 \times C_{UAV}
 \end{aligned} \tag{4.13}$$

which means that the battery capacities $B = 5, 10, 15, 20, 25 \times C_{UAV} < 27.01 \times C_{UAV}$ are not feasible. For $B = 35, 40, 45, 50 \times C_{UAV}$, UAV can visit all CH robots as the case with no priority set, i. e., $E_{ACH}^{\pi^*}(u) = 0$. For $B = 30 \times C_{UAV}$, the optimal strategy with priority set of CH 1, 2 and 3 is same with the optimal strategy with priority set of CH 1 and 2 because UAV with those battery capacities desists from visiting none of CH 1, 2, 3.

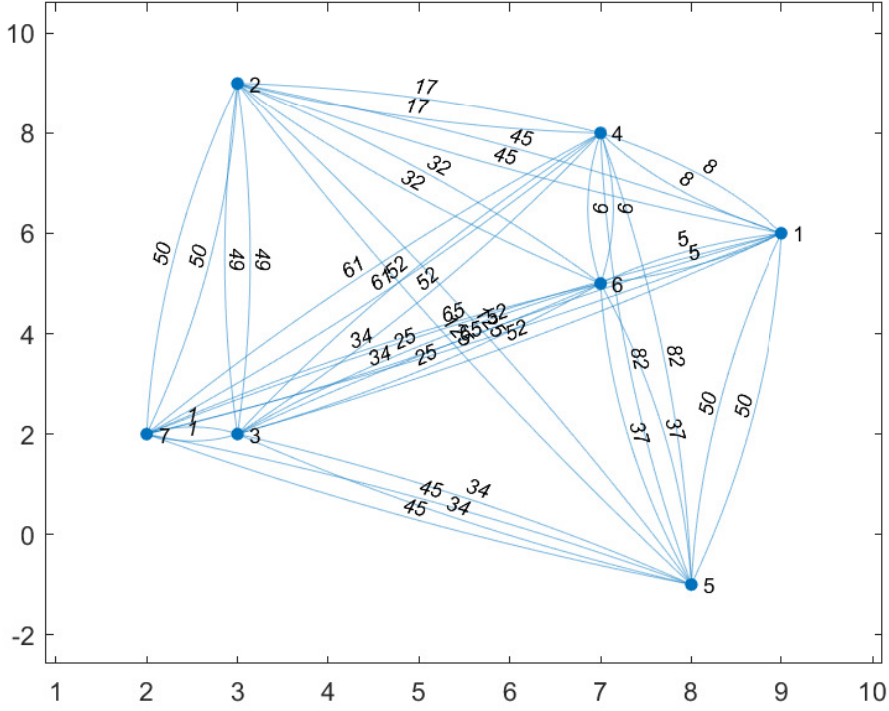


Figure 4.4: Nodes show that the locations of the 7 CH robots. The weight of a link shows the square of distance between the two nodes connected via that link.

4.3.2.6 Selecting Nearest Cluster Heads Strategy (SNCHS)

UAV selects the nearest 3 CH robots which are CH robot 3, 5, 7 in this 7-CH robot scenario. Therefore, UAV desists from visiting CH robot 1, 2, 4, 6 which results in

$$\begin{aligned}
 E_{ACH}^{\pi^*}(u) &= [(5 + 25 + 1 + 8) + (50 + 8) + (9 + 25 + 1 + 8) + (25 + 1 + 8)] \times C_{CH} \\
 &= 164 \times C_{CH}
 \end{aligned} \tag{4.14}$$

total energy consumption. Thus, UAV consumes

$$\begin{aligned}
 E_{UAV}^{\pi^*}(u) &= \|\xi_0 - \xi_7\| + \|\xi_7 - \xi_3\| + \|\xi_3 - \xi_5\| + \|\xi_5 - \xi_0\| \\
 &= (\sqrt{8} + 1 + \sqrt{34} + \sqrt{65}) \times C_{UAV} \\
 &\approx 17.72 \times C_{UAV},
 \end{aligned} \tag{4.15}$$

which implies SNCHS is feasible if $B \geq 17.72 \times C_{UAV}$.

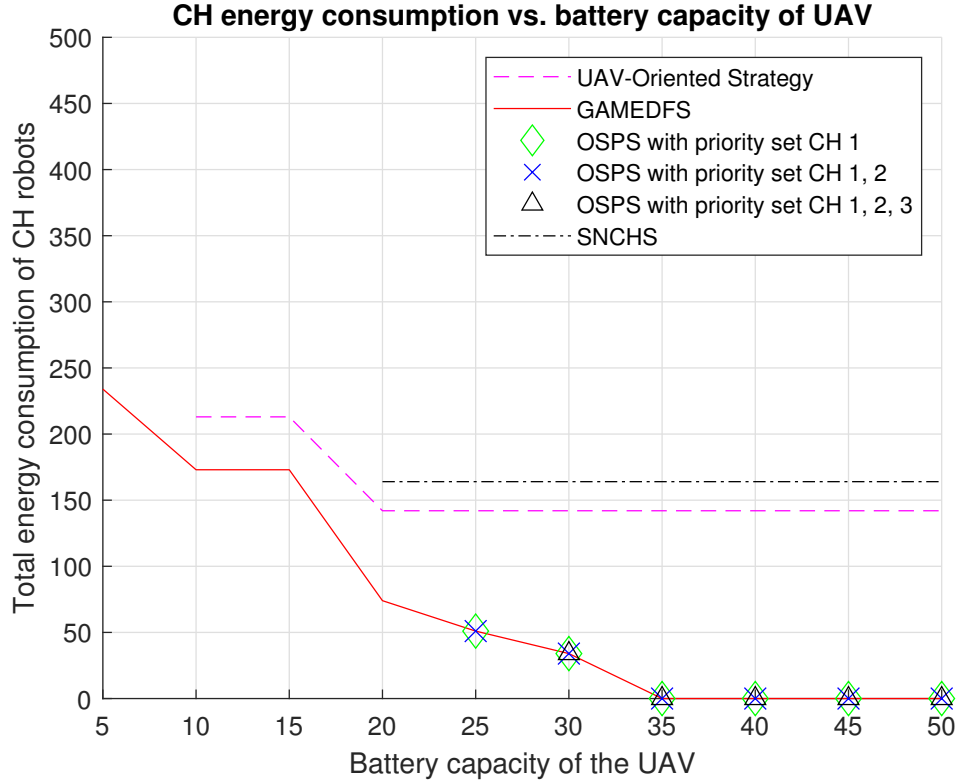


Figure 4.5: The total energy consumption of the 7 CH robots in Figure 4.4 under UAV-Oriented Strategy, GAMEDFS, OSPS and SNCHS for varying battery capacities of the UAV from $B = 5 \times C_{UAV}$ to $B = 50 \times C_{UAV}$. The units for energy consumption of the UAV and total energy consumption of the nonvisited CH robots are C_{UAV} and C_{CH} , respectively. These constants depend on the type of the UAV and the CH robots.

4.3.2.7 Performance Comparison

We compare the performances of UAV-Oriented strategy and our optimal strategy for battery capacity varying from $B = 5$ to $B = 50$ in configuration in Figure 4.4. From Table 4.4 and Figure 4.4, optimal strategy performs much better than UAV-Oriented strategy. Even for $B = 20$, optimal strategy consumes nearly half of the energy consumed by UAV-Oriented strategy. On the other hand, SNCHS consumes more than the energy consumed by UAV-Oriented strategy.

Table 4.3: The table shows indices of the nonvisited CH robots depending on battery capacity of the UAV and the priority set in the 7-CH robot scenario in Figure 4.4. "None" implies that UAV visits all CH robots if $B = 35, 40, 45, 50$. "no priority" means that the UAV can desist from any CH robots. "×" implies that visiting that priority set with that battery capacity is infeasible.

Priority set	B=5	B=10	B=15	B=20	B=25
no priority	1-7	1,2,4-6	1,2,4-6	1,2,4,5	2,5
CH 1	×	×	×	×	2,5
CH 1,2	×	×	×	×	×
CH 1-3	×	×	×	×	×
Priority set	B=30	B=35	B=40	B=45	B=50
no priority	5	None	None	None	None
CH 1	5	None	None	None	None
CH 1,2	5	None	None	None	None
CH 1-3	5	None	None	None	None

4.3.3 10-CH case

In Figure 4.6 shows locations of the 10 CH robots and weights of links between them. With respect to this initial position of UAV (0,0), positions of CH robots are $(\xi_1, \xi_2, \xi_3, \xi_4, \xi_5, \xi_6, \xi_7, \xi_8, \xi_9, \xi_{10}) = ((6, -7), (-5, 3), (2, 4), (-4, 7), (-2, 2), (2, -7), (-1, -2), (4, -8), (-1, 5), (7, -6))m$.

4.3.3.1 UAV-Oriented Strategy

By applying UAV-Oriented strategy, the UAV travels only to CH robot 7 ($\xi_7 = (-1, -2)$) and collects all data of the CH robots from there if

$$\begin{aligned}
B &= 2 \times \|\xi_7 - \xi_0\| \\
&= (2 \times \sqrt{(-1-0)^2 + (2-0)^2}) \times C_{UAV} \\
&\approx 4.47 \times C_{UAV} \\
&< 5 \times C_{UAV},
\end{aligned} \tag{4.16}$$

Table 4.4: The table shows the total energy consumption of the nonvisited CH robots depending on battery capacity of the UAV and the priority set in the 7-CH robot scenario in Figure 4.4. "no priority" means that the UAV can desist from any CH robots. "×" implies that visiting that priority set with that battery capacity is infeasible.

Priority set	B=5	B=10	B=15	B=20	B=25
no priority	234	173	173	74	51
CH 1	×	×	×	×	51
CH 1,2	×	×	×	×	×
CH 1-3	×	×	×	×	×
Priority set	B=30	B=35	B=40	B=45	B=50
no priority	34	0	0	0	0
CH 1	34	0	0	0	0
CH 1,2	34	0	0	0	0
CH 1-3	34	0	0	0	0

In this case, total energy consumed by CH robots is $E_{ACH}^{\pi^{UAV-Oriented}}(u) = 491 \times C_{CH}$.

4.3.3.2 Optimal Strategy with no priori set (GAMEDFS)

The performance of optimal strategy with no priority set (equivalent to GAMEDFS proposed in Chapter 3) with battery capacities varying from $B = 5$ to $B = 50$ in the configuration in Figure 4.6. In Figure 4.7, by applying optimal strategy, the UAV with $B = 45 \times C_{UAV}$ or $B = 50 \times C_{UAV}$ can visit all CH robots, i. e., $E_{ACH}^{\pi^{GAMEDFS}}(u) = 0$. In the configuration in Figure 4.6, the minimum energy required for the UAV to visit all CH robots is $E_{UAV}^{\pi^{GAMEDFS}}(u) \approx 42.02 \times C_{UAV}$.

The UAV with $B = 40 \times C_{UAV}$ desists from visiting CH robot 2 which results in $E_{ACH}^{\pi^{GAMEDFS}}(u) = 10 \times C_{CH}$ and $E_{UAV}^{\pi^{GAMEDFS}}(u) \approx 39.21 \times C_{UAV}$. The UAV with $B = 35 \times C_{UAV}$ desists from visiting CH robot 2 and 4 which results in $E_{ACH}^{\pi^{GAMEDFS}}(u) = 23 \times C_{CH}$ and $E_{UAV}^{\pi^{GAMEDFS}}(u) \approx 34.29 \times C_{UAV}$. The UAV with $B = 30 \times C_{UAV}$ desists from visiting CH robot 2, 3, 4 and 9 which results in $E_{ACH}^{\pi^{GAMEDFS}}(u) = 63 \times C_{CH}$ and $E_{UAV}^{\pi^{GAMEDFS}}(u) \approx 28.83 \times C_{UAV}$. The UAV with

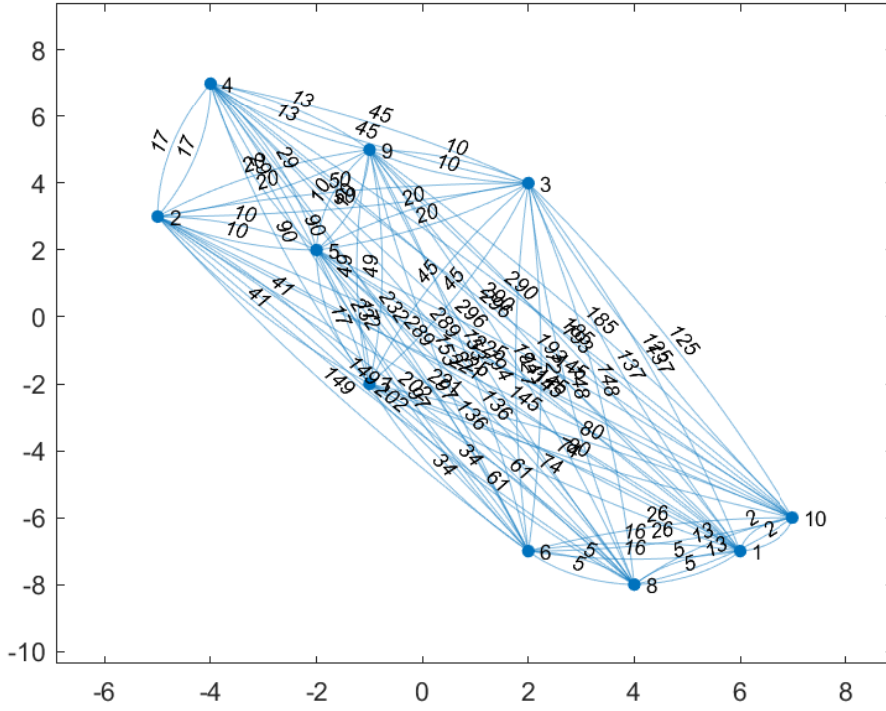


Figure 4.6: Nodes show that the locations of the 10 CH robots. The weight of a link shows the square of distance between the two nodes connected via that link.

$B = 25 \times C_{UAV}$ desists from visiting CH robot 2, 3, 4, 5 and 9 which results in $E_{ACH}^{\pi^{GAMEDFS}}(u) = 103 \times C_{CH}$ and $E_{UAV}^{\pi^{GAMEDFS}}(u) \approx 23.17 \times C_{UAV}$. The UAV with $B = 20 \times C_{UAV}$ desists from visiting CH robot 1, 2, 3, 4, 5, 9 and 10 which results in $E_{ACH}^{\pi^{GAMEDFS}}(u) = 115 \times C_{CH}$ and $E_{UAV}^{\pi^{GAMEDFS}}(u) \approx 19.25 \times C_{UAV}$. The UAV with $B = 15 \times C_{UAV}$ visits only CH robot 6 which results in $E_{ACH}^{\pi^{GAMEDFS}}(u) = 135 \times C_{CH}$ and $E_{UAV}^{\pi^{GAMEDFS}}(u) \approx 14.56 \times C_{UAV}$. The UAV with $B = 10 \times C_{UAV}$ visits only CH robot 5 and 7 which results in $E_{ACH}^{\pi^{GAMEDFS}}(u) = 334 \times C_{CH}$ and $E_{UAV}^{\pi^{GAMEDFS}}(u) \approx 9.19 \times C_{UAV}$. The UAV with $B = 5 \times C_{UAV}$ visit only CH robot 7 which results in $E_{ACH}^{\pi^{GAMEDFS}}(u) = 342 \times C_{CH}$ and $E_{UAV}^{\pi^{GAMEDFS}}(u) \approx 4.47 \times C_{UAV}$. Even with $B = 5$, optimal strategy performs better than no strategy and UAV-oriented strategy.

4.3.3.3 Optimal Strategy with Priori Set {CH 1}

If the priority set consists of CH 1, UAV must visit CH 1, for which it needs

$$\begin{aligned}
E_{UAV}^{\pi^*}(u) &= \|\xi_0 - \xi_1\| + \|\xi_1 - \xi_0\| \\
&= (2 \times \sqrt{85}) \times C_{UAV} \\
&\approx 18.44 \times C_{UAV}
\end{aligned} \tag{4.17}$$

which means that the battery capacities $B = 5, 10, 15 \times C_{UAV} < 18.44 \times C_{UAV}$ are not feasible. For $B = 45, 50 \times C_{UAV}$, UAV can visit all CH robots as the case with no priority set, i. e., $E_{ACH}^{\pi^*}(u) = 0$. For $B = 25, 30, 35, 40 \times C_{UAV}$, the optimal strategy with priority set of CH robot 1 is same with GAMEDFS because UAV with those battery capacities does not desist from visiting CH 1 robot. However, for $B = 20 \times C_{UAV}$, optimal strategy with priority set of CH1 differs from optimal strategy with no priority set. By applying the optimal strategy with priority set of CH robot 1, UAV with $B = 20 \times C_{UAV}$ desists from visiting CH 2, 3, 4, 5, 6, 7, 8 and 9 instead of desisting from CH 1, 2, 3, 4, 5, 9 and 10. In this case, the energy consumption of CH robots is

$$\begin{aligned}
E_{ACH}^{\pi^*}(u) &= [(\|\xi_2 - \xi_5\|^2 + \|\xi_5 - \xi_0\|^2) + \|\xi_3 - \xi_0\|^2 + \|\xi_5 - \xi_0\|^2 + (\|\xi_4 - \xi_5\|^2 \\
&\quad + \|\xi_5 - \xi_0\|^2) + \|\xi_7 - \xi_0\|^2 + (\|\xi_6 - \xi_8\|^2 + \|\xi_8 - \xi_1\|^2) + (\|\xi_9 - \xi_5\|^2 \\
&\quad + \|\xi_5 - \xi_0\|^2) + \|\xi_8 - \xi_1\|^2 \\
&= [(10 + 8) + 20 + 8 + (20 + 8) + 5 + (5 + 5) + 5 + (10 + 8)] \times C_{CH} \\
&= 112 \times C_{CH}
\end{aligned} \tag{4.18}$$

4.3.3.4 Optimal Strategy with Priori Set {CH 1, 2}

If the priority set consists of CH robot 1 and 2, then the UAV must visit CH robot 1 and 2, for which it needs

$$\begin{aligned}
E_{UAV}^{\pi^*}(u) &= \|\xi_0 - \xi_1\| + \|\xi_1 - \xi_2\| + \|\xi_2 - \xi_0\| \\
&= (\sqrt{85} + \sqrt{221} + \sqrt{34}) \times C_{UAV} \\
&\approx 29.92 \times C_{UAV}
\end{aligned} \tag{4.19}$$

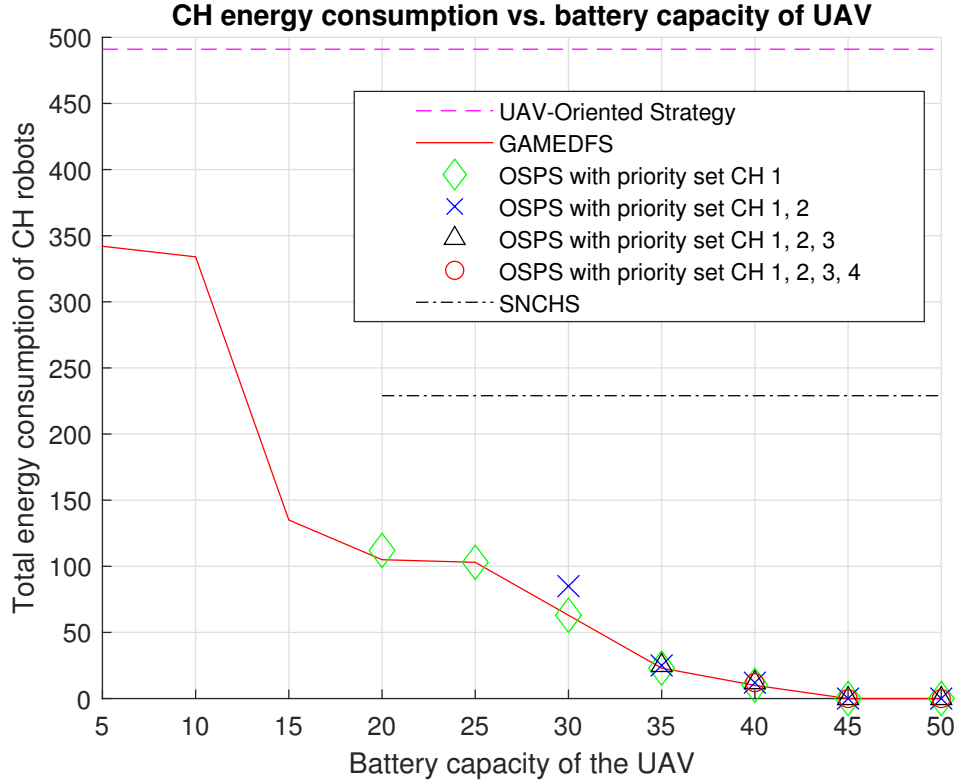


Figure 4.7: The total energy consumption of the 10 CH robots in Figure 4.6 under UAV-oriented Strategy, GAMEDFS, OSPS and SNCHS for varying battery capacities of the UAV from $B = 5 \times C_{UAV}$ to $B = 50 \times C_{UAV}$. The units for energy consumption of the UAV and total energy consumption of the nonvisited CH robots are C_{UAV} and C_{CH} , respectively. These constants depend on the type of the UAV and the CH robots.

which means that the battery capacities $B = 5, 10, 15, 20, 25 \times C_{UAV} < 29.92 \times C_{UAV}$ are not feasible. For $B = 45, 50 \times C_{UAV}$, UAV can visit all CH robots as the case with no priority set, i.e., $E_{ACH}^{\tau^*}(u) = 0$. However, for $B = 30, 35, 40 \times C_{UAV}$, the optimal strategy with priority set of CH 1 and 2 differs from the optimal strategy with priority set of CH 1 because UAV with those battery capacities cannot desist from visiting not only CH 1 but also CH 2. By applying optimal strategy with priority set of CH 1 and CH 2, UAV with $B = 40 \times C_{UAV}$ desists from visiting CH 6, 7 and 10 instead of desisting from CH 2. In this case, total energy consumed by CH robots is

$$\begin{aligned}
E_{ACH}^{\pi^*}(u) &= \|\xi_7 - \xi_0\|^2 + \|\xi_6 - \xi_8\|^2 + \|\xi_{10} - \xi_1\|^2 \\
&= [5 + 5 + 2] \times C_{CH} \\
&= 12 \times C_{CH}
\end{aligned} \tag{4.20}$$

By applying optimal strategy with priority set of CH 1 and 2, UAV with $B = 35 \times C_{UAV}$ desists from visiting CH 4, 6, 7 and 10 instead of desisting from CH 2 and 4. In this case, the energy consumption of CH robots is

$$\begin{aligned}
E_{ACH}^{\pi^*}(u) &= \|\xi_7 - \xi_0\|^2 + \|\xi_6 - \xi_8\|^2 + \|\xi_{10} - \xi_1\|^2 + \|\xi_4 - \xi_9\|^2 \\
&= [5 + 5 + 2 + 13] \times C_{CH} \\
&= 25 \times C_{CH}
\end{aligned} \tag{4.21}$$

By applying optimal strategy with priority set of CH 1, 2 and 3, UAV with $B = 30 \times C_{UAV}$ desists from visiting CH 3, 4, 5, 6, 7, 8, 9 and 10 instead of desisting from CH 2, 3, 4 and 9. In this case, total energy consumption of CH robots is

$$\begin{aligned}
E_{ACH}^{\pi^*}(u) &= \|\xi_4 - \xi_2\|^2 + \|\xi_5 - \xi_0\|^2 + \|\xi_3 - \xi_0\|^2 + (\|\xi_9 - \xi_5\|^2 + \|\xi_5 - \xi_0\|^2) \\
&\quad + \|\xi_7 - \xi_0\|^2 + (\|\xi_6 - \xi_8\|^2 + \|\xi_8 - \xi_1\|^2) + \|\xi_8 - \xi_1\|^2 + \|\xi_{10} - \xi_1\|^2 \\
&= [17 + 8 + 20 + (10 + 8) + 5 + (5 + 5) + 5 + 2] \times C_{CH} \\
&= 85 \times C_{CH}
\end{aligned} \tag{4.22}$$

4.3.3.5 Optimal Strategy with Priors Set {CH 1, 2, 3}

If the priority set consists of CH robot 1, 2 and 3, then the UAV must visit CH robot 1, 2 and 3, for which it needs

$$\begin{aligned}
E_{UAV}^{\pi^*}(u) &= \|\xi_0 - \xi_1\| + \|\xi_1 - \xi_3\| + \|\xi_3 - \xi_2\| + \|\xi_2 - \xi_0\| \\
&= (\sqrt{85} + \sqrt{137} + \sqrt{50} + \sqrt{34}) \times C_{UAV} \\
&\approx 33.83 \times C_{UAV}
\end{aligned} \tag{4.23}$$

which means that the battery capacities $B = 5, 10, 15, 20, 25, 30 \times C_{UAV} < 33.83 \times C_{UAV}$ are not feasible. For $B = 45, 50 \times C_{UAV}$, UAV can visit all CH robots as the case with no priority set, i.e., $E_{ACH}^{\pi^*}(u) = 0$. For $B = 35, 40 \times C_{UAV}$, optimal strategy

with priority set of CH 1, 2 and 3 is the same as optimal strategy with priority set of CH 1 and 2 because UAV with those battery capacities does not desist from visiting none of CH 1, 2 and 3.

4.3.3.6 Optimal Strategy with Priori Set {CH 1, 2, 3, 4}

If the priority set consists of CH robot 1, 2, 3 and 4, then the UAV must visit CH robot 1, 2, 3 and 4, for which it needs

$$\begin{aligned}
E_{UAV}^{\pi^*}(u) &= \|\xi_0 - \xi_1\| + \|\xi_1 - \xi_3\| + \|\xi_3 - \xi_4\| + \|\xi_4 - \xi_2\| + \|\xi_2 - \xi_0\| \\
&= (\sqrt{85} + \sqrt{137} + \sqrt{45} + \sqrt{17} + \sqrt{34}) \times C_{UAV} \\
&\approx 37.59 \times C_{UAV}
\end{aligned} \tag{4.24}$$

which means that the battery capacities $B = 5, 10, 15, 20, 25, 30, 35 \times C_{UAV} < 37.59 \times C_{UAV}$ are not feasible. For $B = 45, 50 \times C_{UAV}$, UAV can visit all CH robots as the case with no priority set, i.e., $E_{ACH}^{\pi^*}(u) = 0$. For $B = 40 \times C_{UAV}$, optimal strategy with priority set of CH 1, 2, 3 and 4 is the same as optimal strategy with priority set of CH 1, 2 and 3 because UAV with those battery capacities does not desist from visiting none of CH 1, 2, 3 and 4.

4.3.3.7 Selecting Nearest Cluster Heads Strategy (SNCHS)

UAV selects the nearest 4 CH robots, CH robot 3, 5, 7, 9 in this 7-CH robot scenario. Therefore, UAV desists from visiting CH robot 1, 2, 4, 6, 8, 10 which results in

$$\begin{aligned}
E_{ACH}^{\pi^*}(u) &= [(5 + 5 + 34 + 5) + (10 + 8) + (20 + 8) + (34 + 5) + (5 + 34 + 5) \\
&\quad + (2 + 5 + 5 + 34 + 5)] \times C_{CH} \\
&= 229 \times C_{CH}
\end{aligned} \tag{4.25}$$

total energy consumption. Thus, UAV consumes

$$\begin{aligned}
E_{UAV}^{\pi^*}(u) &= \|\xi_0 - \xi_7\| + \|\xi_7 - \xi_5\| + \|\xi_5 - \xi_9\| \\
&\quad + \|\xi_9 - \xi_3\| + \|\xi_3 - \xi_0\| \\
&= [\sqrt{5} + \sqrt{17} + \sqrt{10} + \sqrt{10} + \sqrt{20}] \times C_{UAV} \\
&\approx 17.16 \times C_{UAV},
\end{aligned} \tag{4.26}$$

which implies SNCHS is feasible if $B \geq 17.16 \times C_{UAV}$.

Table 4.5: The table shows indices of the nonvisited CH robots depending on battery capacity of UAV and priority set in the 10-CH robot scenario in Figure 4.6. "None" implies that UAV visits all CH robots if $B = 45$ or $B = 50$. "no priority" means that UAV can desist from any CH robots. "×" implies that visiting that priority set with that battery capacity is infeasible.

Priority set	B=5	B=10	B=15	B=20	B=25
no priority	1-6,8-10	1-4,6,8-10	1-5,7-10	1-5,9,10	2-5,9
CH 1	×	×	×	2-9	2-5,9
CH 1,2	×	×	×	×	×
CH 1-3	×	×	×	×	×
CH 1-4	×	×	×	×	×
	B=30	B=35	B=40	B=45	B=50
no priority	2-4,9	2,4	2	None	None
CH 1	2-4,9	2,4	2	None	None
CH 1,2	3-10	4,6,7,10	6,7,10	None	None
CH 1-3	×	4,6,7,10	6,7,10	None	None
CH 1-4	×	×	6,7,10	None	None

4.3.3.8 Performance Comparison

In this subsection, we compare the performances of UAV-Oriented strategy and our optimal strategy with various priority sets for battery capacities varying from $B = 5$ to $B = 50$ in the configuration in Figure 4.6. From Table 4.6 and Figure 4.6, optimal strategy performs much better than UAV-Oriented strategy. Even for $B = 15$, optimal strategy consumes nearly one fourth of the energy consumed by UAV-Oriented strategy. Besides this, SNCHS consumes less than half of the energy consumed by UAV-Oriented strategy.

Table 4.6: The table shows total energy consumption of (the nonvisited) CH robots depending on battery capacity of UAV and priority set in the 10-CH robot scenario in Figure 4.6. "no priority" means that UAV can desist from any CH robots. "×" implies that visiting that priority set with that battery capacity is infeasible.

Priority set	B=5	B=10	B=15	B=20	B=25
no priority	342	334	135	105	103
CH 1	×	×	×	112	103
CH 1,2	×	×	×	×	×
CH 1-3	×	×	×	×	×
CH 1-4	×	×	×	×	×
Priority set	B=30	B=35	B=40	B=45	B=50
no priority	63	23	10	0	0
CH 1	63	23	10	0	0
CH 1,2	85	25	12	0	0
CH 1-3	×	25	12	0	0
CH 1-4	×	×	12	0	0

CHAPTER 5

EFFICIENCY-AWARE AND ENERGY-AWARE DATA COLLECTION VIA A UAV WITH LIMITED-CAPACITY BATTERY IN ROBOTIC WIRELESS SENSOR NETWORKS

5.1 System Model and Problem Definition

This section focuses on defining our problem and generates our system approach.

5.1.1 Motivation and Problem Definition

We will present here a motivating scenario and formulate the problem based on this motivation.

This chapter tackles an M -clustered robotic network and one UAV with limited-capacity battery. This network is responsible of collecting data from sensor nodes monitoring environmental changes.

In each cluster, a cluster head (CH) robot allocates tasks to cluster member (CM) robot nodes which execute their assigned tasks and send the resultant data (environmental monitoring data) to their own CH robot. *CH robots are responsible for collecting data from CM robots to send data to UAV. which visits a varying portion of CH robots depending on their locations, their data efficiencies and its battery capacity (Figure 5.1).* Unless UAV visits each CH robot, each nonvisited CH robot sends its data one nonvisited neighbor CH via multiple hops. $S \triangleq \{1, 2, \dots, M\}$ denotes the index set of CH robots. B denotes battery capacity of UAV.

CH robots consume large amount of energy for aggregating and transmitting its data

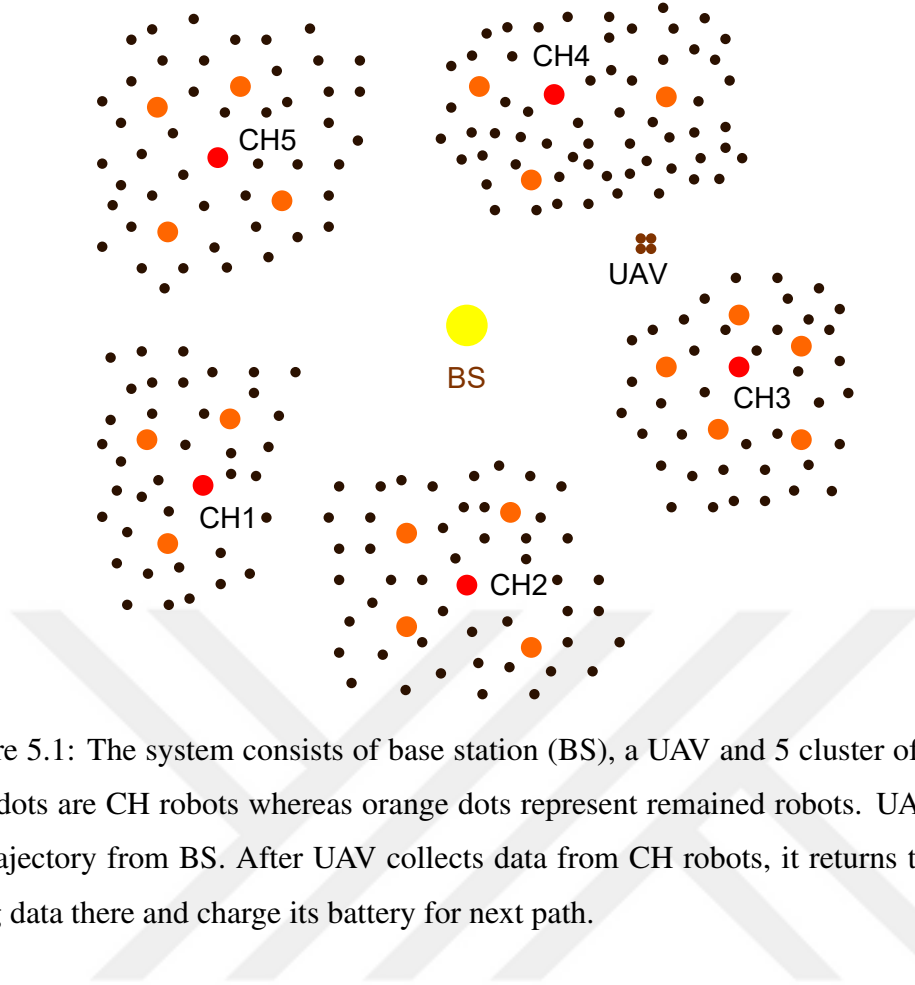


Figure 5.1: The system consists of base station (BS), a UAV and 5 cluster of robots. Red dots are CH robots whereas orange dots represent remained robots. UAV starts its trajectory from BS. After UAV collects data from CH robots, it returns to BS to bring data there and charge its battery for next path.

to their neighboring CH robots or UAV in case of not being visited by the UAV. If one CH robot moved like CM robot, energy remained in battery of that CH robot would decrease below the critical energy level quickly, which causes frequent CH election that consumes too much energy and time. Therefore, it may cause CH robots assigning CM robots with tasks very efficiently to give up serving as a CH robot. Hence, the following assumption is made.

Assumption 10. *For avoiding extra energy consumption, CH robots do not move while they performs as CH.*

Assumption 11. *Each CH robot has same amount of data to send to UAV or forward another CH robot without latency.*

$\xi_0 \triangleq (x_0, y_0)$ denotes initial position of UAV. $\xi_i \triangleq (x_i, y_i)$ denotes position of CH robot i . We assume that UAV consumes energy proportional to its travelled distance.

Its energy consumption from CH robot i to j is defined as

$$\begin{aligned} E_{UAV}(i, j) &\triangleq C_{UAV} \|\xi_i - \xi_j\| \\ &= C_{UAV} \sqrt{(x_i - x_j)^2 + (y_i - y_j)^2} \end{aligned} \quad (5.1)$$

where C_{UAV} is the constant ratio between its travelled distance and energy consumed by UAV. On the other hand, we assume that the energy consumed by a CH robot is proportional to the square of the distance between itself and the next hop. To illustrate, energy consumed by CH robot i to send data to the CH robot j is defined as

$$\begin{aligned} E_{CH}(i, j) &\triangleq C_{CH} \|\xi_i - \xi_j\|^2 \\ &= C_{CH} [(x_i - x_j)^2 + (y_i - y_j)^2] \end{aligned} \quad (5.2)$$

where C_{CH} is the constant ratio between the energy consumption of one CH robot and the square of distance between it and the next hop.

The related literature assumes that each CH node has enough energy for transmitting its data to base station, initial position of UAV. UAV may pass at close proximity of a CH robot during the path. In worst case, some CH robots can send their data to UAV while it is standing on the base station before starting trajectory. This motivate us to make Assumption 12.

Assumption 12. *CH robots have enough energy to send their data to UAV directly if the UAV stands at its initial position on the base station.*

Assumption 13. *CH robots sends data to UAV or another CH robot with constant rate.*

5.1.2 Problem Formulation

We aim at planning the path for UAV to fulfill with limited-capacity battery. By optimal path planning, UAV aims to minimize their total joint cost of data efficiencies and energy consumptions. To formulate our problem precisely, we make following definitions.

Definition 20. *Path Set, P , is set of all linear paths between initial position of UAV and positions of M CH robots, $P \triangleq \{p(\xi_0, \xi_1), p(\xi_0, \xi_2), \dots, p(\xi_0, \xi_M), \dots, p(\xi_i, \xi_j),$*

$\dots, p(\xi_M, \xi_{M-1})\}$ where $p(\xi_i, \xi_j)$ denotes the linear path from CH robot i to j and its length equals to $\|\xi_i - \xi_j\|$.¹

Definition 21. *Strategy of UAV, π is defined as set of linear paths that UAV follows to collect data, i.e., $\pi \subseteq P$.*

Definition 22. *Energy consumption of UAV with strategy π , E_{UAV}^π is energy consumed by UAV with strategy π , i. e.,*

$$E_{UAV}^\pi \triangleq \left[\sum_{j=1}^M \sum_{i=1}^M C_{UAV} \|\xi_i - \xi_j\| I_{\{p(\xi_i, \xi_j) \in \pi\}} \right], \quad (5.3)$$

where $I_{\{X\}}$ is an indicator function becoming 1 if X is true event.

Definition 23. *The set of nonvisited CH robots under strategy π is defined as the set of nonvisited CH robots under strategy π and it is denoted by S_{non}^π .*

Definition 24. *Energy consumed to forward data of CH robot i under strategy π , u_i , denoted by $E_i^\pi(u_i)$, is energy consumed for forwarding unit data of nonvisited CH robot i until a visited CH robot with data forwarding strategy u_i .²*

In our problem, all CH robots collect data from other cluster member (CM) robots in their clusters where these CM robots can collect data from sensor nodes surrounding them. Here, quality of data may vary depending on the sensors in different regions and the CM robots. As each CH robot can collect data from their CM members in different qualities, the efficiency of data may be different for different CH robots after each CH robot evaluates its collected data. In this work, we consider both energy consumed by CH robots and quality of data at CH robots. Therefore, we make the following definition.

Definition 25. *Data efficiency of CH robot i , denoted by η_i , is a quality measure of data evaluated by CH robot i ; it takes a value between 0 (0% efficient) and 1 (100% efficient).³*

¹ $p(\xi_0, \xi_j)$ is the linear path from initial position of UAV to CH robot j ; $p(\xi_i, \xi_0)$ is linear path from CH robot i to initial position of UAV.

² $E_i^\pi(u_i) = 0$ for each visited CH robot i under strategy π .

³ The variance between the amount of data collected by different CH robots can also be considered in this definition implicitly. For example, a new term can be defined as $\zeta_i \triangleq \eta_i \times D_i$ where D_i is the amount of data collected by CH robot i . As it can be seen, ζ_i instead of η_i makes no change in the structure of our problem.

Definition 26. *Total cost of CH robots under strategies π, u , denoted by $J(u, \pi)$, is defined as*

$$J(u, \pi) \triangleq \sum_{i \in S_{non}^{\pi}} (\eta_i \times E_i^{\pi}(u_i)). \quad (5.4)$$

Under Assumptions 10-13, the problem is defined more precisely as follows.

Problem 3. *Minimizing total joint cost of energy consumption and data efficiencies of nonvisited CH robots via UAV with limited-capacity battery*

$$\begin{aligned} \min_{\pi, u \subseteq P} \quad & J(u, \pi) \\ \text{s.t.} \quad & E_{UAV}^{\pi} \leq B \end{aligned}$$

Remark 12. *In this problem, if UAV has insufficient battery capacity for visiting each CH robot, UAV has tendency of desisting from CH robots which have lower efficiency of data collected from their clusters among the CH robots which consume close energy each other for data forwarding. In other words, UAV desists from visiting a farther CH robot i with lower data efficiency than another nearer CH robot j with higher data efficiency if CH robot i has lower joint cost of data efficiency and energy consumption than CH robot j which differs our problem from the problems in the related literature.*

5.2 Joint Energy-Efficiency Cost Minimization Problem by UAV with Limited-Capacity Battery

First, we tackle this problem by modeling it as a travel salesman problem (TSP) for finding the minimum battery capacity sufficient for visiting each CH robot. To find this capacity, we apply genetic algorithm (GA).

By choosing an optimal subset of CH robots to visit, UAV aims to minimize total joint costs of data efficiencies and energy consumptions of the nonvisited CH robots that will be transmitting data by multiple hops through other nonvisited CH until a visited CH node. This chapter considers not only a constraint in battery capacity of UAV and total energy consumed by CH robots for forwarding data but also different efficiency of data for different CH robot.

To show the difference between our problem and the orienteering problem approach, we first formulate the problem as orienteering problem, the problem in (5.5), and then make the following proposition.

Maximizing the sum of efficiencies of data collected from CH robots via a UAV with limited-capacity battery

$$\begin{aligned} \max_{\pi \subseteq P} \quad & \sum_{i \in S - S_{non}^{\pi}} \eta_i \\ \text{s.t.} \quad & E_{UAV}^{\pi} \leq B \end{aligned} \quad (5.5)$$

Proposition 3. *Optimal solution for the orienteering problem in (5.5) does not guarantee optimality for Problem 3.*

Proof. As the sum of data efficiencies of all CH robots is

$$\sum_{i \in S} \eta_i = \sum_{i \in S - S_{non}^{\pi}} \eta_i + \sum_{i \in S_{non}^{\pi}} \eta_i, \quad (5.6)$$

which yields that the problem in (5.5) is equivalent to problem in (5.7).

$$\begin{aligned} \max_{\pi \subseteq P} \quad & \left[\sum_{i \in S} \eta_i - \sum_{i \in S_{non}^{\pi}} \eta_i \right] \\ \text{s.t.} \quad & E_{UAV}^{\pi} \leq B \end{aligned} \quad (5.7)$$

As the sum of data efficiencies of all CH robots, $\sum_{i \in S} \eta_i$, is constant, problem in (5.7) is equivalent to problem in (5.8).

$$\begin{aligned} \min_{\pi \subseteq P} \quad & \sum_{i \in S_{non}^{\pi}} \eta_i \\ \text{s.t.} \quad & E_{UAV}^{\pi} \leq B \end{aligned} \quad (5.8)$$

The problem in (5.8) does not consider energy consumption of the nonvisited CH robots and their data forwarding strategies which have already been considered in Problem 3. As an optimal solution to our problem, UAV can prefer a CH robot which has slightly lower data efficiency but consumes much more energy for forwarding data if not visited, which is not possible in the problem in (5.8). Hence, it is proved. \square

Proposition 3 shows the importance of data forwarding strategy for each nonvisited CH robot. In next subsection, we study optimal strategies for nonvisited CH robots to forward their data to another CH robot until a visited CH robot.

5.2.1 Data Forwarding Strategy for CH Robots

A visited CH robot i does not need data forwarding strategy and so $u_i = \emptyset$. However, a nonvisited CH robot i should look for the shortest path to each visited CH robot and take minimum of all shortest paths.⁴ Hence, they can obtain optimum data forwarding strategies. Notice that each nonvisited CH robot considers each visited CH robot as possible targets.

Theorem 3. *Optimal data forwarding strategy is the minimum-energy shortest path for each nonvisited CH robot to forward data until one visited CH robot.*

Proof. From Definition 26, Problem 3 under the battery constraint can be written as

$$\min_{\pi, u \subseteq P} J(u, \pi) = \min_{\pi, u \subseteq P} \sum_{i \in S_{non}^{\pi}} (\eta_i \times E_i^{\pi}(u_i)). \quad (5.9)$$

For a given strategy of UAV π satisfying $E_{UAV}^{\pi} \leq B$, Problem 3 can be converted into

$$\min_{u \subseteq P} J(u, \pi) = \min_{u \subseteq P} \sum_{i \in S_{non}^{\pi}} (\eta_i \times E_i^{\pi}(u_i)). \quad (5.10)$$

There is no hop constraint to forward data in our Problem 3; therefore, choosing a path for forwarding data brings no cost other than the joint cost which is squarely proportional to the path length. Hence, we can make superposition in the cost optimization problem. Thus, (5.9) turns into

$$\min_{u \subseteq P} J(u, \pi) = \sum_{i \in S_{non}^{\pi}} \min_{u_i \subseteq P} (\eta_i \times E_i^{\pi}(u_i)). \quad (5.11)$$

As η_i is independent from the strategy u_i , (5.11) turns into

$$\min_{u \subseteq P} J(u, \pi) = \sum_{i \in S_{non}^{\pi}} \eta_i \times \left(\min_{u_i \subseteq P} E_i^{\pi}(u_i) \right). \quad (5.12)$$

The shortest path which considers squares of distances from Equation (5.2) is optimal to minimize $E_i^{\pi}(u_i)$, the energy consumed to forward unit data of a nonvisited CH robot i . Therefore, the minimum-energy shortest path is optimal data forwarding

⁴ From Equation (5.2), squares of the distances between CH robots are considered to calculate shortest paths between CH robots.

strategy for each nonvisited CH robot, whereby the total joint cost can be minimized. Hence, it is proved. \square

Remark 13. *By using shortest path for nonvisited CH robot i , we can find an optimal data forwarding strategy which achieves minimum energy consumed by nonvisited CH robot i under strategy π , i. e.,*

$$\gamma_i^\pi = \min_{u_i \subseteq P} \eta_i \times E_i^\pi(u_i) \quad (5.13)$$

for a nonvisited CH robot i .

In the next subsection, we investigate the problem to obtain the structure of optimal strategy for the UAV.

5.2.2 Optimal Strategy for the UAV

Unless UAV has enough battery capacity for visiting each CH robot, considering Problem 3 as an orienteering problems provides no guarantee for obtaining an optimal strategy as it shown by Proposition 3. We should consider minimizing both energy consumed by UAV and the joint cost of data efficiency and energy consumed by each nonvisited CH robot.

Let B_{TSP} denote minimum battery capacity sufficient for visiting each CH robot. UAV with battery capacity $B < B_{TSP}$ requires going without visiting some CH robots. Our problem is selecting the CH robots to go without visiting those CH robots for minimizing the sum of joint cost of data efficiency and energy consumed by non-visited CH robots.

Definition 27 will help us describe Algorithm 4.

Definition 27. *K -element combinations of the CH robots, denoted by S_a^K , is K -element subset of the M -element set of all CH robots, i. e., $S_a^K \subseteq S$ and $|S_a^K| = K$ for $1 \leq a \leq \binom{M}{K}$. $S^K(B)$ denotes set of all feasible K -element combinations that UAV with battery capacity B can visit.*

Theorem 4. *Algorithm 4 is optimal for Problem 3.*

Algorithm 4 Efficiency and Energy-Aware Data Collection Strategy (EEADCS)

#Comment: Battery capacity of UAV is sufficient for visiting all CH robots, i.e.,

$$B \geq B_{TSP}.$$

if $B \geq B_{TSP}$ **then**

Look for an optimal strategy by considering the problem as a TSP.

Output: π^{EEADCS} becomes a genetic algorithm-based strategy for TSP whereby UAV visits all CH robots.

#Comment: Battery capacity of UAV is insufficient for visiting all CH robots, i.e., $B < B_{TSP}$.

else

for $K = (M - 1) : 1$ **do**

Find all $\binom{M}{K}$ combinations of CH robots.

for $a = 1 : \binom{M}{K}$ **do**

if $\min_{\pi} E_{UAV}^{\pi} \leq B$ for S_a^K **then**

Comment: S_a^K is a feasible set that UAV with B can visit. #.

$$S_a^K \subset S^K(B)$$

From Theorem 3 and Remark 13, apply minimum-energy shortest path strategy for each CH robot $i \in S - S_a^K$. Find $\sum_{i \in S - S_a^K} \gamma_i^{\pi}$.

else

Comment: S_a^K is an infeasible set that UAV with B cannot visit. #.

$$S_a^K \not\subset S^K(B)$$

end if

end for

if $S^K(B) \neq \emptyset$ **then**

Find $\min_{S_a^K \in S^K(B)} \sum_{i \in S - S_a^K} \gamma_i^{\pi}$

end if

end for

Find $\min_K \left[\min_{S_a^K \in S^K(B)} \sum_{i \in S - S_a^K} \gamma_i^{\pi} \right]$.

Output: π^{EEADCS} is a genetic algorithm-based strategy for TSP in which UAV visits the CH robots in the combination S_a^K found on previous step.

end if

Proof. If UAV has enough battery capacity for visiting each CH robot, i.e., $B \geq B_{TSP}$, then the problem turns into the TSP problem. In this case, a genetic algorithm-based TSP strategy can provide an optimal solution for Problem 3.

If UAV have insufficient battery capacity for visiting each CH robot, i.e., $B < B_{TSP}$, the UAV needs to go without visiting a portion of CH robots. Therefore, we need to consider various combinations of CH robots $S_a^K \subseteq S$ starting with the combinations with $K = M - 1$ CH robots.

Among these K -element combinations, we need to consider the set of all combinations $S_a^K \in S^K(B)$ for which the UAV can visit each CH robot in the combination S_a^K from Definition 27. From Theorem 3, the minimum-energy shortest path strategy is the optimum data forwarding strategy for each nonvisited CH robot in one combination. It is optimal to take the combination with minimum cost among the joint costs of energy consumptions and data efficiencies of all CH combinations with K CH robots.

A combination with K_1 CH robots may have less joint cost than a combination with K_2 CH robots where $K_1 < K_2$. Therefore, to guarantee optimality, we continue with all combinations with less ($M - 2$, $M - 3$, so on) CH robots until the combinations with 1 CH robot. Hence, it is proved. \square

5.3 Numerical Results

Performances of the strategies will be evaluated for varying number of CH robots and varying battery capacities. We consider 5-CH, 7-CH, and 10-CH robot scenarios by randomly generating locations of CH robots. To generate various data efficiencies, we use the following equation $\eta_i = 1 - \frac{i}{20}$, which prevent efficiencies from being close to each other.

In these scenarios, we observe that the path length for the UAV to visit all CH robots is less than 50 units. This means that the battery capacity of the UAV sufficient to visit all CH robots is less than $50 \times C_{UAV}$ ⁵ Performances of UAV-oriented strategy in [75],

⁵ Remind that C_{UAV} denotes energy consumed by UAV per unit distance travel.

GAMEDFS in [76] (our previous work in Chapter 3) and our optimal (EEADCS) strategy are evaluated. *We find the energy consumed by UAV and joint cost of energy consumption and data efficiencies of nonvisited CH robots.*

5.3.1 5-CH case

Figure 5.2 shows locations of 5 CH robots and the weights of the links between them. Positions of CH robots are $(\xi_1, \xi_2, \xi_3, \xi_4, \xi_5) = ((-8, 5), (2, 2), (6, 10), (-2, -3), (-5, -5))m$ where $(0, 0)$ is initial position of UAV. Data efficiencies of CH robots are taken as $(\eta_1, \eta_2, \eta_3, \eta_4, \eta_5) = (0.95, 0.90, 0.85, 0.80, 0.75) m$.

5.3.1.1 UAV-Oriented Strategy

By applying UAV-Oriented strategy, UAV visits just CH robot 2 ($\xi_2 = (2, 2)$) and collect all data of CH robots from there if

$$\begin{aligned}
 B &= 2 \times \|\xi_2 - \xi_0\| \\
 &= 2 \times \sqrt{(2-0)^2 + (2-0)^2} \times C_{UAV} \\
 &\approx 5.66 \times C_{UAV} < 10 \times C_{UAV},
 \end{aligned} \tag{5.14}$$

by which we can calculate joint costs of data efficiencies and energy consumptions of nonvisited CH robots under UAV-Oriented strategy as follows

$$\begin{aligned}
 J(u, \pi^{UAV-O}) &= \eta_1 \times \|\xi_1 - \xi_2\|^2 + \eta_3 \times \|\xi_3 - \xi_2\|^2 \\
 &+ \eta_4 \times \|\xi_4 - \xi_2\|^2 + \eta_5 \times \|\xi_5 - \xi_2\|^2 \\
 &= (0.95 \times 109 + 0.85 \times 80 + 0.80 \times 41 \\
 &+ 0.75 \times 98) \times C_{CH} \\
 &= 277.85 \times C_{CH}
 \end{aligned} \tag{5.15}$$

in the configuration in Figure 5.2. If $B = 5$, then the UAV-oriented strategy cannot be applied since UAV cannot travel to CH robot 2 and the other CH robots are farther to origin than CH robot 2.

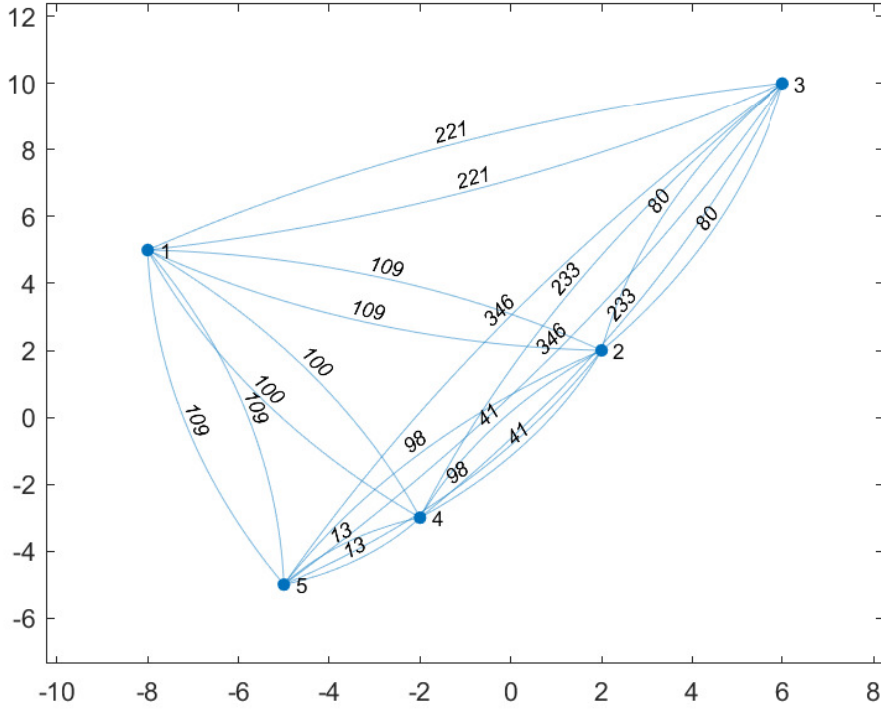


Figure 5.2: Nodes show locations of 5 CH robots. The weight of a link shows square of distance between two nodes connected by the link.

5.3.1.2 GAMEDFS

In this subsection, we obtain the numerical results for performance of GAMEDFS proposed in Chapter 3 with battery capacities varying from $B = 5$ to $B = 50$ in the configuration in Figure 5.2. In Figure 5.3, by applying GAMEDFS, the UAV with $B = 45 \times C_{UAV}$ or $B = 50 \times C_{UAV}$ can visit all CH robots, i. e., $J(u, \pi^{GAMEDFS}) = 0$. In the configuration in Figure 5.2, the energy required for the UAV to visit all CH robots is $E_{UAV}^{\pi^{GAMEDFS}}(u) \approx 44.29 \times C_{UAV}$. The UAV with $B = 35$ or $B = 40 \times C_{UAV}$ goes without visiting CH robot 3 which results in

$$\begin{aligned}
 J(u, \pi^{GAMEDFS}) &= 0.85 \times 80 \times C_{CH} \\
 &= 68 \times C_{CH}
 \end{aligned} \tag{5.16}$$

Thus, the UAV consumes $E_{UAV}^{\pi^{GAMEDFS}}(u) \approx 30.92 \times C_{UAV}$. The UAV with $B = 30 \times C_{UAV}$ goes without visiting CH robot 3 and 5 which results in

$$\begin{aligned} J(u, \pi^{GAMEDFS}) &= (0.85 \times 80 + 0.75 \times 13) \times C_{CH} \\ &= 77.75 \times C_{CH} \end{aligned} \quad (5.17)$$

Thus, the UAV consumes $E_{UAV}^{\pi^{GAMEDFS}}(u) \approx 26.87 \times C_{UAV}$. The UAV with $B = 25 \times C_{UAV}$ goes without visiting CH robot 3, 2 and 5 which results in

$$\begin{aligned} J(u, \pi^{GAMEDFS}) &= (0.85 \times (80 + 8) + 0.90 \times 8 + 0.75 \times 13) \times C_{CH} \\ &= 91.75 \times C_{CH} \end{aligned} \quad (5.18)$$

and $E_{UAV}^{\pi^{GAMEDFS}}(u) \approx 23.04 \times C_{UAV}$. The UAV with $B = 20 \times C_{UAV}$ goes without visiting CH robot 3 and 1 which results in

$$\begin{aligned} J(u, \pi^{GAMEDFS}) &= (0.85 \times 80 + 0.95 \times 89) \times C_{CH} \\ &= 152.55 \times C_{CH} \end{aligned} \quad (5.19)$$

and $E_{UAV}^{\pi^{GAMEDFS}}(u) \approx 19.94 \times C_{UAV}$. UAV with $B = 15 \times C_{UAV}$ goes without visiting CH robot 3, 5 and 1 which results in

$$\begin{aligned} J(u, \pi^{GAMEDFS}) &= (0.85 \times 80 + 0.75 \times 13 + 0.95 \times 89) \times C_{CH} \\ &= 162.30 \times C_{CH} \end{aligned} \quad (5.20)$$

and $E_{UAV}^{\pi^{GAMEDFS}}(u) \approx 12.84 \times C_{UAV}$. UAV with $B = 10 \times C_{UAV}$ goes without visiting CH robot 1, 2, 3, and 5 which results in

$$\begin{aligned} J(u, \pi^{GAMEDFS}) &= (0.85 \times (80 + 8) + 0.90 \times 8 + 0.75 \times 13 + 0.95 \times 89) \times C_{CH} \\ &= 176.30 \times C_{CH} \end{aligned} \quad (5.21)$$

and $E_{UAV}^{\pi^{GAMEDFS}}(u) \approx 7.21 \times C_{UAV}$. UAV with $B = 5 \times C_{UAV}$ can travel to no CH robot which results in

$$\begin{aligned} J(u, \pi^{GAMEDFS}) &= (0.85 \times (80 + 8) + 0.90 \times 8 + 0.80 \times (13 + 13) + 0.75 \times 13 \\ &\quad + 0.95 \times 89) \times C_{CH} \\ &= 196.70 \times C_{CH} \end{aligned} \quad (5.22)$$

5.3.1.3 EEADCS

EEADCS has taken same decisions with GAMEDFS for all battery capacity values varying from $B = 5$ to $B = 50$ in the configuration of Figure 3.8.

Although CH 4 robot has the second lowest data efficiency among all CH robots, UAV still prefers to visit CH 4 with lower battery capacities because CH 4 forwards data of CH 5. For $B = 10$, UAV goes without visiting CH 2 instead of CH 4 because visiting CH 4 reduces the joint cost of data efficiency and energy consumed by CH robots more than visiting CH 2.

Please notice that if CH 4 were located at the position $(-2, -2)$ instead of $(-2, -3)$, then CH 4 and CH 2 would have the same distance to origin. In that case, the UAV would go without visiting CH 4 instead of CH 2 because CH 2 and CH 3 have better data efficiency than CH 4 and CH 5.

In case that data efficiencies of all CH robots are equal, GAMEDFS has already been shown to be optimal in Chapter 3. With efficiencies generated with the formula $\eta_i = 1 - \frac{i}{20}$, the performance of strategies still depends more on positions of CH robots. It can be expected since if a route is infeasible because of battery capacity of UAV, minimizing the data efficiencies of the nonvisited CH robots lose its importance. Here, data efficiencies of the CH robots do not have an affect on the hard constraint of battery capacity of UAV as locations of CH robots do.

5.3.1.4 Performance Comparison

Table 3.2 presents indices of nonvisited CH robots in Figure 3.8. Similarly, Table 3.3 presents total joint cost of energy consumption and data efficiencies of the nonvisited CH robots. From these tables, we can observe how UAV decides to go without visiting a subset of CH robots depending on its battery capacity in Figure 3.8. Moreover, the sum of joint cost of consumed energy and data efficiencies of nonvisited CH robots varies with battery capacity of UAV and so desisting decisions made by UAV. Furthermore, joint costs of nonvisited CH robots depend on positions and data efficiencies of the CH robots.

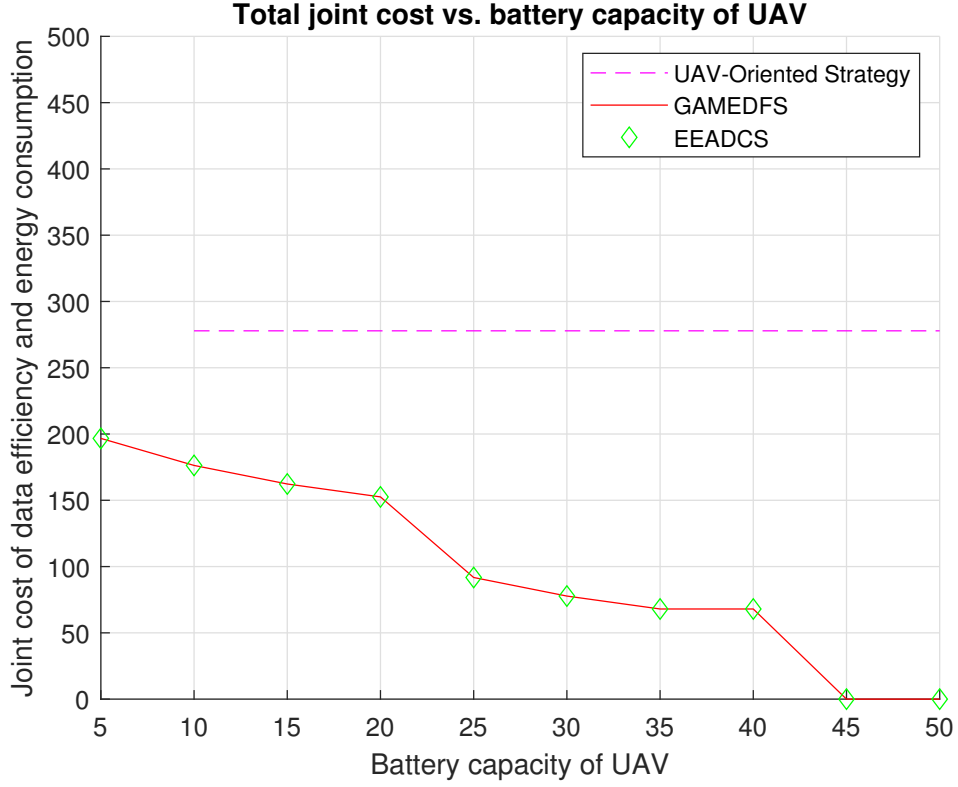


Figure 5.3: Total joint cost of data efficiency and energy consumption of the 5 CH robots in Figure 3.8 under UAV-Oriented strategy, GAMEDFS and EEADCS, vs. battery capacity of UAV from $B = 5 \times C_{UAV}$ to $B = 50 \times C_{UAV}$. The units for energy consumption of the UAV and total joint cost of the CH robots are C_{UAV} and C_{CH} , respectively. These constants depend on the type of the UAV and the CH robots.

5.3.2 6-CH case

Figure 5.4 shows locations of 6 CH robots and the weights of the links between them. Positions of the CH robots are $(\xi_1, \xi_2, \xi_3, \xi_4, \xi_5, \xi_6) = ((1, 2), (5, 4), (9, 2), (1, -2), (5, -4), (9, -2))m$ where $(0, 0)$ is initial position of UAV. Data efficiencies of CH robots are taken as $(\eta_1, \eta_2, \eta_3, \eta_4, \eta_5, \eta_6) = (0.95, 0.90, 0.85, 0.80, 0.75, 0.70)m$.

5.3.2.1 UAV-Oriented Strategy

By applying UAV-Oriented strategy, UAV visits just CH robot 2 ($\xi_2 = (5, -4)$) and collect all data of CH robots from there if $B \approx 12.81 \times C_{UAV}$, by which we can

Table 5.1: The table shows indices of the nonvisited CH robots depending on battery capacity of UAV in Figure 5.2. "None" implies that UAV visits all CH robots if $B = 45$ or $B = 50$. "×" implies that the UAV-oriented Strategy is infeasible for that battery capacity.

Strategy	B = 5	B = 10	B = 15	B = 20	B = 25
UAV-Oriented	×	1,3-5	1,3-5	1,3-5	1,3-5
GAMEDFS	1-5	1-3,5	1,3,5	2-5	2,3,5
EEADCS	1-5	1-3,5	1,3,5	2-5	2,3,5
Strategy	B = 30	B = 35	B = 40	B = 45	B = 50
UAV-Oriented	1,3-5	1,3-5	1,3-5	1,3-5	1,3-5
GAMEDFS	1-5	3	3	None	None
EEADCS	3,5	3	3	None	None

Table 5.2: The table shows total joint cost of energy consumption and data efficiencies of the nonvisited CH robots depending on battery capacity of UAV in Figure 5.3. "×" implies that the UAV-oriented strategy is infeasible for that battery capacity.

Strategy	B = 5	B = 10	B = 15	B = 20	B = 25
UAV-Oriented	×	277.85	277.85	277.85	277.85
GAMEDFS	196.70	176.30	162.30	152.55	91.75
EEADCS	196.70	176.30	162.30	152.55	91.75
Strategy	B = 30	B = 35	B = 40	B = 45	B = 50
UAV-Oriented	277.85	277.85	277.85	277.85	277.85
GAMEDFS	77.75	68.00	68.00	0	0
EEADCS	77.75	68.00	68.00	0	0

calculate total joint cost of data efficiency and energy consumed by each nonvisited CH robot under UAV-Oriented strategy as follows.

$$\begin{aligned}
J(u, \pi^{UAV-O}) &= \eta_1 \times \|\xi_1 - \xi_2\|^2 + \eta_3 \times \|\xi_3 - \xi_2\|^2 + \eta_4 \times \|\xi_4 - \xi_2\|^2 \\
&+ \eta_5 \times \|\xi_5 - \xi_2\|^2 + \eta_6 \times \|\xi_6 - \xi_2\|^2 \\
&= 162 \times C_{CH}
\end{aligned} \tag{5.23}$$

If $B = 5, 10$, UAV can travel to CH robot 1 ($\xi_1 = (1, 2)$), closer to the origin than CH robot 2, which results in

$$\begin{aligned}
 J(u, \pi^{UAV-O}) &= \eta_2 \times \|\xi_2 - \xi_1\|^2 + \eta_3 \times \|\xi_3 - \xi_1\|^2 + \eta_4 \times \|\xi_4 - \xi_1\|^2 \\
 &+ \eta_5 \times \|\xi_5 - \xi_1\|^2 + \eta_6 \times \|\xi_6 - \xi_1\|^2 \\
 &= 180.20 \times C_{CH}
 \end{aligned} \tag{5.24}$$

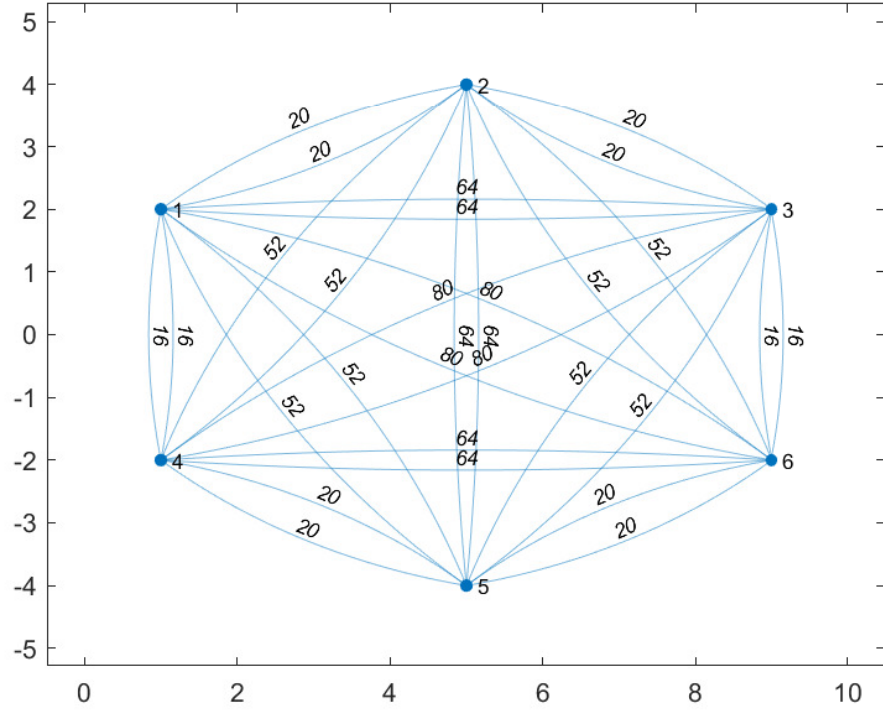


Figure 5.4: Nodes show the locations of the 6 CH robots. The weight of a link shows square of distance between two nodes connected by the link.

5.3.2.2 GAMEDFS

In this subsection, we obtain the numerical results for performance of GAMEDFS proposed in Chapter 3 with battery capacities varying from $B = 5$ to $B = 50$ in the configuration in Figure 5.4. In Figure 5.5, by applying GAMEDFS, UAV with $B = 30, 35, 40, 45, 50 \times C_{UAV}$ can visit all CH robots, i. e., $J(u, \pi^{GAMEDFS}) = 0$. In the configuration in Figure 5.4, the energy required for UAV to visit all CH robots

is $E_{UAV}^{\pi^*}(u) \approx 26.36 \times C_{UAV}$. UAV with $B = 25 \times C_{UAV}$ goes without visiting CH robot 5 and 6 which results in

$$\begin{aligned} J(u, \pi^{GAMEDFS}) &= (0.75 \times 20 + 0.70 \times 16) \times C_{CH} \\ &= 26.20 \times C_{CH} \end{aligned} \quad (5.25)$$

and $E_{UAV}^{\pi^*}(u) \approx 22.36 \times C_{UAV}$. UAV with $B = 20 \times C_{UAV}$ goes without visiting CH robot 3, 5 and 6 which results in

$$\begin{aligned} J(u, \pi^{GAMEDFS}) &= (0.85 \times 20 + 0.75 \times 20 + 0.70 \times (16 + 20)) \times C_{CH} \\ &= 57.20 \times C_{CH} \end{aligned} \quad (5.26)$$

and $E_{UAV}^{\pi^*}(u) \approx 16.16 \times C_{UAV}$. UAV with $B = 15 \times C_{UAV}$ can visit only CH 1 and CH 2 which results in

$$\begin{aligned} J(u, \pi^{GAMEDFS}) &= (0.85 \times 20 + 0.80 \times 5 + 0.75 \times (20 + 20) \\ &\quad + 0.70 \times (16 + 20)) \times C_{CH} \\ &= 76.20 \times C_{CH} \end{aligned} \quad (5.27)$$

and $E_{UAV}^{\pi^*}(u) \approx 13.41 \times C_{UAV}$. UAV with $B = 5, 10 \times C_{UAV}$ can visit only CH 1 and CH 4 which results in

$$\begin{aligned} J(u, \pi^{UAV-O}) &= 0.90 \times 20 + 0.85 \times (20 + 20) + 0.75 \times 20 \\ &\quad + 0.70 \times (20 + 20) \\ &= 95 \times C_{CH} \end{aligned} \quad (5.28)$$

and $E_{UAV}^{\pi^*}(u) = 8.47 \times C_{UAV}$. UAV with $B = 5 \times C_{UAV}$ can visit only CH 1 which results in

$$\begin{aligned} J(u, \pi^{UAV-O}) &= 0.90 \times 20 + 0.85 \times (20 + 20) + 0.80 \times 5 + 0.75 \times (20 + 5) \\ &\quad + 0.70 \times (20 + 20 + 5) \\ &= 106.25 \times C_{CH} \end{aligned} \quad (5.29)$$

and $E_{UAV}^{\pi^*}(u) = 4.47 \times C_{UAV}$.

5.3.2.3 EEADCS

EEADCS has taken same decisions with GAMEDFS for all battery capacity values varying from $B = 5$ to $B = 50$ in the configuration of Figure 5.4.

Although CH 4 has the low data efficiency among all CH robots, UAV still prefers to visit CH 4 for low battery capacity values except $B = 5, 15$ as it can forward data from CH 5, CH 6 which is very important for energy consumption of UAV. As CH 1 has highest data efficiency and close to origin, UAV visits it for all battery capacities.

In case that data efficiencies of all CH robots are equal, GAMEDFS has already been shown to be optimal in Chapter 3. With efficiencies generated with the formula $\eta_i = 1 - \frac{i}{20}$, the performance of strategies still depends more on positions of CH robots. It can be expected since if a route is infeasible because of battery capacity of UAV, minimizing sum of data efficiencies of the nonvisited CH robots lose its importance. Here, data efficiencies of the CH robots do not have an affect on the hard constraint of battery capacity of UAV as locations of CH robots do.

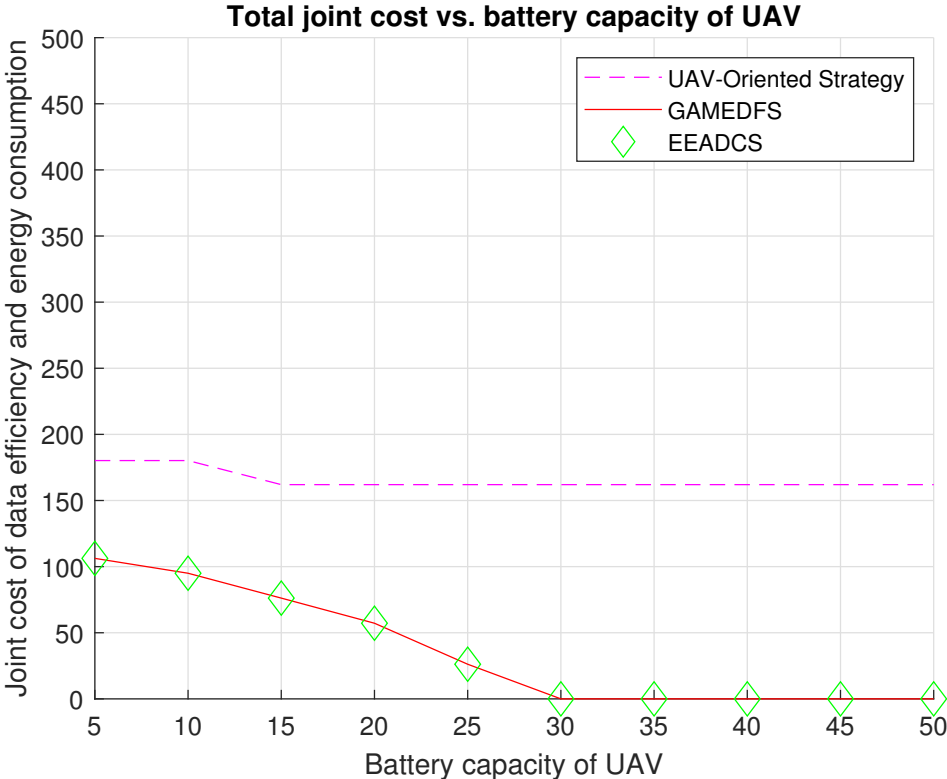


Figure 5.5: Total joint cost of data efficiency and energy consumption of the 6 CH robots in Figure 5.4 under UAV-Oriented strategy, GAMEDFS and EEADCS, vs. battery capacity of UAV from $B = 5 \times C_{UAV}$ to $B = 50 \times C_{UAV}$. The units for energy consumption of the UAV and total joint cost of the CH robots are C_{UAV} and C_{CH} , respectively. These constants depend on the type of the UAV and the CH robots.

5.3.2.4 Performance Comparison

Table 5.3 presents indices of nonvisited CH robots in Figure 5.4. Similarly, Table 5.4 presents total joint cost of energy consumption and data efficiencies of the nonvisited CH robots. From these tables, we can observe how UAV decides to go without visiting a subset of CH robots depending on its battery capacity in Figure 5.4. Moreover, the sum of joint cost of consumed energy and data efficiencies of nonvisited CH robots varies with battery capacity of UAV and so desisting decisions made by UAV. Furthermore, joint costs of nonvisited CH robots depend on positions and data efficiencies of the CH robots.

Table 5.3: The table shows indices of the nonvisited CH robots depending on battery capacity of UAV in Figure 5.4. "None" implies that the UAV visits all CH robots if $B = 25, 30, 35, 40, 45, 50$. "×" implies that the UAV-oriented strategy is infeasible for that battery capacity.

Strategy	B = 5	B = 10	B = 15	B = 20	B = 25
UAV-Oriented	2-6	2-6	1,3-6	1,3-6	1,3-6
GAMEDFS	2-6	2,3,5,6	3-6	3,5,6	5,6
EEADCS	2-6	2,3,5,6	3-6	3,5,6	5,6
Strategy	B = 30	B = 35	B = 40	B = 45	B = 50
UAV-Oriented	1,3-6	1,3-6	1,3-6	1,3-6	1,3-6
GAMEDFS	None	None	None	None	None
EEADCS	None	None	None	None	None

5.3.3 7-CH case

Figure 5.6 shows locations of 7 CH robots and the weights of the links between them. Positions of the CH robots are $(\xi_1, \xi_2, \xi_3, \xi_4, \xi_5, \xi_6, \xi_7) = ((9, 6), (3, 9), (3, 2), (7, 8), (8, -1), (7, 5), (2, 2))m$ where $(0, 0)$ is initial position of UAV. Data efficiencies of CH robots are taken as $(\eta_1, \eta_2, \eta_3, \eta_4, \eta_5, \eta_6, \eta_7) = (0.95, 0.90, 0.85, 0.80, 0.75, 0.70, 0.65)m$.

Table 5.4: The table shows total joint cost of energy consumption and data efficiencies of the nonvisited CH robots depending on battery capacity of UAV in Figure 5.5. "×" implies that the UAV-oriented strategy is infeasible for that battery capacity.

Strategy	B = 5	B = 10	B = 15	B = 20	B = 25
UAV-Oriented	180.20	180.20	162	162	162
GAMEDFS	106.25	95	76.20	57.20	26.20
EEADCS	106.25	95	76.20	57.20	26.20
Strategy	B = 30	B = 35	B = 40	B = 45	B = 50
UAV-Oriented	162	162	162	162	162
GAMEDFS	0	0	0	0	0
EEADCS	0	0	0	0	0

5.3.3.1 UAV-Oriented Strategy

By applying UAV-Oriented strategy, UAV visits just CH robot 6 ($\xi_6 = (7, 5)$) and collect all data of CH robots from there if $B \approx 17.2 \times C_{UAV}$. by which we can calculate total joint cost of data efficiency and energy consumed by each nonvisited CH robot under UAV-Oriented strategy as follows.

$$\begin{aligned}
J(u, \pi^{UAV-O}) &= \eta_1 \times \|\xi_1 - \xi_6\|^2 + \eta_2 \times \|\xi_2 - \xi_6\|^2 + \eta_3 \times \|\xi_3 - \xi_6\|^2 \\
&\quad + \eta_4 \times \|\xi_4 - \xi_6\|^2 + \eta_5 \times \|\xi_5 - \xi_6\|^2 + \eta_7 \times \|\xi_7 - \xi_6\|^2 \\
&= 111.85 \times C_{CH}
\end{aligned} \tag{5.30}$$

If $B = 10$ or $B = 15$, UAV can travel to CH robot 3, closer to the origin than CH robot 6, which results in

$$\begin{aligned}
J(u, \pi^{UAV-O}) &= \eta_1 \times \|\xi_1 - \xi_3\|^2 + \eta_2 \times \|\xi_2 - \xi_3\|^2 + \eta_4 \times \|\xi_4 - \xi_3\|^2 \\
&\quad + \eta_5 \times \|\xi_5 - \xi_3\|^2 + \eta_6 \times \|\xi_6 - \xi_3\|^2 + \eta_7 \times \|\xi_7 - \xi_3\|^2 \\
&= 178.75 \times C_{CH}
\end{aligned} \tag{5.31}$$

However, if $B = 5$, UAV-oriented strategy cannot be applied since it can visit no CH robot.

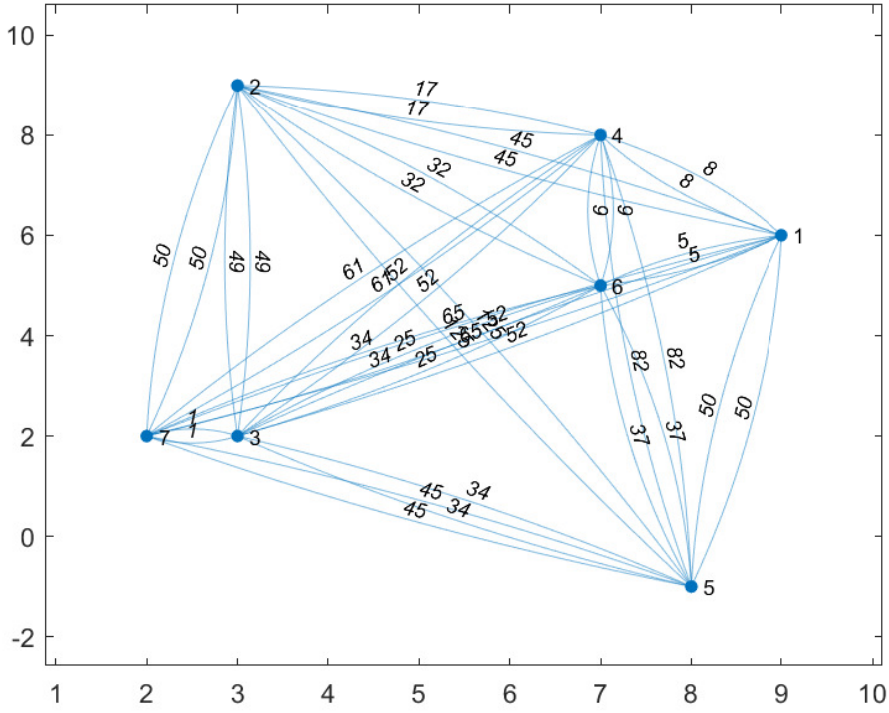


Figure 5.6: Nodes show the locations of the 7 CH robots. The weight of a link shows square of distance between two nodes connected by the link.

5.3.3.2 GAMEDFS

In this subsection, we obtain the numerical results for performance of GAMEDFS proposed in Chapter 3 with battery capacities varying from $B = 5$ to $B = 50$ in the configuration in Figure 5.6. In Figure 5.7, by applying GAMEDFS, UAV with $B = 35 \times C_{UAV}$ or $B = 40 \times C_{UAV}$ or $B = 45 \times C_{UAV}$ or $B = 50 \times C_{UAV}$ can visit all CH robots, i. e., $J(u, \pi^{GAMEDFS}) = 0$. In the configuration in Figure 3.12, the energy required for UAV to visit all CH robots is $E_{UAV}^{\pi^*}(u) \approx 34.42 \times C_{UAV}$. UAV with $B = 30 \times C_{UAV}$ goes without visiting CH robot 5 which results in

$$\begin{aligned}
 J(u, \pi^{GAMEDFS}) &= 0.75 \times 34 \times C_{CH} \\
 &= 25.50 \times C_{CH}
 \end{aligned} \tag{5.32}$$

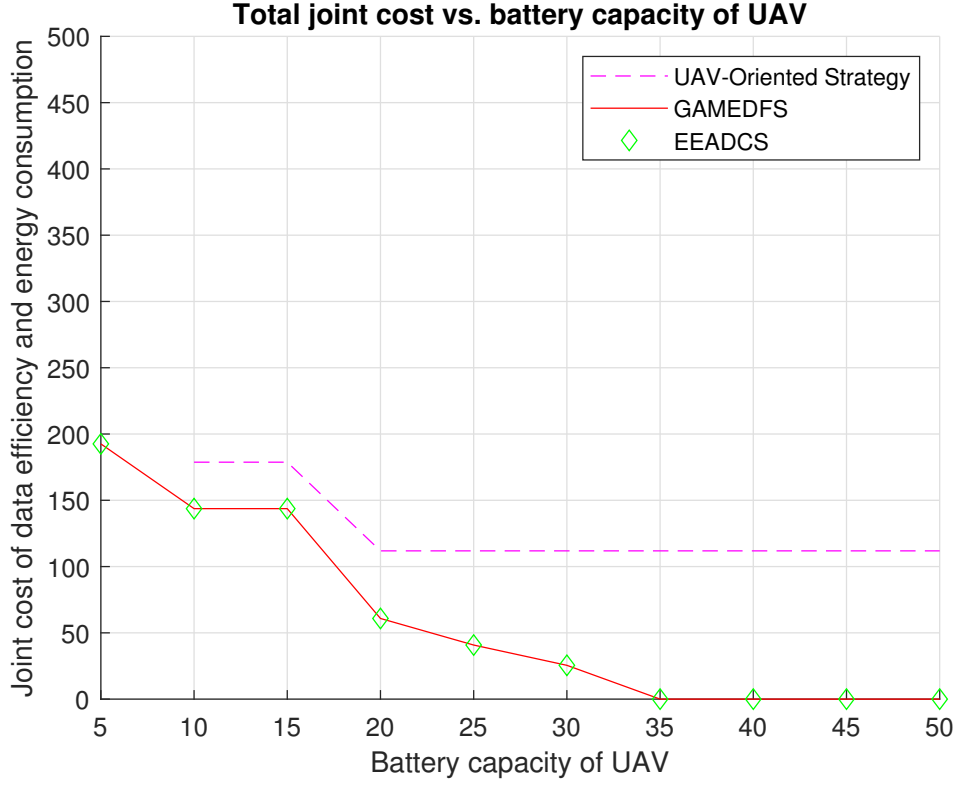


Figure 5.7: Total joint cost of data efficiency and energy consumption of the 7 CH robots in Figure 5.6 under UAV-Oriented strategy, GAMEDFS and EEADCS, vs. battery capacity of UAV from $B = 5 \times C_{UAV}$ to $B = 50 \times C_{UAV}$. The units for energy consumption of the UAV and total joint cost of the CH robots are C_{UAV} and C_{CH} , respectively. These constants depend on the type of the UAV and the CH robots.

and $E_{UAV}^{\pi^*}(u) \approx 27.50 \times C_{UAV}$. UAV with $B = 25 \times C_{UAV}$ goes without visiting CH robot 2 and 5 which results in

$$\begin{aligned} J(u, \pi^{GAMEDFS}) &= (0.90 \times 17 + 0.75 \times 34) \times C_{CH} \\ &= 40.80 \times C_{CH} \end{aligned} \quad (5.33)$$

and $E_{UAV}^{\pi^*}(u) \approx 24.52 \times C_{UAV}$. UAV with $B = 20 \times C_{UAV}$ goes without visiting CH robot 1, 2, 4 and 5 which results in

$$\begin{aligned} J(u, \pi^{GAMEDFS}) &= (0.95 \times 5 + 0.90 \times (17 + 9) + 0.80 \times 9 + 0.75 \times 34) \times C_{CH} \\ &= 60.85 \times C_{CH} \end{aligned} \quad (5.34)$$

and $E_{UAV}^{\pi^*}(u) \approx 17.43 \times C_{UAV}$. UAV with $B = 10 \times C_{UAV}$ or $B = 15 \times C_{UAV}$ goes without visiting CH robot 1, 2, 4, 5 and 6 which results in

$$\begin{aligned} J(u, \pi^{GAMEDFS}) &= 0.95 \times (5 + 25) + 0.90 \times 50 + 0.80 \times (9 + 25) + 0.75 \times 34 \\ &\quad + 0.70 \times 25 \\ &= 143.70 \times C_{CH} \end{aligned} \quad (5.35)$$

and $E_{UAV}^{\pi^*}(u) \approx 7.43 \times C_{UAV}$. UAV with $B = 5 \times C_{UAV}$ can visit no CH robot which results in

$$\begin{aligned} J(u, \pi^{GAMEDFS}) &= (0.95 \times (5 + 25 + 1 + 8) + 0.90 \times (50 + 8) + 0.85 \times (1 + 8) \\ &\quad + 0.80 \times (9 + 25 + 1 + 8) + 0.75 \times (34 + 1 + 8) \\ &\quad + 0.70 \times (25 + 1 + 8) + 0.65 \times 8) \times C_{CH} \\ &= 192.55 \times C_{CH} \end{aligned} \quad (5.36)$$

5.3.3.3 EEADCS

EEADCS has taken same decisions with GAMEDFS for all battery capacity values varying from $B = 5$ to $B = 50$ in the configuration of Figure 5.6.

Although CH 6 has the second lowest data efficiency among all CH robots, UAV still prefers to visit CH 6 with lower battery capacities because CH 6 robot is very close to CH 1 and CH 4 so CH 6 forwards their data.

As CH 2 is very far from origin and CH 7 is closest CH robot to the origin $(0, 0)$, UAV with $B = 15$ still prefers CH 7 instead of CH 2. If CH 2 were located at the position $(3, 6)$ instead of $(3, 9)$, then UAV with $B = 15$ would prefer CH 2 instead of CH 7 to reduce the joint cost of data efficiency and energy consumption of CH robots.

In case that data efficiencies of all CH robots are equal, GAMEDFS has already been shown to be optimal in Chapter 3. With efficiencies generated with the formula $\eta_i = 1 - \frac{i}{20}$, the performance of strategies still depends more on positions of CH robots. It can be expected since if a route is infeasible because of battery capacity of UAV, minimizing sum of data efficiencies of the nonvisited CH robots lose its importance. Here, data efficiencies of the CH robots do not have an affect on the hard constraint of battery capacity of UAV as locations of CH robots do.

5.3.3.4 Performance Comparison

Table 5.5 presents indices of nonvisited CH robots in Figure 5.6. Similarly, Table 5.6 presents total joint cost of energy consumption and data efficiencies of the nonvisited CH robots. From these tables, we can observe how UAV decides to go without visiting a subset of CH robots depending on its battery capacity in Figure 5.6. Moreover, the sum of joint cost of consumed energy and data efficiencies of nonvisited CH robots varies with battery capacity of UAV and so desisting decisions made by UAV. Furthermore, joint costs of nonvisited CH robots depend on positions and data efficiencies of the CH robots.

Table 5.5: The table shows indices of the nonvisited CH robots depending on battery capacity of UAV in Figure 5.6. "None" implies that the UAV visits all CH robots if $B = 35, 40, 45, 50$. " \times " implies that the UAV-oriented strategy is infeasible for that battery capacity.

Strategy	B = 5	B = 10	B = 15	B = 20	B = 25
UAV-Oriented	\times	1,2,4-7	1,2,4-7	1-5,7	1-5,7
GAMEDFS	1-7	1,2,4-6	1,2,4-6	1,2,4,5	2,5
EEADCS	1-7	1,2,4-6	1,2,4-6	1,2,4,5	2,5
Strategy	B = 30	B = 35	B = 40	B = 45	B = 50
UAV-Oriented	1-5,7	1-5,7	1-5,7	1-5,7	1-5,7
GAMEDFS	5	None	None	None	None
EEADCS	5	None	None	None	None

5.3.4 8-CH case

Figure 5.8 shows locations of 8 CH robots and the weights of the links between them. Positions of CH robots are $(\xi_1, \xi_2, \xi_3, \xi_4, \xi_5, \xi_6, \xi_7, \xi_8) = ((7, 1), (8, 1), (5, 1), (1, 1), (3, -1), (10, -1), (2, -1), (9, -1))m$ where $(0, 0)$ is initial position of UAV. Data efficiencies of CH robots are taken as $(\eta_1, \eta_2, \eta_3, \eta_4, \eta_5, \eta_6, \eta_7, \eta_8) = (0.95, 0.90, 0.85, 0.80, 0.75, 0.70, 0.65, 0.60)m$.

Table 5.6: The table shows total joint cost of energy consumption and data efficiencies of the nonvisited CH robots depending on battery capacity of UAV in Figure 5.7. "×" implies that the UAV-oriented strategy is infeasible for that battery capacity.

Strategy	B = 5	B = 10	B = 15	B = 20	B = 25
UAV-Oriented	×	178.75	178.75	111.85	111.85
GAMEDFS	192.55	143.70	143.70	60.85	40.80
EEADCS	192.55	143.70	143.70	60.85	40.80
Strategy	B = 30	B = 35	B = 40	B = 45	B = 50
UAV-Oriented	111.85	111.85	111.85	111.85	111.85
GAMEDFS	25.50	0	0	0	0
EEADCS	25.50	0	0	0	0

5.3.4.1 UAV-Oriented Strategy

By applying UAV-Oriented strategy, UAV visits just CH robot 3 ($\xi_3 = (5, 1)$) and collect all data of CH robots from there if $B \approx 10.2 \times C_{UAV}$, by which we can calculate total joint cost of data efficiency and energy consumed by each nonvisited CH robot under UAV-Oriented strategy as follows.

$$\begin{aligned}
 J(u, \pi^{UAV-O}) &= \eta_1 \times \|\xi_1 - \xi_3\|^2 + \eta_2 \times \|\xi_2 - \xi_3\|^2 + \eta_4 \times \|\xi_4 - \xi_3\|^2 + \eta_5 \times \|\xi_5 - \xi_3\|^2 \\
 &\quad + \eta_6 \times \|\xi_6 - \xi_3\|^2 + \eta_7 \times \|\xi_7 - \xi_3\|^2 + \eta_8 \times \|\xi_8 - \xi_3\|^2 \\
 &= 67.05 \times C_{CH}
 \end{aligned} \tag{5.37}$$

If $B = 10$, UAV can travel to CH robot 5, closer to the origin than CH robot 3, which results in

$$\begin{aligned}
 J(u, \pi^{UAV-O}) &= \eta_1 \times \|\xi_1 - \xi_5\|^2 + \eta_2 \times \|\xi_2 - \xi_5\|^2 + \eta_3 \times \|\xi_3 - \xi_5\|^2 + \eta_4 \times \|\xi_4 - \xi_5\|^2 \\
 &\quad + \eta_6 \times \|\xi_6 - \xi_5\|^2 + \eta_7 \times \|\xi_7 - \xi_5\|^2 + \eta_8 \times \|\xi_8 - \xi_5\|^2 \\
 &= 114.85 \times C_{CH}
 \end{aligned} \tag{5.38}$$

If $B = 5$, UAV can travel to CH robot 7, closer to the origin than CH robot 3 and 5, which results in

$$\begin{aligned}
 J(u, \pi^{UAV-O}) &= \eta_1 \times \|\xi_1 - \xi_7\|^2 + \eta_2 \times \|\xi_2 - \xi_7\|^2 + \eta_3 \times \|\xi_3 - \xi_7\|^2 + \eta_4 \times \|\xi_4 - \xi_7\|^2 \\
 &\quad + \eta_5 \times \|\xi_5 - \xi_7\|^2 + \eta_6 \times \|\xi_6 - \xi_7\|^2 + \eta_8 \times \|\xi_8 - \xi_7\|^2 \\
 &= 153.55 \times C_{CH}
 \end{aligned} \tag{5.39}$$

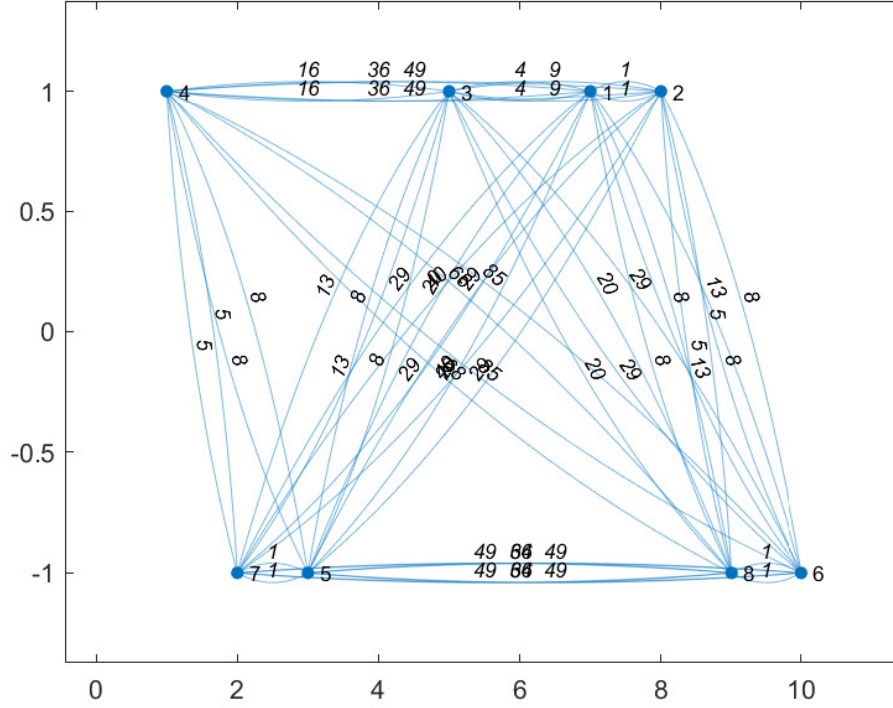


Figure 5.8: Nodes show the locations of the 8 CH robots. The weight of a link shows square of distance between two nodes connected by the link.

5.3.4.2 GAMEDFS

We obtain the numerical results for performance of GAMEDFS proposed in Chapter 3 with battery capacities varying from $B = 5$ to $B = 50$ in the configuration in Figure 5.8. In Figure 5.9, by applying GAMEDFS, UAV with $B = 25, 30, 35, 40, 45, 50 \times C_{UAV}$ can visit all CH robots, i. e., $J(u, \pi^{GAMEDFS}) = 0$. In Figure 5.8, the energy required for UAV to visit all CH robots is $E_{UAV}^*(u) \approx 21.48 \times C_{UAV}$. UAV with

$B = 20 \times C_{UAV}$ goes without visiting CH robot 6 which results in

$$\begin{aligned} J(u, \pi^{GAMEDFS}) &= 0.70 \times 1 \times C_{CH} \\ &= 0.70 \times C_{CH} \end{aligned} \quad (5.40)$$

and $E_{UAV}^{\pi^*}(u) \approx 19.89 \times C_{UAV}$. UAV with $B = 15 \times C_{UAV}$ goes without visiting CH robot 2, 4, 6 and 8 which results in

$$\begin{aligned} J(u, \pi^{GAMEDFS}) &= (0.90 \times 1 + 0.80 \times 2 + 0.70 \times (8 + 1) + 0.60 \times 8) \times C_{CH} \\ &= 13.60 \times C_{CH} \end{aligned} \quad (5.41)$$

and $E_{UAV}^{\pi^*}(u) \approx 14.81 \times C_{UAV}$. UAV with $B = 10 \times C_{UAV}$ visit only CH 4, 5, 7 which results in

$$\begin{aligned} J(u, \pi^{GAMEDFS}) &= (0.95 \times (4 + 8) + 0.90 \times (1 + 4 + 8) + 0.85 \times 8 \\ &\quad + 0.70 \times (36 + 1) + 0.60 \times 36) \times C_{CH} \\ &= 71.70 \times C_{CH} \end{aligned} \quad (5.42)$$

and $E_{UAV}^{\pi^*}(u) \approx 7.48 \times C_{UAV}$. UAV with $B = 5 \times C_{UAV}$ visit only CH 7 which results in

$$\begin{aligned} J(u, \pi^{GAMEDFS}) &= (0.95 \times (4 + 13) + 0.90 \times (1 + 4 + 13) + 0.85 \times 13 + 0.80 \times 2 \\ &\quad + 0.75 \times 1 + 0.70 \times (49 + 1) + 0.60 \times 49) \times C_{CH} \\ &= 110.15 \times C_{CH} \end{aligned} \quad (5.43)$$

and $E_{UAV}^{\pi^*}(u) \approx 4.46 \times C_{UAV}$.

5.3.4.3 EEADCS

EEADCS has taken same decisions with GAMEDFS for all battery capacity values varying from $B = 5$ to $B = 50$ in the configuration of Figure 5.8.

Although CH 5 has the low data efficiency among all CH robots, UAV still prefers to visit CH 5 with lower battery capacities because many CH robots forward their data to CH 5 robot for lower battery capacities of UAV.

As CH 2 is very far from origin and CH 7 is closest CH robot to the origin $(0, 0)$, UAV with $B = 5$ still prefers CH 7 instead of CH 2. If CH 4 were located at the position

(2, 1) instead of (1, 1), then UAV with $B = 15$ would prefer CH 4 instead of CH 7 to reduce the joint cost of data efficiency and energy consumption of CH robots.

In case that data efficiencies of all CH robots are equal, GAMEDFS has already been shown to be optimal in Chapter 3. With efficiencies generated with the formula $\eta_i = 1 - \frac{i}{20}$, the performance of strategies still depends more on positions of CH robots. It can be expected since if a route is infeasible because of battery capacity of UAV, minimizing sum of data efficiencies of the nonvisited CH robots lose its importance. Here, data efficiencies of the CH robots do not have an affect on the hard constraint of battery capacity of UAV as locations of CH robots do.

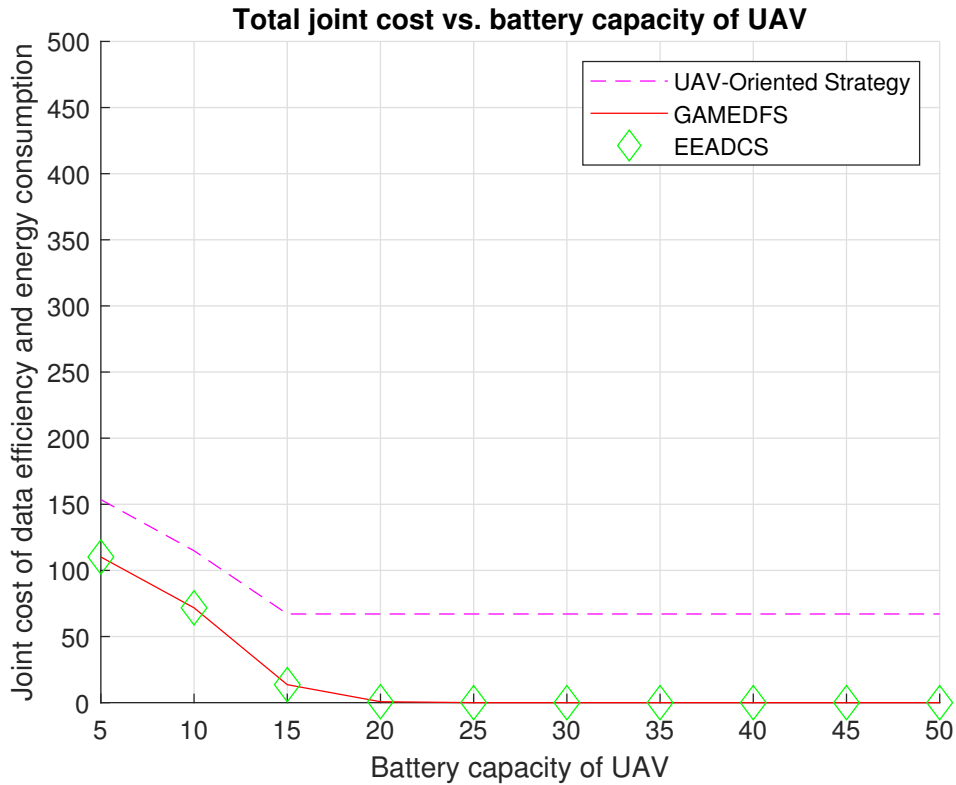


Figure 5.9: Total joint cost of data efficiency and energy consumption of the 8 CH robots in Figure 5.8 under UAV-Oriented strategy, GAMEDFS and EEADCS, vs. battery capacity of UAV from $B = 5 \times C_{UAV}$ to $B = 50 \times C_{UAV}$. The units for energy consumption of the UAV and total joint cost of the CH robots are C_{UAV} and C_{CH} , respectively. These constants depend on the type of the UAV and the CH robots.

5.3.4.4 Performance Comparison

Table 5.7 presents indices of nonvisited CH robots in Figure 5.8. Similarly, Table 5.8 presents total joint cost of energy consumption and data efficiencies of the nonvisited CH robots. From these tables, we can observe how UAV decides to go without visiting a subset of CH robots depending on its battery capacity in Figure 5.8. Moreover, the sum of joint cost of consumed energy and data efficiencies of nonvisited CH robots varies with battery capacity of UAV and so desisting decisions made by UAV. Furthermore, joint costs of nonvisited CH robots depend on positions and data efficiencies of the CH robots.

Table 5.7: The table shows indices of the nonvisited CH robots depending on battery capacity of UAV in Figure 5.8. "None" implies that the UAV visits all CH robots if $B = 25, 30, 35, 40, 45, 50$. "×" implies that the UAV-oriented strategy is infeasible for that battery capacity.

Strategy	B = 5	B = 10	B = 15	B = 20	B = 25
UAV-Oriented	1-6,8	1-4,6-8	1,2,4-8	1,2,4-8	1,2,4-8
GAMEDFS	1-6,8	1-3,6,8	2,4,6,8	6	None
EEADCS	1-6,8	1-3,6,8	2,4,6,8	6	None
Strategy	B = 30	B = 35	B = 40	B = 45	B = 50
UAV-Oriented	1,2,4-8	1,2,4-8	1,2,4-8	1,2,4-8	1,2,4-8
GAMEDFS	None	None	None	None	None
EEADCS	None	None	None	None	None

5.3.5 9-CH case

Figure 5.10 shows locations of 9 CH robots and the weights of the links between them. Positions of CH robots are $(\xi_1, \xi_2, \xi_3, \xi_4, \xi_5, \xi_6, \xi_7, \xi_8, \xi_9) = ((4, 8), (3, 6), (6, 7), (5, 5), (3, -4), (6, -3), (9, -4), (4, -7), (8, -7))m$ where $(0, 0)$ is initial position of UAV. Data efficiencies of CH robots are taken as $(\eta_1, \eta_2, \eta_3, \eta_4, \eta_5, \eta_6, \eta_7, \eta_8, \eta_9) = (0.95, 0.90, 0.85, 0.80, 0.75, 0.70, 0.65, 0.60, 0.55)m$.

Table 5.8: The table shows total joint cost of energy consumption and data efficiencies of the nonvisited CH robots depending on battery capacity of UAV in Figure 5.9. "×" implies that the UAV-oriented strategy is infeasible for that battery capacity.

Strategy	B = 5	B = 10	B = 15	B = 20	B = 25
UAV-Oriented	153.55	114.85	67.05	67.05	67.05
GAMEDFS	110.15	71.70	13.60	0.70	0
EEADCS	110.15	71.70	13.60	0.70	0
Strategy	B = 30	B = 35	B = 40	B = 45	B = 50
UAV-Oriented	67.05	67.05	67.05	67.05	67.05
GAMEDFS	0	0	0	0	0
EEADCS	0	0	0	0	0

5.3.5.1 UAV-Oriented Strategy

By applying UAV-Oriented strategy, UAV visits just CH robot 6 ($\xi_6 = (6, -3)$) and collect all data of CH robots from there if $B \approx 13.41 \times C_{UAV}$, by which we can calculate total joint cost of data efficiency and energy consumed by each nonvisited CH robot under UAV-Oriented strategy as follows.

$$\begin{aligned}
 J(u, \pi^{UAV-O}) &= \eta_1 \times \|\xi_1 - \xi_6\|^2 + \eta_2 \times \|\xi_2 - \xi_6\|^2 + \eta_3 \times \|\xi_3 - \xi_6\|^2 + \eta_4 \times \|\xi_4 - \xi_6\|^2 \\
 &\quad + \eta_5 \times \|\xi_5 - \xi_6\|^2 + \eta_7 \times \|\xi_7 - \xi_6\|^2 + \eta_8 \times \|\xi_8 - \xi_6\|^2 + \eta_9 \times \|\xi_9 - \xi_6\|^2 \\
 &= 373.75 \times C_{CH}
 \end{aligned} \tag{5.44}$$

If $B = 10$, UAV can travel to CH robot 5 ($\xi_5 = (3, -4)$), closer to the origin than CH robot 6, which results in

$$\begin{aligned}
 J(u, \pi^{UAV-O}) &= \eta_1 \times \|\xi_1 - \xi_5\|^2 + \eta_2 \times \|\xi_2 - \xi_5\|^2 + \eta_3 \times \|\xi_3 - \xi_5\|^2 + \eta_4 \times \|\xi_4 - \xi_5\|^2 \\
 &\quad + \eta_6 \times \|\xi_6 - \xi_5\|^2 + \eta_7 \times \|\xi_7 - \xi_5\|^2 + \eta_8 \times \|\xi_8 - \xi_5\|^2 + \eta_9 \times \|\xi_9 - \xi_5\|^2 \\
 &= 850.25 \times C_{CH}
 \end{aligned} \tag{5.45}$$

For $B = 5$, UAV-oriented strategy cannot be applied since it can visit no CH robot.

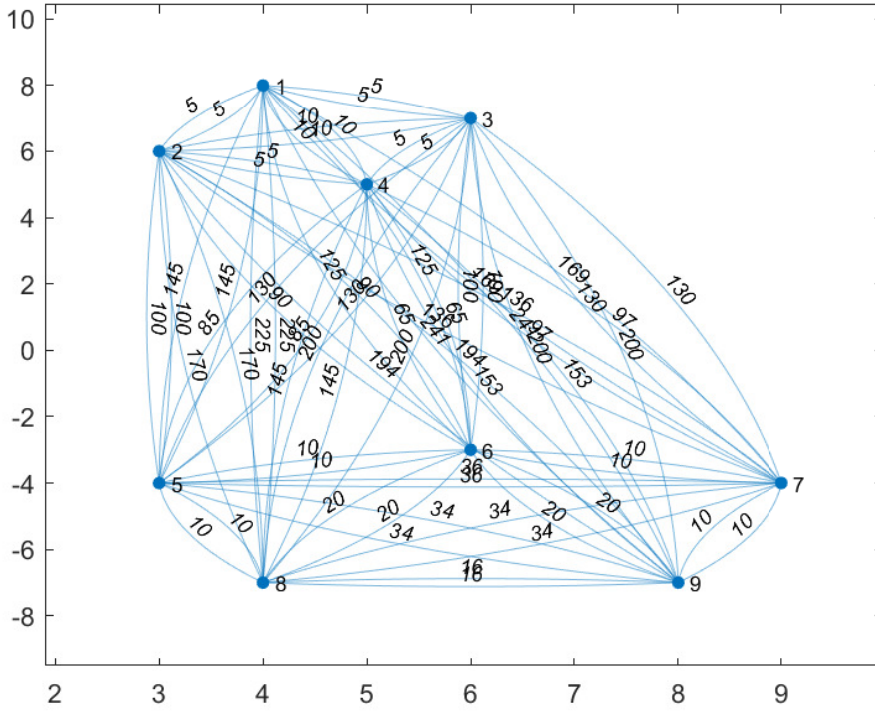


Figure 5.10: Nodes show the locations of the 9 CH robots. The weight of a link shows square of distance between two nodes connected by the link.

5.3.5.2 GAMEDFS

In this subsection, we obtain the numerical results for performance of GAMEDFS proposed in Chapter 3 with battery capacities varying from $B = 5$ to $B = 50$ in the configuration in Figure 5.10. In Figure 5.11, by applying GAMEDFS, UAV with $B = 40, 45, 50 \times C_{UAV}$ can visit all CH robots, i. e., $J(u, \pi^{GAMEDFS}) = 0$. In the configuration in Figure 5.10, the energy required for UAV to visit all CH robots is $E_{UAV}^{\pi^*}(u) \approx 39.97 \times C_{UAV}$. UAV with $B = 35 \times C_{UAV}$ goes without visiting CH robot 7 and 9 which results in

$$\begin{aligned}
 J(u, \pi^{GAMEDFS}) &= (0.65 \times 10 + 0.55 \times 20) \times C_{CH} \\
 &= 17.50 \times C_{CH}
 \end{aligned} \tag{5.46}$$

and $E_{UAV}^{\pi^*}(u) \approx 34.11 \times C_{UAV}$. UAV with $B = 30 \times C_{UAV}$ goes without visiting CH robot 7, 8 and 9 which results in

$$\begin{aligned} J(u, \pi^{GAMEDFS}) &= (0.65 \times 10 + 0.60 \times 10 + 0.55 \times 20) \times C_{CH} \\ &= 23.50 \times C_{CH} \end{aligned} \quad (5.47)$$

and $E_{UAV}^{\pi^*}(u) \approx 29.64 \times C_{UAV}$. UAV with $B = 25 \times C_{UAV}$ goes without visiting CH robot 1,3, 7, 8 and 9 which results in

$$\begin{aligned} J(u, \pi^{GAMEDFS}) &= (0.95 \times 5 + 0.85 \times 5 + 0.65 \times 10 + 0.60 \times 10 + 0.55 \times 20) \times C_{CH} \\ &= 32.50 \times C_{CH} \end{aligned} \quad (5.48)$$

and $E_{UAV}^{\pi^*}(u) \approx 23.71 \times C_{UAV}$. UAV with $B = 20 \times C_{UAV}$ goes without visiting CH robot 3, 5, 6, 7, 8 and 9 which results in

$$\begin{aligned} J(u, \pi^{GAMEDFS}) &= (0.85 \times 5 + 0.75 \times 25 + 0.70 \times (10+25) + 0.65 \times (10+10+25) \\ &\quad + 0.60 \times (10 + 25) + 0.55 \times (16 + 10 + 25)) \times C_{CH} \\ &= 118.30 \times C_{CH} \end{aligned} \quad (5.49)$$

and $E_{UAV}^{\pi^*}(u) \approx 19.18 \times C_{UAV}$. UAV with $B = 15 \times C_{UAV}$ can visit only CH 2 which results in

$$\begin{aligned} J(u, \pi^{GAMEDFS}) &= (0.95 \times 5 + 0.85 \times 5 + 0.80 \times 5 + 0.75 \times 25 + 0.70 \times (10+25) \\ &\quad + 0.65 \times (10 + 10 + 25) + 0.60 \times (10 + 25) \\ &\quad + 0.55 \times (16 + 10 + 25)) \times C_{CH} \\ &= 127.05 \times C_{CH} \end{aligned} \quad (5.50)$$

and $E_{UAV}^{\pi^*}(u) \approx 13.41 \times C_{UAV}$. UAV with $B = 10 \times C_{UAV}$ can visit only CH 5 which results in

$$\begin{aligned} J(u, \pi^{GAMEDFS}) &= (0.95 \times (5 + 45) + 0.90 \times 45 + 0.85 \times (5 + 50) + 0.80 \times 50 \\ &\quad + 0.70 \times 10 + 0.65 \times (10 + 10) + 0.60 \times 10 \\ &\quad + 0.55 \times (16 + 10)) \times C_{CH} \\ &= 222.05 \times C_{CH} \end{aligned} \quad (5.51)$$

and $E_{UAV}^{\pi^*}(u) = 10.00 \times C_{UAV}$. UAV with $B = 5 \times C_{UAV}$ can visit no CH robot which results in

$$\begin{aligned}
J(u, \pi^{GAMEDFS}) &= (0.95 \times (5 + 45) + 0.90 \times 45 + 0.85 \times (5 + 50) + 0.80 \times 50 \\
&\quad + 0.75 \times 25 + 0.70 \times (10 + 25) + 0.65 \times (10 + 10 + 25) \\
&\quad + 0.60 \times (10 + 25) + 0.55 \times (16 + 10 + 25)) \times C_{CH} \\
&= 303.30 \times C_{CH}
\end{aligned} \tag{5.52}$$

5.3.5.3 EEADCS

EEADCS has taken same decisions with GAMEDFS for all battery capacity values varying from $B = 5$ to $B = 50$ in the configuration of Figure 5.10.

Although CH 6 has the low data efficiency among all CH robots, UAV still prefers to visit CH 6 for $B = 20, 25, 30, 35$ because it can forward data from CH 7, CH 8, CH 9 and it is the closest CH robot to the set of CH 1, CH 2, CH 3, CH 4, which is very important for the energy consumption of the UAV.

UAV still prefers to visit CH 2 and CH 5 with lower battery capacities because many CH robots forward their data to CH 2 or CH 5 robot for lower battery capacities of UAV. If $B = 15$, UAV prefers CH 2 to CH 5 because CH 2 is further from origin than CH 5 and it forwards data of CH 1, CH 3 and CH 4, which has higher efficiency than CH 6, CH 7, CH 8 and CH 9. If CH 2 were much closer to origin than CH 5, then UAV may prefer to visit CH 5 to reduce the total joint cost.

In case that data efficiencies of all CH robots are equal, GAMEDFS has already been shown to be optimal in Chapter 3. With efficiencies generated with the formula $\eta_i = 1 - \frac{i}{20}$, the performance of strategies still depends more on positions of CH robots. It can be expected since if a route is infeasible because of battery capacity of UAV, minimizing sum of data efficiencies of the nonvisited CH robots lose its importance. Here, data efficiencies of the CH robots do not have an affect on the hard constraint of battery capacity of UAV as locations of CH robots do.

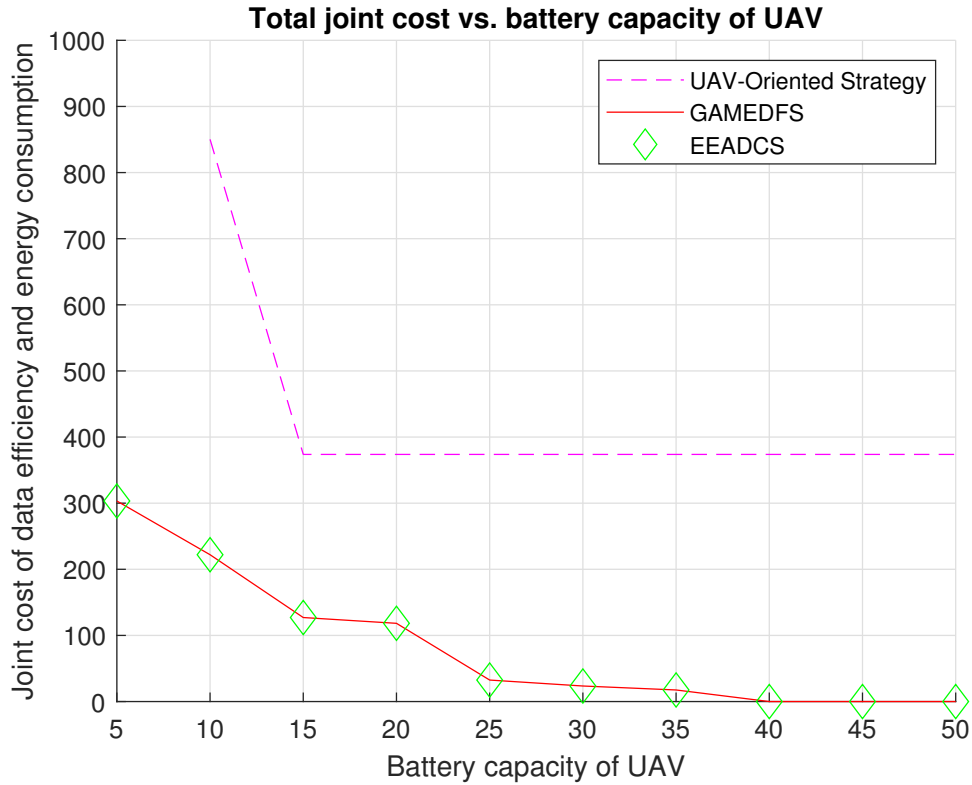


Figure 5.11: Total joint cost of data efficiency and energy consumption of the 9 CH robots in Figure 5.10 under UAV-Oriented strategy, GAMEDFS and EEADCS, vs. battery capacity of UAV from $B = 5 \times C_{UAV}$ to $B = 50 \times C_{UAV}$. The units for energy consumption of the UAV and total joint cost of the CH robots are C_{UAV} and C_{CH} , respectively. These constants depend on the type of the UAV and the CH robots.

5.3.5.4 Performance Comparison

Table 5.9 presents indices of nonvisited CH robots in Figure 5.10. Similarly, Table 5.10 presents total joint cost of energy consumption and data efficiencies of the nonvisited CH robots. From these tables, we can observe how UAV decides to go without visiting a subset of CH robots depending on its battery capacity in Figure 5.10. Moreover, the sum of joint cost of consumed energy and data efficiencies of nonvisited CH robots varies with battery capacity of UAV and so desisting decisions made by UAV. Furthermore, joint costs of nonvisited CH robots depend on positions and data efficiencies of the CH robots.

Table 5.9: The table shows indices of the nonvisited CH robots depending on battery capacity of UAV in Figure 5.10. "None" implies that the UAV visits all CH robots if $B = 25, 30, 35, 40, 45, 50$. "×" implies that the UAV-oriented strategy is infeasible for that battery capacity.

Strategy	B = 5	B = 10	B = 15	B = 20	B = 25
UAV-Oriented	×	1-4,6-9	1-5,7-9	1-5,7-9	1-5,7-9
GAMEDFS	1-9	1-4,6-9	1,3-9	3,5-9	1,3, 7-9
EEADCS	1-9	1-4,6-9	1,3-9	3,5-9	1,3, 7-9
Strategy	B = 30	B = 35	B = 40	B = 45	B = 50
UAV-Oriented	1-5,7-9	1-5,7-9	1-5,7-9	1-5,7-9	1-5,7-9
GAMEDFS	7-9	7,9	None	None	None
EEADCS	7-9	8,9	None	None	None

Table 5.10: The table shows total joint cost of energy consumption and data efficiencies of the nonvisited CH robots depending on battery capacity of UAV in Figure 5.11. "×" implies that the UAV-oriented strategy is infeasible for that battery capacity.

Strategy	B = 5	B = 10	B = 15	B = 20	B = 25
UAV-Oriented	×	850.25	373.75	373.75	373.75
GAMEDFS	303.30	222.05	127.05	118.30	32.50
EEADCS	303.30	222.05	127.05	118.30	32.50
Strategy	B = 30	B = 35	B = 40	B = 45	B = 50
UAV-Oriented	373.75	373.75	373.75	373.75	373.75
GAMEDFS	23.50	17.50	0	0	0
EEADCS	23.50	17.00	0	0	0

5.3.6 10-CH case

Figure 3.18 shows locations of 10 CH robots and weights of links between them. Positions of CH robots are $(\xi_1, \xi_2, \xi_3, \xi_4, \xi_5, \xi_6, \xi_7, \xi_8, \xi_9, \xi_{10}) = ((6, -7), (-5, 3), (2, 4), (-4, 7), (-2, 2), (2, -7), (-1, -2), (4, -8), (-1, 5), (7, -6))m$ where $(0, 0)$ is initial position of UAV. Data efficiencies of CH robots are taken as $(\eta_1, \eta_2, \eta_3, \eta_4, \eta_5, \eta_6,$

$$\eta_7, \eta_8, \eta_9, \eta_{10}) = (0.95, 0.90, 0.85, 0.80, 0.75, 0.70, 0.65, 0.60, 0.55, 0.50)m.$$

5.3.6.1 UAV-Oriented Strategy

By applying UAV-Oriented strategy, UAV travels only to CH robot 7 ($\xi_7 = (-1, -2)$) and collect all data of the CH robots from there if $B \approx 4.47 \times C_{UAV} < 5 \times C_{UAV}$. by which we can calculate the joint cost of data efficiency and energy consumption of nonvisited CH robots under UAV-Oriented strategy as follows.

$$\begin{aligned} J(u, \pi^{UAV-O}) &= \eta_1 \times \|\xi_1 - \xi_7\|^2 + \eta_2 \times \|\xi_2 - \xi_7\|^2 + \eta_3 \times \|\xi_3 - \xi_7\|^2 \\ &+ \eta_4 \times \|\xi_4 - \xi_7\|^2 + \eta_5 \times \|\xi_5 - \xi_7\|^2 + \eta_6 \times \|\xi_6 - \xi_7\|^2 \\ &+ \eta_8 \times \|\xi_8 - \xi_7\|^2 + \eta_9 \times \|\xi_9 - \xi_7\|^2 + \eta_{10} \times \|\xi_{10} - \xi_7\|^2 \\ &= 357.55 \times C_{CH} \end{aligned} \quad (5.53)$$

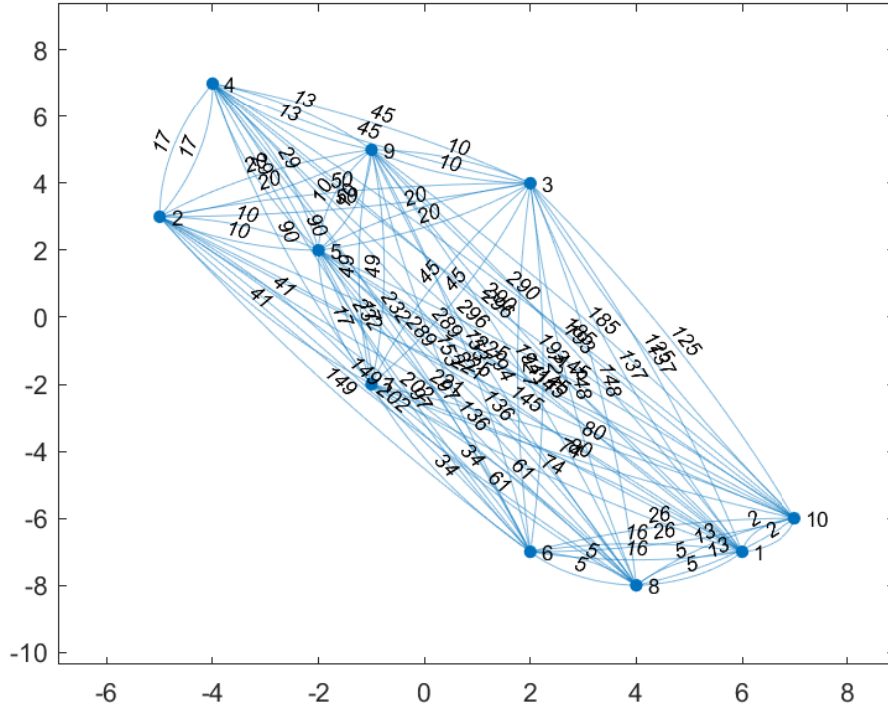


Figure 5.12: Nodes show locations of 10 CH robots. The weight of a link shows square of distance between two nodes connected by the link.

5.3.6.2 GAMEDFS

In this subsection, we obtain numerical results for the performance of GAMEDFS proposed in Chapter 3 with battery capacities varying from $B = 5$ to $B = 50$ in the configuration in Figure 5.12. In Figure 5.13, by applying optimal strategy, the UAV with $B = 45 \times C_{UAV}$ or $B = 50 \times C_{UAV}$ can visit all CH robots, i. e., $J(u, \pi^{GAMEDFS}) = 0$. In the configuration in Figure 5.12, minimum energy required for UAV to visit each CH robot is $E_{UAV}^{\pi^{GAMEDFS}}(u) \approx 42.02 \times C_{UAV}$.

The UAV with $B = 40 \times C_{UAV}$ goes without visiting CH robot 2 which results in

$$\begin{aligned} J(u, \pi^{GAMEDFS}) &= 0.90 \times 10 \\ &= 9 \times C_{CH} \end{aligned} \quad (5.54)$$

and $E_{UAV}^{\pi^{GAMEDFS}}(u) \approx 39.21 \times C_{UAV}$. The UAV with $B = 35 \times C_{UAV}$ goes without visiting CH robot 2 and 4 which results in

$$\begin{aligned} J(u, \pi^{GAMEDFS}) &= (0.90 \times 10 + 0.80 \times 13) \times C_{CH} \\ &= 19.40 \times C_{CH} \end{aligned} \quad (5.55)$$

and $E_{UAV}^{\pi^{GAMEDFS}}(u) \approx 34.29 \times C_{UAV}$. The UAV with $B = 30 \times C_{UAV}$ goes without visiting CH robot 2, 3, 4 and 9 which results in

$$\begin{aligned} J(u, \pi^{GAMEDFS}) &= (0.90 \times 10 + 0.85 \times 20 + 0.80 \times (13 + 10) + 0.55 \times 10) \times C_{CH} \\ &= 49.90 \times C_{CH} \end{aligned} \quad (5.56)$$

and $E_{UAV}^{\pi^{GAMEDFS}}(u) \approx 28.83 \times C_{UAV}$. The UAV with $B = 25 \times C_{UAV}$ goes without visiting CH robot 2, 3, 4, 5 and 9 which results in

$$\begin{aligned} J(u, \pi^{GAMEDFS}) &= (0.90 \times (10 + 8) + 0.85 \times 20 + 0.80 \times (13 + 10 + 8) \\ &\quad + 0.75 \times 8 + 0.55 \times (10 + 8)) \times C_{CH} \\ &= 73.90 \times C_{CH} \end{aligned} \quad (5.57)$$

and $E_{UAV}^{\pi^{GAMEDFS}}(u) \approx 23.17 \times C_{UAV}$. The UAV with $B = 20 \times C_{UAV}$ goes without visiting CH robot 1, 2, 3, 4, 5, 9 and 10 which results in

$$\begin{aligned} J(u, \pi^{GAMEDFS}) &= (0.95 \times 5 + 0.90 \times (10 + 8) + 0.85 \times 20 + 0.80 \times (13 + 10 + 8) \\ &\quad + 0.75 \times 8 + 0.55 \times (10 + 8) + 0.50 \times (2 + 5)) \times C_{CH} \\ &= 82.15 \times C_{CH} \end{aligned} \quad (5.58)$$

and $E_{UAV}^{\pi^{GAMEDFS}}(u) \approx 19.25 \times C_{UAV}$. The UAV with $B = 15 \times C_{UAV}$ visits only CH robot 6 which results in

$$\begin{aligned}
J(u, \pi^{GAMEDFS}) &= (0.95 \times (5 + 5) + 0.90 \times (10 + 8) + 0.85 \times 20 \\
&+ 0.80 \times (13 + 10 + 8) + 0.75 \times 8 + 0.60 \times 5 \\
&+ 0.55 \times (10 + 8) + 0.65 \times 5 + 0.50 \times (2 + 5 + 5)) \times C_{CH} \\
&= 95.65 \times C_{CH}
\end{aligned} \tag{5.59}$$

and $E_{UAV}^{\pi^{GAMEDFS}}(u) \approx 14.56 \times C_{UAV}$. The UAV with $B = 10 \times C_{UAV}$ visits only CH robot 5 and 7 which results in

$$\begin{aligned}
J(u, \pi^{GAMEDFS}) &= (0.95 \times (5 + 5 + 34) + 0.90 \times (10 + 8) + 0.85 \times 20 \\
&+ 0.80 \times (13 + 10 + 8) + 0.70 \times 34 + 0.55 \times (10 + 8) \\
&+ 0.60 \times (5 + 34) + 0.50 \times (2 + 5 + 5 + 34)) \times C_{CH} \\
&= 179.65 \times C_{CH}
\end{aligned} \tag{5.60}$$

and $E_{UAV}^{\pi^{GAMEDFS}}(u) \approx 9.19 \times C_{UAV}$. The UAV with $B = 5 \times C_{UAV}$ visit only CH robot 7 which results in

$$\begin{aligned}
J(u, \pi^{GAMEDFS}) &= (0.95 \times (5 + 5 + 34) + 0.90 \times (10 + 8) + 0.85 \times 20 \\
&+ 0.80 \times (13 + 10 + 8) + 0.75 \times 8 + 0.70 \times 34 + 0.55 \times (10 + 8) \\
&+ 0.60 \times (5 + 34) + 0.50 \times (2 + 5 + 5 + 34)) \times C_{CH} \\
&= 185.65 \times C_{CH}
\end{aligned} \tag{5.61}$$

and $E_{UAV}^{\pi^{GAMEDFS}}(u) \approx 4.47 \times C_{UAV}$.

5.3.6.3 EEADCS

EEADCS has taken same decisions with GAMEDFS for all battery capacity values varying from $B = 5$ to $B = 50$ except $B = 20$ in the configuration of Figure 5.12.

Under the GAMEDFS, the UAV with $B = 20 \times C_{UAV}$ goes without visiting CH robot 1, 2, 3, 4, 5, 9 and 10 which results in $J(u, \pi^{GAMEDFS}) = 82.15 \times C_{CH}$. Besides, under the GAMEDFS, the UAV with $B = 25 \times C_{UAV}$ goes without visiting CH robot 2, 3, 4, 5, 9 and 10 which results in $J(u, \pi^{GAMEDFS}) = 73.90 \times C_{CH}$. On the other

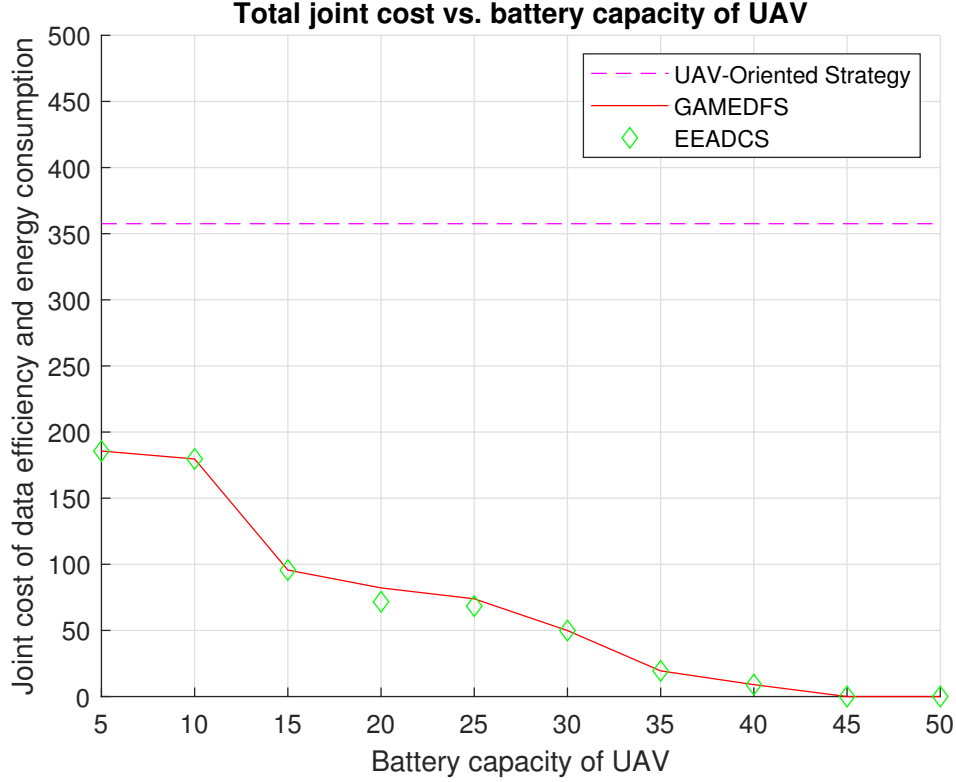


Figure 5.13: Total joint cost of data efficiency and energy consumption of 10 CH robots in Figure 5.12 under UAV-Oriented strategy, GAMEDFS and EEADCS, vs. battery capacity of UAV from $B = 5 \times C_{UAV}$ to $B = 50 \times C_{UAV}$. The units for energy consumption of the UAV and total joint cost of the CH robots are C_{UAV} and C_{CH} , respectively. These constants depend on the type of the UAV and the CH robots.

hand, under EEADCS, UAV with $B = 20 \times C_{UAV}$ goes without visiting CH robot 1, 2, 3, 4, 7, 8, 9 and 10 which results in $J(u, \pi^{EEADCS}) = 71.65 \times C_{CH}$ and

$$\begin{aligned} E_{UAV}^{\pi^{EEADCS}}(u) &= \|\xi_0 - \xi_6\| + \|\xi_6 - \xi_5\| + \|\xi_5 - \xi_0\| \\ &\approx 19.96 \times C_{UAV} \end{aligned} \quad (5.62)$$

Moreover, under the EEADCS, the UAV with $B = 25 \times C_{UAV}$ goes without visiting CH robot 1, 2, 3, 4, 8, 9 and 10 which results in $J(u, \pi^{EEADCS}) = 68.40 \times C_{CH}$ and

$$\begin{aligned} E_{UAV}^{\pi^{EEADCS}}(u) &= \|\xi_0 - \xi_7\| + \|\xi_7 - \xi_6\| + \|\xi_6 - \xi_5\| + \|\xi_5 - \xi_0\| \\ &\approx 24.79 \times C_{UAV} \end{aligned} \quad (5.63)$$

Although CH 6 and CH 8 have the low data efficiency among all CH robots, UAV still

prefers to visit CH 6 and CH 8 with lower battery capacities because CH 6 and CH 8 are very close to CH 1 and CH 10 so CH 6 and CH 8 forwards their data. Even only visiting CH 6 reduces the sum of joint costs of data efficiency and consumed energy of each CH robot because UAV can collect data from CH 8, CH 1 and CH 10 at CH 6. On the other hand, although CH 2 and CH 3 have the high data efficiency among all CH robots, UAV with lower battery capacities go without visiting them instead of CH 6 and CH 8 because CH 2 and CH 3 do not forward data of another CH robot as CH 6 and CH 8 do.

Although CH 5 and CH 7 have the low data efficiency among all CH robots, UAV still prefers to visit CH 5 and CH 7 with low battery capacities $B = 10$ because CH 5 and CH 7 are much closer to origin than the other CH robots.

For $B = 5$, visiting CH 7 is the only feasible path. Please notice that if CH 5 were located at the position $(-1, 2)$ instead of $(-2, 2)$ and CH 3 is not visited by UAV, then CH 3 would send its data to CH robot 5 instead of directly sending to the origin. For UAV with $B = 5$, CH 5 would forward data from CH 2, CH 4, CH 9 and CH 3 whereas CH 7 would forward data from CH 6, CH 8, CH 1 and CH 10. Compared with visiting no CH robot, the UAV would reduce the joint cost

$$5 \times [0.75 + (0.90 + 0.80 + 0.55 + 0.85)] \times C_{CH} = 3.85 \times C_{CH} \quad (5.64)$$

by visiting only CH 5 at position $(-1, 2)$ whereas the UAV would reduce the joint cost

$$5 \times [0.65 + (0.70 + 0.60 + 0.95 + 0.50)] \times C_{CH} = 3.40 \times C_{CH} \quad (5.65)$$

by visiting only CH 7 at the position $(-1, -2)$. Therefore, UAV with $B = 5$ would prefer CH 5 instead of CH 7 to reduce the joint cost of data efficiency and energy consumption of CH robots.

In case that data efficiencies of all CH robots are equal, GAMEDFS has already been shown to be optimal in Chapter 3. With efficiencies generated with the formula $\eta_i = 1 - \frac{i}{20}$, the performance of strategies still depends more on positions of CH robots. It can be expected since if a route is infeasible because of battery capacity of UAV, minimizing the data efficiencies of the nonvisited CH robots lose its

importance. Here, data efficiencies of the CH robots do not have an affect on the hard constraint of battery capacity of UAV as locations of CH robots do.

5.3.6.4 Performance Comparison

Table 5.11 presents indices of nonvisited CH robots in Figure 5.12. Similarly, Table 5.12 presents total joint cost of energy consumption and data efficiencies of the nonvisited CH robots. From these tables, we can observe how UAV decides to go without visiting a subset of CH robots depending on its battery capacity in Figure 5.12. Moreover, the sum of joint cost of consumed energy and data efficiencies of nonvisited CH robots varies with battery capacity of UAV and so desisting decisions made by UAV. Furthermore, joint costs of nonvisited CH robots depend on positions and data efficiencies of the CH robots.

Table 5.11: The table shows indices of the nonvisited CH robots depending on battery capacity of UAV in Figure 5.12. "None" implies that the UAV visits all CH robots if $B = 45$ or $B = 50$.

Strategy	B = 5	B = 10	B = 15	B = 20	B = 25
UAV-O	1-6,8-10	1-6,8-10	1-6,8-10	1-6,8-10	1-6,8-10
GAMEDFS	1-6,8-10	1-4,6,8-10	1-5,7-10	1-5,9,10	2-5,9
EEADCS	1-6,8-10	1-4,6,8-10	1-5,7-10	1-4,7-10	1-4,8-10
Strategy	B = 30	B = 35	B = 40	B = 45	B = 50
UAV-O	1-6,8-10	1-6,8-10	1-6,8-10	1-6,8-10	1-6,8-10
GAMEDFS	2-4,9	2,4	2	None	None
EEADCS	2-4,9	2,4	2	None	None

Table 5.12: The table shows total joint cost of energy consumption and data efficiencies of the nonvisited CH robots depending on battery capacity of UAV in Figure 5.13.

Strategy	B = 5	B = 10	B = 15	B = 20	B = 25
UAV-Oriented	357.55	357.55	357.55	357.55	357.55
GAMEDFS	185.65	179.65	95.65	82.15	73.90
EEADCS	185.65	179.65	95.65	71.65	68.40
Strategy	B = 30	B = 35	B = 40	B = 45	B = 50
UAV-Oriented	357.55	357.55	357.55	357.55	357.55
GAMEDFS	49.90	19.40	9.00	0	0
EEADCS	49.90	19.40	9.00	0	0



CHAPTER 6

SENSITIVITY ANALYSIS UNDER HOP CONSTRAINTS FOR DATA FORWARDING

We evaluated the performance of the strategies for various battery capacities and various hop constraints (for data forwarding) in the 5-CH robot, 7-CH robot, and 10-CH robot scenarios in Section 3.4.

In these scenarios, remind that the path length for UAV to visit all CH robots is less than 50 units, which yields that battery capacity of UAV sufficient to visit all CH robots is less than $50 \times C_{UAV}$. We evaluate the performances of UAV-oriented strategy in [75], GAMEDFS in [76] (the strategy proposed in Chapter 3) and EEADCS (the strategy proposed in Chapter 5). *We calculate energy consumed by UAV and joint cost of energy consumptions and data efficiencies of the nonvisited CH robots under various hop constraints.*

Remind that Problem 3 does not have any hop constraints. In this chapter, we make the sensitivity analysis of EEADCS (the strategy proposed in Chapter 5) with respect to hop constraints for data forwarding and evaluate the performance of EEADCS for various battery capacities and various hop constraints (for data forwarding). We tackle the energy-aware and efficiency-aware data collection problem under various hop constraints.

By adding a constraint for maximum number of hops, Problem 3 turns into Problem 4.

Problem 4. *Minimizing total joint cost of energy consumption and data efficiencies of nonvisited CH robots via UAV with limited-capacity battery*

$$\begin{aligned}
 & \min_{\pi, u \subseteq P} J(u, \pi) \\
 & \text{s.t.} \quad E_{UAV}^{\pi} \leq B \\
 & \quad n_{max}(\pi, u) \leq N_{hop}
 \end{aligned}$$

where $n_{max}(\pi, u)$ denotes the number of hops made by forwarded data under strategies π and u ; N_{hop} denotes the maximum number of hops that forwarded data can be made.

From Section 3.4, the number of hops made by forwarded data under strategies π^{EEADCS} and u can be given as follows. In 5-CH robot scenario in Figure 6.1, $n_{max}(\pi^{EEADCS}, u) = 2$; In 7-CH robot scenario in Figure 6.3, $n_{max}(\pi^{EEADCS}, u) = 4$; In 10-CH robot scenario in Figure 6.5, $n_{max}(\pi^{EEADCS}, u) = 4$. Therefore, in this chapter, we will investigate the performances of EEADCS with lower number of hop constraints. To illustrate, we will choose $N_{hop} = 3, 2, 1$ for 7-CH robot scenario in Figure 6.3. If we choose $N_{hop} = 4$ for 7-CH robot scenario in Figure 6.3, we can observe no difference in the performance of EEADCS.

In Section 6.1, we will investigate the performance of EEADCS with 1-hop constraint in 5-CH robot scenario in Figure 6.1. In Section 6.2, we will investigate the performance of EEADCS with 3-hop constraint, EEADCS with 2-hop constraint and EEADCS with 1-hop constraint in 7-CH robot scenario in Figure 6.3. In Section 6.3, we will investigate the performance of EEADCS with 3-hop constraint, EEADCS with 2-hop constraint and EEADCS with 1-hop constraint in 10-CH robot scenario in Figure 6.5. The performance of EEADCS with no hop constraints will be also given in the scenarios in Section 6.1, Section 6.2 and Section 6.3 for the comparison. Hence, we will analyse how much our proposed strategy EEADCS is sensitive with respect to the constraints on the maximum number of hops made by forwarded data of a nonvisited CH robot.

6.1 5-CH case

In this 5-CH scenario in Figure 6.1, Table 6.1 indicates that at least one nonvisited CH robot forwards its data via 2-hop (more than 1-hop) under GAMEDFS and EEADCS for the following battery capacities of UAV $B = 5, 10, 25$. For the following battery capacities of UAV $B = 15, 20, 30, 35, 40$, each nonvisited CH robot forwards its data via at most one hop under GAMEDFS and EEADCS. On the other hand, UAV-Oriented Strategy is a single-hop strategy so we do not need to consider it again. Remind that $J(u, \pi^{UAV-O}) = 277.85 \times C_{CH}$ for $B > 5.66 \times C_{UAV}$.

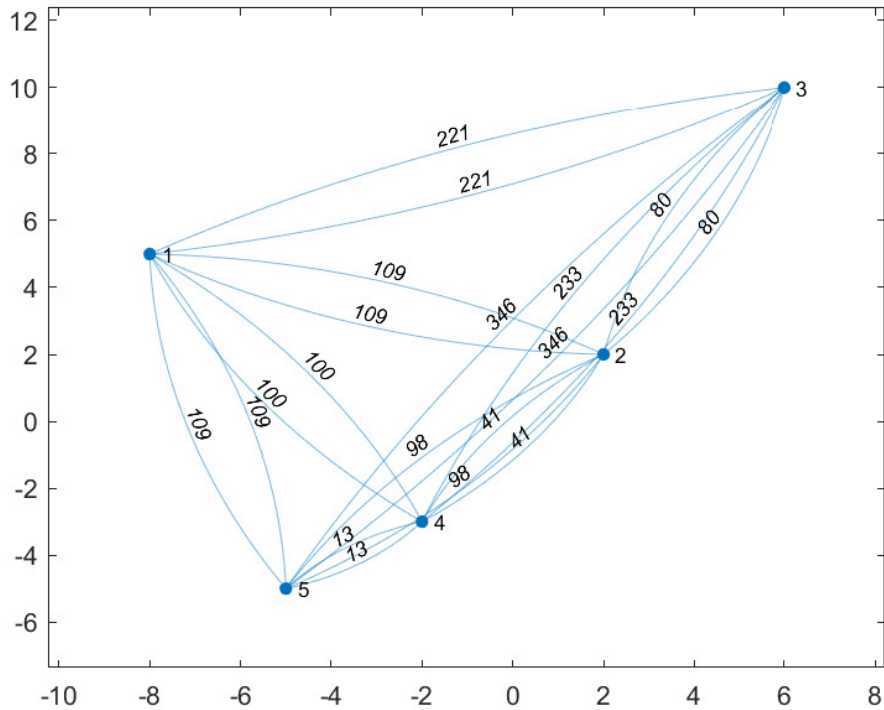


Figure 6.1: Nodes show locations of 5 CH robots. The weight of a link shows square of distance between two nodes connected by the link.

6.1.1 EEADCS with 1-hop constraint

In this subsection, under maximum 1-hop constraint, we obtain the numerical results for the performance of EEADCS with battery capacities varying from $B =$

5, 10, 25 in the configuration in Figure 6.1 (The other battery capacities make no difference). The UAV with $B = 25 \times C_{UAV}$ goes without visiting CH robot 3, 4 and 5 which results in

$$\begin{aligned} J(u, \pi^{EEADCS}) &= (0.85 \times 80 + 0.80 \times 13 + 0.75 \times 50) \times C_{CH} \\ &= 115.90 \times C_{CH} \end{aligned} \quad (6.1)$$

and $E_{UAV}^{\pi^{EEADCS}}(u) \approx 22.70 \times C_{UAV}$. UAV with $B = 10 \times C_{UAV}$ goes without visiting CH robot 3, 4, 5 and 1 which results in

$$\begin{aligned} J(u, \pi^{EEADCS}) &= (0.85 \times 80 + 0.80 \times 13 + 0.75 \times 50 + 0.95 \times 89) \times C_{CH} \\ &= 201.45 \times C_{CH} \end{aligned} \quad (6.2)$$

and $E_{UAV}^{\pi^{EEADCS}}(u) \approx 5.66 \times C_{UAV}$. UAV with $B = 5 \times C_{UAV}$ can visit no CH robot which results in

$$\begin{aligned} J(u, \pi^{EEADCS}) &= (0.85 \times 136 + 0.90 \times 8 + 0.80 \times 13 + 0.75 \times 50 \\ &\quad + 0.95 \times 89) \times C_{CH} \\ &= 255.25 \times C_{CH} \end{aligned} \quad (6.3)$$

6.1.2 Performance Comparison

Table 6.1 presents indices of nonvisited CH robots in Figure 6.1. Similarly, Table 6.2 presents total joint cost of energy consumption and data efficiencies of the nonvisited CH robots. From these tables, we can observe how UAV decides to go without visiting a subset of CH robots depending on its battery capacity in Figure 6.1. Moreover, the sum of joint cost of consumed energy and data efficiencies of nonvisited CH robots varies with battery capacity of UAV and so desisting decisions made by UAV. Furthermore, joint costs of nonvisited CH robots depend on positions and data efficiencies of the CH robots.

EEADCS makes different decision than EEADCS (with no hop constraint) only for $B = 10$ and $B = 25$. In these cases, EEADCS go without visiting CH robot 4 instead of CH robot 2. Besides, the total joint cost change due to change in data

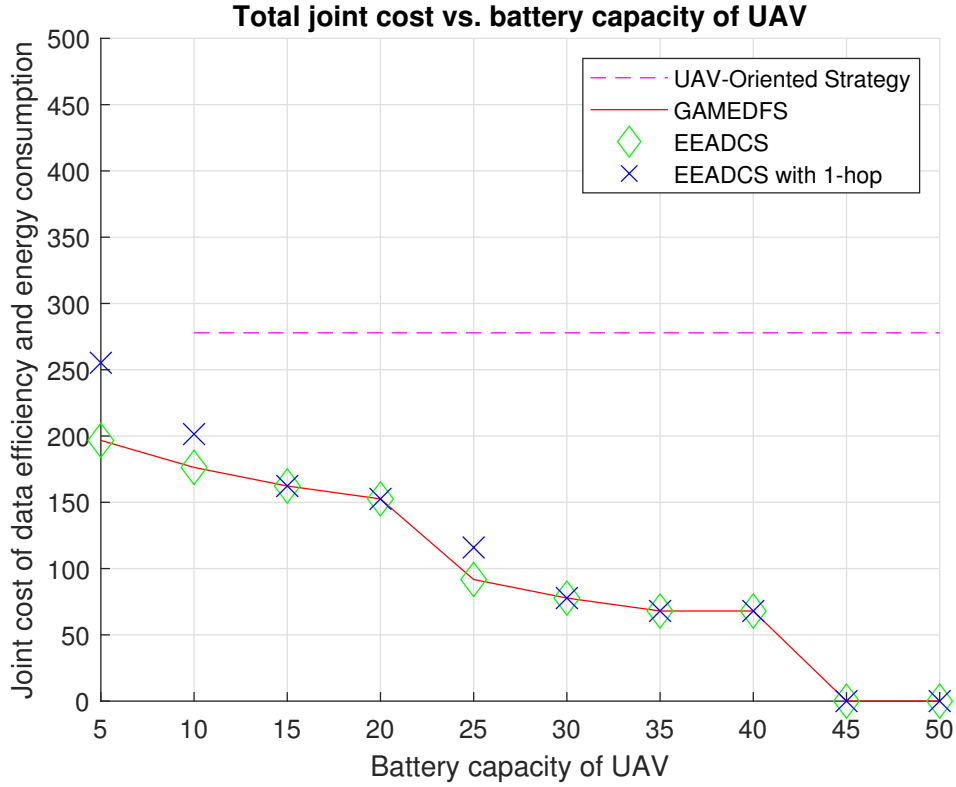


Figure 6.2: Total joint cost of data efficiency and energy consumption of the 5 CH robots in Figure 6.1 under UAV-Oriented strategy, GAMEDFS and EEADCS (with various hop constraints), for varying battery capacities of UAV. The units for energy consumption of the UAV and total joint cost of the CH robots are C_{UAV} and C_{CH} , respectively. These constants depend on the type of the UAV and the CH robots.

forwarding strategies of some CH robots for some battery capacity values under 1-hop constraints. We can make the following remarks. For minimizing the joint cost of nonvisited CH robots that are very far from the rest of the CH robots and its initial position, UAV should not go without visiting the next CH robots to these far nonvisited CH robots. Similarly, minimizing the joint cost of the nonvisited CH robots which have much higher efficiency than the other CH robots, the UAV should not go without visiting the next CH robots to these nonvisited CH robots with high data efficiencies.

Comparing EEADCS under 1-hop constraint and no hop constraint, we can make the following remarks. Especially under 1-hop constraint, EEADCS has result in more energy consumption than EEADCS with no hop constraint because no nonvisited

CH robot can forward its data. In fact, they need to transmit their data directly to a nonvisited CH robot or UAV at origin. As the battery capacity of UAV decreases, hops required for forwarding data optimally is increased. Therefore, the difference in the cost between EEADCS under 1-hop constraint and no hop constraint increases for low battery capacities.

Table 6.1: The table shows indices of the nonvisited CH robots depending on battery capacity of UAV in Figure 6.1. "None" implies that UAV visits all CH robots if $B = 45$ or $B = 50$. "×" implies that the UAV-oriented Strategy is infeasible for that battery capacity.

Strategy	B = 5	B = 10	B = 15	B = 20	B = 25
UAV-Oriented	×	1,3-5	1,3-5	1,3-5	1,3-5
GAMEDFS	1-5	1-3,5	1,3,5	1,3	2,3,5
EEADCS	1-5	1-3,5	1,3,5	1,3	2,3,5
EEADCS with 1-hop	1-5	1,3-5	1,3,5	1,3	3,4,5
Strategy	B = 30	B = 35	B = 40	B = 45	B = 50
UAV-Oriented	1,3-5	1,3-5	1,3-5	1,3-5	1,3-5
GAMEDFS	3,5	3	3	None	None
EEADCS	3,5	3	3	None	None
EEADCS with 1-hop	3,5	3	3	None	None

6.2 7-CH case

In this 7-CH scenario in Figure 6.3, Table 6.3 indicates that at least one nonvisited CH robot forwards its data via more than one hop (maximum 4-hop) under GAMEDFS and EEADCS for the following battery capacities of UAV $B = 5, 10, 15$. For the following battery capacities of UAV $B = 20, 25, 30$, each nonvisited CH robot forwards its data via at most one hop under GAMEDFS and EEADCS. On the other hand, UAV-Oriented Strategy is a single-hop strategy so we do not need to consider it again. Remind that $J(u, \pi^{UAV-O}) = 111.85 \times C_{CH}$ for $B > 17.2 \times C_{UAV}$ and $J(u, \pi^{UAV-O}) = 178.75 \times C_{CH}$ for $5.65 < B \leq 17.2 \times C_{UAV}$.

Table 6.2: The table shows total joint cost of energy consumption and data efficiencies of the nonvisited CH robots depending on battery capacity of UAV in Figure 6.2. "×" implies that the UAV-oriented strategy is infeasible for that battery capacity.

Strategy	B = 5	B = 10	B = 15	B = 20	B = 25
UAV-Oriented	×	277.85	277.85	277.85	277.85
GAMEDFS	196.70	176.30	162.30	152.55	91.75
EEADCS	196.70	176.30	162.30	152.55	91.75
EEADCS with 1-hop	255.25	201.45	162.30	152.55	115.90
Strategy	B = 30	B = 35	B = 40	B = 45	B = 50
UAV-Oriented	277.85	277.85	277.85	277.85	277.85
GAMEDFS	77.75	68.00	68.00	0	0
EEADCS	77.75	68.00	68.00	0	0
EEADCS with 1-hop	77.75	68.00	68.00	0	0

6.2.1 EEADCS with 3-hop constraint

In this subsection, under maximum 3-hop constraint, we obtain the numerical results for the performance of EEADCS with battery capacities varying from $B = 5$ in the configuration in Figure 3.12 (The other battery capacities make no difference). UAV with $B = 5 \times C_{UAV}$ can travel to no CH robot which result in $J(u, \pi^{EEADCS}) = 199.55 \times C_{CH}$. Here, data forwarding strategies of CH 1 and CH 4 robots change only for $B = 5$. Their data is forwarded to CH 6, then forwarded to CH 3 and then forwarded directly to origin. (CH 7 is removed from their data forwarding path).

6.2.2 EEADCS with 2-hop constraint

In this subsection, under maximum 2-hop constraint, we obtain the numerical results for the performance of EEADCS with battery capacities varying from $B = 5$ in the configuration in Figure 3.12 (The other battery capacities make no difference). UAV with $B = 5 \times C_{UAV}$ can visit no CH robot which results in $J(u, \pi^{EEADCS}) = 240.65 \times C_{CH}$. Here, data forwarding strategies of CH 1, CH4, CH5 and CH 6 robots change only for $B = 5$. Their data is forwarded to CH 3 and then directly to origin.

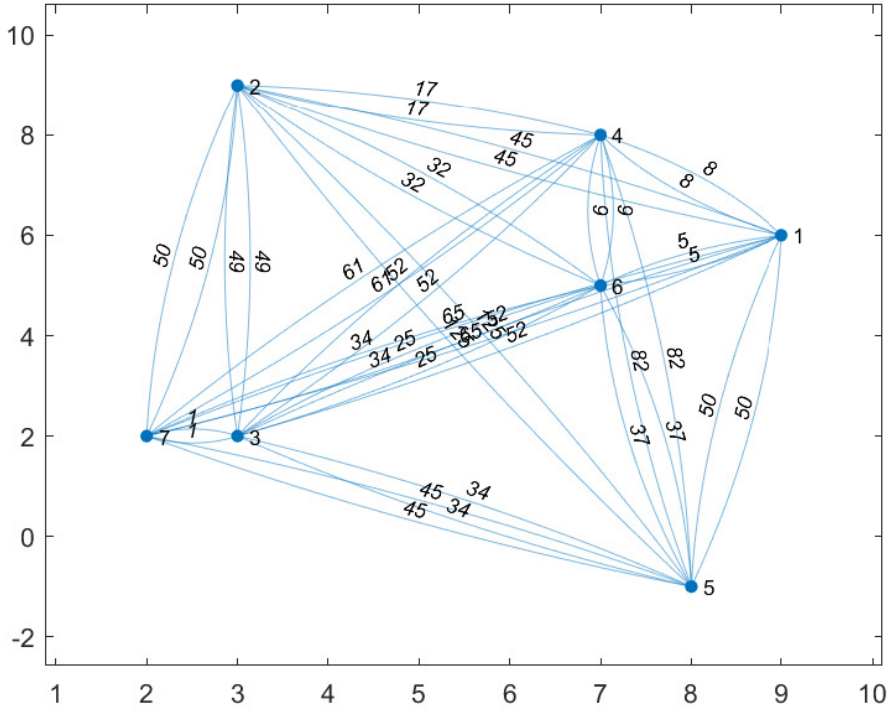


Figure 6.3: Nodes show locations of 7 CH robots. The weight of a link shows square of distance between two nodes connected by the link.

(CH 7 is removed from their data forwarding paths. Moreover, CH 6 and CH 7 is removed from their data forwarding paths of CH 1 and CH 4).

6.2.3 EEADCS with 1-hop constraint

In this subsection, under maximum 1-hop constraint, we obtain the numerical results for the performance of EEADCS with battery capacities varying from $B = 5, 10, 15$ in the configuration in Figure 6.3 (The other battery capacities make no difference). UAV with $B = 10 \times C_{UAV}$ or $B = 15 \times C_{UAV}$ goes without visiting CH robot 1, 2, 4, 5 and 6 which results in

$$\begin{aligned}
 J(u, \pi^{EEADCS}) &= (0.95 \times 52 + 0.90 \times 50 + 0.80 \times 52 + 0.75 \times 34 \\
 &\quad + 0.70 \times 25) \times C_{CH} \\
 &= 179 \times C_{CH}
 \end{aligned} \tag{6.4}$$

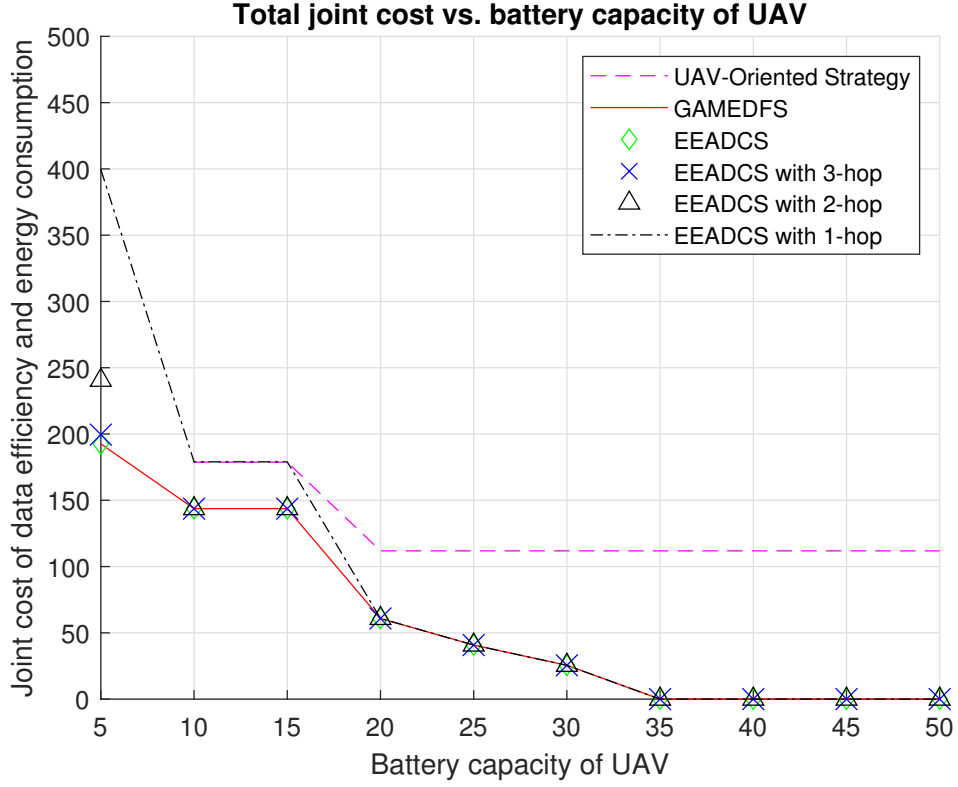


Figure 6.4: Total joint cost of data efficiency and energy consumption of the 7 CH robots in Figure 6.3 under UAV-Oriented strategy, GAMEDFS and EEADCS (with various hop constraints), for varying battery capacities of UAV. The units for energy consumption of the UAV and total joint cost of the CH robots are C_{UAV} and C_{CH} , respectively. These constants depend on the type of the UAV and the CH robots.

and $E_{UAV}^{\pi^*}(u) \approx 7.43 \times C_{UAV}$. UAV with $B = 5 \times C_{UAV}$ can travel to no CH robot which result in

$$\begin{aligned}
 J(u, \pi^{EEADCS}) &= (0.95 \times 117 + 0.90 \times 90 + 0.85 \times 13 + 0.80 \times 113 + 0.75 \times 65 \\
 &\quad + 0.70 \times 74 + 0.65 \times 8) \times C_{CH} \\
 &= 399.35 \times C_{CH}
 \end{aligned} \tag{6.5}$$

(Each CH robot transmits data directly to UAV standing in the origin).

6.2.4 Performance Comparison

Table 6.3 presents indices of nonvisited CH robots in Figure 6.3. Similarly, Table 6.4 presents total joint cost of energy consumption and data efficiencies of the nonvisited CH robots. From these tables, we can observe how UAV decides to go without visiting a subset of CH robots depending on its battery capacity in Figure 6.3. Moreover, the sum of joint cost of consumed energy and data efficiencies of nonvisited CH robots varies with battery capacity of UAV and so desisting decisions made by UAV. Furthermore, joint costs of nonvisited CH robots depend on positions and data efficiencies of the CH robots.

EEADCS with 1-hop, EEADCS with 2-hop and EEADCS with 3-hop make no different decision than EEADCS (with no hop constraint); however, the total joint cost changes due to change in data forwarding strategies of some CH robots for some battery capacity values under hop-constraints. We can make the following remarks. While minimizing the sum of joint costs of each nonvisited CH robot, UAV should keep battery constraint. As CH 3 and CH 7 robots are close to initial location of UAV, the UAV can visit only them independent from their joint cost of data efficiency&energy consumption and the hop constraint.

Comparing EEADCS under 1-hop constraint, 2-hop constraint, 3-hop constraint and no hop constraint, we can make the following remarks. Especially under 1-hop constraint, EEADCS has result in more energy consumption than EEADCS with no hop constraint because none of the nonvisited CH robots can forward their data. In fact, they need to send their data directly to a nonvisited CH robot or UAV at origin. Especially under 2-hop constraint and 3-hop constraint, EEADCS has result in more energy consumption than EEADCS with no hop constraint because some of the nonvisited CH robots can forward their data with removing some nonvisited CH robots from their data forwarding paths. As the battery capacity of the UAV decreases, the hops required for forwarding data optimally is increased. Therefore, the difference in the cost between EEADCS under 1-hop constraint, 2-hop constraint, 3-hop constraint and no hop constraint increases for low battery capacities.

Table 6.3: The table shows indices of the nonvisited CH robots depending on battery capacity of UAV in Figure 6.3. "None" implies that the UAV visits all CH robots if $B = 35, 40, 45, 50$. " \times " implies that the UAV-oriented strategy is infeasible for that battery capacity.

Strategy	B = 5	B = 10	B = 15	B = 20	B = 25
UAV-Oriented	\times	1,2,4-7	1,2,4-7	1-5,7	1-5,7
GAMEDFS	1-7	1,2,4-6	1,2,4-6	1,2,4,5	2,5
EEADCS	1-7	1,2,4-6	1,2,4-6	1,2,4,5	2,5
EEADCS with 3-hop	1-7	1,2,4-6	1,2,4-6	1,2,4,5	2,5
EEADCS with 2-hop	1-7	1,2,4-6	1,2,4-6	1,2,4,5	2,5
EEADCS with 1-hop	1-7	1,2,4-6	1,2,4-6	1,2,4,5	2,5
Strategy	B = 30	B = 35	B = 40	B = 45	B = 50
UAV-Oriented	1-5,7	1-5,7	1-5,7	1-5,7	1-5,7
GAMEDFS	5	None	None	None	None
EEADCS	5	None	None	None	None
EEADCS with 3-hop	5	None	None	None	None
EEADCS with 2-hop	5	None	None	None	None
EEADCS with 1-hop	5	None	None	None	None

6.3 10-CH case

In this 10-CH scenario in Figure 6.5, Table 6.5 indicates that at least one nonvisited CH robot forwards its data via more than one hop (maximum 4-hop) under GAMEDFS and EEADCS for the following battery capacities of UAV $B = 5, 10, 15, 20, 25$. For the following battery capacities of UAV $B = 30, 35, 40$, each nonvisited CH robot forwards its data via at most one hop under GAMEDFS and EEADCS. On the other hand, UAV-Oriented Strategy is a single-hop strategy so we do not need to consider it again. Remind that $J(u, \pi^{UAV-O}) = 357.55 \times C_{CH}$.

Table 6.4: The table shows total joint cost of energy consumption and data efficiencies of the nonvisited CH robots depending on battery capacity of UAV in Figure 6.4. "×" implies that the UAV-oriented strategy is infeasible for that battery capacity.

Strategy	B = 5	B = 10	B = 15	B = 20	B = 25
UAV-Oriented	×	178.75	178.75	111.85	111.85
GAMEDFS	192.55	143.70	143.70	60.85	40.80
EEADCS	192.55	143.70	143.70	60.85	40.80
EEADCS with 3-hop	199.55	143.70	143.70	60.85	40.80
EEADCS with 2-hop	240.65	143.70	143.70	60.85	40.80
EEADCS with 1-hop	399.35	179.00	179.00	60.85	40.80
Strategy	B = 30	B = 35	B = 40	B = 45	B = 50
UAV-Oriented	111.85	111.85	111.85	111.85	111.85
GAMEDFS	25.50	0	0	0	0
EEADCS	25.50	0	0	0	0
EEADCS with 3-hop	25.50	0	0	0	0
EEADCS with 2-hop	25.50	0	0	0	0
EEADCS with 1-hop	25.50	0	0	0	0

6.3.1 EEADCS with 3-hop constraint

In this subsection, under maximum 3-hop constraint, we obtain the numerical results for the performance of EEADCS with battery capacities varying from $B = 5$ in the configuration in Figure 6.5 (The other battery capacities make no difference). The UAV with $B = 10 \times C_{UAV}$ visits only CH robot 5 and 7 which results in

$$\begin{aligned}
 J(u, \pi^{EEADCS}) &= (0.95 \times (5 + 5 + 34) + 0.90 \times (10 + 8) + 0.85 \times 20 \\
 &+ 0.80 \times (13 + 10 + 8) + 0.70 \times 34 + 0.55 \times (10 + 8) \\
 &+ 0.60 \times (5 + 34) + 0.50 \times (13 + 5 + 34)) \times C_{CH} \\
 &= 182.65 \times C_{CH}
 \end{aligned} \tag{6.6}$$

and $E_{UAV}^{\pi^{EEADCS}}(u) \approx 9.19 \times C_{UAV}$. The UAV with $B = 5 \times C_{UAV}$ visit only CH robot 7 which results in

which results in

$$\begin{aligned}
J(u, \pi^{EEADCS}) &= (0.95 \times (5 + 5) + 0.90 \times 10 + 0.85 \times 20 + 0.80 \times (13 + 10) \\
&\quad + 0.60 \times 5 + 0.55 \times 10 + 0.50 \times (13 + 5)) \times C_{CH} \\
&= 71.40 \times C_{CH}
\end{aligned} \tag{6.8}$$

and $E_{UAV}^{\pi^{EEADCS}}(u) \approx 24.79 \times C_{UAV}$. The UAV with $B = 20 \times C_{UAV}$ goes without visiting CH robot 1, 2, 3, 4, 7, 8, 9 and 10 which results in

$$\begin{aligned}
J(u, \pi^{EEADCS}) &= (0.95 \times (5 + 5) + 0.90 \times 10 + 0.85 \times 20 + 0.80 \times (13 + 10) \\
&\quad + 0.65 \times 5 + 0.60 \times 5 + 0.55 \times 10 + 0.50 \times (13 + 5)) \times C_{CH} \\
&= 74.65 \times C_{CH}
\end{aligned} \tag{6.9}$$

and $E_{UAV}^{\pi^{EEADCS}}(u) \approx 19.96 \times C_{UAV}$. The UAV with $B = 15 \times C_{UAV}$ visits only CH robot 6 which results in

$$\begin{aligned}
J(u, \pi^{EEADCS}) &= (0.95 \times (5 + 5) + 0.90 \times (10 + 8) + 0.85 \times 20 + 0.80 \times (29 + 8) \\
&\quad + 0.75 \times 8 + 0.60 \times 5 + 0.55 \times (10 + 8) + 0.65 \times 5 \\
&\quad + 0.50 \times (13 + 5)) \times C_{CH} \\
&= 103.45 \times C_{CH}
\end{aligned} \tag{6.10}$$

and $E_{UAV}^{\pi^{EEADCS}}(u) \approx 14.56 \times C_{UAV}$. The UAV with $B = 10 \times C_{UAV}$ travel to just CH robot 5 and 7 which result in

$$\begin{aligned}
J(u, \pi^{EEADCS}) &= (0.95 \times (16 + 34) + 0.90 \times (10 + 8) + 0.85 \times 20 \\
&\quad + 0.80 \times (29 + 8) + 0.70 \times 34 + 0.55 \times (10 + 8) \\
&\quad + 0.60 \times (5 + 34) + 0.50 \times (26 + 34)) \times C_{CH} \\
&= 197.40 \times C_{CH}
\end{aligned} \tag{6.11}$$

and $E_{UAV}^{\pi^{EEADCS}}(u) \approx 9.19 \times C_{UAV}$. The UAV with $B = 5 \times C_{UAV}$ visit only CH robot 7 which results in

$$\begin{aligned}
J(u, \pi^{EEADCS}) &= (0.95 \times (16 + 34) + 0.90 \times (10 + 8) + 0.85 \times 20 \\
&\quad + 0.80 \times (29 + 8) + 0.75 \times 8 + 0.70 \times 34 + 0.55 \times (10 + 8) \\
&\quad + 0.60 \times (5 + 34) + 0.50 \times (26 + 34)) \times C_{CH} \\
&= 203.40 \times C_{CH}
\end{aligned} \tag{6.12}$$

and $E_{UAV}^{\pi^{EEADCS}}(u) \approx 4.47 \times C_{UAV}$.

6.3.3 EEADCS with 1-hop constraint

In this subsection, under maximum 1-hop constraint, we obtain the numerical results for the performance of EEADCS with battery capacities varying from $B = 5$ in the configuration in Figure 6.5 (The other battery capacities make no difference). The UAV with $B = 25 \times C_{UAV}$ goes without visiting CH robot 1, 2, 3, 4, 8, 9 and 10 which results in

$$\begin{aligned}
 J(u, \pi^{EEADCS}) &= (0.95 \times 16 + 0.90 \times 10 + 0.85 \times 20 + 0.80 \times 29 + 0.60 \times 5 \\
 &\quad + 0.55 \times 10 + 0.50 \times 26) \times C_{CH} \\
 &= 85.90 \times C_{CH}
 \end{aligned} \tag{6.13}$$

and $E_{UAV}^{\pi^{EEADCS}}(u) \approx 24.79 \times C_{UAV}$. The UAV with $B = 20 \times C_{UAV}$ goes without visiting CH robot 1, 2, 3, 4, 7, 8, 9 and 10 which results in

$$\begin{aligned}
 J(u, \pi^{EEADCS}) &= (0.95 \times 16 + 0.90 \times 10 + 0.85 \times 20 + 0.80 \times 29 + 0.65 \times 5 \\
 &\quad + 0.60 \times 5 + 0.55 \times 10 + 0.50 \times 26) \times C_{CH} \\
 &= 89.15 \times C_{CH}
 \end{aligned} \tag{6.14}$$

and $E_{UAV}^{\pi^{EEADCS}}(u) \approx 19.96 \times C_{UAV}$. The UAV with $B = 15 \times C_{UAV}$ visits only CH robot 6 which results in

$$\begin{aligned}
 J(u, \pi^{EEADCS}) &= (0.95 \times 16 + 0.90 \times 26 + 0.85 \times 20 + 0.80 \times 65 + 0.75 \times 8 \\
 &\quad + 0.60 \times 5 + 0.55 \times 26 + 0.65 \times 5 + 0.50 \times 26) \times C_{CH} \\
 &= 147.15 \times C_{CH}
 \end{aligned} \tag{6.15}$$

and $E_{UAV}^{\pi^{EEADCS}}(u) \approx 14.56 \times C_{UAV}$. The UAV with $B = 10 \times C_{UAV}$ travels to just CH robot 5 and 7 which result in

$$\begin{aligned}
 J(u, \pi^{EEADCS}) &= (0.95 \times 74 + 0.90 \times 10 + 0.85 \times 20 + 0.80 \times 29 + 0.70 \times 34 \\
 &\quad + 0.55 \times 10 + 0.60 \times 61 + 0.50 \times 80) \times C_{CH} \\
 &= 225.40 \times C_{CH}
 \end{aligned} \tag{6.16}$$

and $E_{UAV}^{\pi^{EEADCS}}(u) \approx 9.19 \times C_{UAV}$. The UAV with $B = 5 \times C_{UAV}$ visit only CH robot 7 which results in

$$\begin{aligned}
 J(u, \pi^{EEADCS}) &= (0.95 \times 74 + 0.90 \times 34 + 0.85 \times 20 + 0.80 \times 65 + 0.75 \times 8 \\
 &\quad + 0.70 \times 34 + 0.55 \times 26 + 0.60 \times 61 + 0.50 \times 80) \times C_{CH} \\
 &= 290.60 \times C_{CH}
 \end{aligned} \tag{6.17}$$

and $E_{UAV}^{\pi^{EEADCS}}(u) \approx 4.47 \times C_{UAV}$.

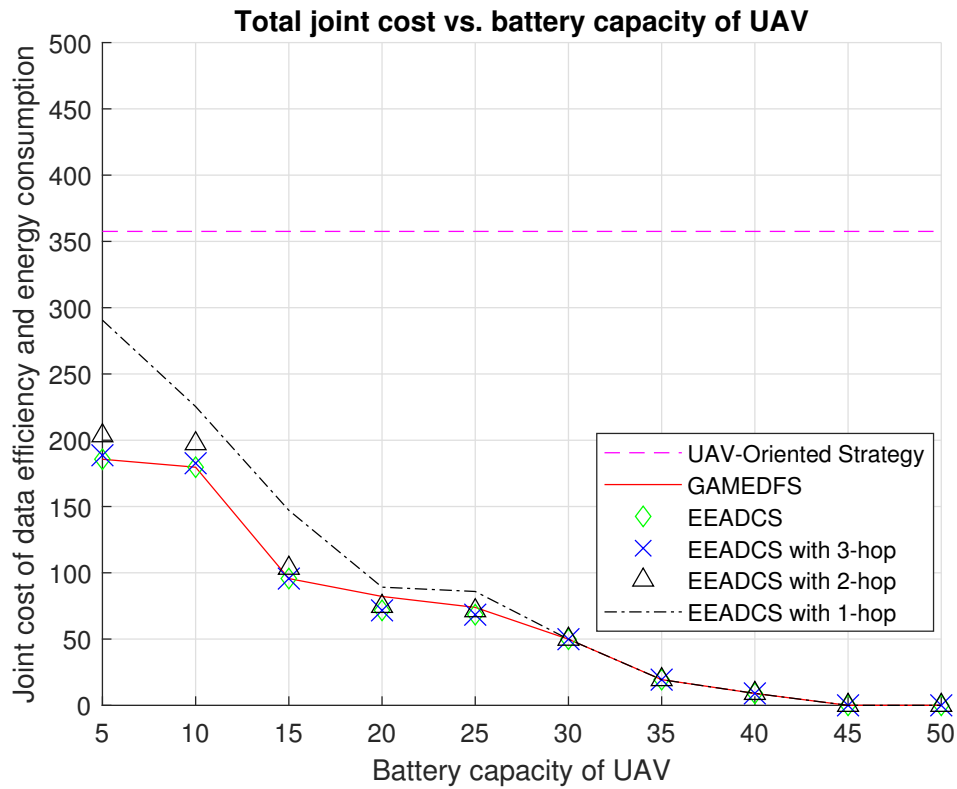


Figure 6.6: Total joint cost of data efficiency and energy consumption of the 10 CH robots in Figure 6.5 under UAV-Oriented strategy, GAMEDFS and EEADCS (with various hop constraints), for varying battery capacities of UAV. The units for energy consumption of the UAV and total joint cost of the CH robots are C_{UAV} and C_{CH} , respectively. These constants depend on the type of the UAV and the CH robots.

6.3.4 Performance Comparison

Table 6.5 presents indices of nonvisited CH robots in Figure 6.5. Similarly, Table 6.6 presents total joint cost of energy consumption and data efficiencies of the nonvisited CH robots. From these tables, we can observe how UAV decides to go without visiting a subset of CH robots depending on its battery capacity in Figure 6.5. Moreover, the sum of joint cost of consumed energy and data efficiencies of nonvisited CH robots varies with battery capacity of UAV and so desisting decisions made by UAV. Furthermore, joint costs of nonvisited CH robots depend on positions and data efficiencies of the CH robots.

EEADCS with 1-hop, EEADCS with 2-hop and EEADCS with 3-hop make no different decision than EEADCS (with no hop constraint); however, the total joint cost changes due to change in data forwarding strategies of some CH robots for some battery capacity values under hop-constraints. We can make the following remarks. While minimizing the joint cost of nonvisited CH robots, UAV should keep battery constraint. As CH 5 and CH 7 robots are close to initial location of UAV, the UAV can visit only them independent from their joint cost of data efficiency&energy consumption and the hop constraint.

Comparing EEADCS under 1-hop constraint, 2-hop constraint, 3-hop constraint and no hop constraint, we can make the following remarks. Especially under 1-hop constraint, EEADCS has result in more energy consumption than EEADCS with no hop constraint because no nonvisited CH robot can forward its data. In fact, it need to transmit its data directly to one of visited CH robots or UAV at origin. Especially under 2-hop constraint and 3-hop constraint, EEADCS has result in more energy consumption than EEADCS with no hop constraint because some of the nonvisited CH robots can forward their data with removing some nonvisited CH robots from their data forwarding paths. As the battery capacity of the UAV decreases, the hops required for forwarding data optimally is increased. Therefore, the difference in the cost between EEADCS under 1-hop constraint, 2-hop constraint, 3-hop constraint and no hop constraint increases for low battery capacities.

Table 6.5: The table shows indices of the nonvisited CH robots depending on battery capacity of UAV in Figure 6.5. "None" implies that the UAV visits all CH robots if $B = 45$ or $B = 50$.

Strategy	B = 5	B = 10	B = 15	B = 20	B = 25
UAV-O	1-6,8-10	1-6,8-10	1-6,8-10	1-6,8-10	1-6,8-10
GAMEDFS	1-6,8-10	1-4,6,8-10	1-5,7-10	1-5,9,10	2-5,9
EEADCS	1-6,8-10	1-4,6,8-10	1-5,7-10	1-4,7-10	1-4,8-10
EEADCS with 3-hop	1-6,8-10	1-4,6,8-10	1-5,7-10	1-4,7-10	1-4,8-10
EEADCS with 2-hop	1-6,8-10	1-4,6,8-10	1-5,7-10	1-4,7-10	1-4,8-10
EEADCS with 1-hop	1-6,8-10	1-4,6,8-10	1-5,7-10	1-4,7-10	1-4,8-10
Strategy	B = 30	B = 35	B = 40	B = 45	B = 50
UAV-O	1-6,8-10	1-6,8-10	1-6,8-10	1-6,8-10	1-6,8-10
GAMEDFS	2-4,9	2,4	2	None	None
EEADCS	2-4,9	2,4	2	None	None
EEADCS with 3-hop	2-4,9	2,4	2	None	None
EEADCS with 2-hop	2-4,9	2,4	2	None	None
EEADCS with 1-hop	2-4,9	2,4	2	None	None

Table 6.6: The table shows total joint cost of energy consumption and data efficiencies of the nonvisited CH robots depending on battery capacity of UAV in Figure 6.6.

Strategy	B = 5	B = 10	B = 15	B = 20	B = 25
UAV-Oriented	357.55	357.55	357.55	357.55	357.55
GAMEDFS	185.65	179.65	95.65	82.15	73.90
EEADCS	185.65	179.65	95.65	71.65	68.40
EEADCS with 3-hop	188.65	182.65	95.65	71.65	68.40
EEADCS with 2-hop	203.40	197.40	103.45	74.65	71.40
EEADCS with 1-hop	290.60	225.40	147.15	89.15	85.90
Strategy	B = 30	B = 35	B = 40	B = 45	B = 50
UAV-Oriented	357.55	357.55	357.55	357.55	357.55
GAMEDFS	49.90	19.40	9.00	0	0
EEADCS	49.90	19.40	9.00	0	0
EEADCS with 3-hop	49.90	19.40	9.00	0	0
EEADCS with 2-hop	49.90	19.40	9.00	0	0
EEADCS with 1-hop	49.90	19.40	9.00	0	0



CHAPTER 7

CONCLUSION

In this work, we investigate a data collection problem via an unmanned aerial vehicle (UAV) with limited battery capacity in a robot network divided into several robot clusters. In each cluster, a cluster head (CH) robot allocates tasks to the remaining robots in the cluster and collects data from them and then transmits data to the UAV directly or indirectly (by sending its data to another CH robot to forward to the UAV). In this network, UAV visits some of the CH robots or all of them depending on their locations and the battery capacity of the UAV. If the UAV cannot visit all of CH robots due to the limited battery capacity, then the CH robots not visited by the UAV transmit their data to one of the neighbor CH robot. The aim of the UAV is to minimize the total energy consumption of the CH robots by planning a path.

We propose a two-stage solution for this problem. First, we consider the problem as a traveling salesman problem (TSP) by taking unlimited battery capacity for the UAV. In the second stage, we remove some of the CH robots from the path in order to reduce the energy consumption of the UAV up to the battery capacity of the UAV. We handle the problem by using an approach and obtain the optimal strategy for this problem. Our strategy is compared with the approaches in the close literature for varying number of clusters. The numerical results show that our approach performs much better than the approach in the close literature for various number of CH robots and various battery capacities of the UAV. Hence, our strategy minimizes the total energy consumption of the CH robots optimally depending on the locations of the CH robots and the battery capacity of the UAV.

In our work, we consider the amount and accuracy of all data from all CH robots equally; however, the amount and accuracy of data from different CH robots may

differ due to many factors such as difference in the performance of robots and sensors. Therefore, in future work, we plan to consider the problem with varying amount of data for different CH robots. In this scenario, the UAV also evaluates the decision efficiencies of the CH robots which allocates tasks to the other robots. The problem can also be considered under the assumption that visiting a certain specific portion of CH robots are mandatory for the UAV. As the intensity of the acquisition signal can be reduced due to forwarding, this will be our consideration of the near future. This will possibly include the relay cost, i.e., the energy consumed by the CH robot to forward the data received by other CH robot/s.

Then, we investigate another data collection problem by an UAV with limited battery capacity in a robot network divided into clusters. In each cluster, a CH robot allocates tasks to the remaining robots in the cluster and collects data from them and then transmit data to the UAV directly or indirectly. In this network, UAV visits a varying portion of CH robots depending on its battery capacity, positions of the CH robots and the priority sets of CH robots. The nonvisited CH robots forwards their data to another CH robot. By planning an optimal trajectory, UAV aims to minimize the energy consumed by CH robots. First, we consider this problem as a travel salesman problem by taking unlimited battery capacity for the UAV. In the second stage, we remove some of the CH robots from the path in order to reduce the energy consumption of the UAV upto the battery capacity of the UAV. We handle the problem by using an approach and obtain the optimal strategy for this problem. Our strategy is compared with the approaches in the close literature for varying number of clusters. The numerical results show that our approach performs much better than the approach in the close literature for various number of CH robots and various battery capacities of the UAV. Hence, with our strategy, the UAV plans an optimal trajectory to minimize the energy consumed by CH robots depending on its battery capacity, positions of CH robots and the priority sets of CH robots.

Finally, we investigate another data collection problem by a UAV with limited battery capacity in a clustered robot network. In each cluster, a CH robot allocates tasks to the remaining robots in the cluster and collects data from them and then transmit data to the UAV directly or indirectly. In this network, UAV visits a varying portion of CH robots depending on its battery capacity, data efficiencies and positions of the

CH robots. The nonvisited CH robots forwards their data to another CH robot. UAV aims to minimize total energy consumption of CH robots by also considering the data efficiencies of CH robots. First, we consider this problem as a travel salesman problem by taking unlimited battery capacity for the UAV. In the second stage, we remove In case that UAV has insufficient battery capacity, it desist from some CH robots to reduce its energy consumption below its battery capacity. We handle the problem analytically and obtain an optimal strategy for this problem. Our strategy is compared with the approaches in the close literature for varying number of clusters. The numerical results show that our approach performs much better than the approach in the close literature for various number of CH robots, various battery capacities of the UAV and data efficiencies of CH robots. *Hence, with our strategy, the UAV plans an optimal trajectory to minimize the joint cost of data efficiencies and energy consumed by nonvisited CH robots depending on its battery capacity, positions of CH robots and data efficiencies of CH robots.*

As future work, we can develop our work in the following directions. First, we may consider to apply such a constraint to the problem that a CH robot can forward data of a limited number of CH robots. The motivation behind this constraint comes from the fact that if a CH robot forwards data of many other CH robots, then its energy will decrease very fast, which will cause CH elections to be repeated very frequently. Second, the altitude can be considered during the trajectory planning because it can affect the energy consumption of UAV very much especially when it visits the CH robots close to each other. It can also affect the energy consumption for the visited CH robots to transmit their data, which has been neglected in this thesis (If the altitude is much lower than the distance between the CH robots, then we can neglect the energy consumption of CH robots which is proportional to the square of the distance). Third, mobility can be considered for the CH robots, at least for a subset of them. There may be some cases where at least a portion of CH robots need to move for completing their tasks other than their CH missions. Lastly, as the obtained solutions are not scalable, suboptimal heuristic solutions can be searched.



REFERENCES

- [1] J. Lin, W. Yu, N. Zhang, X. Yang, H. Zhang, and W. Zhao, "A Survey on Internet of Things: Architecture, Enabling Technologies, Security and Privacy, and Applications", *IEEE Internet of Things Journal*, vol. 4, no. 5, Oct. 2017.
- [2] P. Kamalinejad, C. Mahapatra, Z. Sheng, S. Mirabbasi, V.C.M. Leung, Y.L. Guan, "Wireless Energy Harvesting for the Internet of Things", *IEEE Communications Magazine*, vol. 53, 2015, pp. 102-108.
- [3] C.W. Tsai, T.P. Hong, G.N. Shiu, "Metaheuristics for the lifetime of WSN: A review", *IEEE Sensor Journal*, vol. 16, 2016, pp. 2812-2831.
- [4] C. Gomez, J. Paradells, "Urban Automation Networks: Current and Emerging Solutions for Sensed Data Collection and Actuation in Smart Cities", *Sensors* 2015, vol. 15, pp. 22874-22898.
- [5] Y. Zhang, L. Sun, H. Song, X. Cao, "Ubiquitous WSN for Healthcare: Recent Advances and Future Prospects", *IEEE Internet of Things Journal*, vol. 1, no. 4, Aug. 2014.
- [6] T. Wark, P. Corke, P. Sikka, L. Klingbeil, Y. Guo, C. Crossman, P. Valencia, D. Swain, G. Bishop-Hurley, "Transforming Agriculture through Pervasive Wireless Sensor Networks", *IEEE Pervasive Computing*, 2007, 6.
- [7] J. Valente, D. Sanz, A. Barrientos, J. del Cerro, A. Ribeiro, C. Rossi, "An Air-Ground Wireless Sensor Network for Crop Monitoring", *Sensors* 2011, 11, pp. 6088-6108.
- [8] C. Chaiwatpongsakorn, M. Lu, T.C. Keener, S.-J. Khang, "The deployment of carbon monoxide wireless sensor network (CO-WSN) for ambient air monitoring", *International Journal of Environmental Research and Public Health* 2014, 11, pp. 6246-6264.

- [9] Ahmed I., A. Alfa, "Optimization Techniques for Design Problems in Selected Areas in WSNs: A Tutorial", *Sensors*, vol. 17, no. 8: 1761, 2017.
- [10] S. Shue, J. Conrad, "Survey of Robotic Applications in Wireless Sensor Networks", *Proceedings of IEEE Southeastcon 2013*, 4-7 April 2013, pp.1-5.
- [11] Luthy, K.A.; Grant, E.; Henderson, T.C. Leveraging RSSI for Robotic Repair of Disconnected Wireless Sensor Networks. In Proceedings of the 2007 IEEE International Conference on Robotics and Automation, Roma, Italy, 10–14 April 2007; pp. 3659–3664.
- [12] Xu, L.; Falcon, R.; Nayak, A.; Stojmenovic, I., "Servicing wireless sensor networks by mobile robots", *IEEE Communications Magazine*, vol. 50, pp. 147-154, 2012.
- [13] Sheu, J.; Hsieh, K.; Cheng, P., "Design and Implementation of Mobile Robot for Nodes Replacement in Wireless Sensor Networks", *Journal of Information Science and Engineering*, vol. 24, pp. 393-410, 2008.
- [14] Zhang, Y.; Wang, L., "A particle filtering method for odor-source localization in Wireless Sensor Network with mobile robot", *In Proceedings of the 2010 29th Chinese Control Conference (CCC)*, Kunming, China, 29-31 July 2010; pp. 4821-4825.
- [15] Yuan, B; Orłowska, M.; Sadiq, S., "On the Optimal Robot Routing Problem in Wireless Sensor Networks", *IEEE Transactions on Knowledge and Data Engineering.*, vol. 19, pp. 1252-1261, 2007.
- [16] Tekdas, O.; Isler, V.; Lim, J.H.; Terzis, A., "Using mobile robots to harvest data from sensor fields", *IEEE Wireless Communications.*, 19, 22-28, 2009.
- [17] Mkhwanazi, X.; Hanh, L.; Blake, E., "Clustering between Data Mules for Better Message Delivery" *In Proceedings of the IEEE 26th International Conference on Advanced Information Networking and Applications*, Fukuoka, Japan, 26-29 March 2012; pp. 209-214.
- [18] Wong, R.; Xiao, J.; Joseph, S.L.; Shan, Z., "Data association for simultaneous localization and mapping in robotic wireless sensor networks", *In Proceed-*

ings of the 2010 IEEE/ASME International Conference on Advanced Intelligent Mechatronics (AIM), Montreal, QC, Canada, 6-9 July 2010; pp. 459-464.

- [19] Yao, Z.; Gupta, K., "Distributed roadmaps for robot navigation in sensor networks", *In Proceedings of the 2010 IEEE International Conference on Robotics and Automation (ICRA)*, Anchorage, AK, USA, 3-7 May 2010; pp. 3078-3083.
- [20] Fu, S.; Kuai, X.; Zheng, Z.; Yang, G.; Hou, Z., "Compressive sensing approach based mapping and localization for mobile robot in an indoor wireless sensor network", *In Proceedings of the 2010 International Conference on Networking, Sensing and Control*, Chicago, IL, USA, 10-12 April 2010; pp. 122-127.
- [21] Kuai, X.; Yang, K.; Fu, S.; Zheng, R; Yang, G., "Simultaneous localization and mapping (SLAM) for indoor autonomous mobile robot navigation in wireless sensor networks", *In Proceedings of the 2010 International Conference on Networking, Sensing and Control*, Chicago, IL, USA, 10-12 April 2010; pp. 128-132.
- [22] Gasparri, A.; Pascucci, F., "An Interlaced Extended Information filter for Self-Localization in Sensor Networks", *IEEE Transactions on Wireless Communications*, 9, pp. 1491-1504, 2010.
- [23] Mezei, I.; Malbasa, V.; Stojmenovic, I., "Robot to Robot: Communication Aspects of Coordination in Robot Wireless Networks", *IEEE Robotics and Automation Magazine*, 17, pp. 63-69, 2010.
- [24] Romeo, L.; Petitti, A.; Marani, R.; Milella, A. "Internet of Robotic Things in Smart Domains: Applications and Challenges", *Sensors* 2020, 20, 3355.
- [25] Cobano, J.A.; Martinez-Dios, J.R.; Conde, R.; Sanchez-Matamoros, J.M.; Ollero, A., "Data retrieving from heterogeneous wireless sensor network nodes using UAVs", *Journal of Intelligent and Robotic Systems.*, vol. 60, 133-151, 2020.
- [26] Heinzelman, W.B.; Chandrakasan, A.P.; Balakrishnan, H. "Energy efficient communication protocol for wireless microsensor networks", *In Proceedings of the 33rd Annual Hawaii International Conference on System Sciences*, Maui, HI, USA, 7-10 January; pp. 1-10.

- [27] Heinzelman, W.B.; Chandrakasan, A.P.; Balakrishnan, H., "An application-specific protocol architecture for wireless microsensor networks", *IEEE Transactions on Wireless Communications*, vol. 1, 660-670, 2004.
- [28] M. M. Shirmohammadi, K. Faez, and M. Chhardoli, "LELE: Leader election with load balancing energy in wireless sensor network", in *Proceedings of IEEE International Conference on Communications and Mobile Computing*, Sep. 2009, pp. 106-110.
- [29] F. Ayughi, K. Faez, and Z. Eskandari, "A non location aware version of modified LEACH algorithm based on residual energy and number of neighbors", in *Proceedings of IEEE International Conference in Advanced Communications Technologies*, Feb. 2010, pp. 1076-1080.
- [30] T. Camp, J. Boleng, and V. Davies, "A survey of mobility models for ad hoc network research", *Wireless Communications and Mobile Computing (WCMC): Special issue on Mobile Ad Hoc Networking: Research, Trends and Applications*, vol. 2, no. 5, pp. 483-502, 2002.
- [31] Sanchez M, Manzoni P, Anejos, "A java based simulator for ad-hoc networks", *Future Generation Computer Systems*, vol. 17, no. 5, 2001, pp. 573-583.
- [32] O. Younis and S. Fahmy, "Distributed Clustering in Ad-hoc Sensor Networks: A Hybrid, Energy-Efficient Approach", in *Proceedings of IEEE INFOCOM 2004*, Hong Kong, March 2004.
- [33] O. Younis and S. Fahmy, "HEED: A Hybrid, Energy-Efficient, Distributed Clustering Approach for Ad Hoc Sensor Networks", *IEEE Transaction on Mobile Computing*, vol. 3, no. 4, October-December 2004.
- [34] Kamimura, J.; Wakamiya, N.; Murata, M., "Energy-Efficient Clustering Method for Data Gathering in Sensor Networks", *Proceedings of the First Workshop on Broadband Advanced Sensor Networks (BaseNets2004)*, San Jose, California, USA, 25-29 October 2004, pp. 31-36.
- [35] Labroche, N.; Monmarche, N.; Venturini, G., "A new clustering algorithm based on the ants chemical recognition system", in *Proceedings of European Associ-*

ation for Artificial Intelligence 2002, Lyon, France, 21-26 July 2002; pp. 345-349.

- [36] Muhamad, W.N.W.; Dimayati, K.; Mohamad, R.; Haron, M.A.; Sarnin, S.S.; Wahab, N.A.; Aizi, N.H.A., "Evaluation of stable clusterhead election (SCHE) routing protocol for wireless sensor networks", *In Proceedings of the 2008 IEEE International RF and Microwave Conference*, Kuala Lumpur, Malaysia, 2-4 December 2008; pp. 101-105.
- [37] Ali, M.S.; Dey, T.; Biswas, R., "ALEACH: Advanced LEACH routing protocol for wireless microsensor networks", *In Proceedings of the 2008 International Conference on Electrical and Computer Engineering*, Dhaka, Bangladesh, 20-22 December 2008; pp. 909-914.
- [38] Hu, J.; Jin, Y.; Dou, L., "A time-based cluster-head selection algorithm for LEACH", *In Proceedings of the 2008 IEEE Symposium on Computers and Communications*, Marrakech, Morocco, 6-9 July 2008; pp. 1172-1176.
- [39] Zhao, L.; Liang, Q., "Distributed and energy efficient self-organization for on-off wireless sensor networks", *In Proceedings of the 15th IEEE International Symposium on Personal Indoor and Mobile Radio Communications (PIMRC)*, Barcelona, Spain, 5-8 September 2004; pp. 211-215.
- [40] Hu, X.; Luo, J.; Xia, Z.; Hu, M., "Adaptive algorithm of cluster head in wireless sensor network based on LEACH", *In Proceedings of IEEE 3rd International Conference on Communication Software and Networks*, Xi'an, China, 27-29 May 2011; pp. 14-18.
- [41] Azim, A.; Islam, M.M., "A dynamic round-time based fixed low energy adaptive clustering hierarchy for wireless sensor networks", *In Proceedings of the 2009 IEEE 9th Malaysia International Conference on Communications (MICC)*, Kuala Lumpur, Malaysia, 14-17 December 2009; pp. 922-926.
- [42] Sun, Z.G.; Zheng, Z.W.; Xu, S.J., "An efficient routing protocol based on two step cluster head selection for wireless sensor networks", *In Proceedings of the 2009 5th International Conference on Wireless Communications, Networking and Mobile Computing*, Beijing, China, 24-26 September 2009; pp. 1-5.

- [43] Mahmood, D.; Javaid, N.; Mahmood, S.; Qureshi, S.; Memon, A.M.; Zaman, T, "MODLEACH: A variant of LEACH for WSNs", *In Proceedings of the 2013 Eighth international conference on broadband and wireless computing, communication and applications*, Compiegne, France, 28-30 October 2013; pp. 158-163.
- [44] G. Smaragdakis, I. Matta, and A. Bestavros, "SEP: A stable election protocol for clustered heterogeneous wireless sensor networks", *in Proceedings of 2nd International Workshop Sensor Actor Network Protocols Applications. (SANPA)*, August 2004, pp. 1-11.
- [45] Q. Li, Q. Zhu, and M. Wang, "Design of a distributed energy-efficient clustering algorithm for heterogeneous wireless sensor networks", *Computer Communications*, vol. 29, no. 12, pp. 2230-2237, Aug. 2006.
- [46] K. Cengiz, T. Dag, "Energy Aware Multi-Hop Routing Protocol for WSNs", *IEEE Access*, Vol. 6, February 2018, pp. 2622 - 2633.
- [47] T. Rault, A. Bouabdallah, Y. Challal, "Energy efficiency in wireless sensor networks: a top-down survey", *Computer Networks*, vol. 67, pp. 104-122, 2014.
- [48] V. Mor and H. Kumar, "Energy efficient wireless mobile networks: A review", *in Proceedings of IEEE International Conference on Optim., Reliable, Information Technologies*, February 2014, pp. 281-285.
- [49] Jinhua Zhu, "PEER: a progressive energy efficient routing protocol for wireless ad hoc networks", *24th Annual Joint Conference of the IEEE Computer and Communications Societies (IEEE INFOCOM 2005)*, pp. 1887- 1896, March 13-17, 2005.
- [50] A. Venkateswaran, V. Sarangan, T.F. La Portaand, R. Acharya, "A Mobility-Prediction-Based Relay Deployment Framework for Conserving Power in MANETs", *IEEE Transactions on Mobile Computing*, vol.8, no.6, pp.750-765, June 2009.
- [51] Floriano De Rango, Marco Fotino and Salvatore Marano, "EEOLSR: Energy Efficient OLSR Routing Protocol For Mobile Adhoc Networks", *IEEE Military Communications Conference*, pp 1-7, Nov. 16- 19, 2008.

- [52] Thomas Clausen, Philippe Jacquet, Cédric Adjih, Anis Laouiti, Pascale Minet, et al.. "Optimized Link State Routing Protocol (OLSR)", pp. 1-53, 2003. (inria-00471712)
- [53] E. Amar and S. Boumerdassi, "A scalable mobility-adaptive location service with Kalman-based prediction", *2011 IEEE Wireless Communications and Networking Conference (WCNC)*, pp.593-598, March 28-31,2011.
- [54] R.A. Hunjet, "Power and Placement: Increasing Mobile Adhoc Network Capacity and Power Efficiency", *Telecommunication Networks and Applications Conference (ATNAC) 2008*, pp. 198-203, Dec. 7-10, 2008.
- [55] Prabha, M.; Darly, S.S.; Rabi, B.J., "Energy conservative mobile sink path routing for wireless sensor networks", *In Proceedings of the 2019 International Conference on Smart Structures and Systems(ICSSS)*, Chennai, India, 14-15 March 2019; pp. 1-6.
- [56] Wen, W.; Zhao, S.; Shang, C.; Chang, C.Y., "EAPC: Energy-aware path construction for data collection using mobile sink in wireless sensor networks", *IEEE Sensors Journal*, vol. 18, pp. 890-901, 2017.
- [57] Salarian, H.; Chin, K.W.; Naghdy, F., "An energy-efficient mobile-sink path selection strategy for wireless sensor networks", *IEEE Transactions on Vehicular Technologies.*, vol. 63, pp. 2407-2419, 2013.
- [58] Wang, J.; Gao, Y.; Liu, W.; Sangaiah, A.K.; Kim, H.J., "Energy Efficient Routing Algorithm with Mobile Sink Support for Wireless Sensor Networks", *Sensors*, vol. 19, 1494, 2019.
- [59] Wang, J.; Cao, J.; Ji, S.; Park, J.H., "Energy-efficient cluster-based dynamic routes adjustment approach for wireless sensor networks with mobile sinks", *J. Supercomput.* 73, pp. 3277-3290, 2017.
- [60] Sasirekha, S.; Swamynathan, S., "Cluster-chain mobile agent routing algorithm for efficient data aggregation in wireless sensor network", *J. Commun. Netw.*, vol. 19, pp. 392–401 2017.

- [61] Rady, A.; Shokair, M.; El-Rabaie, E.L.M.; Saad, W.; Benaya, A., "Energy-efficient routing protocol based on sink mobility for wireless sensor networks", *IET Wireless Sensor Systems*, vol. 9, 405-415, 2019.
- [62] Jafri, M.R.; Javaid, N.; Javaidand, A.; Khan, Z.A., "Maximizing the lifetime of multi-chain PEGASIS using sink mobility", *World Applied Sciences Journal*, vol. 21, pp. 1283-1289, 2013.
- [63] He, X.; Fu, X.; Yang, Y., "Energy-Efficient Trajectory Planning Algorithm Based on Multi-Objective PSO for the Mobile Sink in Wireless Sensor Networks", *IEEE Access*, vol. 7, pp. 176204-176217, 2019.
- [64] K. Almiani, A. Viglas, and L. Libman, "Energy-efficient data gathering with tour length-constrained mobile elements in wireless sensor networks", in *Proceedings of 35th IEEE Local Computer Networks Conference (LCN)*, October 2010, pp. 582–589.
- [65] Mehto, A.; Tapaswi, S.; Pattanaik, K.K., "PSO-Based Rendezvous Point Selection for Delay Efficient Trajectory Formation for Mobile Sink in Wireless Sensor Networks", in *Proceedings of the International Conference on COMMunication Systems and NETWORKS (COMSNETS)*, Bengaluru, India, 5-9 January 2020; pp. 252-258.
- [66] Zhong, J.; Huang, Z.; Feng, L.; Du, W.; Li, Y., "A hyper-heuristic framework for lifetime maximization in wireless sensor networks with a mobile sink", *IEEE/CAA Journal of Automatic Sinica*, vol. 7, pp. 223-236, 2019.
- [67] Sahoo, B.M.; Rout, R.K.; Umer,S.; Pandey, H.M., "ANT Colony Optimization based Optimal Path Selection and Data Gathering in WSN", in *Proceedings of the 2020 International Conference on Computation, Automation and Knowledge Management (ICCAKM)*, Dubai, United Arab Emirates, 9–11 January 2020; pp. 113–119.
- [68] Coloni, A., Dorigo, M., Maniezzo, V., "Distributed optimization by ant colonies", in *Proceedings of ECAL91-European Conference on Artificial Life*, Paris, France. Elsevier, Amsterdam, pp. 134–142, 1991.

- [69] Colorni, A., Dorigo, M., Maniezzo, V., "An investigation of some properties of an ant algorithm", *In Manner, R., Manderick, B. (Eds.), Proceedings of the Parallel Problem Solving from Nature Conference (PPSN 92)*, Brussels, Belgium. Elsevier, Amsterdam, pp. 509–520, 1992.
- [70] Dorigo, M., Maniezzo, V., Colorni, A., "Ant System: Optimization by a Colony of Cooperating Agents", *IEEE Transactions on Systems, Man, and Cybernetics-Part B Cybernetics*, vol. 26, no. 1, pp. 29-41, February 1996.
- [71] Thiruchelvi, A.; Karthikeyan, N., "Pair-based sink relocation and route adjustment in mobile sink WSN integrated IoT", *IET Communications*, vol. 14, pp. 365-375, 2020.
- [72] Liu, Q., Zhang, K., Liu, X., et al.: "Grid routing: an energy-efficient routing protocol for WSNs with single mobile sink", *International Journal of Sensor Networks*, 2017, 25, pp. 232-243.
- [73] Khan, A.W., Bangash, J.I., Ahmed, A., Abdullah, A. H., "QDVGDD: Query-Driven Virtual Grid based Data Dissemination for wireless sensor networks using single mobile sink", *Wireless Networks*, vol. 25, pp. 241-253, (2019).
- [74] Wen, W.; Shang, C.; Chang, C.Y.; Roy, D.S., "DEDC: Joint Density-Aware and Energy-Limited Path Construction for Data Collection Using Mobile Sink in WSNs", *IEEE Access*, vol. 8, pp. 78942-78955, 2020.
- [75] Vera-Amaro, R.; Rivero-Ángeles, M.E.; Luviano-Juárez, A., "Data Collection Schemes for Animal Monitoring Using WSNs-Assisted by UAVs: WSNs-Oriented or UAV-Oriented", *Sensors*, vol. 20, 262, 2020.
- [76] Gul, O. M. and Erkmén, A. M. "Energy-efficient Cluster-Based Data Collection by a UAV with a Limited-Capacity Battery in Robotic Wireless Sensor Networks", (*MDPI*) *Sensors*, vol. 20 (10), pp. 1-35, October 2020.
- [77] Golden, B. L. , Levy, L. , Vohra, R., "The orienteering problem", *Naval Research Logistics*, 34 (3), pp. 307–318, 1987.
- [78] A. G. Hoong, C. Laua and P. Vansteenwegen, "Orienteering Problem: A survey of recent variants, solution approaches and applications", *European Journal of Operational Research*, pp. 315-332, 2016.

- [79] Vansteenwegen, P. , Souffriau, W. , and Van Oudheusden, D., "The orienteering problem: A survey", *European Journal of Operational Research*, 209 (1), pp. 1-10, 2011.
- [80] E. Fountoulakis; G. S. Paschos; N. Pappas, "UAV Trajectory Optimization for Time Constrained Applications", *IEEE Networking Letters*, vol. 2, no. 3, September 2020, pp 136-139.
- [81] Sevkli, Z. , and Sevilgen, F. E., "StPSO: Strengthened particle swarm optimization", *Turkish Journal of Electrical Engineering & Computer Sciences*, vol. 18, no. 6, pp. 1095-1114.
- [82] Sevkli, Z. , and Sevilgen, F. E., "Discrete particle swarm optimization for the orienteering problem", *Proceedings of IEEE congress on evolutionary computation (CEC 2010)*, Barcelona, Spain, pp. 3234-3241, 2010.
- [83] Chekuri, C. , Korula, N. , & Pál, M. (2012). Improved algorithms for orienteering and related problems", *ACM Transactions on Algorithms*, vol. 8 , pp. 661-670.
- [84] Y. C.Liang, S.Kulturel-Konak,M.H.Lo, "A multiple-level variable neighborhood search approach to the orienteering problem", *Journal of Industrial and Production Engineering*, vol. 30, no. 4, pp. 238-247, 2013.
- [85] Kulturel-Konak, S. , Norman, B. A. , Coit, D. W. , & Smith, A. E., "Exploiting tabu-search memory in constrained problems", *INFORMS Journal on Computing*, vol. 16, no. 3, pp. 241-254.
- [86] Ramirez-Marquez, J. E. , Kulturel-Konak, S. , & Sanseverino, C. M. R., "Probabilistic solution discovery algorithm for the orienteering problem", *International Journal of Industrial and Systems Engineering*, 6 (1), 45-61, 2010 .
- [87] Campos, V. , Martí, R. , Sánchez-Oro, J. , & Duarte, A., "GRASP with path relinking for the orienteering problem", *Journal of the Operational Research Society*, 65 (12), pp. 1800-1813, 2014.
- [88] Resende, M. G. C. , & Ribeiro, C. C., "Greedy randomized adaptive search procedure", In F. Glover, & G. Kochenberger (Eds.), *State-of-the-art handbook in meta- heuristics*, *Kluwer Academic Publishers*, pp. 219-250, 2003.

- [89] Marinakis, Y. , Politis, M. , Marinaki, M. , & Matsatsinis, N., "A memetic-GRASP algorithm for the solution of the orienteering problem" In H. A. Le Thi, T. P. Dinh, & N. T. Nguyen (Eds.), *Modelling, computation and optimization in information systems and management sciences. In Advances in Intelligent Systems and Computing*, 360, pp. 105-116, Springer, 2015.
- [90] Chao, I.-M. , Golden, B. L. ,& Wasil, E. A. , "A fast and effective heuristic for the orienteering problem", *European Journal of Operational Research*, vol. 88, no. 3, pp. 475-489, 1996.
- [91] Tsiligirides, T., "Heuristic methods applied to orienteering", *Journal of the Operational Research Society*, vol. 35, no. 9, pp. 797-809, 1984 .





CURRICULUM VITAE

PERSONAL INFORMATION

Surname, Name : Gül, Ömer Melih
Nationality : Turkish (TC)
Date and Place of Birth : 29 November 1989, Istanbul, Turkey
Marital Status : Single
Phone : +90 312 210 45 90
E-mail : omgul@metu.edu.tr

EDUCATION

Degree	Institution	Year of Graduation
M.S.	METU, Electrical&Electronics Engineering	2014
B.S.	METU, Electrical&Electronics Engineering	2012
High School	Kocaeli Science High School	2007

PROFESSIONAL EXPERIENCE

Year	Place	Enrollment
2012- 2020	METU, Dept. of Electrical&Electronics Engineering	Research Assistant

FOREIGN LANGUAGES

Advanced English, Beginner German

PUBLICATIONS

International Journal Publications

1. Gul, O. M. and Erkmen, A. M. "Efficiency-aware and Energy-aware Cluster-Based Data Collection via UAV with Limited-Capacity Battery in Robotic Wireless Sensor Networks", submitted.
2. Gul, O. M. and Erkmen, A. M. "Energy-efficient Cluster-Based Data Collection by a UAV with a Limited-Capacity Battery in Robotic Wireless Sensor Networks", (MDPI) Sensors, vol. 20 (10), pp. 1-35, October 2020.
3. Gul, O. M., "Average Throughput of Myopic Policy for Opportunistic Access Over Block Fading Channels", IEEE Networking Letters, vol. 1, no. 1. pp. 38-41, March 2019.
4. Gul, O. M., Demirekler, M., "Asymptotically Throughput Optimal Scheduling for Energy Harvesting Wireless Sensor Networks", IEEE Access, vol. 6, pp. 45004-45020, September 2018.
5. Gul, O. M., Demirekler, M., "Average Throughput Performance of Myopic Policy in Energy Harvesting Wireless Sensor Networks", (MDPI) Sensors, vol. 17, no. 10., pp. 1-20, September 2017.

International Conference Publications

1. Gul, O. M., "Achieving Near-Optimal Fairness in Energy Harvesting Wireless Sensor Networks", in the Proceedings of 24th Annual IEEE International Symposium on Computers and Communications (IEEE ISCC 2019), 29 June-3 July 2019, Barcelona, Spain, pp. 1-6.
2. Gul, O. M., "Asymptotically Optimal Scheduling for Energy Harvesting Wireless Sensor Networks", in the Proceedings of 28th Annual IEEE International Symposium on Personal, Indoor and Mobile Radio Communications (IEEE PIMRC 2017), 08-13 October 2017, Montreal, QC, Canada, pp. 1-7.

3 Gul, O. M. and Uysal-Biyikoglu, E., "Achieving Nearly 100% Throughput without Feedback in Energy Harvesting Wireless Networks", in the Proceedings of IEEE International Symposium on Information Theory (IEEE ISIT 2014), 29 June-4 July 2014, Honolulu, Hawaii, USA, pp. 1171-1175.

4. Gul, O. M. and Uysal-Biyikoglu, E., "A Randomized Scheduling Algorithm for Energy Harvesting Wireless Sensor Networks Achieving Nearly 100% Throughput", in the Proceedings of IEEE Wireless Communication & Networking Conference (IEEE WCNC 2014), 6-9 April 2014, Istanbul, Turkey, pp. 2456-2461.

International Conference Abstracts

1. Gul, O. M. and Erkmen, A. M. "Achieving Asymptotically Optimal Throughput in Centralized Mobile Robot Networks without Dispatching Feedback", 28th European Conference on Operational Research, Poznan/Poland, (2016).

2. Nalcaci, G., Ozmen, A., Weber, G. W., and Gul, O. M., "Load Forecasting Using Multivariate Adaptive Regression Splines for Turkish Electricity System", 28th European Conference on Operational Research, Poznan/Poland, (2016).

INTERNATIONAL AWARDS

1. Finalist in the Best Poster Competition (with Theme: Response and Recovery from COVID-19) in the 2021 IEEE Rising Stars Global Conference.

2. Third Place at 2019 Lance Stafford Larson Outstanding Student Paper Award, organized by the IEEE Computer Society.